Water Science and Application 7

A Peculiar River

Geology, Geomorphology, and Hydrology of the Deschutes River, Oregon

Water Science and Application 7

A Peculiar River

Geology, Geomorphology, and Hydrology of the Deschutes River, Oregon

Jim E. O'Connor
Gordon E. Grant
Editors

American Geophysical Union
Washington, DC

A Peculiar River: Geology, Geomorphology, and Hydrology of the Deschutes River
Water Science and Application 7

Library of Congress Cataloging-in-Publication Data

A peculiar river : geology, geomorphology, and hydrology of the
Deschutes River, Oregon / Gordon E. Grant, Jim E. O'Connor, editors.
p. cm. -- (Water science and application ; 7)
Includes bibliographical references.
ISBN 0-87590-356-8
1. Deschutes River (Or.) I. Grant, Gordon, 1953- II. O'Connor, Jim E., 1959-
III. Series.

GB1227.D55P54 2003
551.48'3'0979562--dc21 2003048069

ISBN 0-87590-356-8
ISSN 1526-758X

Printed in the United States of America.

CONTENTS

FOREWORD

Fashions in science as in society come and go. One hundred years ago, geographers wrote treatises on individual rivers with simple two or three word titles such as "The...River." While this great tradition endures, it is carried on primarily by journalists whose orientation is less scientific and certainly less quantitative than much of the earth sciences expects today. Perhaps more common now are detailed studies of portions of rivers, or syntheses of observations on diverse rivers in hopes of discerning generalizations. Of course, recent trends should not obscure the need for both approaches.

Seen as a continuum, the characteristics and behavior of a river at any point are a consequence of forces generated both upstream and downstream. Thus, unique features of a river and its valley may be locally determined or the consequence of a continuum of processes operating over broader scales. Abstraction of observations and generalizations from river features provide insights and useful tools for the study and management of rivers. At the same time, broad geographic studies of rivers provides tests of the validity of generalization, revelations of the truly unique, and insights that sometimes only the unique can provide. Study of the Deschutes River satisfies these three criteria as well as a fourth—the study of the basin as a whole and its recent geologic history provides a context within which to analyze a practical problem: the impact of dams on a river system.

The Deschutes is odd, probably unique. It is a large river for which 80% of the mean annual flow is from groundwater; in the two greatest floods in this century 70% of the peak discharge came from 26% of the drainage area, the peak flood flows are less than five times the mean annual flow, and the annual sediment load is only 4-6 tonnes per square kilometer per year. A spatial mix of geology, topography, and climate produces these striking and unusual phenomena. Mount Hood on the northwestern boundary of the drainage basin attains an elevation of 3200 m and the annual precipitation along this Cascade Range boundary is over 2000 mm. To the east, sparsely dissected plains of Columbia River basalt and older, deeply eroded, volcanic ranges bake in a dramatic semi-arid landscape.

The dramatic juxtaposition of geology, topography, and climate creates a virtual textbook of landforms and geomorphic processes. These become even more vivid as the geologic history is explored revealing Quaternary, Holocene, and very recent episodic events of immense magnitude. Along with active volcanism and tectonism, the present riverine landscape reflects this episodic geomorphic history, as remnants of fluviatile features, huge bars and boulders, mantle the landscape. On the basis of stratigraphic, sedimentary, hydraulic, and hydrologic evidence these studies show that a number of flood discharges in the past 4,500 years exceeded by four-fold or more known floods of the historic past, the last 150 years. For example, the stage of the "Outhouse" flood, about 4,500 years ago, was 3 to 4 m above the highest flood of record at twice the discharge.

In sum, the papers in this volume tell a fascinating story about a striking, sometimes intimidating, landscape. In our search for generalizations about rivers, as about many phenomena, study of anomalies serves both to question generalities and as a laboratory in which to study special landforms and the diverse processes that produce those landforms. With its large groundwater influence and unique geologic, climatologic and topographic setting, the Deschutes River is a fine laboratory.

But the history of the landscape, the processes that molded it and the characteristic features left behind by these processes in the Deschutes valley here serve an important additional purpose. It is the coherent background story that provides the basis for evaluating the effect of a large three-dam complex on the Deschutes River. The authors' conclusion that the dams and reservoirs have had little effect on the sedimentary regimen or channel morphology and behavior of the river could not have been reached in the absence of a knowledge of the origin of the rock and sedimentary features comprising the valley of the Deschutes. Matching lines of comparative evidence are used to support this finding. For the current hydrologic regimen, studies include observation of materials moved by several of the largest floods of record, computations of bedload sediment rating curves and thresholds of movement of varied particle sizes by modern flows, and comparisons of channel changes shown on aerial photographs. Comparable stratigraphic, particle size and morphologic observation of dated paleo-landscape features coupled with computations of paleoflood magnitudes from slackwater and terrace deposits demonstrate that pre-historic events far exceeded the magnitude and geomorphic effect of even the largest events in the historic record. To the chagrin of some, the evidence clearly indicates that more rare events of large magnitude dominate in molding this landscape.

Reconstruction of the paleohydrology and associated morphology provides the framework within which modern processes operate and their relative scale and significance. The interrelationship between past and present is important in distinguishing and measuring the impact of human activity. The study of this "peculiar" river, so characterized 100 years ago, also demonstrates the value and potentially fascinating context of those volumes traditionally titled "The...River."

M. G. Wolman

Introduction

Jim E. O'Connor

U.S. Geological Survey, Portland, Oregon

Gordon E. Grant

U.S. Forest Service, Corvallis, Oregon

INTRODUCTION

...the Deschutes is of especial interest to geographers, as it exhibits certain peculiarities not commonly met with.

This observation by geographer *Israel C. Russell* [1905, p. 20] replayed in our minds repeatedly during our studies of the Deschutes River in central Oregon. Studies by Russell and others alerted us to some peculiar aspects of the Deschutes, such as the remarkably steady spring-fed flow and extensive groundwater system. These attributes led other early chroniclers to describe the river's flow as being "...more remarkably uniform than that of any other river in the United States comparable with it in size, and its economic value is almost incalculable" [*Henshaw et al.*, 1914, p. 12]. Some of that value has been realized over the past century with the development of agriculture, hydropower, water supply, river recreation, and a blue-ribbon recreational fishery, the latter complementing a Native American fishery that has persisted for millennia.

Nevertheless, we were not prepared for other peculiarities, such as the role of extreme events in controlling channel and valley geomorphology, the paucity of historic changes to the lower river after nearly fifty years of upstream impoundment, and the remarkably low rates of sediment production and transport within the basin. In hindsight, we can see that all these aspects of the river system are connected and perhaps even predictable, given sufficient understanding of rivers and river processes. For us, however, these connections were unexpected and forced us towards achieving "consilience" in our understanding of the Deschutes River, which in the words of inductionist *Whewell* [1840] is the "jumping together" of "facts and fact-based theory across disciplines to create a common groundwork of explanation."

A Peculiar River
Water Science and Application 7

Published in 2003 by the American Geophysical Union
10.1029/007WS01

The purpose of this monograph is to describe this groundwork of understanding by linking together several separate but related studies from a variety of disciplines into an integrated view of the geology, hydrology, geomorphology, and ecology of the Deschutes River. Although presented together, these studies did not result from an organized plan to understand the entire Deschutes River basin. Instead, the research was initially prompted by the Federal Energy Regulatory Commission (FERC) relicensing of the Pelton-Round Butte Hydroelectric Project (FERC Project No. 2030) (Figure 1), and centered on a specific question focused on a particular reach of river: "What effect has flow regulation and reduced sediment input had on the Deschutes River downstream of the Pelton-Round Butte dam complex?" Given the abundant literature on this issue for a variety of rivers, we expected this study to reveal evidence of channel armoring and incision downstream of the dam complex. To our surprise, this did not turn out to be the case-there is little evidence of change in channel bed texture and morphology since dam construction, even with the 1996 passage of the largest flood in 135 years. Only then (in the process of defending our unexpected results) were we inspired to step back and look at the river system from a broader perspective.

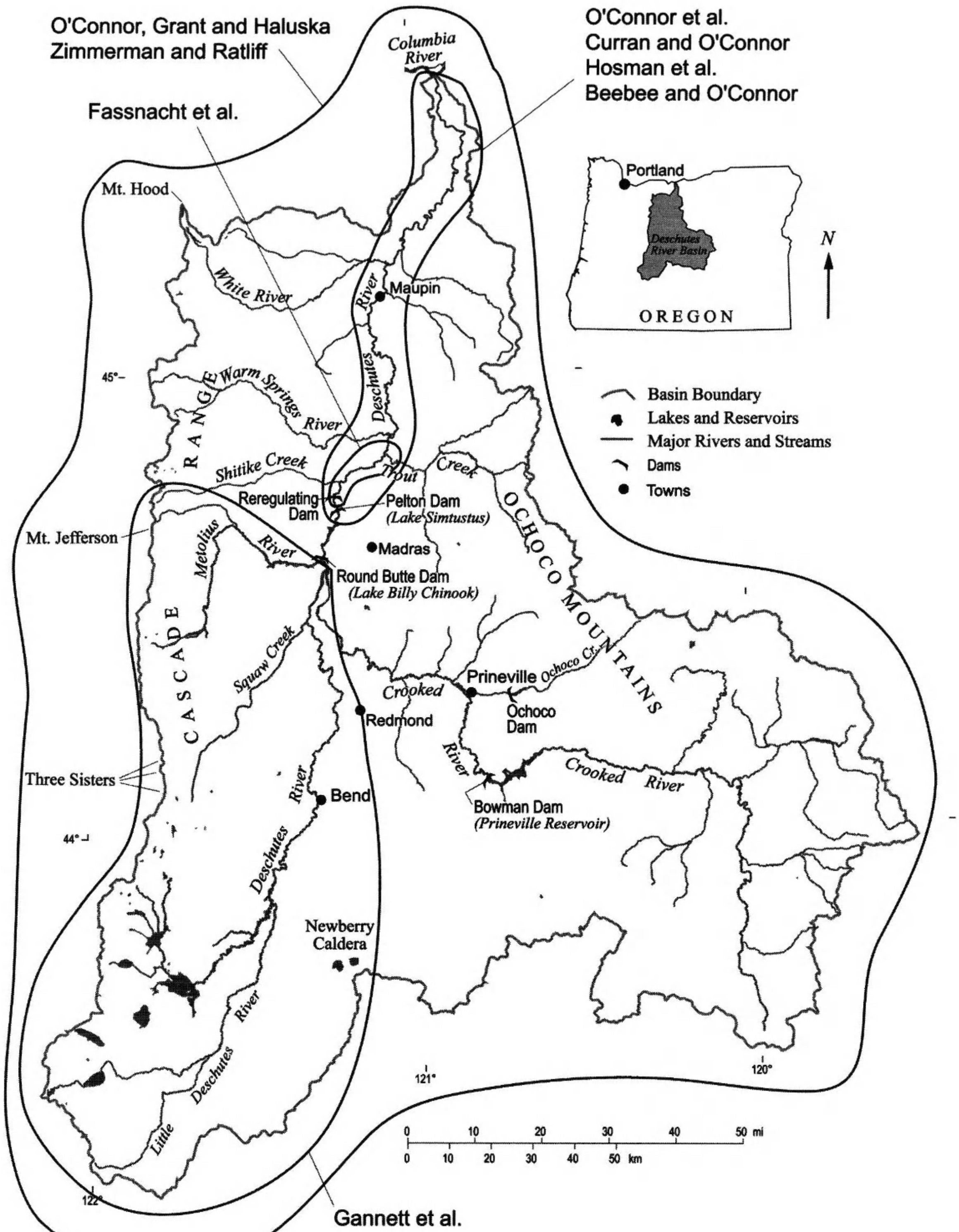

Figure 1. Map of the Deschutes River basin, Oregon, showing areas reported on by individual contributions to this volume.

This wider view, carried out in a range of studies, illuminated the role of geologic setting and history in limiting the effectiveness of modern processes, such as those likely to be affected by dam operations, in shaping the present channel and valley bottom of the Deschutes River.

Some might argue that we conducted our research backwards—that the likelihood of such research surprises might have been smaller if we first understood the broader setting of the river basin before launching into detailed analyses of reach-scale conditions. But such an approach might not have been more efficient. The first reach-scale studies targeted the specific issues that needed to be addressed for understanding the downstream effects of the Pelton-Round Butte dam complex. The results indicating that the response of Deschutes River was different from most dammed rivers focused our broader-scale studies toward understanding the landscape-level mechanisms involved. Without these targets, results of these basin-scale studies might not have been relevant to the specific issues generated by the dam relicensing. In reality, the process was iterative, requiring investigators to think about processes and events at multiple temporal and spatial scales. Inevitably, we revisited studies and reinterpreted results multiple times until we achieved what we feel is some measure of "consilience" in our understanding of the Deschutes River. Together, these studies and their reports paint a coherent picture of the river.

Why report this work in a single volume? One pragmatic reason, of course, is that readers interested in various aspects of the geology, geomorphology and hydrology of the Deschutes River will be able to find overview papers as well as detailed reports between one pair of book covers. But as we struggled to convince ourselves and others that this body of work represented more than an interesting case study, we came to understand that such a volume is the only way in which an integrated perspective of a unique river system can be presented without the intellectual fragmentation of separate offerings spread throughout the literature. We were inspired by the unexpected connections of observations and findings at many different temporal and spatial scales that developed between studies, the "jumping together" in the words of Whewell.

In our view, development of these atmosphere-to-basin-to-cobble linkages was a major product of our efforts on the Deschutes River—one that transcends just the Deschutes River and is applicable to understanding rivers worldwide. While such an approach is not necessarily new, only in a volume such as this can we fully lay out these connections as well as the underlying studies. Our intent is that this volume serves as an example of a holistic approach to understanding rivers—one that recognizes that each river is unique and will respond differently to environmental conditions depending on its current landscape setting as well as its history. This type of approach is increasingly needed, not just to evaluate the hundreds of dams scheduled to be relicensed in the next decades, but also to provide the technical underpinning to decisions related to new dam construction

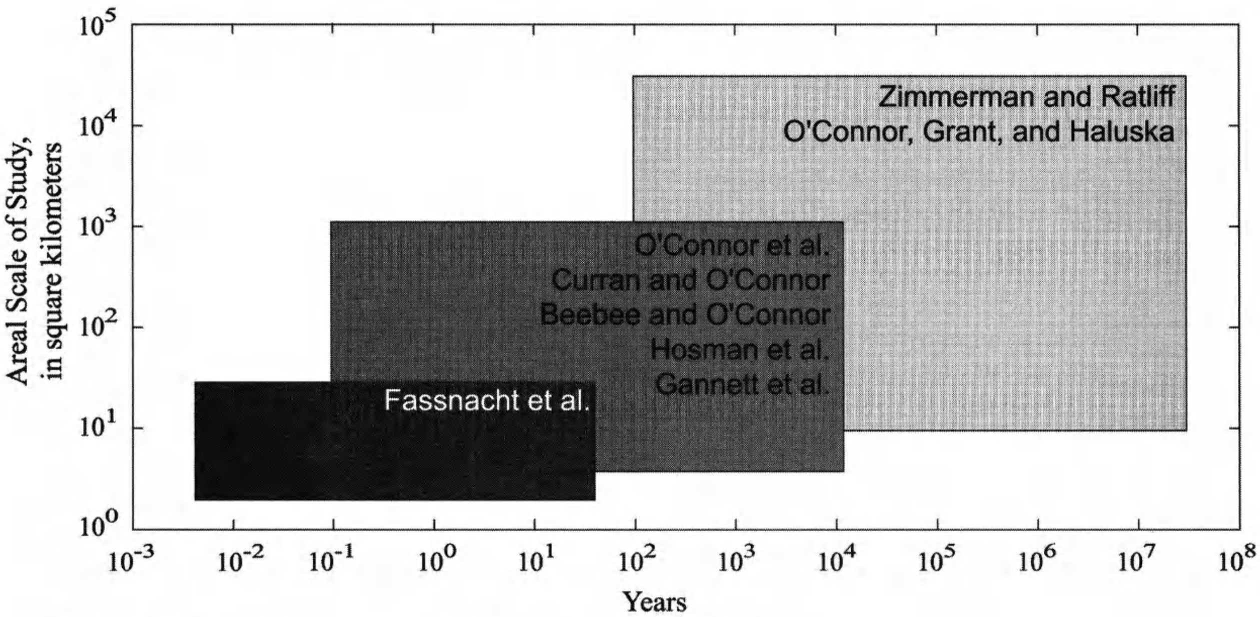

Figure 2. Approximate temporal and spatial domains of volume contributions.

(particularly in the developing world), dam removal, and river restoration efforts worldwide. If we had to distill the message of this volume down to a single line, it would read: A river is not a river is not a river; nor are all dams created equal; but an understanding of the geological and geomorphic context around both rivers and dams provides a sound framework for interpreting their behaviors and effects.

This volume is composed of nine separately authored papers arranged in three sections. The contributions were ordered so that findings and results from early papers form points of departure for subsequent papers. Consequently, the temporal and spatial scales of described features and processes generally diminish as the reader progresses through the book (Figure 2). The first section is a series of three overview papers describing the geology, hydrology, and fish of the Deschutes River basin. The second section contains four papers focusing on the geomorphology and geologic history of the 160 km of the Deschutes River downstream of the Pelton-Round Butte dam complex. The final section is composed of two papers that specifically address the effects of the dam complex on the lower Deschutes River, and evaluates these results with respect to global observations of the effects of dams on rivers. Each section is preceded by a brief introduction summarizing linkages between individual contributions.

Finally, we come back to Russell's observation that the Deschutes River is of "especial interest" because of its peculiarities. We hope that the papers contained in this volume are of interest because of the remarkable peculiarities of the Deschutes River and the understanding that we have developed of the river basin over the last seven years of studies. Moreover, we hope that this volume is of interest because of the linkages between the studies in the volume, and how, in total, such studies frame an understanding of a river. After all, few readers will visit or conduct research on the Deschutes River, but many will strive to understand other rivers, each peculiar in its own way.

Acknowledgments. Individual papers acknowledge funding sources, assistance, and reviewers, but several entities and individuals were important in the process of planning, conducting, and reporting the research presented in this volume. Portland General Electric directly or indirectly funded many of the studies, provided logistical support, and supplied data for many of the studies. In particular, Julie Keil, Don Ratliff, and John Esler of the P.G.E. hydropower licensing team supported our studies while allowing us to work independently. Eric Schuster and Walt Wolff of P.G.E. assisted with the logistics of working on the river. Major additional sources of funding included the U.S. Geological Survey, the Pacific Northwest Forestry Sciences Laboratory of the U.S.D.A. Forest Service, Oregon Department of Water Resources, and Oregon State University.

We thank all the authors for their contributions and patience in dealing with a long review and publication process. All the contributions were improved with the assistance of the more than twenty external reviewers. Kathryn Ronnenberg of the Forestry Sciences Laboratory edited the text, prepared many of the figures and maps, and performed final text formatting. Sarah Lewis of the Dept. of Geosciences at Oregon State University assisted with a range of editorial, graphics, and organizational tasks. Completion of this volume was aided by the staff and publications committee at the American Geophysical Union, including John Costa of the publications committee, Allan Graubard, A.G.U. books acquisition editor, and Terence Mulligan, who prepared the final layout.

REFERENCES

Henshaw, F. F., J. H. Lewis, and E. J. McCaustland, Deschutes River, Oregon, and its utilization, *U.S. Geol. Surv. Water Supply Pap.* 344, 200 pp., 1914.

Russell, I. C., Preliminary report on the geology and water resources of central Oregon, *U.S. Geol. Surv. Bull.* 252, 138 pp., 1905.

Whewell, W., *The Philosophy of the Inductive Sciences, Founded Upon Their History,* John W. Parker, London, two volumes, 1840.

Jim E. O'Connor, U.S. Geological Survey, 10615 SE Cherry Blossom Drive, Portland, OR, 97216

Gordon E. Grant, U.S. Forest Service, 3200 Jefferson Way Corvallis, OR 97331

Section I

Geology, Hydrology and Fish of the Deschutes River Basin

To understand a river, one must understand something of its watershed. While this simple concept applies to all rivers, it is particularly true for the Deschutes River. The peculiarities of the Deschutes discussed in later chapters of this book derive, in large part, from the unique context, history and processes of its drainage basin—the subject of this section.

At the largest scale, this context comes from the basin's climatic and tectonic setting. The Deschutes River drains the leeward side of a young, uplifted volcanic arc squarely in the path of the westerly prevailing winds at a temperate latitude not far from a marine source of moisture. The many unusual aspects of the river's discharge and sediment regimes, as described in the papers in this section, follow logically (though not obviously) from this geography. The combination of abundant moisture plus highly permeable, undissected, and layered lava flows in the southwestern portion of the basin gives rise to a laterally extensive, deep groundwater system, which supports the extraordinarily stable discharge regime, as discussed in *Gannett et al.* Limited surface runoff in this area is reflected in the low drainage densities and gentle slopes; these factors coupled with the young and unweathered rocks result in extremely low sediment production and delivery to channels, as described in *O'Connor, Grant and Haluska.* Low temperature springs fed by the deep groundwater system provide ideal habitat for coldwater fish species, such as bull trout, that could not otherwise survive in an arid landscape, as *Zimmerman and Ratliff* point out. All of these aspects owe to the basin's geoclimatic setting.

The papers in this section provide background and context for interpreting the finer-scaled processes discussed in later chapters. All emphasize the theme of geologic control. The geologic, geomorphic, and hydrologic framework for the basin is explored in the overview chapter by *O'Connor, Grant and Haluska*, who demonstrate how both landscape evolution, as reflected in the topography, and the modern hydrology and sediment transport regimes of the Deschutes River are intimately linked to the underlying geological setting. Geologic controls on the flow regime are described more extensively in the paper by *Gannett et al.*, who identify the sources, flow paths, and residence times of water in the upper Deschutes River basin through analyses of hydrologic records, water temperature, and isotopic tracers. They show how the combination of long groundwater flow paths, high groundwater recharge rates, and a large, laterally extensive unsaturated zone contribute to dampening peak flows and diminishing seasonal and interannual variability in discharge, leading to highly stable flows. Finally, in the sole ecological chapter in this volume, *Zimmerman and Ratliff* consider how even the distribution and population dynamics of fish assemblages are related to the geology.

The themes that emerge from this section—the strong influence of geology, the seasonally and spatially varying sources of water, the exceedingly small sediment production from the upper basin—are fundamental to understanding the Deschutes River and its response to dams, as discussed in subsequent sections.

A Peculiar River
Water Science and Application 7
10.1029/007WS02

Overview of Geology, Hydrology, Geomorphology, and Sediment Budget of the Deschutes River Basin, Oregon

Jim E. O'Connor

U.S. Geological Survey, Portland, Oregon

Gordon E. Grant

U.S. Forest Service, Corvallis, Oregon

Tana L. Haluska

U.S. Geological Survey, Portland, Oregon

Within the Deschutes River basin of central Oregon, the geology, hydrology, and physiography influence geomorphic and ecologic processes at a variety of temporal and spatial scales. Hydrologic and physiographic characteristics of the basin are related to underlying geologic materials. In the southwestern part of the basin, Quaternary volcanism and tectonism has created basin fills and covered and deranged the surficial hydrologic system, resulting in a relatively low-relief lava-covered landscape with runoff emerging largely from extensive groundwater systems fed by Cascade Range precipitation. The remarkably steady flows of the entire Deschutes River, as depicted in annual and peak flow hydrographs, are due primarily to buffering by the extensive groundwater system of this part of the basin. The eastern part of the basin is primarily underlain by Tertiary volcanic, volcaniclastic, and sedimentary rocks that have weathered into dissected uplands with generally greater slopes and drainage densities than of that of the southwestern part of the basin. Surficial runoff is more seasonal and less voluminous from this more arid part of the basin. The northern part of the basin has been sharply etched by several hundred meters of late Cenozoic incision, resulting in the greatest relief and drainage density of anywhere in the basin. For large floods, such as those of December 1964 and February 1996, more than half of the peak flow at the mouth of the Deschutes River is derived from the northern part of the basin. Modern sediment yield for much of the Deschutes River basin, as determined from reservoir surveys, is exceptionally low and is related to regional slope and drainage properties. Broad-scale sediment budget calculations indicate that more than 50 percent of the sediment produced in the Deschutes River basin produced under modern, pre-impoundment, conditions is from the northern part of the basin. There is ample evidence, however, of much greater sediment yields and large pulses of downstream sediment delivery during Quaternary episodes of volcanism and glaciation.

INTRODUCTION

The Deschutes River is remarkable. Its uniform, spring-fed hydrologic regime has long impressed geographers and hydrologists [e.g., *Russell*, 1905; *Henshaw et al.*, 1914]. Partly in conjunction with the stable flow regime, modern sediment production is exceptionally low over much of the basin. These two factors have combined to create an unusually stable geomorphic system over human time scales. Consequently, as will be seen in following chapters, it is a river system in which impoundments have had few apparent geomorphic effects on the downstream channel and valley bottom of the Deschutes River system.

A Peculiar River
Water Science and Application 7

Published in 2003 by the American Geophysical Union
10.1029/007WS03

However, the Deschutes River basin has not been similarly quiescent over geologic time scales. Extensive volcanism, regional and local tectonism, landslides, and cataclysmic floods have all left their mark across the landscape. Moreover, as is the case for most large basins, the resulting geomorphic characteristics, such as topography, hydrology, and sediment yield, vary widely. The modern Deschutes River, with its stable hydrologic and geomorphic regime and rich aquatic ecosystems, is the combined result of (1) these past processes and events and (2) the present regime of sediment and water yield established by the regional geology. To understand the Deschutes River and its response to impoundment, it is necessary to understand this geologic and hydrologic context.

This paper provides an overview of the geologic, hydrologic, and geomorphic setting of the Deschutes River basin, with special emphasis on aspects that have influenced how the river has responded to impoundment by the Pelton-Round Butte dam complex. This overview sets the stage for companion studies of the valley bottom, channel, and fish ecology of the Deschutes River, which comprise the other papers in this volume.

GEOLOGY, TOPOGRAPHY, HYDROLOGY, AND SEDIMENT TRANSPORT OF THE DESCHUTES RIVER

The Deschutes River drains 26,860 km^2 of north-central Oregon[1], first flowing south from its Cascade Range headwaters, then northward for nearly 300 km along the eastern margin of the Cascade Range before joining the Columbia River 160 km east of Portland (Figure 1). Its principle tributaries, the Crooked and Metolius Rivers, join the Deschutes River at 185 and 180 km, respectively, from the Columbia River confluence. Portland General Electric and the Confederated Tribes of Warm Springs generate 427 megawatts of power from the Pelton-Round Butte dam complex, a set of three hydroelectric dams located 160 to 180 km upstream from the Columbia River confluence.

[1] The drainage area reported by *Hubbard et al.* [1998, p. 118] for the U.S. Geological Survey gage "Deschutes River at Moody, near Biggs, Oregon (station number 14103000)", 2.25 km upstream from the Deschutes River confluence with the Columbia River, is "10,500 mi^2, approximately". Our estimate of the drainage basin area, from a geographic information system analysis of the basin outline portrayed in Figure 1 (derived from a 30-meter resolution digital elevation model) is 26,860 km^2 (10,370 mi^2). We will use the 26,860 km^2 value for discussion and analysis.

Geologic Setting

The Deschutes River basin is formed in sedimentary, igneous, and metamorphic rocks, whose ages range from more than 250 million years old to as young as 1300 years old (Plate 1). The vast majority, however, are Cenozoic volcanic rocks (less than 65 million years old), and almost all of these rocks are lavas of various compositions or other eruptive products. In general, bedrock ages become progressively younger from east to west across the basin. Mesozoic (250 to 65 million years old) and Paleozoic (more than 250 million years old) sedimentary and volcanic rocks crop out in a small area at the eastern edge of the Deschutes River basin. Most of the Ochoco Mountains, a low mountain range forming much of the eastern flank of the basin, and the Mutton Mountains, which trend northwest across the north-central part of the basin, are underlain by weathered volcanic, volcaniclastic, and sedimentary rocks of the John Day and Clarno Formations. These rocks date from about 55 to 20 million years old and are remnants of ancient volcanic highlands and their eruptive products [*Robinson et al.*, 1984; *Walker and Robinson*, 1990; *Taylor*, 1990].

Much of the northern and eastern parts of the Deschutes River basin is underlain by the Columbia River Basalt Group (CRBG), a series of accordantly layered basalt flows erupted primarily between 17 and 14.5 million years ago and covering 165,000 km^2 of southern Washington, northern Oregon, and western Idaho [*Tolan et al.*, 1989]. The CRBG in the eastern part of the Deschutes River basin issued from vents in the John Day River basin, whereas CRBG in the northern Deschutes River basin originated as flows that came westward down the ancestral Columbia Plain from numerous vents in eastern Washington, eastern Oregon, and western Idaho, filling the Columbia Plain with up to 600 m of lava, locally separated by thin sedimentary interbeds [*Newcomb*, 1969; *Smith*, 1986, 1991]. The contemporaneous "Prineville chemical-type" basalt flows (mapped as part of the CRBG in Figure 2, although geographically and chemically distinct from the CRBG [*Goles*, 1986; *Reidel et al.*, 1989; *Hooper et al.*, 1993]) erupted near the location of Bowman Dam in the central part of the basin and flowed northward along an ancestral Crooked River to where they are interbedded with the CRBG that filled the Columbia Plain from the north. The distribution of the CRBG and contemporaneous basalt flows indicates that by 17 million years ago, the present overall geometry of the northern Deschutes River basin had been established with northward drainage through lowlands bounded by the Ochoco Mountains on the east and the ancestral Cascade Range on the west [*Smith*, 1986].

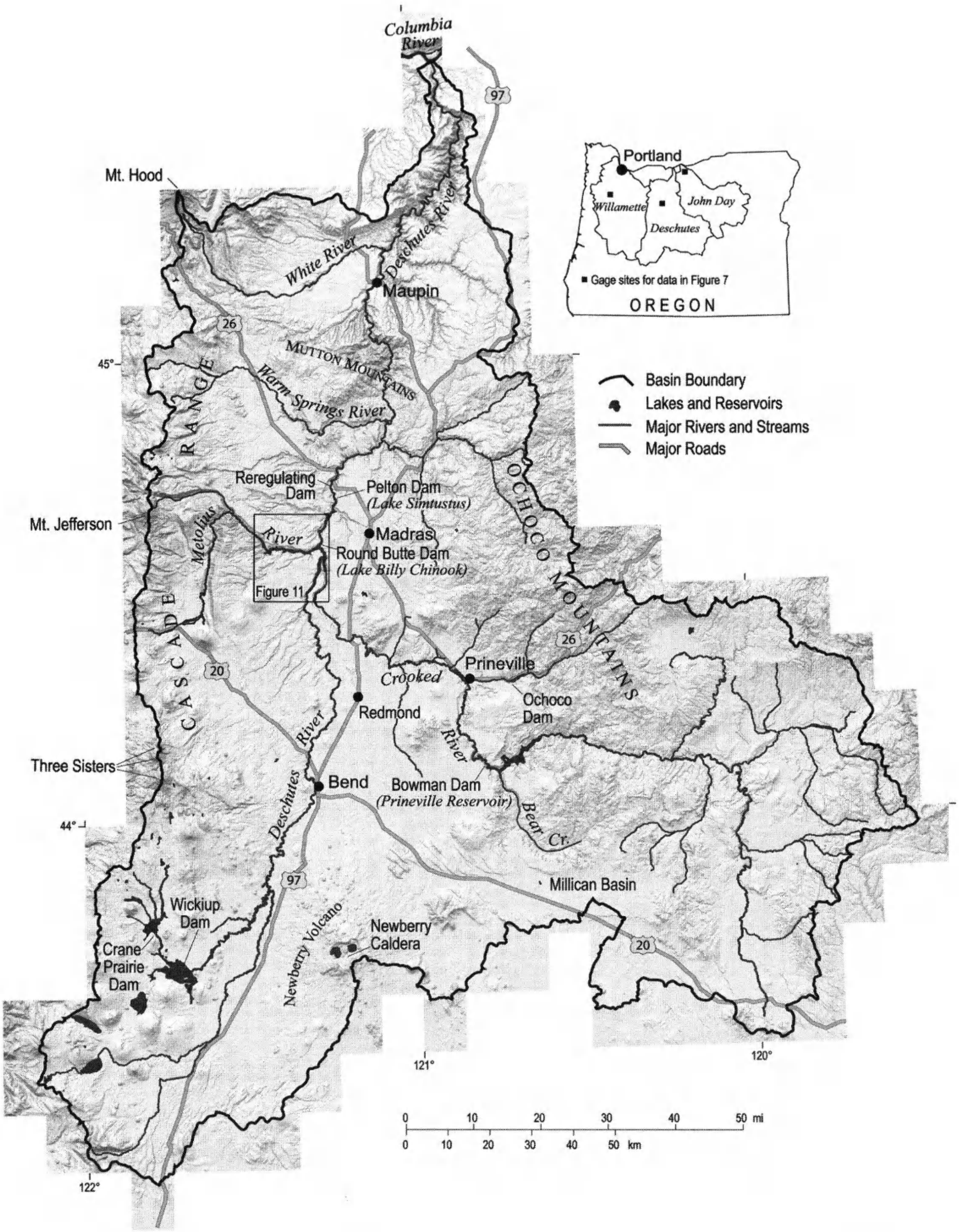

Figure 1. Location map showing major physiographic and cultural features of the Deschutes River basin. Hillshade topographic base derived from U.S. Geological Survey 30-m resolution digital elevation data.

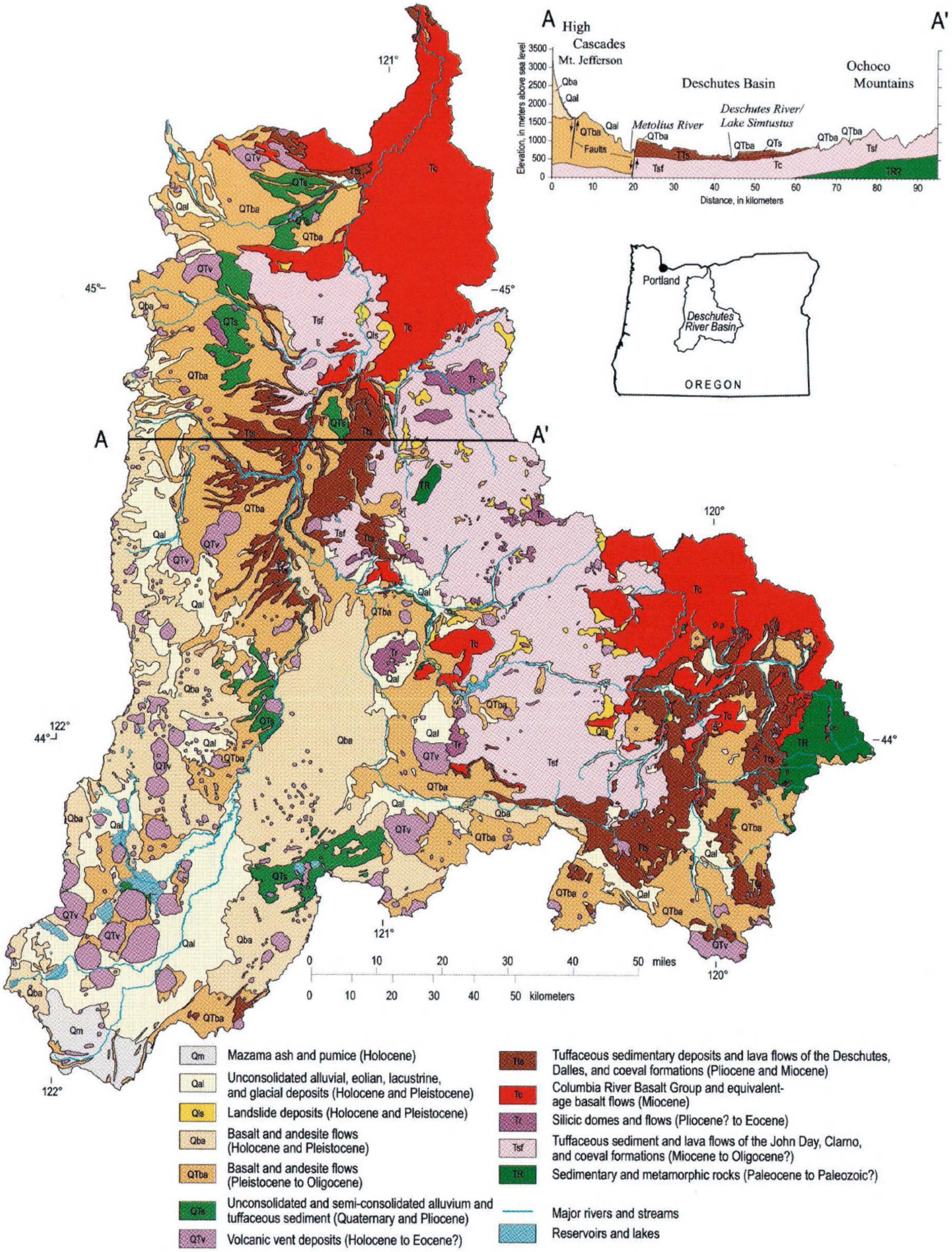

Plate 1. Geologic map of the Deschutes River basin, map units and descriptions generalized from *Walker and MacLeod* [1991]. Cross-section after *Smith* [1986].

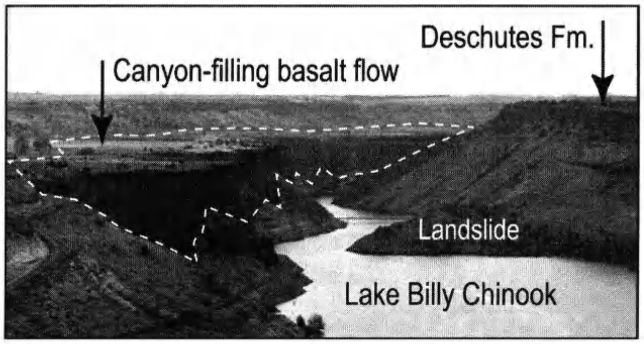

Figure 2. View south up the Crooked River arm of Lake Billy Chinook, impounded behind Round Butte Dam. A basalt flow, age 1.19±0.08 Ma [*Smith*, 1986], has partly filled the canyon previously incised into lava flows, pyroclastic deposits, and fluvial sand and gravel of the Deschutes Formation. The top of the intercanyon basalt flow is 140 m above lake; top of Deschutes Formation is 210 m above lake. Photograph by J.E. O'Connor, 1998.

Deformation during and after emplacement of the Columbia River Basalt Group resulted in isolated basins that accumulated sediment, ignimbrite, and airfall tuffs shed eastward from the emerging Cascade Range and from volcanic highlands in the eastern part of the Deschutes River basin [*Smith*, 1986; *Smith et al.*, 1989]. These deposits formed primarily between 15 and 4 million years ago and include the Simtustus, Deschutes, and Dalles Formations in the central and northern parts of the Deschutes River basin, and the Rattlesnake Ash Flow Tuff in the southeastern Deschutes River basin [*Smith*, 1986, 1991; *Smith et al.*, 1989]. Basalt flows and gravel deposits within the Deschutes Formation near Madras show that the course of the Deschutes River 7.4 to 4.0 million years ago was similar to the present course [*Smith*, 1986, 1987a].

Near the top or capping the Deschutes and Dalles Formations are widespread basalt flows, including the basalt of Juniper Flat near Maupin [2.77±0.36 Ma; R.M. Conrey, unpublished data, cited in *Sherrod and Scott*, 1995] and the Agency Plains basalt flow north of Madras [5.31±0.05 Ma; *Smith and Hayman*, 1987]. These Pliocene basalt flows cover vast surfaces on the uplands, indicating that the landscape at the time was incised little if at all, and that the Deschutes River and its tributaries were flowing at an elevation near the present canyon rims near Madras and Maupin. Specific evidence is found at Round Butte, near Round Butte Dam, where a 3.97±0.05-million-year-old basalt flow invaded Deschutes River gravel about 275 m above the present river level [*Smith*, 1986, 1987b].

The Deschutes and Dalles Formations grade westward into Miocene volcanic rocks of the Cascade Range [*Smith et al.*, 1989]. These rocks are in turn overlain by the active volcanic arc of the present Cascade Range that forms the western boundary of the Deschutes River basin. Volcanism along the crest of the range, as well as at numerous vents that pepper the eastern flank of the range, has resulted in a largely constructional topography of young volcanoes and lava flows that are mostly less than 2 million years old [Plate 1; *Taylor*, 1990; *Walker and MacLeod*, 1991].

Extensive lava flows from Newberry Volcano south of Bend flowed into and partly filled the Crooked and Deschutes River canyons between 1.2 and <0.4 million years ago [Figure 2; *Russell*, 1905; *Stearns*, 1931; *Smith*, 1986, 1991; *Bishop and Smith*, 1990; *Sherrod et al.*, in press]. Their distribution and thickness show that by 1.2 million years ago, the Deschutes River system had incised to near its present elevation near Round Butte Dam. Similarly, a 0.9±0.1 million year old basalt flow from Stacker Butte [*Shannon and Wilson Inc.*, 1973, cited in *Bela*, 1982], flowed down the north valley wall of the Columbia River to near present river level near the mouth of the Deschutes, indicating that local base level at the Columbia-Deschutes confluence has not changed substantially in the last million years. The 275 m of incision between about 4 and 1 million years ago indicates a period of regional incision and canyon formation affecting at least the north half of the Deschutes River basin, during which downcutting averaged nearly 0.1 mm/yr. Repeated episodes of incision through the subsequent canyon-filling lava flows (Figure 2) were at even more rapid rates.

Topography and Drainage Network

The overall topography and drainage network development within the Deschutes River basin is the result of this geologic history. To frame discussion of the overall geologic, topographic and hydrologic characteristics of the basin, we have subdivided the watershed into three terranes on the basis of general geologic and topographic characteristics (Figures 3 and 4).

Eastern Highlands Terrane. The Ochoco Mountains and high lava plains form the southeastern part of the Deschutes River basin. This region, largely drained by the Crooked River, is underlain by a variety of rocks, but the main Ochoco Mountains are formed primarily of the John Day and Clarno Formations (unit Tsf on Plate 1). These formations are mainly composed of weathered lava flows and poorly consolidated claystone, siltstone, and volcanic ash-flow tuff deposited between 55 and 20 million years ago. The John Day and Clarno Formations are susceptible to landsliding, and almost all of the landslides in the Deschutes

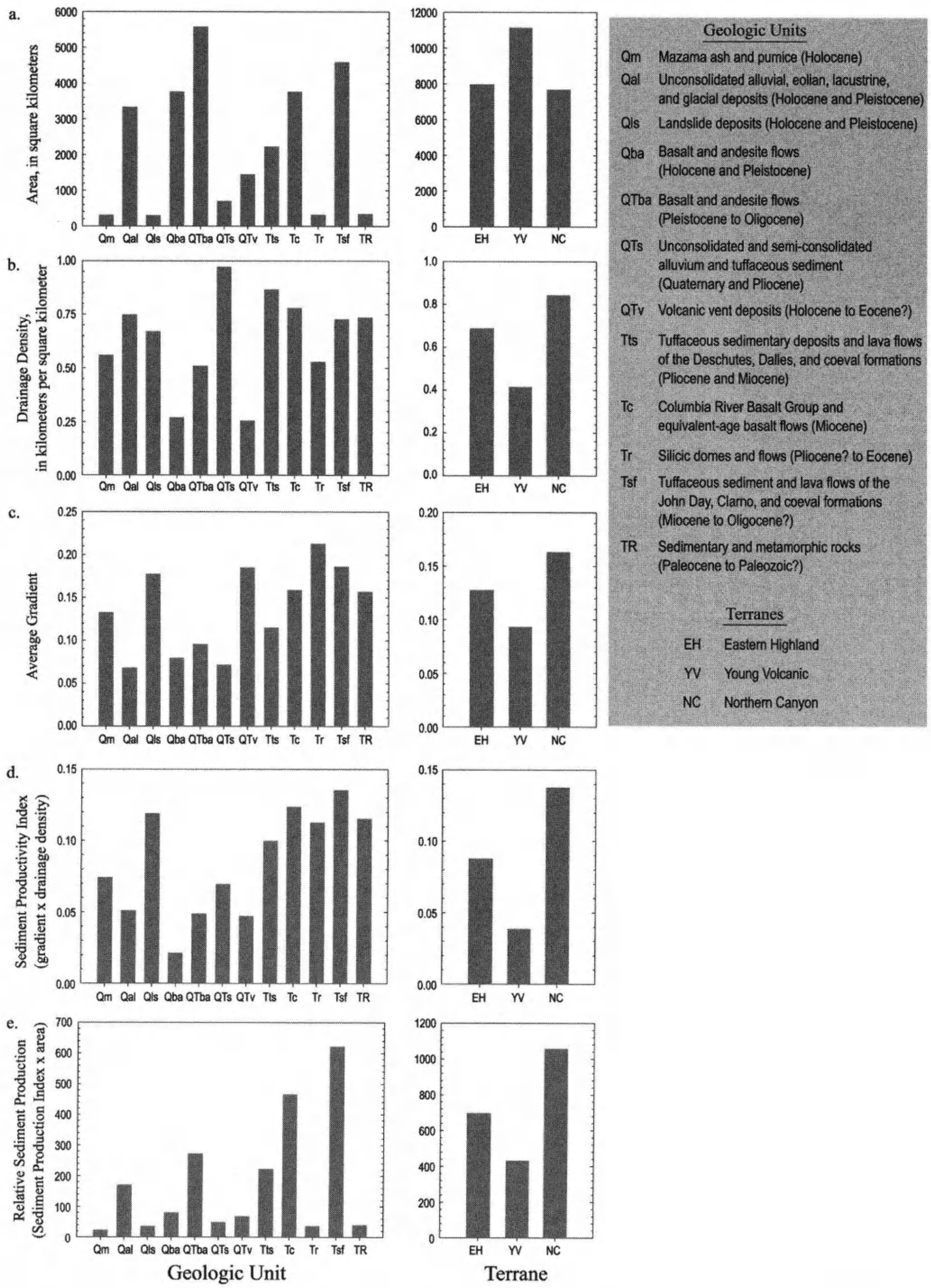

Figure 3. Geomorphic and physiographic attributes of each of the twelve major geologic units (Plate 1) and three terranes (Figure 4) within the Deschutes River basin. (a) Area of surface exposure. (b) Drainage density, from U.S. Geological Survey 1:100,000 digital hydrography. (c) Average hillslope gradient, calculated from U.S. Geological Survey 30-meter digital elevation data. (d) Sediment Production Index (SPI), calculated as the product of mean gradient and drainage density. (e) Relative potential for sediment production, calculated as the product of SPI and area.

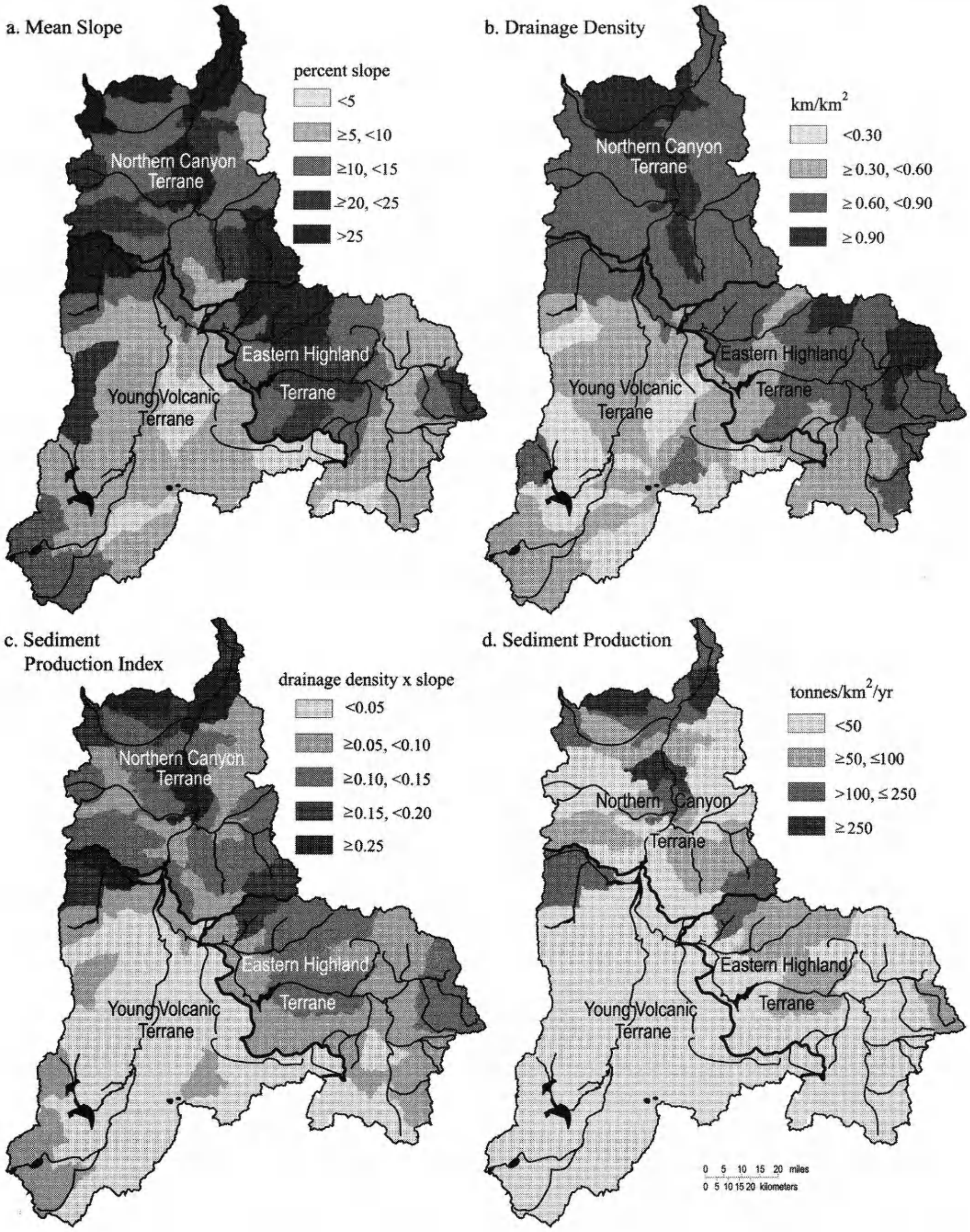

Figure 4. Distribution of geomorphic attributes and estimated sediment production for 100 approximately equal-sized subbasins of the Deschutes River basin. (a) Mean subbasin hillslope gradient, calculated from U.S. Geological Survey 30-meter digital elevation data (depicted in Figure 1). In many subbasins there are areas of significantly higher and lower slopes. (b) Subbasin drainage density, from mapped watercourses shown by U.S. Geological Survey 1:100,000 digital hydrography (shown on Figure 6). (c) Sediment Production Index (SPI), calculated as the product of mean gradient and drainage density as depicted (in a generalized fashion) in 4a and 4b (where slope is expressed as a fraction). (d) Calculated sediment yields, developed from empirical relation between SPI and surveyed accumulations in Deschutes River basin reservoirs (shown in Figure 14).

River basin are within these units (Plate 1). This landscape is one of the oldest in the Deschutes River basin, and more than 10 million years of weathering has produced a well-integrated hydrologic network in the erodible rocks of the region. The Ochoco Mountains have a high density of stream channels (Figure 4b) that connect steep hillslopes and source channels to trunk channels flowing within alluvial valleys.

Young Volcanic Terrane. The southern and southwestern part of the basin, drained by the Deschutes and Metolius Rivers upstream of the Pelton-Round Butte dam complex, is bounded by the high and rugged Cascade Range on the west, the western margin of Newberry Volcano lava flows on the east, and indistinct low divides between the Klamath Basin and the Basin and Range Province to the south. The Young Volcanic terrane is underlain by young volcanic rocks (units QTba, Qba and QTv on Plate 1) and basin-filling deposits (unit Qal) that have accumulated behind drainage-blocking lava flows and fault scarps. Pleistocene glacial deposits and outwash locally mantle uplands along the east flank of the Cascade Range. Pumice from Mount Mazama (Crater Lake) forms a widespread surface layer in the southern part of the province (mapped as unit Qm on Plate 1 where it obscures the underlying bedrock). The largely constructional volcanic landscape coupled with Quaternary faulting and channel-damming lava flows has resulted in a sparse and locally disconnected surface channel network traversing low-relief alluvial and lacustrine basins (Figures 4a and 4b).

Northern Canyon Terrane. The northern part of the Deschutes River basin is composed of dissected tablelands formed along the eastern rampart of the Cascade Range and the western Columbia River Plain. The central axis of the basin consists of sharply etched canyons rimmed by young basalt flows and incised into basin-filling sediment and older volcanic and volcaniclastic rocks. From Lake Billy Chinook downstream, the Deschutes River is deeply incised within a canyon variously carved into the relatively soft John Day and Clarno Formations, cliff-forming CRBG basalts, and younger strata of the Simtustus, Deschutes, and Dalles Formations with their capping basalt flows. Large tributaries from the west drain the Cascade Range, whereas tributaries from the east drain tablelands of CRBG and landslide-dominated uplands of the John Day and Clarno Formations. This terrane has the highest average slope and drainage density of the entire basin (Figures 3 and 4).

Geology, Topography, and Drainage Pattern. Topographic and stream-network properties in the basin result from the strong correspondence of geomorphic properties, such as slope and drainage density, with geology. This correspondence gives each of the terranes its distinct topographic and hydrologic characteristics (Figures 3 and 4). The older rock units that underlie most of the uplands of the Eastern Highlands and Northern Canyons have the greatest average slope. Of the widely distributed units, the John Day and Clarno Formations (grouped on Plate 1 as unit Tsf) and the CRBG (unit Tc on Plate 1) have the greatest average hillslope gradients. Late Tertiary and Quaternary vent complexes (unit QTv) also have relatively high average gradients. The older high-relief uplands underlain by the John Day and Clarno Formations and the CRBG also have relatively high drainage densities (Figure 3). The greatest drainage densities in the Deschutes River basin have developed on the poorly consolidated and unconsolidated Tertiary and Quaternary sedimentary rocks. These units (Tts and QTs on Plate 1), which were deposited during times of basin filling, regional aggradation, and higher base levels, are now densely drained by closely spaced channels, especially in the Northern Canyons province. In contrast, the young volcanic rocks (units Qba, QTba, and QTv of Plate 1), which characterize the Young Volcanic terrane, have drainage densities typically less than half that of most other units in the basin (Figure 3).

Hydrology

The unique hydrologic characteristics of the Deschutes River basin are largely controlled by the geology, topography, and stream network [see also *Gannett et al.*, this volume]. Average annual runoff for the 26,860 km^2 basin is $5.2 \cdot 10^9$ m^3, which is equivalent to about 0.19 m over the entire drainage area. By far the largest portion of this water is derived from the high Cascade Range along the western part of the drainage basin, where high elevation and oceanward position promote greater precipitation and substantial winter snowpack (Figure 5). Farther east within the Cascade Range rain shadow, annual precipitation and runoff diminish rapidly, resulting in semi-arid rainfall and runoff conditions for much of the basin (Figures 5 and 6).

Near its confluence with the Columbia River, the Deschutes River has a mean monthly flow ranging from 124 m^3/s in August to 213 m^3/s in February (Figure 6, Deschutes River at Moody, 1965-1996). Prior to regulation, the highest monthly averages were in early spring and resulted primarily from snowmelt in the Cascade Range. Lowest flows are typically during the late summer months of July, August, and September. The relatively small range between low and high flows is unusual and was noted by *Russell* [1905], who wrote that:

> "The Deschutes is of especial interest to geographers, as it exhibits certain peculiarities not commonly met with.

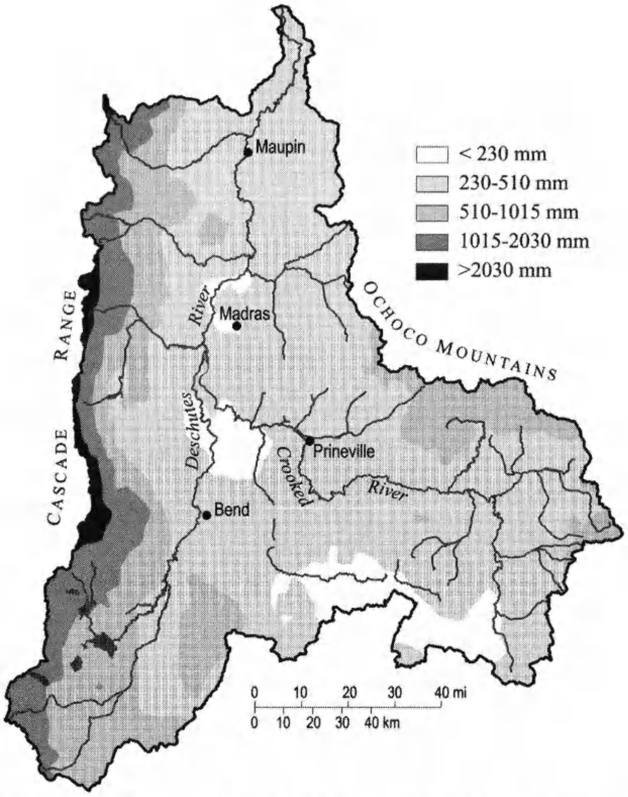

Figure 5. Mean annual precipitation in the Deschutes River basin for the period 1961-1990. From data provided by the Spatial Climate Analysis Service, Oregon State University. (http://www.ocs.orst.edu/prism/prism_new.html; August, 2001).

Although flowing from high mountains on which precipitation varies conspicuously with seasonal changes and where snow melts rapidly as the heat of summer increases, its volume, throughout a large section of its course, is practically constant throughout the year."

and by *Henshaw et al.* [1914, p. 12] who more specifically observed:

"The flow of the river is more remarkably uniform than that of any other river in the United States comparable with it in size, and its economic value is almost incalculable. At the mouth of the stream the maximum discharge is only six times the minimum. Ocular evidence of this uniformity of flow is presented by the low grass-grown banks between which the river flows for much of its course."

The steadiness of flow is illustrated by comparing the annual hydrographs and flood peak records of the Deschutes River basin with those of the adjacent and similar-sized basins to the west (Willamette Basin) and east (John Day Basin) (Figures 7 and 8). For the John Day River, the mean monthly discharge for April is more than thirty times that for September. Likewise for the Willamette River, the mean monthly discharge for January is about ten times that for August. In contrast, the Deschutes River varies only by a factor of 1.5 between the months of greatest and least flow. Just as the annual response to flow is tempered in the Deschutes River basin, so is the response to individual climatic events. The maximum meteorologic peak discharge for the Deschutes River just downstream from the Pelton-Round Butte dam complex was 540 m^3/s on February 8, 1996[2]—less than five times the mean flow of 125 m^3/s. In contrast, the largest flood discharges on both the Willamette and John Day Rivers have been more than twenty times the rivers' mean flows (Figure 8).

The uncommonly steady flow of the Deschutes River is due primarily to the poorly integrated surficial drainage system along the eastern flank of the Cascade Range in the southern and western parts of the Deschutes River basin. Much of the seasonal precipitation and snow melt infiltrates into extensive groundwater systems within the highly permeable young volcanic fields and basin fill deposits, emerging months to years later in large springs at the headwaters of the Metolius River, along the lower Crooked River, and between River Mile (RM) 100 and 120 on the Deschutes River[3] [*Russell*, 1905; *Henshaw et al.*, 1914; *Stearns*, 1931; *Manga*, 1996, 1997; *Gannett et al.*, 2001, *Gannett et al.*, this volume]. Consequently, there is little monthly or seasonal variation in flow for many headwater drainages in the southern and western parts of the Deschutes River basin (Figure 6). As a result, the annual hydrograph of the Deschutes River shows minimal seasonal variation near the Pelton-Round Butte dam complex, where springs contribute the majority of the total flow volume [*Gannett et al.*, this volume]. In contrast, seasonal flow variations are much greater in the headwater basins of the older, steeper, and more dissected terrain in the eastern Deschutes River basin (Figure 6), but because the total volume of flow from these more arid drainages is small, they do not substantially affect the annual distribution of flow in the lower Deschutes River. Some additional flow regulation is provided by the abundant lakes and glaciers in Cascade Range headwaters, and also

[2] The February 8, 1996, flow was not substantially attenuated by the Pelton-Round Butte dam complex [*Fassnacht*, 1998]. A larger flow (640 m^3/s) on July 16, 1983, resulted from a short accidental release from the Pelton-Round Butte dam complex.

[3] Units given are metric except for locations, which are given as river miles (RM), or miles upstream from the river mouth as marked on USGS topographic maps. These values are close to, but not necessarily the same as, actual distances along the present channel. Fractional river miles given herein are based on interpolations between these published river miles.

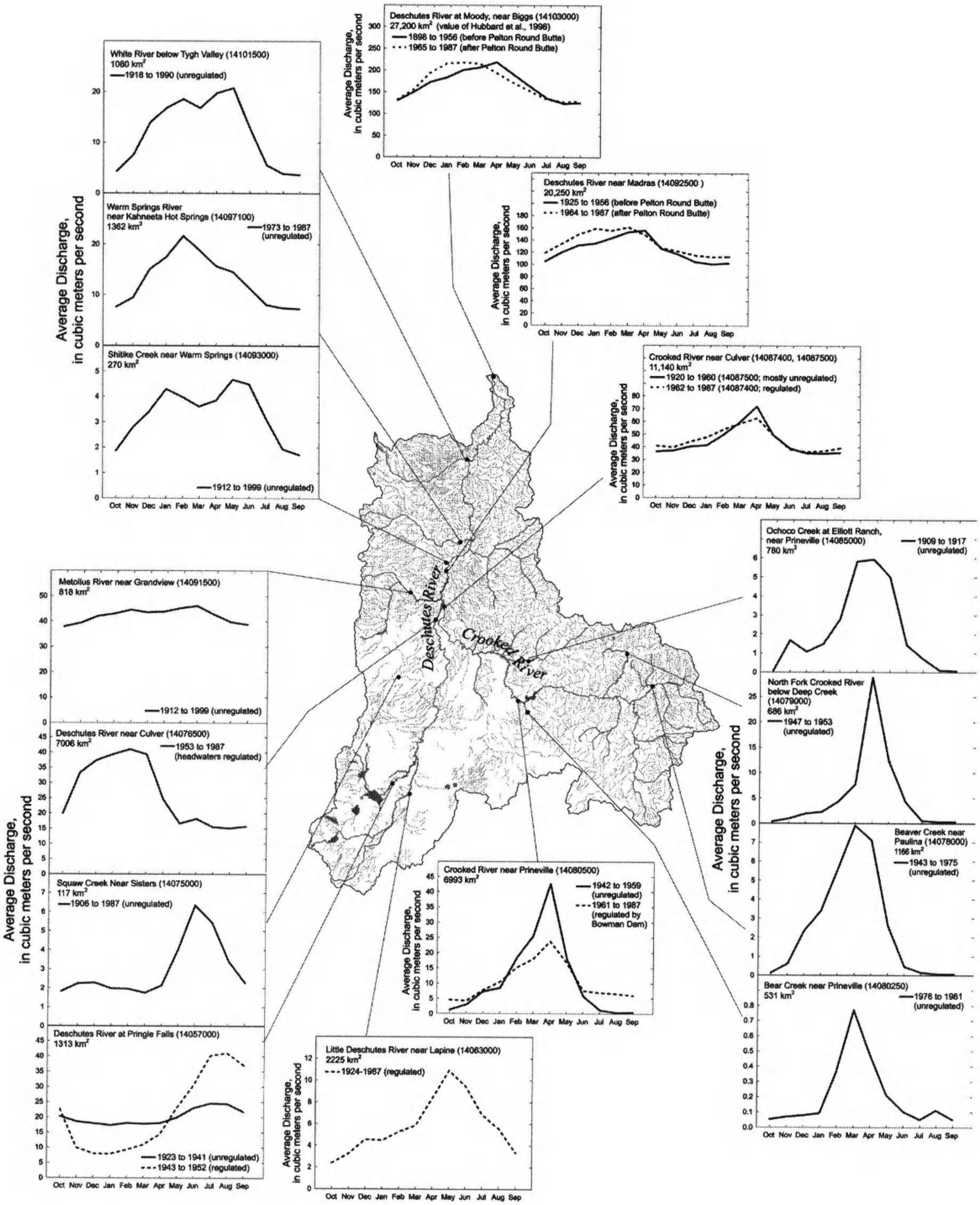

Figure 6. Hydrography and representative annual hydrographs for U.S. Geological Survey stream gaging stations in the Deschutes River basin. Data from *Moffatt et al.* [1990] and the U.S. Geological Survey National Water Information System (http://water.usgs.gov/nwis).

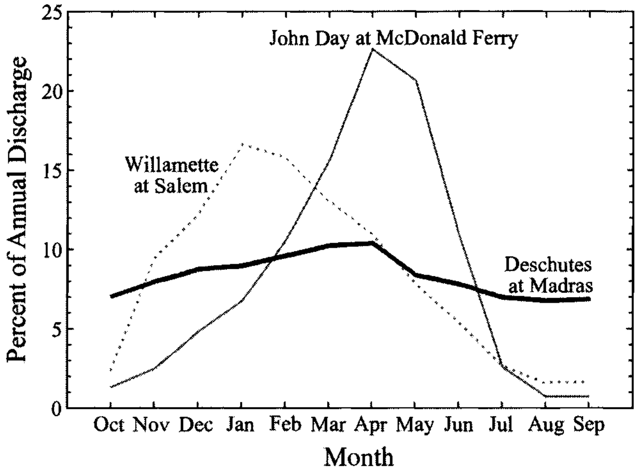

Figure 7. Mean monthly discharges for the John Day River at McDonald Ferry (station No. 14048000, period of record 1905-1987, drainage area 19,630 km^2), Deschutes River near Madras (14092500, 1925-1956, 20,250 km^2), and Willamette River at Salem (14191000, 1910-1941, 18,855 km^2). Discharges are expressed in terms of percent of annual flow to emphasize differences in seasonal distribution of runoff. Periods of record selected to minimize effects of upstream dams. Data from *Moffatt* et al. [1990]. Basin locations shown in Figure 1.

by two storage reservoirs in the Crooked River system and three reservoirs in the Deschutes River headwaters.

Steady discharge and muted response to individual meteorologic events are pronounced for flow entering Lake Billy Chinook at the Pelton-Round Butte dam complex, where the largest flows are less than five times the mean annual flow. However, flow response to individual runoff events becomes progressively greater downstream in the Northern Canyons terrane. For example, large inflows to the Deschutes River from Cascade Range tributaries (primarily Shitike Creek, Warm Springs River, and White River) during the February 1996 flood (the largest flood in nearly 100 years of record) increased the peak discharge from 540 m^3/s (Deschutes River near Madras) to 1990 m^3/s (Deschutes River at Moody), an increase of a factor of 3.7 despite only a 26 percent increase in drainage area. Similar increases occurred during the December 1964 flood, although more runoff was captured by storage reservoirs during this event [*Beebee and O'Connor*, this volume; *Hosman et al.*, this volume]. The large peak flows generated in the Northern Canyons terrane result from the steeper and more dissected tributary drainages and the absence of an extensive regional groundwater system such as found in the southern Deschutes River basin. This heightened storm response of the Northern Canyons tributaries is reflected in the early winter peaks and the greater month-to-month variation of the annual hydrographs for Shitike Creek, Warm Springs River, and White River compared to Cascade Range stations in the Deschutes River headwaters (Figure 6).

Regional Sediment Production and Transport

Together, the geology, geomorphology, and hydrology of the Deschutes River basin substantially influence the type and quantity of sediment delivered to the Deschutes River as well as the frequency of sediment movement. There are few data on actual sediment delivery in the Deschutes River basin, so the following discussion is largely qualitative and founded on consideration of the overall geologic history as well as current geomorphic and hydrologic characteristics. In a later section, we apply sparse sediment-transport measurements and the record of modern sediment delivery to Lake Billy Chinook, Prineville Reservoir, and Ochoco Reservoir to provide quantitative support for the inferences derived here from more general observations.

Within the Young Volcanic terrane of the southern and southwestern parts of the basin, the primarily basaltic and andesitic volcanic rocks are generally unweathered and do not produce large volumes of sediment. These lava flows typically break down to gravel (by physical weathering processes such as freeze-thaw) and clay (through chemical weathering). Modern processes produce very little sand. Reworked tephra, ash, and Mazama pumice also contribute in some degree to bedload. The low drainage density (Figure 4b) coupled with the small and steady surface flows in this part of the basin (Figure 6) result in only infrequent sediment transport in the river systems draining this terrane. In the southern part of the basin, much of the transported sediment is probably trapped in lakes and alluvial basins formed behind young lava flows and by basin-range faulting.

Nevertheless, large volumes of sediment have been produced episodically in the Young Volcanic terrane during periods of extensive glaciation and during large volcanic eruptions. Large glaciers and ice sheets covered much of the high Cascade Range during Pleistocene ice ages [*Crandell*, 1965; *Scott*, 1977]. These glaciers eroded and transported a substantial volume of gravel, sand, and silt derived from erodible Cascade Range stratovolcanoes and formed large moraines and outwash plains near their termini. These deposits compose much of the alluvium along the eastern flank of the Cascade Range (Plate 1, unit Qal). Sand and gravel outwash terraces can be traced from moraines down many of the tributaries to the Deschutes and Metolius Rivers [e.g. *Scott*, 1977; *Sherrod et al.*, in press], indicating that at times of peak sediment production there was abundant sand and gravel delivered continuously to the Metolius and Deschutes Rivers.

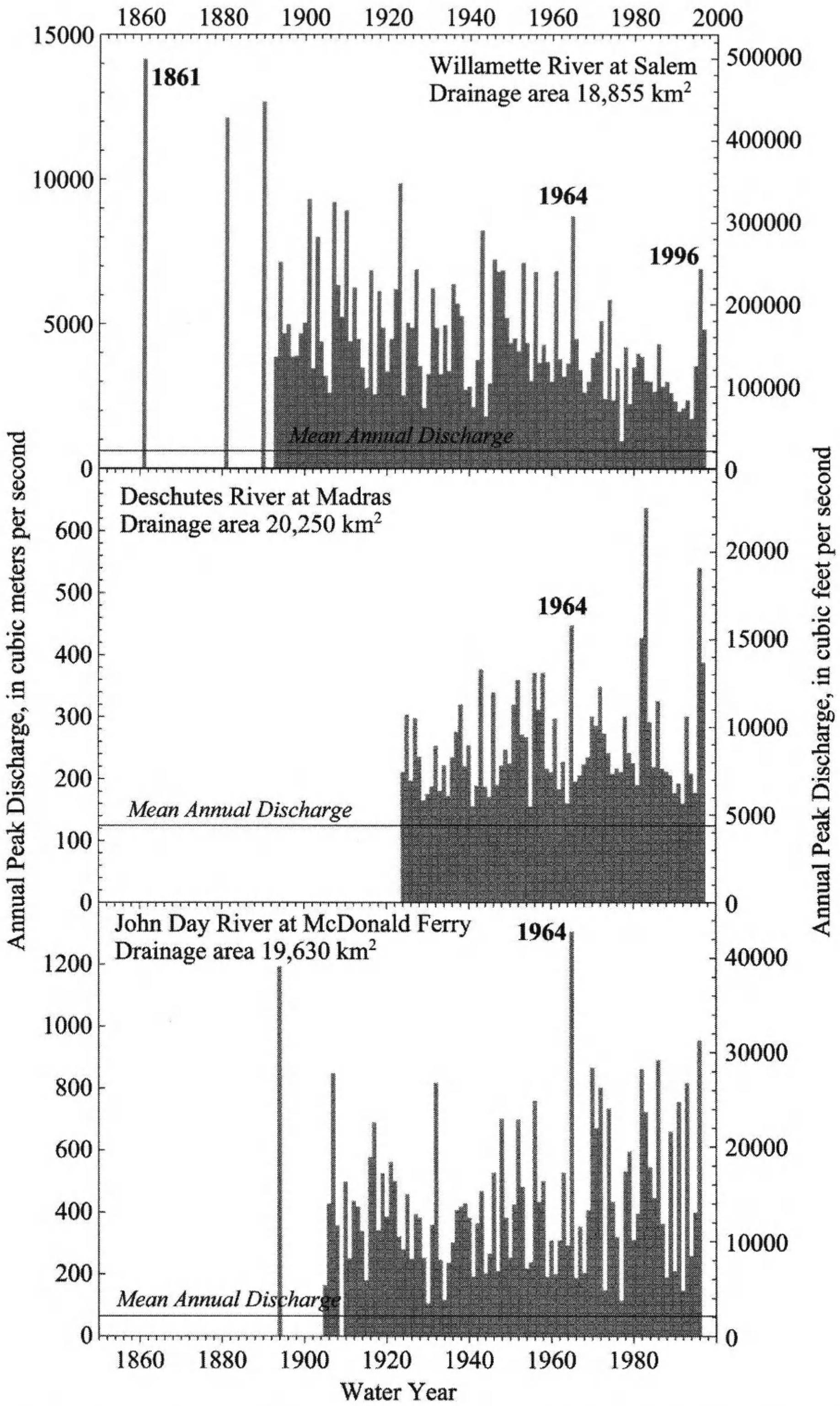

Figure 8. Annual peak discharges for the Willamette (station No. 14191000), Deschutes (14092500), and John Day (14048000) Rivers. Basin locations shown in Figure 1.

Most of the remaining glacial deposits, however, are perched on ridgetops, lava flows, and hillslopes away from active channels, so that little of this sediment now makes its way into modern channels.

Large volcanic eruptions have also episodically fed immense quantities of sediment to the Deschutes and Metolius Rivers. During the last 500,000 years, major eruptions from volcanic centers west of Bend [*Hill and Taylor*, 1989], Mount Jefferson [*Beget*, 1981; *Conrey*, 1991] and Mount Mazama [Crater Lake; *Sarna-Wojcicki and Davis*, 1991] have spread vast quantities of fallout ash and pumice over large parts of the Deschutes River basin, but the thickest accumulations have been along the eastern flank of the Cascade Range in the upper Deschutes and Metolius drainages. Several individual pumice and ash falls from the Tumalo volcanic center west of Bend are locally thicker than 10 m [*Hill and Taylor*, 1989]. The 7500-year-old Mazama pumice is sufficiently thick to obscure the underlying geology over more than 250 km^2 of the southern margin of the Deschutes River basin (unit Qm on Plate 1). Sand- and gravel-sized pumice is readily mobilized from hillslopes and transported downstream; consequently, during the decades following these major eruptions, there were likely periods of greatly enhanced sediment transport of silt-sized tephra and sand- and gravel-sized pumice grains, resulting in substantial channel aggradation. Pyroclastic flows (hot gas-rich flows of volcanic rock fragments) and lahars (volcanic debris flows) from Cascade Range eruptions have likely also episodically introduced large quantities of sand and gravel directly into the upper Deschutes and Metolius Rivers [e.g. *Smith*, 1986; *Hill and Taylor*, 1989]. Although there is sparse stratigraphic record of such events in Quaternary deposits above Lake Billy Chinook, deposits from a >75 ka[4] lahar from Mount Jefferson are preserved along the lower Deschutes River [*O'Connor et al.*, this volume].

Within the Eastern Highlands terrane, including the Ochoco Mountains and high lava plains of the southeastern part of the Deschutes River basin, the deeply weathered lava flows and poorly consolidated claystone, siltstone, and ashflow tuffs of the John Day and Clarno Formations are highly erodible, producing silt and clay from extensively dissected uplands. The fine-grained material produced in the uplands locally accumulates as valley fill along larger tributaries. Over geologic time scales, however, the dense stream network within this province efficiently conveys abundant fine-grained sediment from the eroding highlands into the Crooked and Deschutes Rivers.

The distinctly different hydrologic character of the Eastern Highland terrane of the Deschutes River basin likely amplifies sediment transport efficiency. The Crooked River has a more arid hydrologic regime with less total runoff but significantly greater month-to-month variation than does the upper Deschutes River (Figure 6). Prior to construction of Prineville Reservoir, the mean March flow of the Crooked River near Prineville was 100 times the mean August flow, whereas the variation for the Deschutes River near Culver is less than a factor of three [Figure 6; *Moffatt et al.*, 1990]. Because the ability to entrain and transport sediment increases exponentially with discharge, the flashier flows of the Crooked River probably expedited sediment delivery to the Deschutes River under pre-dam conditions.

As in the Young Volcanic terrane, there has probably been significant variation in the sediment delivery from the Ochoco Mountains over geologic and historic time scales. During the last 0.5 million years, the drainage area of the Crooked River has also been repeatedly blanketed by eastward drifting plumes of ash and pumice from Cascade Range eruptions. These deposits were probably eroded rapidly from steep hillslopes and moved into the channel system. There were no glaciers in the Ochoco Mountains during Pleistocene glacial periods, but the colder climates may have enhanced rates of weathering and hillslope sediment production. Pleistocene sand and gravel terraces 15 meters above the modern floodplain near Prineville reflect regional stream aggradation and increased sediment delivery that probably resulted from glacial climates.

Historic incision of fine-grained valley alluvium in the Crooked River basin has formed extensive gully networks [*Russell*, 1905; *Buckley*, 1992; *Welcher*, 1993] that continue to erode headward up the stream channel network (Figure 9). Incision has been widely attributed to overgrazing [e.g.

Figure 9. Bear Creek eroding fine-grained valley alluvium in the Crooked River drainage. Cut bank is about 3 m high. Photograph by J.E. O'Connor, 1998.

[4] "ka" = kilo-annum, or thousands of years before present.

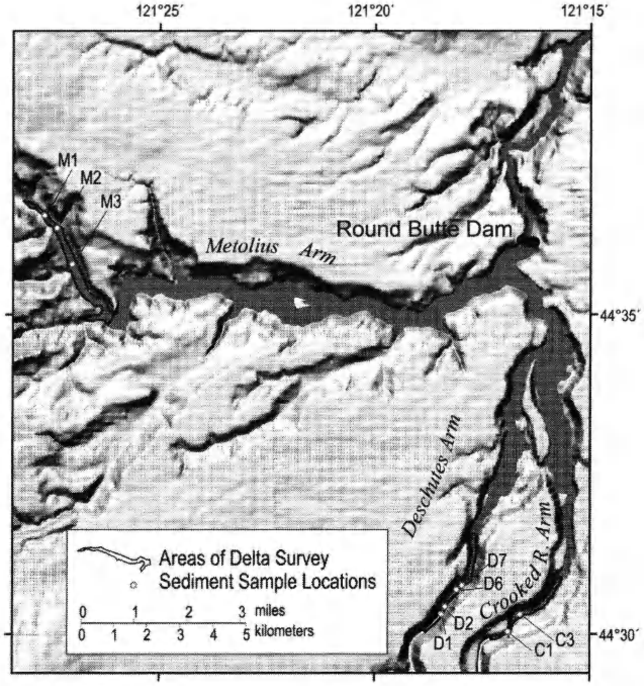

Figure 10. Location of delta surveys and sediment samples in Lake Billy Chinook. Survey and sample location data from Portland General Electric (Scott Lewis and Gary Reynolds, Portland General Electric, 1998 written communication). Hillshade topographic base from U.S. Geological Survey 30-m digital elevation data.

reconnaissance diving by Scott Lewis (Portland General Electric, oral communication, 1998) revealed local accumulation of silt, sand, and gravel up to 2 m thick, which is about the maximum uncertainty associated with comparing pre- and post-reservoir bathymetry.

The volumes of each of the Deschutes and Crooked River deltas were calculated by multiplying the average change in area for each pair of adjacent cross sections by the distance between each pair. Using this approach, the estimated volume of the delta where the Crooked River enters Lake Billy Chinook is about 627,000 m^3, and that for the Deschutes River is about 622,400 m^3 (Table 1). Composition of the deltas is not completely known, but reconnaissance augering and analysis of ten samples from the delta surfaces show that all three deltas are primarily composed of sand and gravel at their apices and become finer-grained farther and deeper into the reservoir (Figures 11 and 12). The Deschutes River delta is coarsest, having a pebbly delta apex that grades downstream to mostly sand. The Crooked River delta is distinctly finer than both the Deschutes and Metolius River deltas, with the upstream part of the delta formed primarily of sand, grading downstream to mostly silt and clay. These analyses support qualitative observations during reconnaissance diving and collection of the samples (Scott Lewis, written communication, 1998) that the Crooked River delta is primarily composed of silt, fine sand, and organic detritus; and the Deschutes River delta is composed of coarse sand with minor gravel at the delta apex grading to fine sand at the downstream crest of the delta.

Reservoir sediment volumes have also been measured by the Bureau of Reclamation for Prineville and Ochoco Reservoirs in the Crooked River drainage (Table 1; Ronald Ferrari, U.S. Bureau of Reclamation, written communication, 1999). In Prineville Reservoir, behind Bowman Dam on the Crooked River, a May 1998 survey indicated that about 5,657,400 m^3 had accumulated since the December 1960 closure of the dam. Ochoco Reservoir accumulated about 3,802,000 m^3 of sediment between January 1920 closure and a June 1990 survey. There are no available sediment-size data for these reservoirs.

These volume estimates were converted to masses by assuming *in situ* sediment densities of 1.3 to 1.5 tonnes/m^3 for sediment in Lake Billy Chinook and about 1.1 tonnes/m^3 for the presumably finer sediment in Ochoco and Prineville Reservoirs, for which large parts of their source areas are underlain by the John Day and Clarno Formations (Table 1). These sediment density values were based on empirical observations of reservoir sediment density presented in *Vanoni* [1975, pp. 38-44], which show that the density of reservoir deposits composed primarily of sand and gravel typically ranges between 1.3 and 1.5 tonnes/m^3. The 1.1 tonnes/m^3 density assumed for Ochoco and Prineville Reservoirs corresponds to an assumed sediment composition of silt and fine sand.

Sediment Yield. These measurements of reservoir sediment accumulation provide for independent decadal-scale estimates of modern sediment yield for parts of the basin (Table 1). The yield contributing to the Deschutes and Crooked River arms to Lake Billy Chinook for the 34-year period between 1964 and 1998 is remarkably low–on the order of 4 to 6 tonnes/km^2·yr. The yield from the Metolius arm is even lower. These low sediment yield values are all the more notable because the 34-year period that they encompass includes the two largest flow events in the last 140 years. Sediment yield in the upper Crooked River basin is substantially higher, ranging from 26 tonnes/km^2·yr in Prineville Reservoir (also including the sediment delivered by both the 1964 and 1996 floods) to 80 tonnes/km^2·yr for Ochoco Reservoir (only including the 1964 flood, but representing a much longer duration than the other reservoirs).

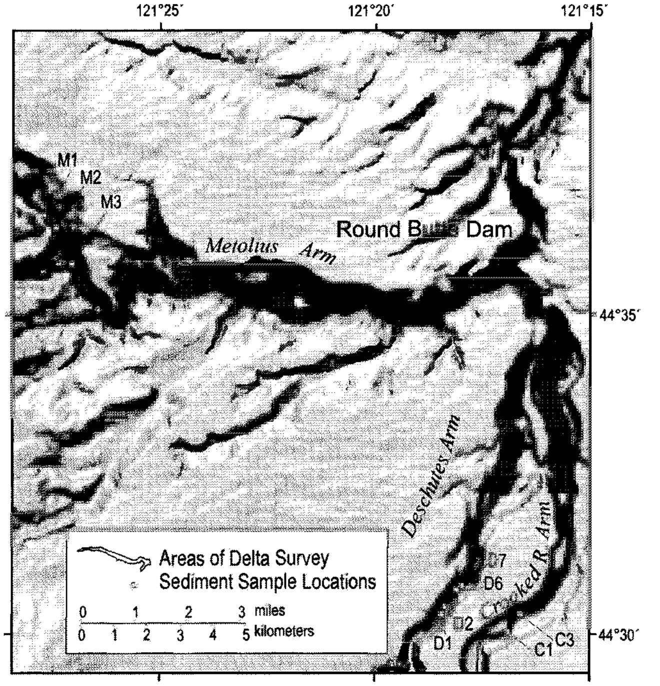

Figure 10. Location of delta surveys and sediment samples in Lake Billy Chinook. Survey and sample location data from Portland General Electric (Scott Lewis and Gary Reynolds, Portland General Electric, 1998 written communication). Hillshade topographic base from U.S. Geological Survey 30-m digital elevation data.

reconnaissance diving by Scott Lewis (Portland General Electric, oral communication, 1998) revealed local accumulation of silt, sand, and gravel up to 2 m thick, which is about the maximum uncertainty associated with comparing pre- and post-reservoir bathymetry.

The volumes of each of the Deschutes and Crooked River deltas were calculated by multiplying the average change in area for each pair of adjacent cross sections by the distance between each pair. Using this approach, the estimated volume of the delta where the Crooked River enters Lake Billy Chinook is about 627,000 m^3, and that for the Deschutes River is about 622,400 m^3 (Table 1). Composition of the deltas is not completely known, but reconnaissance augering and analysis of ten samples from the delta surfaces show that all three deltas are primarily composed of sand and gravel at their apices and become finer-grained farther and deeper into the reservoir (Figures 11 and 12). The Deschutes River delta is coarsest, having a pebbly delta apex that grades downstream to mostly sand. The Crooked River delta is distinctly finer than both the Deschutes and Metolius River deltas, with the upstream part of the delta formed primarily of sand, grading downstream to mostly silt and clay. These analyses support qualitative observations during reconnaissance diving and collection of the samples (Scott Lewis, written communication, 1998) that the Crooked River delta is primarily composed of silt, fine sand, and organic detritus; and the Deschutes River delta is composed of coarse sand with minor gravel at the delta apex grading to fine sand at the downstream crest of the delta.

Reservoir sediment volumes have also been measured by the Bureau of Reclamation for Prineville and Ochoco Reservoirs in the Crooked River drainage (Table 1; Ronald Ferrari, U.S. Bureau of Reclamation, written communication, 1999). In Prineville Reservoir, behind Bowman Dam on the Crooked River, a May 1998 survey indicated that about 5,657,400 m^3 had accumulated since the December 1960 closure of the dam. Ochoco Reservoir accumulated about 3,802,000 m^3 of sediment between January 1920 closure and a June 1990 survey. There are no available sediment-size data for these reservoirs.

These volume estimates were converted to masses by assuming *in situ* sediment densities of 1.3 to 1.5 tonnes/m^3 for sediment in Lake Billy Chinook and about 1.1 tonnes/m^3 for the presumably finer sediment in Ochoco and Prineville Reservoirs, for which large parts of their source areas are underlain by the John Day and Clarno Formations (Table 1). These sediment density values were based on empirical observations of reservoir sediment density presented in *Vanoni* [1975, pp. 38-44], which show that the density of reservoir deposits composed primarily of sand and gravel typically ranges between 1.3 and 1.5 tonnes/m^3. The 1.1 tonnes/m^3 density assumed for Ochoco and Prineville Reservoirs corresponds to an assumed sediment composition of silt and fine sand.

Sediment Yield. These measurements of reservoir sediment accumulation provide for independent decadal-scale estimates of modern sediment yield for parts of the basin (Table 1). The yield contributing to the Deschutes and Crooked River arms to Lake Billy Chinook for the 34-year period between 1964 and 1998 is remarkably low–on the order of 4 to 6 tonnes/km^2·yr. The yield from the Metolius arm is even lower. These low sediment yield values are all the more notable because the 34-year period that they encompass includes the two largest flow events in the last 140 years. Sediment yield in the upper Crooked River basin is substantially higher, ranging from 26 tonnes/km^2·yr in Prineville Reservoir (also including the sediment delivered by both the 1964 and 1996 floods) to 80 tonnes/km^2·yr for Ochoco Reservoir (only including the 1964 flood, but representing a much longer duration than the other reservoirs).

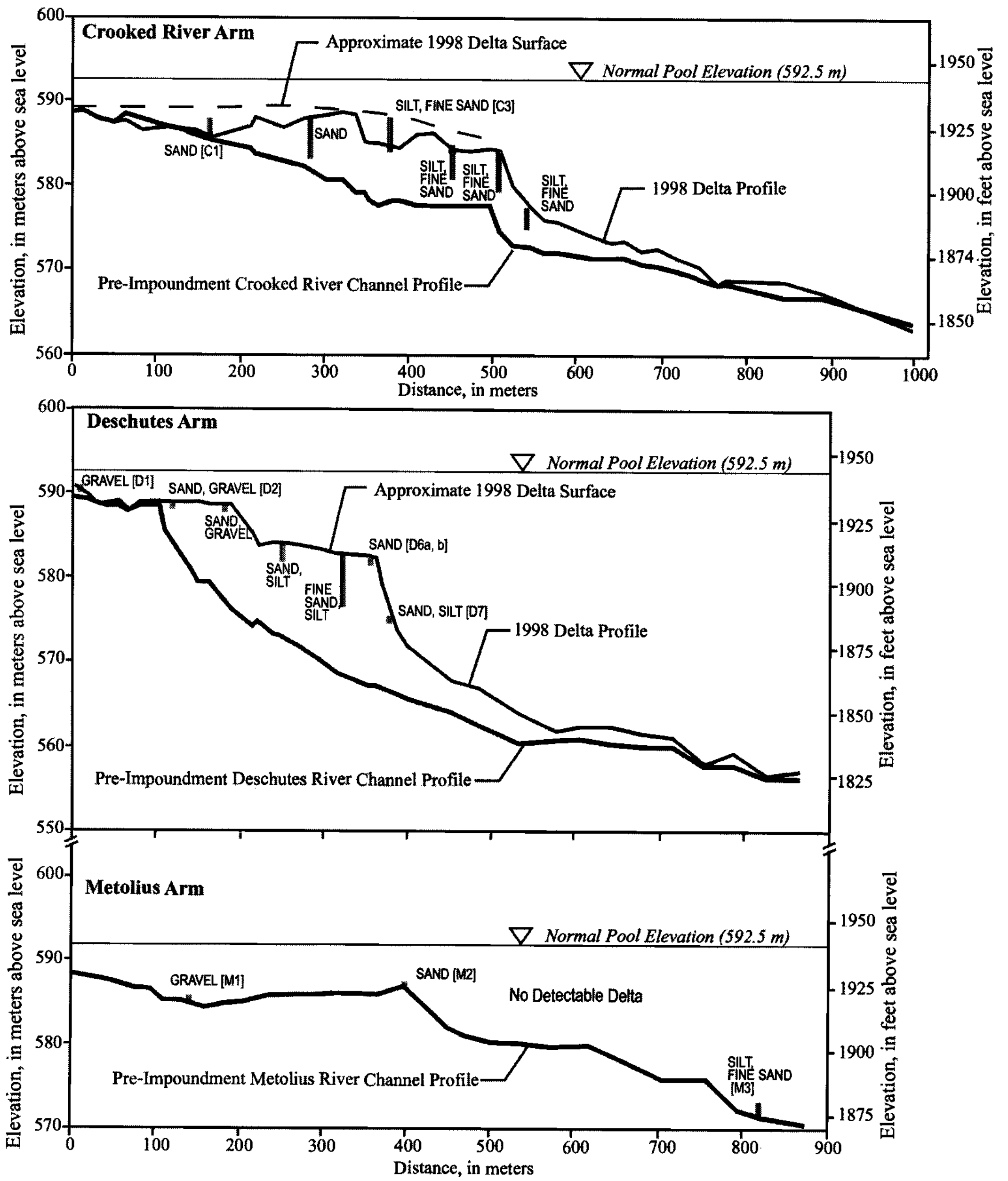

Figure 11. Upper 1 km of longitudinal profiles of the three arms of Lake Billy Chinook, showing pre-impoundment river profile, present delta profiles over the former channel thalwegs, and dominant substrate composition along each delta. Areas of surveys shown on Figure 10. There was no detectable difference between the present reservoir bottom and the former channel profile in the Metolius arm, although there has been up to 1.5 m of deposition locally (Scott Lewis, Portland General Electric, written communication, 1998). The approximate delta surface depicted for the Crooked arm represents the overall uppermost elevation of delta deposits along the survey transects. In contrast, the surface of the Deschutes arm delta was more uniform across its breadth. Drawn from data from Portland General Electric (Gary Reynolds, 1998 written communication). Substrate descriptions from subsurface augering conducted by Scott Lewis (Portland General Electric, written communication, 1999; depth indicated by extent of vertical bars). Locations of analyzed samples (with sample designations) shown in Figure 10.

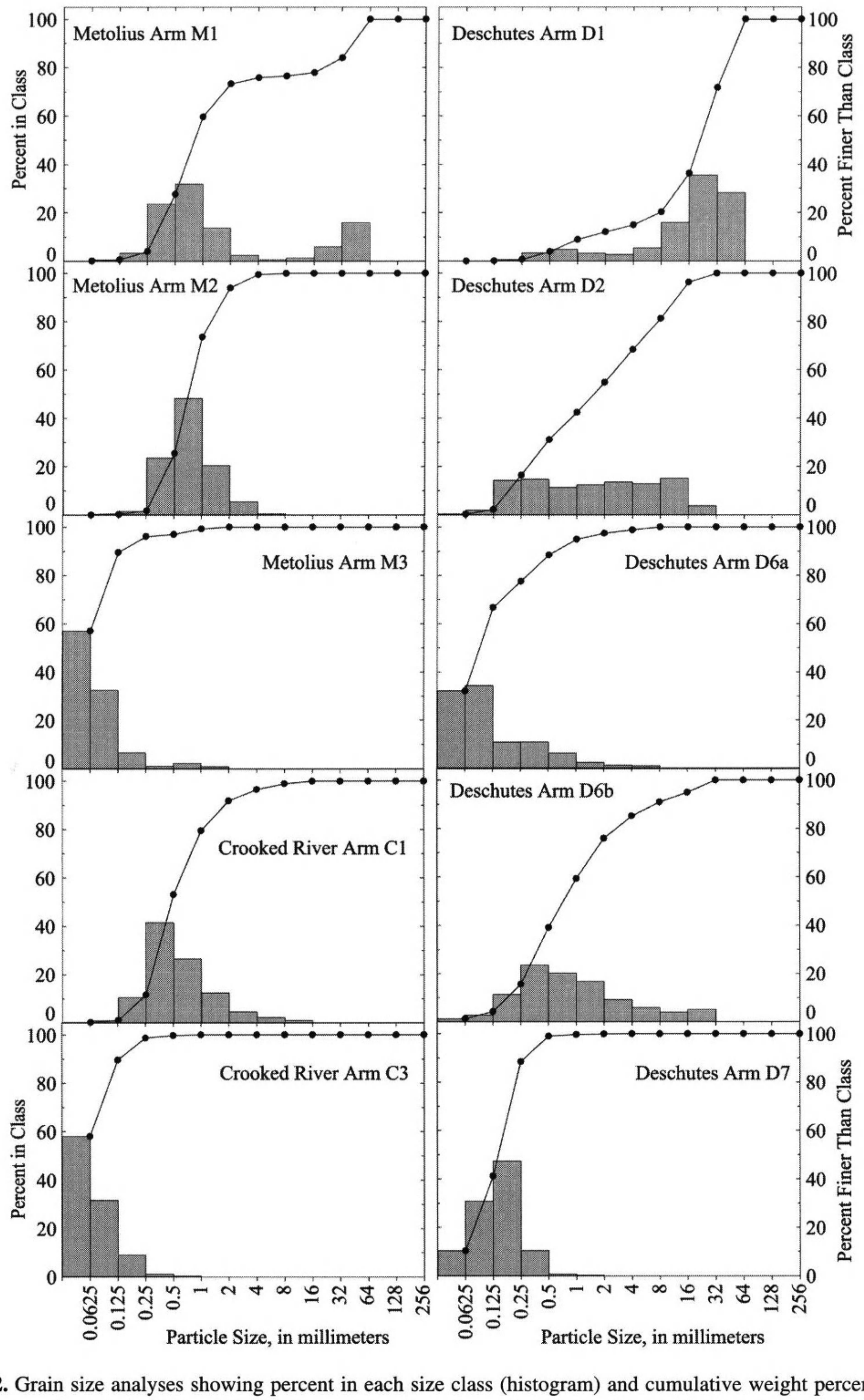

Figure 12. Grain size analyses showing percent in each size class (histogram) and cumulative weight percent (curve) for ten samples from Lake Billy Chinook. Sample locations shown in Figures 10 and 11. Samples collected by Scott Lewis, Portland General Electric. Analyses conducted by U.S. Geological Survey, Vancouver, Washington.

Table 1. Summary of sediment yield estimates determined from Deschutes River basin reservoir surveys.

Reservoir	Contributing Basin Area (km^2)	Closure and Survey Records	Surveyed Sediment Volume (m^3)	Assumed Sediment Density ($tonnes/m^3$)[1]	Sediment Mass (tonnes)	Sediment Yield (tonnes/ yr/km^2)	Unit Area Sediment Production Index (km^{-3})
Deschutes Arm, Lake Billy Chinook	6000	Round Butte Dam closed Jan. 2, 1964; surveyed May 1998	622400	1.44	898700	4.4	0.032
Crooked River Arm, Lake Billy Chinook	3920	Round Butte Dam closed Jan. 2, 1964; surveyed May 1998	627000	1.25	803200	6.1	0.046
Prineville Reservoir	6346	Bowman Dam closed Dec., 1960; surveyed May, 1998[2]	5657400	1.12	6342000	26.0	0.078
Ochoco Reservoir	752	Ochoco Dam closed Jan., 1920; survey date June 1990[2]	3802000	1.12	4262100	80.4	0.136

[1]Estimated from measured and inferred delta composition and empirical observations of reservoir sediment density portrayed in *Vanoni* [1975, pp. 38-44].

[2]Sediment volumes, survey dates, and dam closure information provided by Ronald Ferrari, U.S. Bureau of Reclamation (written communication, 1999)

We have found no other measurements of regional sediment yield for equivalent contributing areas that are as low as the sediment yield of the areas contributing to the Crooked and Deschutes River arms of Lake Billy Chinook (Figure 13). These rates are generally two to seven times less than sediment yields reported by *Judson and Ritter* [1964] for the Columbia and Snake River basins, about seven to fifteen times less than reported for the Klamath River basin (as calculated from data attributed to Janda and Nolan in *Milliman and Syvitiski* [1992]), and more than two orders of magnitude smaller than those predicted by area-based regression equations developed by *Milliman and Syvitiski* [1992] for mountain drainage basins in temperate regions. These low overall rates of sediment yield from the areas contributing to Lake Billy Chinook reflect the predominance of young volcanic rocks (which produce little sediment), limited surficial hydrologic network in many of the sediment source areas, and the absence of modern processes that supply and deliver abundant sediment. The sediment yields of the areas contributing to Ochoco and Prineville Reservoir are more typical of other landscapes, but still lower than for most basins of similar size for which there are sediment yield measurements (Figure 13).

Sediment Budget. Sediment yield values from isolated parts of the basin document regional sediment contributions to the Deschutes River system, but do not fully portray basin-wide patterns of sediment yield. A basin-wide sediment budget is critical to fully evaluate the effects of impoundment on overall sediment flux. In this section we extrapolate the reservoir sediment yield data to the rest of the basin on the basis of basin physiography in order predict the spatial distribution of sediment input into the Deschutes River system and the effects of impoundment on overall sediment supply.

Our approach follows from the premise that in steady-state landscapes dominated by diffusive processes of surficial sediment mobilization (e.g. biogenic activity, rainsplash, soil creep, freeze-thaw action), sediment flux per unit stream length is proportional to the gradient of the flanking hillslope [*Culling*, 1960, 1963; *Hirano*, 1968], although this relation is not necessarily linear in steeper terrains [*Andrews and Buckman*, 1987; *Roering et al.*, 1999]. Consequently, the sediment yield per unit area will be proportional to the product of average slope gradient and drainage density, which we term *the sediment production index* (SPI). To apply this reasoning on a spatially explicit basis, we divided the Deschutes River basin into 100 approximately equal-sized and hydrographically defined subbasins for which area, drainage density, and average hillslope gradient were calculated from digital topographic and hydrographic data (Figure 4a, b). For each subbasin we then calculated the sediment production index as the product of subbasin drainage density and mean hillslope gradient (Figure 4c). Combining the areas now contributing sediment into the Crooked River and Deschutes arms of Lake Billy Chinook, and Prineville and Ochoco Reservoirs, and comparing the calculated sediment production index to actual sediment yields as recorded in the reservoirs yields the regression relation:

$$Q_s = 3.74\ (SPI)^{2.23} (r^2 = 0.98; P = 0.015),$$

where Q_S is sediment yield, in tonnes per square kilometer per year, and SPI is in units of km^{-1} (Figure 14).

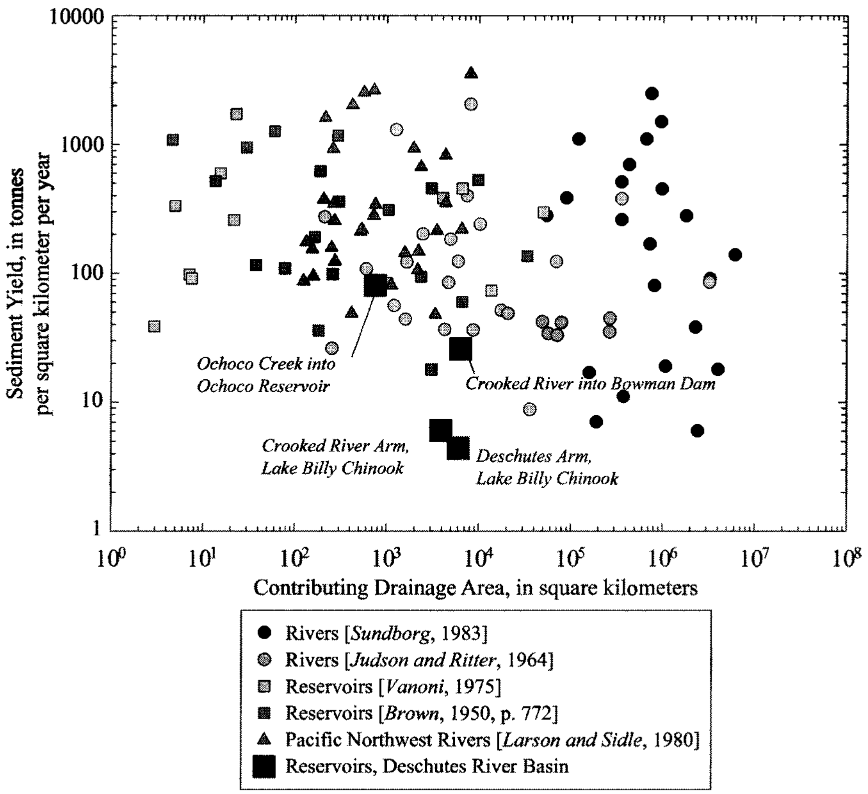

Figure 13. Compilation of sediment yield data from various sources, comparing sediment yield from parts of the Deschutes River basin to yields from other basins. Ochoco Creek and Crooked River sediment yields derived from surveyed sediment volumes behind Ochoco and Bowman Dams (Table 1; Ronald Ferrari, U.S. Bureau of Reclamation, 1999 written communication). Lake Billy Chinook (LBC) volumes measured by Portland General Electric survey crews in 1998 (Figures 10 and 11).

This result is only strictly applicable to transported bedload and suspended sand and silt (>0.002 mm) that drops out rapidly in these large reservoirs. Clay-sized particles probably stay in suspension long enough bypass the reservoirs. This result is also broadly consistent with the central tendencies (on a logarithmic plot) of the annual volumes of suspended load recorded at four U.S. Geological Survey gaging stations for short periods (Figure 14), although these gages also depict the substantial year-to-year variation in sediment transport. The results of a single year of suspended load measurements for White River, a large tributary draining the eastern Cascade Range and entering the Deschutes River downstream of the Pelton-Round Butte dam complex, are consistent with extrapolation of this relation to even higher values of SPI.

By applying this relation to the SPI calculated for each of the 100 subwatersheds (Figure 4d) and summing the resulting estimates of sediment yield downstream, we may estimate the overall downstream sediment flux and the incremental effects of impoundment in the Deschutes River basin (Figure 15). Under pre-impoundment conditions, modern sediment flux downstream of the confluence of the Deschutes, Crooked, and Metolius Rivers, 180 km upstream of the Columbia River confluence, is estimated to have been about 480,000 tonnes/yr. More than half of this volume was from the Crooked River basin. Downstream at the Columbia River confluence, the total annual sediment flux under pre-impoundment conditions is estimated to have been slightly more than 1,200,000 tonnes/yr, indicating that 60 percent of Deschutes River pre-impoundment sediment flux into the Columbia River is derived from below the Pelton-Round Butte dam complex. On the basis of this analysis, Trout Creek, Warm Springs River, and White River are likely to be major sources of sediment along the lower Deschutes River (Figure 15). In addition, the steep and dissected terrain formed where the Deschutes River has incised through the Mutton Mountains, between 120 and 90 km from the Columbia River confluence, (Figures 1 and 4) is also predicted to be an area of substantial sediment production and delivery. Consistent with this prediction is a concentration

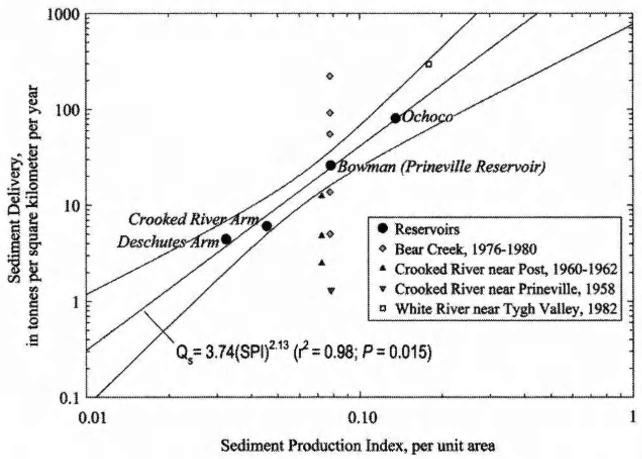

Figure 14. Regression and 95 percent confidence limits between unit Sediment Production Index values (SPI) and measured sediment yields (Table 1) for areas contributing to reservoirs in the Deschutes River basin. Shown for comparison are annual suspended load volumes measured at U.S. Geological Survey streamflow stations within the Deschutes River basin. Suspended load data from U.S. Geological Survey annual reports and water-supply papers.

of tributary fan deposits along this section of Deschutes River [*Curran and O'Connor*, this volume), likely formed by floods and debris flows triggered by summer convective storms precipitating on the numerous short and steep tributaries.

These sediment yield and delivery estimates portrayed in figures 4c, 4d, 13, 14, and 15 represent modern pre- and post-impoundment conditions for the past 50 to 80 years, including the effects of two large regional floods. Nevertheless, the short time window of sedimentation recorded in Lake Billy Chinook and other basin reservoirs does not adequately reflect basin-wide sediment delivery over longer time scales that incorporate periods of volcanism, cataclysmic flooding, and glacial climates. Such events and processes that operate over longer time scales are important in controlling valley geomorphology and the transport of sediment into the Deschutes River system. Thus, a key to assessing the effects of Deschutes River basin dams on river, channel, and valley bottom conditions is the role of the modern sediment transport regime relative to sediment yield and delivery events that occur over geologic

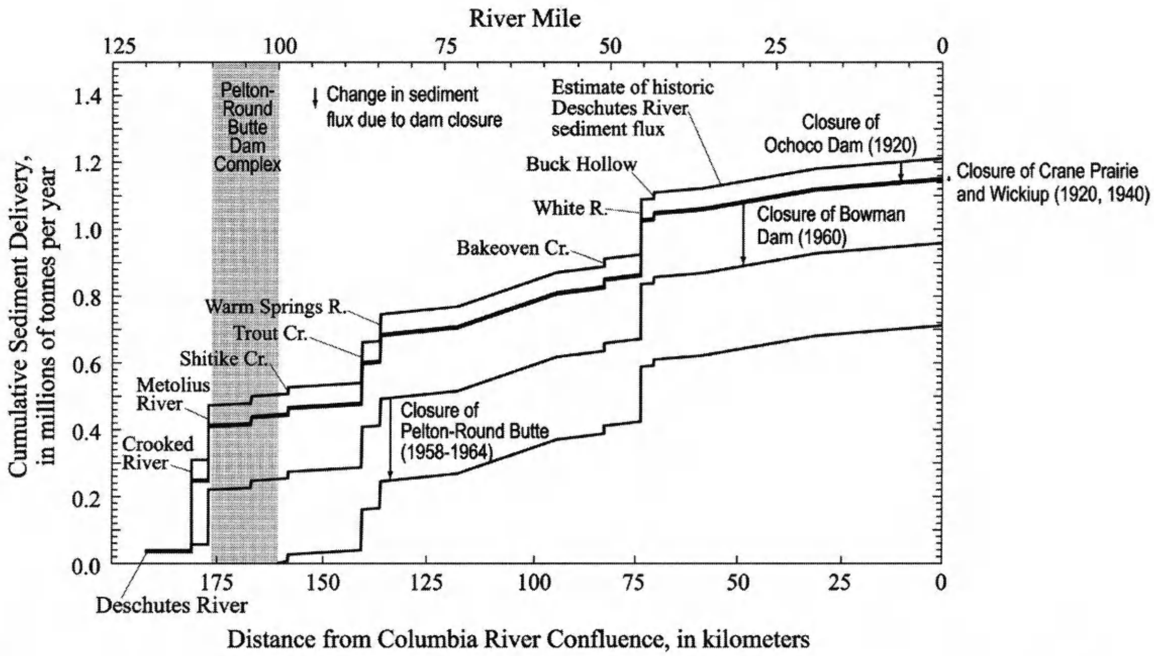

Figure 15. Calculated sediment budget for the lower 200 km of the Deschutes River showing spatial distribution of sediment input and the incremental effects of sediment trapping by upstream reservoirs. Sediment volumes determined on the basis of calculated SPI values (Figure 4) and the empirical relation between SPI and sediment yield shown in Figure 14. Uppermost curve shows calculated cumulative sediment delivery for preimpoundment Deschutes River upstream to Crooked River confluence, and lowest curve shows calculated cumulative sediment delivery after the stepwise reduction resulting from each of the major impoundments in the Deschutes River basin.

time scales. Several papers in this volume explore this matter in greater detail, but the remarkably low sediment transport rates of the modern (both pre- and post-impoundment) Deschutes River basin help tip the scales toward greater importance of rare high-magnitude events.

SUMMARY OF IMPORTANT BASIN-SCALE PROCESSES AND CONDITIONS

The cumulative result of the geologic history of the Deschutes River basin is that the basin has distinct geologic, hydrologic, and geomorphic attributes when compared to other western U.S. rivers. Of these attributes, the remarkably steady flows and low sediment flux are important factors for understanding the geomorphology of the Deschutes River below the Pelton-Round Butte dam complex. These modern processes and conditions, as well as the history of geologic events such as canyon cutting, volcanism, and glaciation, form the framework for the studies of valley geomorphology, channel processes, and fish ecology reported in accompanying papers. The most important aspects of this framework are:

1. The present stream network and valley morphology have resulted from tens of millions of years of tectonic, volcanic, and erosional processes. The overall northward course of the Deschutes River was established by about 12 million years ago. The present canyon of the lower Deschutes River was carved between 4 and 1 million years ago, but there have been subsequent episodes of partial refilling and incision initiated by lava flows, volcaniclastic debris, and glacial outwash.

2. The vast extent of young and permeable volcanic rocks and the poorly developed surface channel network in the southern Deschutes River basin have resulted in a hydrologic system buffered by substantial groundwater flow. Consequently, flow entering the lower Deschutes River is unusually steady–the annual variation of flow is small and the response to regional climatic events is muted compared to other rivers of its size. More than 70 percent of the peak discharges of both the December 1964 and February 1996 flood flows in the lower Deschutes River entered downstream of the Pelton-Round Butte dam complex despite encompassing only 26 percent of the total drainage area.

3. The rock types in the southern and western parts of the Deschutes River basin, especially the Quaternary volcanic rocks, do not produce substantial sediment, and the sediment that has been produced is primarily gravel, silt, and clay deposited as glacial moraines and outwash now preserved on ridgetops and in disconnected alluvial basins. The older and more weathered volcanic rocks of the John Day and Clarno Formations that underlie the Ochoco Mountains are susceptible to landsliding and likely produce more sediment than any of the other broadly defined rock types in the basin. In the northern part of the basin, Tertiary lava flows of the CRBG are relatively resistant to erosion and produce mainly cobble- and gravel-sized material. Aside from the lahar-filled valley of the upper White River draining Mount Hood, there are few sources of sand readily accessible by the modern channel network anywhere in the Deschutes River Basin.

4. The steady stream flows coupled with low sediment supply have resulted in extremely low rates of sediment delivery to the Deschutes River. Sediment yield from the southern part of the Deschutes River basin, determined from reservoir surveys, is the smallest yet reported for basins of such size. The eastern part of the Deschutes River basin, underlain by the weathered and uplifted volcanic and volcaniclastic rocks of the John Day and Clarno Formations has greater sediment yield and is a major source of silt and clay, but most of the areas underlain by these formations are now upstream of reservoirs and do not contribute sediment to the lower Deschutes River. Extrapolation of sediment yield measurements from reservoir surveys on the basis of an empirical relation between sediment yield and physiography leads us to infer that more than 60 percent of the total Deschutes River sediment load was derived from downstream of the Pelton-Round Butte dam complex prior to impoundment in the basin. This also corresponds to the greater relative runoff volumes derived from the lower part of the basin. The Pelton-Round Butte dam complex now traps about 50 percent of the total, basin-wide, pre-impoundment sediment load entering the lower Deschutes River. But because of the large volume of sediment introduced from downstream, this equates to less than 25 percent of the total load at the Columbia River confluence (Figure 15).

5. Most sediment delivered to the Deschutes River over time periods of thousands to millions of years has probably been delivered in pulses by episodic events such as major pumice and ash falls, volcanic debris flows, landslides, or during periods of radically altered basin conditions such as extensive glaciation or short-lived rapid incision. The total volume of sediment, especially sand and gravel, delivered during these episodic events is probably orders of magnitude greater than the volume of sediment that enters the system during more quiescent times, such as those recorded by the 20th century reservoir surveys.

Acknowledgments. This research was funded by the U.S. Geological Survey, U.S.D.A. Forest Service, Oregon State University, and Portland General Electric. Discussions with Don Ratliff, Andrei Sarna-Wojcicki, Marshall Gannett, Gary Smith and David Sherrod have improved our understanding of the geology and hydrology of the Deschutes River basin. Portland General Electric conducted the reservoir surveys and sampling. Previous versions of this report were reviewed by Gary Smith and David Sherrod.

REFERENCES

Andrews, D. J., and R. C. Buckman, Fitting degradation of shoreline scarps by a nonlinear diffusion model, *J. Geophys. Res., 92*, 12,857-12,867, 1987.

Beget, J.E., Evidence of Pleistocene explosive eruptions of Mount Jefferson, Oregon, *EOS, Trans. Am. Geophys. Union* (1981 Fall Meet. Supp.), *62*(45), 1089, 1981.

Bela, J. L., Geologic and neotectonic evaluation of north-central Oregon: The Dalles 1° x 2° quadrangle, *State of Oregon Dept. of Geol. Min. Ind. Geol. Map Ser. GMS-27*, Portland, Oregon, 1982.

Bishop, E. M., and G. A. Smith, A field guide to the geology of Cove Palisades State Park and the Deschutes basin in central Oregon, *Oregon Geol., 52*(1), 3-12, 1990.

Brown, C. B., Sediment transportation, in *Engineering Hydraulics*, edited by H. Rouse, pp. 769-857, John Wiley, New York, 1950.

Buckley, G. L., Desertification of the Camp Creek drainage in central Oregon, 1826-1905, M.A. Thesis, 136 pp., University of Oregon, Eugene, Oregon. 1992.

Conrey, R. M., Geology and petrology of the Mt. Jefferson area, High Cascade Range, Oregon, Ph.D. Dissertation, 357 pp., Washington State University, Pullman, Washington, 1991.

Crandell, D. R., The glacial history of western Washington and Oregon, in *The Quaternary of the United States*, edited by H. E. Wright, Jr., and D.G. Frey, pp. 341-353, Princeton University Press, Princeton, New Jersey, 1965.

Culling, W. E. H., Analytical theory of erosion, *J. Geol., 68*, 1681-1692, 1960.

Culling, W. E. H., Soil creep and the development of hillside slopes, *J. Geol., 71*, 127-161, 1963.

Fassnacht, H., Frequency and magnitude of bedload transport downstream of the Pelton-Round Butte dam complex, lower Deschutes River, Oregon, M. S. Thesis, 311 pp., Oregon State University, Corvallis, Oregon, 1998.

Gannett, M. W., K. E. Lite Jr., D. S. Morgan, and C. A. Collins, Ground-water hydrology of the upper Deschutes Basin, Oregon, *U.S. Geol. Surv. Water-Resour. Inv. Rep. 00-4162*, 78 pp., 2001.

Goles, G. G., Miocene basalts of the Blue Mountain province in Oregon: Part I–Compositional types and their geological setting, *J. Petrol., 27*, 495-520, 1986.

Henshaw, F. F., J. H. Lewis, and E. J. McCaustland, Deschutes River, Oregon, and its utilization, *U.S. Geol. Surv. Water Supply Pap. 344*, 200 pp., 1914.

Hill, B. E., and E. M. Taylor, Oregon Central High Cascade pyroclastic units in the vicinity of Bend, Oregon, in *Guidebook for field trip to the Mount Bachelor-South Sister-Bend area, Central Oregon High Cascades, U.S. Geol. Surv. Open-File Rep. 89-645*, edited by W. E. Scott, C. A. Gardner, and A. M. Sarna-Wojcicki, pp. 51-54, 1989.

Hirano, M., A mathematical model of slope development–an approach to the analytical theory of erosional topography, *J. Geosci., 11*, 13-52, 1968.

Hooper, P. R., W. K. Steele, R. M. Conrey, et al., The Prineville basalt, north-central Oregon, *Oregon Geol., 55*(1), 3-12, 1993.

Hubbard, L. E., T. A. Herrett, J. E. Poole, G. P. Ruppert, and M. L. Courts, Water resources data, Oregon, water year 1997, *U.S. Geol. Surv. Water-Data Rep. OR-97-1*, 416 pp., 1998.

Judson, S., and D. F. Ritter, Rates of regional denudation in the United States, *J. Geophys. Res., 69* (16), 3395-3401, 1964.

Larson, K. R., and R. C. Sidle, Erosion and sedimentation data catalog of the Pacific Northwest, *U.S.D.A. Forest Service Tech. Rep.* R6-WM-050-1981, Portland, Oregon, 64 pp., 1980.

Manga, M., Hydrology of spring-dominated streams in the Oregon Cascades, *Wat. Resour. Res., 32*, 2435-2439, 1996.

Manga, M., A model for discharge in spring-dominated streams and implications for the transmissivity and recharge of Quaternary volcanics in the Oregon Cascades, *Wat. Resour. Res., 33*, 1813-1822, 1997.

Milliman, J. D., and J. P. M. Syvitiski, Geomorphic/tectonic control of sediment discharge to the ocean: the importance of small mountainous rivers, *J. Geol., 100*, 525-544, 1992.

Moffatt, R. L., R. E. Wellman, and J. M. Gordon, Statistical summaries of streamflow data in Oregon: Vol. 1–Monthly and annual streamflow, and flow-duration values, *U.S. Geol. Surv. Open-File Rep. 90-118*, 413 pp., 1990

Newcomb, R. C., Effect of tectonic structure on the occurrence of ground water in the basalt of the Columbia River Group of The Dalles area, Oregon and Washington, *U.S. Geol. Surv. Prof. Pap. 383-C*, 33 pp., 1969.

Reidel, S. P., T. L. Tolan, P. R. Hooper, et al., The Grande Ronde Basalt, Columbia River Basalt Group; stratigraphic descriptions and correlations in Washington, Oregon, and Idaho, in *Volcanism and Tectonism in the Columbia River Flood-Basalt Province, Geol. Soc. Amer. Spec. Pap. 239*, edited by S. P. Reidel and P. R. Hooper, pp. 21-53, 1989.

Robinson, P. T., G. F. Brem, and E. H. McKee, John Day Formation of Oregon–a distal record of early Cascade volcanism, *Geology, 12*, 229-232, 1984.

Roering, J. J, J. W. Kirchner, and W. E. Dietrich, Evidence for nonlinear, diffusive sediment transport on hillslopes and implications for landscape morphology, *Wat. Resour. Res., 35*, 853-870, 1999.

Russell, I. C., Preliminary report on the geology and water resources of central Oregon, *U.S. Geol. Surv. Bull. 252*, 138 pp., 1905.

Sarna-Wojcicki, A. M., and J. O. Davis, Quaternary tephrochronology, in *Quaternary Nonglacial Geology; Conterminous U.S., Geol. Soc. Am., The geology of North America (K-2)*, edited by R. B. Morrison, pp. 93-116, 1991.

Scott, W. E., Quaternary glaciation and volcanism, Metolius River area, Oregon, *Geol. Soc. Am. Bull., 88*, 113-124, 1977.

Shannon and Wilson Inc., *Geologic studies of Columbia River basalt structures and age of deformation, The Dalles-Umatilla region, Washington and Oregon, Boardman Nuclear Project*, report to Portland General Electric Company, Portland, Oregon, 52 pp. 1973.

Sherrod, D. R., and W. E. Scott, Preliminary geologic map of the Mount Hood 30- by 60- minute Quadrangle, northern Cascade Range, Oregon, *U.S. Geol. Surv. Open-File Rep. 95-219*, 28 pp., scale 1: 100,000, 1995.

Sherrod, D. R., E. M. Taylor, M. L. Ferns, et al., Geologic map of the Bend 30′ X 60′ Quadrangle, central Oregon, *U.S. Geol. Surv. Geol. Inv. Map I-2683*, scale 1:100,000, in press.

Smith, G. A., Stratigraphy, sedimentology, and petrology of Neogene rocks in the Deschutes basin, central Oregon: a record of continental-margin volcanism and its influence on fluvial sedimentation in an arc-adjacent basin, Ph.D. Dissertation, 464 pp., Oregon State University, Corvallis, Oregon, 1986.

Smith, G. A., The influence of explosive volcanism on fluvial sedimentation–the Deschutes Formation (Neogene) of central Oregon, *J. Sed. Pet.*, *57*, 613-619, 1987a.

Smith, G. A., Geologic map of the Seekseequa Junction and a portion of the Metolius Bench quadrangles, Jefferson County, Oregon, *State of Oregon Dept. Geol. Min. Ind. Geol. Map Ser. GMS-44*, Portland, Oregon, 1987b.

Smith, G.A., A field guide to depositional processes and facies geometry of Neogene continental volcaniclastic rocks, Deschutes basin, central Oregon, *Oregon Geol.*, *53*(1), 3-20, 1991.

Smith, G. A. and G. A. Hayman, Geologic map of the Eagle Butte and Gateway quadrangles, Jefferson and Wasco Counties, Oregon, *State of Oregon Dept. of Geol. Min. Ind. Geol. Map Ser. GMS-43*, Portland, Oregon, scale 1:24,000, 1987.

Smith, G. A., B. N. Bjornstad, and K. R. Fecht, Neogene terrestrial sedimentation on and adjacent to the Columbia Plateau, Washington, Oregon, Idaho, in *Volcanism and Tectonism in the Columbia River Flood-Basalt Province, Geol. Soc. Am. Spec. Pap. 239*, edited by S. P. Reidel and P. R. Hooper, pp.187-198, 1989.

Stearns, H. T., Geology and water resources of the middle Deschutes River basin, Oregon, *U.S. Geol. Surv. Water Supply Paper 637-D*, pp. 125-220, 1931.

Sundborg, A., Sedimentation problems in river basins, *Nature and Resources*, *19*, 10-21, 1983.

Taylor, E. M., Volcanic history and tectonic development of the central High Cascade Range, Oregon, *J. Geophys. Res.*, *95*, 19,611-19,622, 1990.

Tolan, T. L., S. P. Reidel, M. H. Beeson, et al., Revisions to the estimates of the areal extent and volume of the Columbia River Basalt Group, in *Volcanism and Tectonism in the Columbia River Flood-Basalt Province, Geol. Soc. Amer. Spec. Pap. 239*, edited by S. P. Reidel and P. R. Hooper, pp. 1-20, 1989.

Vanoni, V. A.(editor), *Sedimentation Engineering*, American Society of Civil Engineers, 745 pp., New York, New York, 1975.

Walker, G. W., and N. S. MacLeod, Geologic map of Oregon (1:500,000), U.S. Geol. Surv., 1991.

Walker, G. W., and P. T. Robinson, Paleocene (?), Eocene, and Oligocene (?) rocks of the Blue Mountains region, *U.S. Geol. Surv. Prof. Pap. 1437*, pp. 13-27, 1990.

Welcher, K. E., Holocene channel changes of Camp Creek; an arroyo in eastern Oregon, M.A. Thesis, University of Oregon, Eugene, Oregon, 145 pp., 1993.

Jim E. O'Connor and Tana L. Haluska, U.S. Geological Survey, 10615 SE Cherry Blossom Drive, Portland, OR, 97216

Gordon E. Grant, U.S. Forest Service, 3200 SW Jefferson Way Corvallis, OR 97331

Groundwater Hydrology of the Upper Deschutes Basin and its Influence on Streamflow

Marshall W. Gannett

U.S. Geological Survey, Portland, Oregon

Michael Manga

Department of Earth and Planetary Science, University of California, Berkeley, California

Kenneth E. Lite, Jr.

Oregon Water Resources Department, Salem, Oregon

The remarkable stability of flow in the Deschutes River, relative to other rivers with comparable mean discharges, can be attributed to the substantial fraction of flow that originates as groundwater in the upper Deschutes River basin, the region upstream of Pelton Dam. Indeed, groundwater discharge from the upper basin provides more than three quarters of the total streamflow for the entire Deschutes River basin. In order to understand the factors that result in such a large component of groundwater discharge and the stability of the flow, we develop a conceptual model for the hydrology of the upper basin. The model is based on the regional geology, the distribution and rate of groundwater recharge and discharge, and measurements of hydraulic head, water temperature and isotopic tracers. We show that three hydrogeologic aspects of the upper basin contribute to the stability of flow in the Deschutes River. First, the large vertical and lateral scale of the groundwater system damp out seasonal and longer period variations of discharge. Second, the high permeability of near-surface rocks, combined with the lack of an integrated surface drainage system, permits high recharge rates and thus high groundwater discharge rates, and reduces surface and shallow subsurface runoff. Third, the high storage capacity of the groundwater system filters out large and abrupt changes in recharge, resulting in greatly subdued changes in groundwater discharge. All three factors are responsible for the absence of large peak flows in the upper basin, even during rain on snow events that cause significant flooding elsewhere in Oregon.

INTRODUCTION

The Deschutes River basin encompasses approximately 27,000 km^2 in central Oregon (Figure 1). The river is over 400 km long and has an annual discharge of 170 m^3/s. The western margin of the basin is defined by the volcanic Cascade Range, which includes several large stratovolcanoes with elevations exceeding 3000 meters (m) above sea level. The northern part of the basin is dominated by lava flows of the Columbia River Basalt Group, which form a gently northward-sloping surface, ranging in elevation from approximately 800 to 300 meters, that has been deeply

A Peculiar River
Water Science and Application 7

10.1029/007WS04

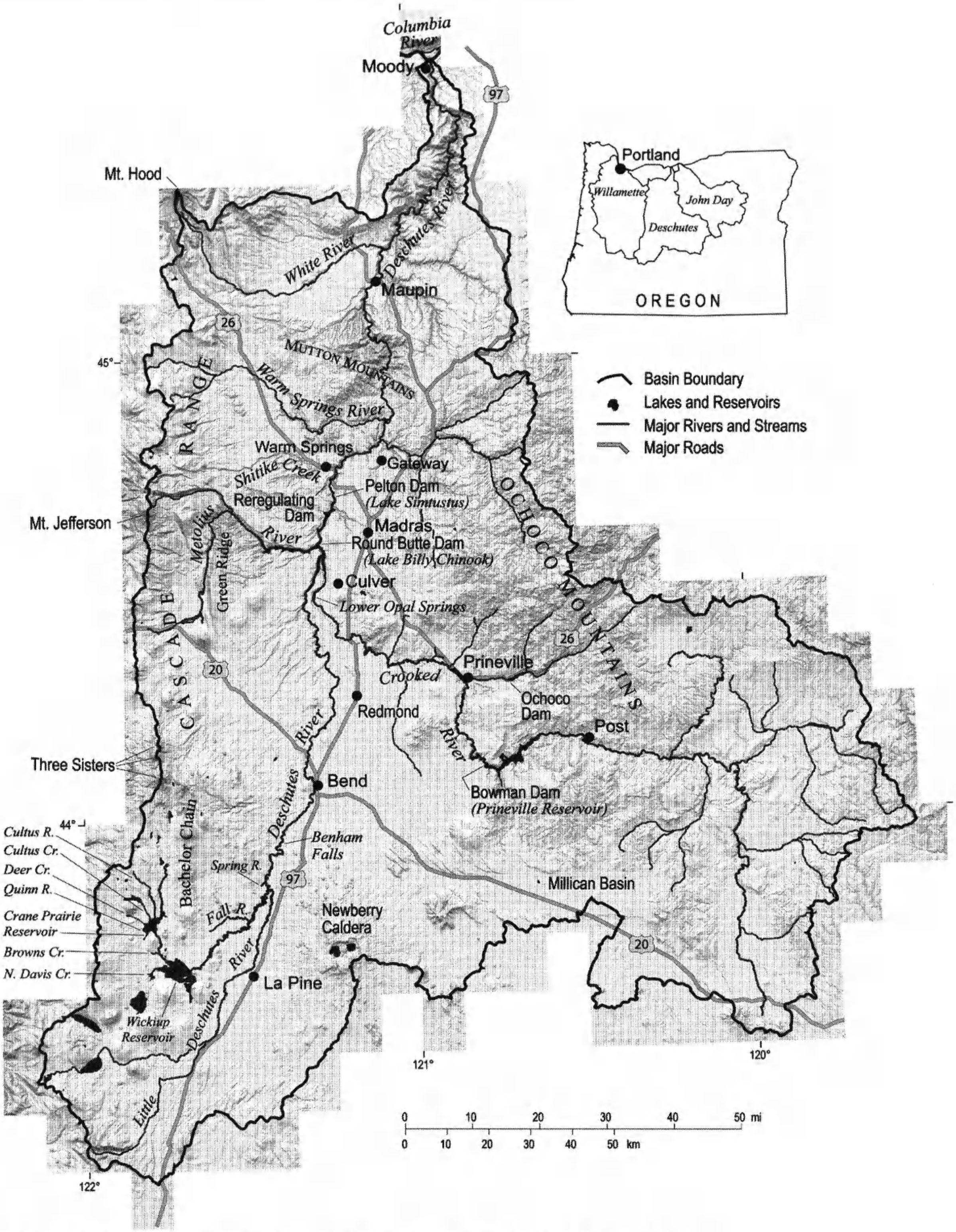

Figure 1. Major geographic and cultural features in the upper Deschutes River basin.

incised by the river. The eastern part of the basin consists of early Tertiary volcanic deposits that have been eroded to form a rugged, dissected terrain with some peaks exceeding an elevation of 2000 m above sea level. The southern part of the basin is dominated by the broad edifice of Newberry Volcano, which rises to 2434 m, 1000 m above the surrounding terrain. Precipitation in the Deschutes River basin ranges from more than 3,800 mm in the Cascade Range, due to orographic effects, to less than 250 mm in the high desert to the east [*Taylor*, 1993]. Most precipitation falls as snow during winter.

The Deschutes River is known for its remarkably stable flow, which is attributed to the influence of the regional geology [*Russell*, 1905; *Henshaw et al.*, 1914; *O'Connor, Grant and Haluska,* this volume]. "In fact, it is considered to be one of the most stable rivers in the United States. Serious floods are extremely rare on the Deschutes." [quotation from page 179 in *Manning,* 1992]. To highlight the stability of the flow of the Deschutes River and its spring-fed tributaries, Tables 1a and 1b compare their flow variability with that of other Oregon streams with comparable mean flows.

The Deschutes River exhibits not only seasonal and interannual stability; it also shows a very muted response to extreme meteorological events. For example, the peak discharge of the Deschutes River near Madras during the largest flood in more than 100 years of record (February 1996) was less than five times the mean annual flow at that location [*O'Connor, Grant and Haluska,* this volume]. For comparison, peak flows during large floods of the Willamette and John Day Rivers, both of which are adjacent to the Deschutes Basin, exceeded twenty times their respective mean annual flows.

The stable flow of the Deschutes River is due primarily to groundwater discharge. A large proportion of the flow in the Deschutes River originates as groundwater discharge to the river and its tributaries upstream of Warm Springs. Much of this discharge occurs from large spring complexes near the confluence of the Deschutes and Crooked Rivers. In addition, a substantial amount of groundwater discharges to tributary streams in and near the margins of the Cascade Range, many of which are largely or entirely spring-fed [*Meinzer*, 1927]. Recognizing this, however, is only the first step in understanding the hydrology of the basin. To understand the hydrologic behavior of the Deschutes River basin and its similarities to and differences from other basins, additional questions must be considered:

What are the principal geologic and hydrologic characteristics of the basin that control the rates and distribution of recharge?

Where are the principal groundwater discharge areas and what are the controlling mechanisms?

What are the principal groundwater flow paths and how do different paths affect the rates and timing of groundwater discharge?

How do the geologic, hydrologic, and climatic characteristics of the basin interact in order to produce the stable flow regime?

In this paper we attempt to address these questions by developing a model of the regional groundwater flow system. First we evaluate gaging records to determine the fraction of streamflow in the Deschutes River that is provided by groundwater. Next we describe the features of the geological setting that govern the regional hydrology. We then

Table 1. Discharge characteristics of rivers in Oregon. Q_{xx} indicates the discharge for which xx percent of discharges are greater.

a) Oregon rivers with mean discharge similar to the Deschutes River. All these rivers except the John Day are regulated.

Stream	Period of Record	Mean Flow (m^3/s)	Q_{10}/Q_{90}
Deschutes near Madras	1923-2000	130	1.7
Deschutes at Moody	1897-2000	164	2.0
Siuslaw at Mapleton	1967-1994	56	40
John Day	1904-2000	59	41
McKenzie near Vida	1910-2000	115	4.0
Willamette near Springfield	1911-1957	163	15
Santiam at Jefferson	1907-2000	221	15

b) Rivers in the upper Deschutes River basin.

Stream	Period of Record	Mean Flow (m^3/s)	Q_{10}/Q_{90}
Spring-fed streams			
Quinn River	1937-1991	0.68	3.6
Browns Creek	1937-1991	1.1	2.2
Cultus River	1938-1991	1.8	2.3
Fall River	1938-1991	4.1	1.8
Runoff-dominated streams			
Deer Creek	1938-1991	0.21	210
Cultus Creek	1938-1991	0.62	580

describe the temporal and spatial pattern of groundwater discharge and recharge in relation to the geological setting. We then use a variety of approaches and measurements, including the distribution of hydraulic head, water temperature, and isotopic tracers, to determine groundwater flow paths and rates. Finally, we use the resulting hydrologic model of the basin to evaluate the factors that govern the dynamic behavior of the groundwater system, and its influence on the surface water hydrology.

GROUNDWATER DISCHARGE TO THE DESCHUTES RIVER

The proportion of flow consisting of groundwater at various locations along the Deschutes River is depicted in Figure 2. This figure was created using groundwater discharge estimates from *Gannett et al.* [2001], which were based primarily on stream gage data and streamflow measurements, and from statistical summaries of streamflow data by *Moffatt et al.* [1990]. The proportion of flow consisting of groundwater was estimated in a variety of ways depending on the type of data available. For spring-fed streams with no tributaries or surface runoff, the entire flow was considered groundwater discharge. For streams with a variety of spring-fed and runoff-fed tributaries, the component of groundwater discharge was estimated from mean monthly flow statistics for the late summer and early fall, when surface runoff is assumed to be negligible. Synoptic sets of stream flow measurements (referred to as "seepage runs") were used to determine groundwater discharge to, and leakage from, selected reaches of most major streams in the basin.

The 4.3 m^3/s flow at the uppermost gage on the river, at River Mile[1] (RM) 244, is entirely groundwater discharge (Table 2). By the next gage, below Crane Prairie reservoir at RM 238, flow from both groundwater and surface-water dominated tributaries raises the mean annual flow to about 5.9 m^3/s, about 5.3 m^3/s of which is groundwater discharge. Flow from numerous springs and spring-fed tributaries raises the mean annual flow to about 21.4 m^3/s by the gage just below Wickiup Reservoir at RM 226. Approximately 20.5 m^3/s, or 96% of the mean annual flow at this point is composed of groundwater discharge. The next long-term stream gage on the river is just above Benham Falls at RM 181. The mean annual flow at Benham Falls is about 41.9 m^3/s. Estimating the proportion of flow at Benham Falls consisting of groundwater discharge, however, is complicated by tributary inflow from the Little Deschutes River, which has

[1]Locations along the Deschutes River are in river miles (RM) upstream of the river mouth as marked on USGS topographic maps.

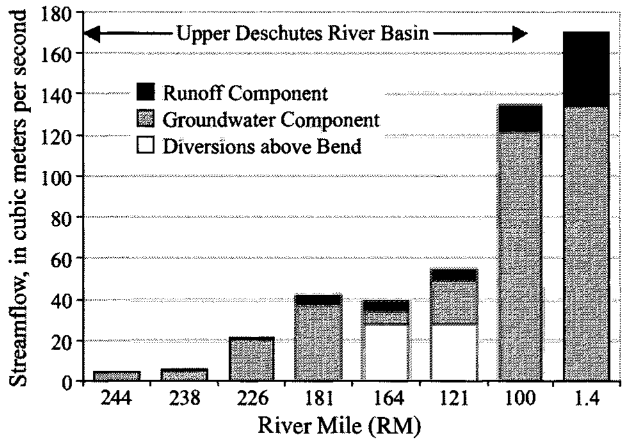

Figure 2. Flow of the Deschutes River broken down by surface water and groundwater components at selected gaging stations. The flows at RM 164 and 121 are offset to reflect diversions above RM 164. Approximately half of the water diverted infiltrates through leaking canals and returns to the river as groundwater discharge above RM 100. For gage locations, see Table 2.

a drainage area of about 2640 km^2 and includes flow from many tributaries. A conservative estimate of the amount of groundwater discharge at the Benham Falls gage, based on seepage runs and gage data from the Little Deschutes River, is 37.6 m^3/s, or about 90% of the mean annual flow.

Evaluating the discharge at the gages downstream of Benham Falls is complicated by irrigation diversion. Between Benham Falls and Bend, average annual irrigation diversions are about 25 to 30 m^3/s. In addition, about 3.2 m^3/s is lost through stream leakage, or direct infiltration of water from the channel to groundwater. The mean annual flow at Bend (RM 164) is 10.7 m^3/s. Between Bend and the downstream gage at Culver (RM 121), the river gains approximately 13 m^3/s from groundwater discharge. The mean annual flow at Culver is 26.3 m^3/s, approximately 21.4 m^3/s (81%) of which originates as groundwater.

Downstream from the Culver gage there is a series of dams and reservoirs (the Pelton-Round Butte Complex) extending to RM 100. Lake Billy Chinook, the reservoir behind the uppermost dam, covers the confluence of the Deschutes, Crooked, and Metolius Rivers. There is substantial groundwater discharge to both the Metolius and Crooked Rivers. Mean annual flow at the gage at Madras (RM 100) below the confluence is 135 m^3/s, 122 m^3/s (91%) of which consists of groundwater discharge. Very little groundwater discharges directly to the main stem of the Deschutes River below the gage at Madras, and most increases in streamflow are due to inflow from three tributaries: Shitike Creek, the Warm Springs River, and the

Table 2. Mean annual discharge and proportion of discharge due to groundwater at selected stream gages.

Gage Location	Station ID	Location (RM)	Mean Annual Discharge (m^3/s)	Discharge from Groundwater (m^3/s)	% of Total Discharge from Groundwater
highest gage, below Snow Cr.	14050000	244	4.3	4.3	100
below Crane Prairie Reservoir	14054000	238	5.9	5.3	90
below Wickiup Reservoir	14056500	226	21.4	20.5	96
above Benham Falls	14064500	181	41.9	37.6*	90*
Irrigation diversions remove ~25-30 m^3/s; stream leakage removes ~3.2 m^3/s					
Bend	14070500	164	10.7	9.6*	90*
River gains ~13 m^3/s from groundwater discharge					
Culver	14076500	121	26.3	21.4	81
Pelton-Round Butte Dam complex, confluence of Crooked and Metolius Rivers					
Madras	14092500	100	135	122	91
Tributary inflow from Shitike Creek, Warm Springs River, and White River					
Moody, near Biggs	14103000	1.4	170	135	80

*See text for qualification of these numbers.

White River. The mean annual flow of the Deschutes River at the gage at Moody, at RM 1.4, is 170 m^3/s. Using conservative estimates of baseflow determined from stream gage data for the above three tributaries, approximately 135 m^3/s, or about 80%, of the mean annual flow of the Deschutes River at Moody consists of groundwater.

GEOLOGIC FRAMEWORK

The distribution of regional groundwater discharge to the Deschutes River is controlled primarily by regional geology (Figure 3). Most of the groundwater that discharges to the Deschutes River system originates in the part of the basin south (upstream) of Warm Springs and extending from the Cascade Range east to the Deschutes River. This region consists almost entirely of Tertiary to Quaternary volcanic deposits and volcanically derived sediments [*Walker and MacLeod*, 1991; *Sherrod et al.*, in press]. The western margin of the basin is defined by the prominent peaks and volcanic highlands of the Cascade Range, which consists largely of lava flows, pyroclastic deposits, and vent complexes, all Quaternary in age. Deposits become progressively older east of the Cascade Range, where deposits of the late Miocene to Pliocene Deschutes Formation dominate. The Deschutes Formation consists largely of lava flows, ash flows, debris flows, and fluvial sediments, many of which originated in the ancestral Cascade Range and were deposited in an arc-adjacent basin [*Smith*, 1986a]. The Deschutes Formation also includes deposits resulting from eruptive activity within this arc-adjacent basin. The boundary between Quaternary Cascade deposits and Pliocene deposits is marked locally by faults from Bend to Green Ridge [*Sherrod and Smith*, 2000]. Elsewhere, Quaternary rocks overlie or on-lap the older rocks.

The most prominent feature of the southern basin is Newberry Volcano, one of the largest Quaternary volcanoes in the conterminous United States, measuring 60 by 30 km at its topographic base [*MacLeod et al.*, 1995]. Basalt and basaltic andesite lava flows from Newberry Volcano extend northward into the central part of the basin, filling canyons of the ancestral Deschutes and Crooked Rivers.

The eastern part of the basin is dominated by deposits of the early Tertiary John Day and Clarno Formations. The John Day Formation consists largely of devitrified silicic pyroclastic material with sparse basaltic and andesitic lava [*Robinson et al.*, 1984] and the Clarno Formation is com-

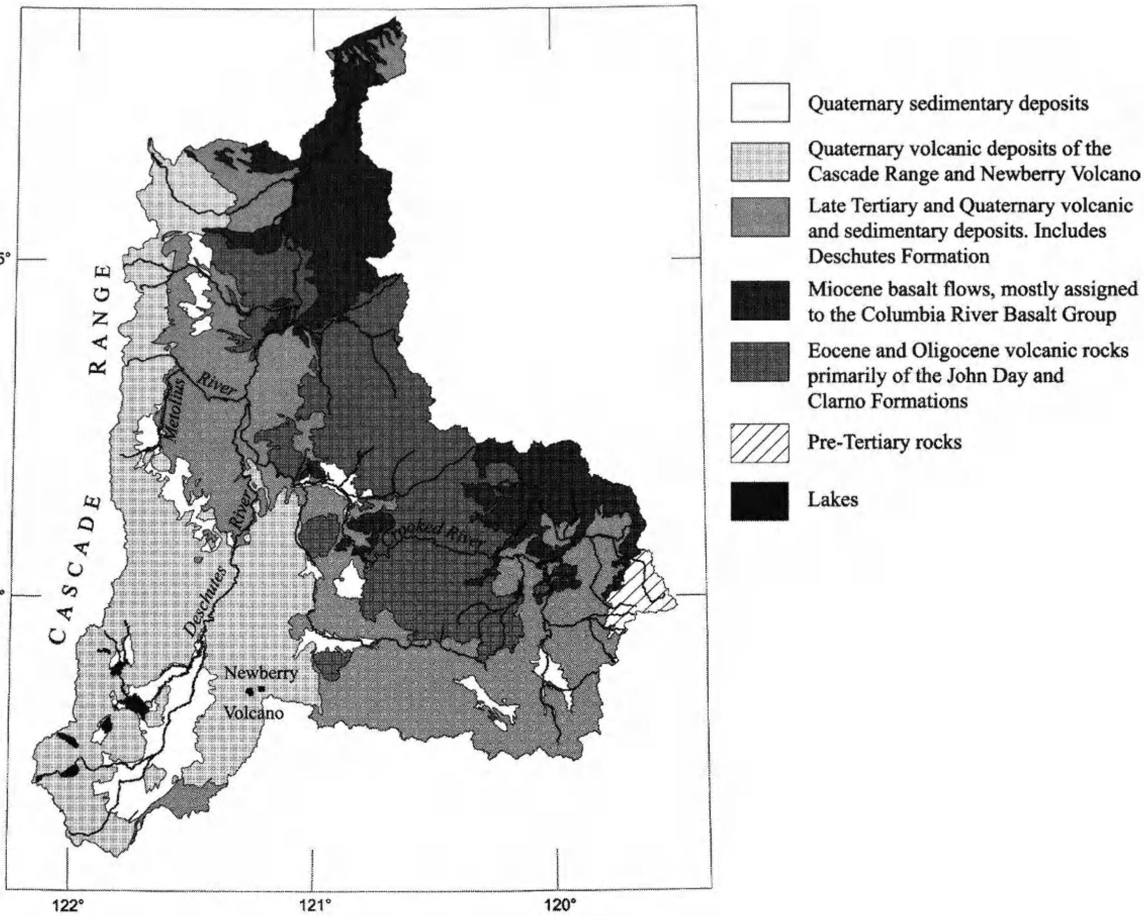

Figure 3. Generalized geologic map of the Deschutes River basin.

posed primarily of andesitic and rhyolitic lava, mudflows, and tuffaceous sediments [*Orr et al.*, 1992]. These units are exposed in a northwest-trending belt extending from the southeastern part of the basin to the Mutton Mountains north of Warm Springs. This belt of Eocene to early Miocene rock forms the boundary of the basin into which the younger Cascade-derived materials were deposited.

Regional groundwater flow into the Deschutes River system occurs almost exclusively in the late Miocene to Pliocene Deschutes Formation and younger deposits of the Cascade Range and Newberry Volcano. These deposits are generally permeable, and the volcanic upland and large peaks of the Cascade Range form the principal recharge area for the basin. The John Day and Clarno Formations, in contrast, have very low permeability due to extensive devitrification and secondary mineralization. These older deposits bound the permeable younger units. Where deposits of the John Day and Clarno Formations occur upgradient of the younger more permeable deposits, they contribute only minimal water to the regional groundwater system due to their low permeability and the fact that they occur primarily in the drier, eastern parts of the basin where little recharge occurs. Where the John Day and Clarno Formations occur downgradient from the younger more permeable deposits, they impede subsurface flow, diverting most groundwater flow out to springs and streams.

The principal area of regional groundwater flow, therefore, includes the southwestern part of the Deschutes River basin extending from the crest of the Cascade Range to the contact with the low-permeability early Tertiary rocks of the John Day and Clarno Formations. In the south-to-north direction, the area extends from Newberry Volcano northward to the point at which the Deschutes River system has cut down to the low permeability rocks. This is the area considered in this paper, and is henceforth referred to as the "upper Deschutes River basin."

The depth to the base of the regional groundwater system in the upper Deschutes River basin is not well known. Temperature logs of deep wells drilled in the Cascade Range and Newberry Volcano are generally isothermal to depths between 100 and 500 m, indicating substantial and rapid groundwater flow with a large downward component [*Swanberg et al.*, 1988; *Blackwell et al.*, 1990; *Blackwell*, 1992; *Ingebritsen et al.*, 1992]. At sufficiently great depths, in places > 500 m, temperature gradients approach the expected conductive heat flow regime indicating little groundwater flow. Analyses of cuttings and cores [*Gannett and Barger*, 1981; *Keith and Barger*, 1988, 1999] suggest that the reduced permeability at these depths is caused by hydrothermal alteration and secondary mineralization.

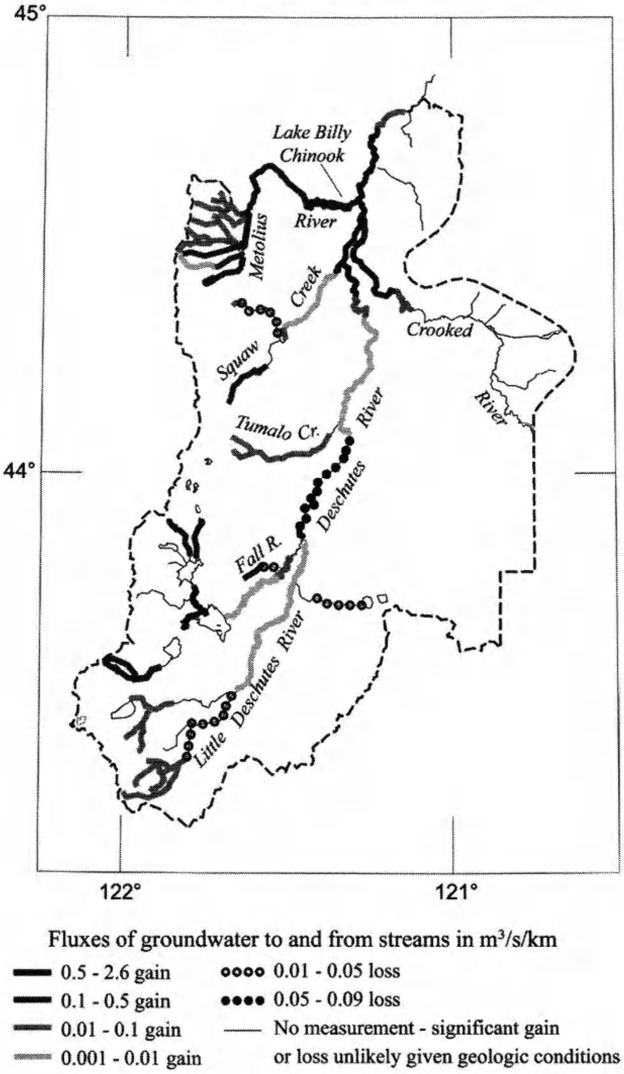

Figure 4. Estimated average fluxes of groundwater to and from streams in the upper Deschutes River basin [modified from *Gannett et al.*, 2001].

Away from the Cascade Range and Newberry Volcano, the base of the active regional groundwater flow system is presumed to be the contact between the Deschutes Formation and the underlying John Day Formation. Except near the margin of the basin, no wells penetrate this contact, and its elevation must be inferred from exposures in the Deschutes River Canyon. The elevation of the contact, where exposed, is about 450 to 550 m above sea level [*Smith*, 1987a, b]. Its geometry beneath most of the Deschutes River basin is not known. Pre-Deschutes Formation rocks dip 5 degrees to the southwest in the Gateway area and the Deschutes Formation itself dips less than 1 degree to the southwest in the same area [*Smith*, 1986b]. A 322 m well in Bend did not penetrate the contact, indicating that it is below an elevation of 730 m at that location. A 445 m well in La Pine penetrated to an elevation below 850 m and does not penetrate the base of the permeable section.

REGIONAL HYDROLOGY

In this section we use a variety of measurements to determine the pattern and rate of groundwater flow and the resulting distribution of groundwater discharge. The measurements and data that we review and discuss have all been published elsewhere, and a more detailed interpretation of the data can be found in the original publications. The goal of the present paper is to integrate previous studies in order to develop a conceptual model of the Deschutes River Basin that can be used to understand the relationship between the geological setting, climate, and the dynamics of the groundwater flow system. Later in the paper, we show how this model can be used to understand how the discharge characteristics of the Deschutes River reflect the hydrogeology of the basin.

Rates and Distribution of Groundwater Discharge and Controlling Factors

There are two principal settings for groundwater discharge in the upper Deschutes River basin: *i)* to streams in and adjacent to the Cascade Range; and *ii)* to the Deschutes and Crooked Rivers in the vicinity of their confluence (Figure 4). We discuss these two settings in order.

Many streams emanating from the Cascade Range are largely or entirely spring-fed [*Meinzer*, 1927]. These streams typically have spring complexes at or near their headwaters and no tributaries. Spring-fed streams have very constant flow, exhibiting only small seasonal fluctuations, with late summer flows comparable to the annual mean flows. For example, the large spring-fed streams in the Cascade Range analyzed by *Manga* [1996] exhibit seasonal deviations from their annual mean flows ranging between only 7 and 47 percent in any given year. By comparison, Table 1 shows that runoff-dominated streams in the basin with comparable mean discharges have annual variations that are about two orders of magnitude greater. Variations in discharge from spring-fed streams are also muted on longer time scales. For example, the ratio of maximum and minimum annual mean flows of Fall River from 1939 and 1991 is 2.5. In contrast, the ratios of maximum and minimum annual mean flows of the Crooked River near Post (1941-1965) and the John Day river near John Day (1969-1991), streams with comparable mean annual flows, are 4.3 and 5.3 respectively.

Some water emanating from the Cascade Range is carried by runoff-dominated streams such as Deer Creek and Cultus Creek. These streams are characterized by large seasonal flow variations and often go dry, or nearly so, in the late summer. Some streams show both groundwater and surface water signatures and exhibit both large seasonal variations and substantial late-season flows.

Combined groundwater discharge to streams emanating from the Cascade Range, including those in the Metolius River drainage, is estimated to average about 74 m^3/s [*Gannett et al.*, 2001]. Groundwater flowing from the Cascade Range that does not discharge to streams in and adjacent to the range eventually discharges near the confluence of the Deschutes, Metolius and Crooked Rivers, the second principal setting for groundwater discharge in the upper Deschutes River basin. Of the approximately 91% of the flow of the Deschutes River at Madras that originates as groundwater, roughly half comes from discharge to the main stem of the Deschutes and lower Crooked Rivers within about 16 km of their confluence.

Synoptic discharge measurements and stream gage data indicate that the Deschutes River gains approximately 12 to 15 m^3/s from groundwater inflow along a 16 km reach upstream of Lake Billy Chinook, the reservoir behind Round Butte Dam that inundates the confluence of the Deschutes, Crooked, and Metolius Rivers. A single set of synoptic discharge measurements indicates that the Crooked River gains approximately 35 m^3/s in the 11 km reach upstream of Lake Billy Chinook. Stream gaging records indicate that this figure is typical of average conditions. Gaging station data indicate that Lake Billy Chinook itself gains, on average, approximately 12 m^3/s. Downstream from Round Butte Dam to the reregulating dam, a distance of about 16 km, the Deschutes River gains an additional 8.9 m^3/s according to discharge measurements by Bolke and Laenen [1989]. An additional 2.2 m^3/s of groundwater inflow are reported by Bolke and Laenen [1989] along the 8 km reach below the reregulating dam (Figure 1). Below this point, the Deschutes River canyon has cut well into to the low-permeability John Day Formation, and no additional significant groundwater inflow has been measured. Thus, total inflow in this area is approximately 70 to 73 m^3/s.

The large amount of groundwater discharge to the Deschutes and Crooked Rivers in the vicinity of their confluence is due to two related factors. First, upstream of Lake Billy Chinook, both rivers have incised canyons hundreds of meters deep into the Deschutes Formation which intercept the regional water table, resulting in spring complexes in the canyon walls. Second, at about the location of Pelton Dam, the Deschutes River has cut entirely through the Deschutes Formation to the much less permeable John Day Formation. A few kilometers north of the reregulating dam, the Deschutes Formation pinches out against the John Day Formation. By this point, virtually all of the northward-flowing regional groundwater has discharged to the Deschutes River system (Figure 5).

Variations in groundwater discharge to the Deschutes and lower Crooked Rivers near their confluence are smaller than variations observed in Cascade streams. No data are available to evaluate seasonal variations, but interannual and decadal scale variations in discharge to the Deschutes in this area can be evaluated using gaging data along the 16 km reach of the Deschutes River upstream from Lake Billy Chinook bracketed by stream gages at Bend and near Culver. During the late summer, the difference in discharge between these two gages can be attributed entirely to groundwater inflow, as tributary inflow is negligible. The difference between the August mean discharges of the two gages can be used as a proxy for groundwater discharge and provides information on temporal variations in groundwater discharge. From 1953 to 1997 the differences between August mean flows at Bend and Culver varied between 9.9 and 14.8 m^3/s and exhibited a decadal-scale pattern of variation similar to that of other streams in the basin (Figure 6). The groundwater discharge to the main stem of the Deschutes River is more constant than that to smaller tributary streams in the Cascade Range, presumably because of the larger scale of flow.

Sources, Distribution, and Rates of Groundwater Recharge

Recharge to the groundwater flow system in the upper Deschutes River basin is by infiltration of precipitation (rainfall and snowmelt). The spatial distribution of recharge from precipitation in the upper Deschutes River basin mimics the spatial distribution of precipitation [*Gannett et al.*, 2001]. Precipitation in the basin is not uniformly distributed,

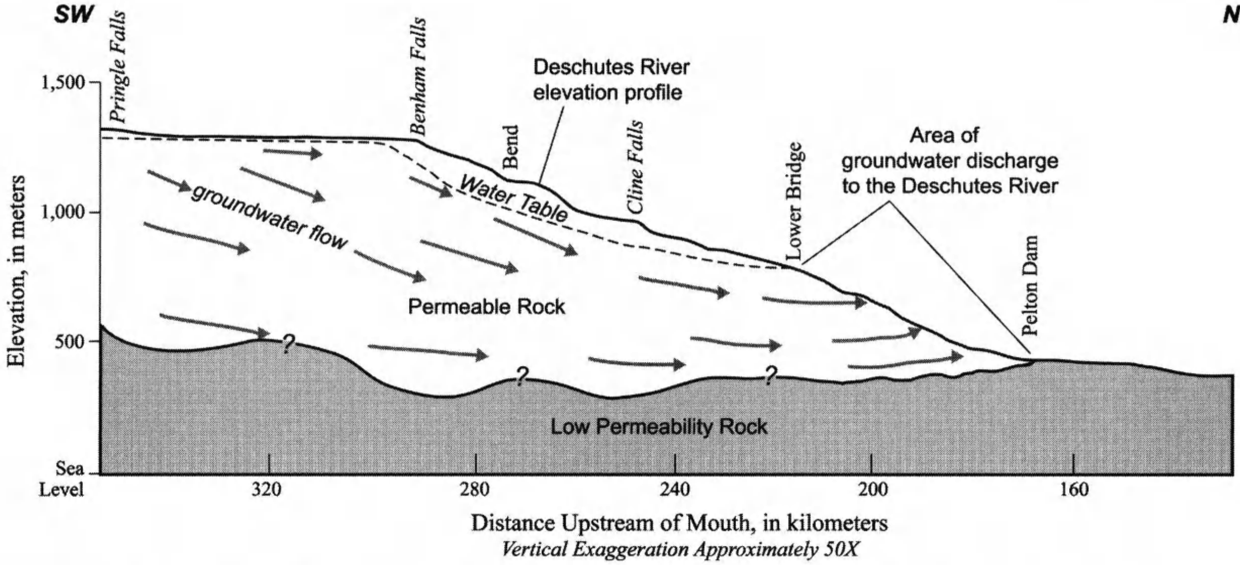

Figure 5. Schematic section along the profile of the Deschutes River showing the influence of low-permeability geologic units on groundwater discharge.

but falls mostly in the Cascade Range due to orographic effects (Figure 7). The large amount of precipitation, in combination with the high permeability of soils and near-surface rocks, makes the Cascade Range the locus of groundwater recharge in the upper Deschutes River basin.

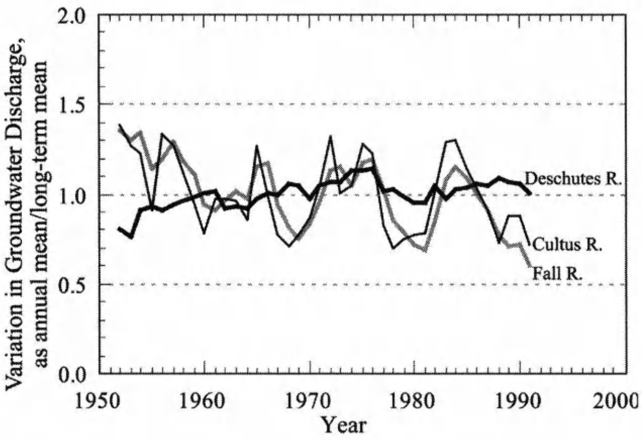

Figure 6. Normalized variations in annual mean groundwater discharge to Fall River, Cultus River, and the Deschutes River between Bend and Culver from 1952 to 1991. Fall River and Cultus River are small, spring-fed tributary streams. Annual mean flows are normalized by dividing them by the long-term mean. Variations from the long-term mean are mainly due to climate influences. The slight upward trend observed in the Deschutes River flow is not climatic and is likely due to canal leakage or effects of Lake Billy Chinook.

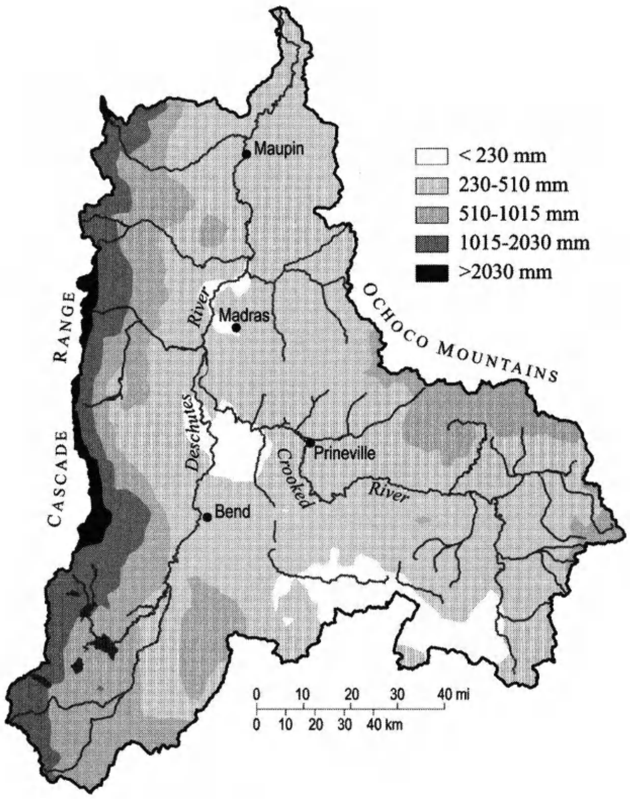

Figure 7. Normal annual precipitation in the Deschutes River basin 1961-1990. Precipitation data are from Taylor [1993].

The spatial and temporal distribution of groundwater recharge to the upper Deschutes River basin from infiltration of precipitation was estimated for water years 1962-1994 by *Boyd* [1996] using the water-balance method of *Bauer and Vaccaro* [1987]. Boyd's calculations were extended through 1997 by *Gannett et al.* [2001]. The estimated annual recharge averaged over the upper basin during this 36-year period ranged from less than 7 cm to nearly 60 cm. The mean recharge for the period was 27 cm/year, which is equivalent to about 100 m^3/s, similar to the estimated groundwater discharge from the upper basin. Recharge averages about 35-40 % of annual precipitation within the basin, and ranges from as much as 70% at high elevations [*Manga*, 1997], to less than 5% at low elevations, where potential evapotranspiration greatly exceeds precipitation.

In order to confirm that much of the groundwater discharged at springs is recharged at high elevations, several studies in the Oregon Cascade Range have compared the stable isotopes of oxygen and hydrogen in precipitation and in spring waters [e.g., *Ingebritsen et al.*, 1994; *James et al.*, 2000]. Because much of the recharge occurs from snowmelt, *James et al.* [2000] collected a large set of snow cores and water from small springs in order to determine the relationship between the isotopic composition of precipitation and elevation, latitude and longitude. The primary control on isotopic variability of the precipitation (i.e., for oxygen, the ratio of ^{18}O to ^{16}O) was found to be elevation [*James*, 1999]. Figure 8 shows the regression relationship between elevation and the oxygen isotopic composition of precipitation in the upper basin (either oxygen or hydrogen isotopes can be used for this analysis, although in the study of *James et al.* [2000] the precision of measurements, relative to their variability, was better for oxygen isotopes). The isotopic compositions of selected spring waters from large cold springs are also shown as a function of the discharge elevation. The isotopic composition of the spring water can be projected to the elevation at which precipitation has a comparable composition to infer a representative or mean recharge elevation. This extrapolation should be reasonable because samples from snow cores and the large springs in Figure 8 fall on the same meteoric water line [see Figure 3 in *James et al.*, 2000], suggesting that evaporation has not significantly affected the isotopic composition of the spring water. The extrapolation also assumes that the discharged

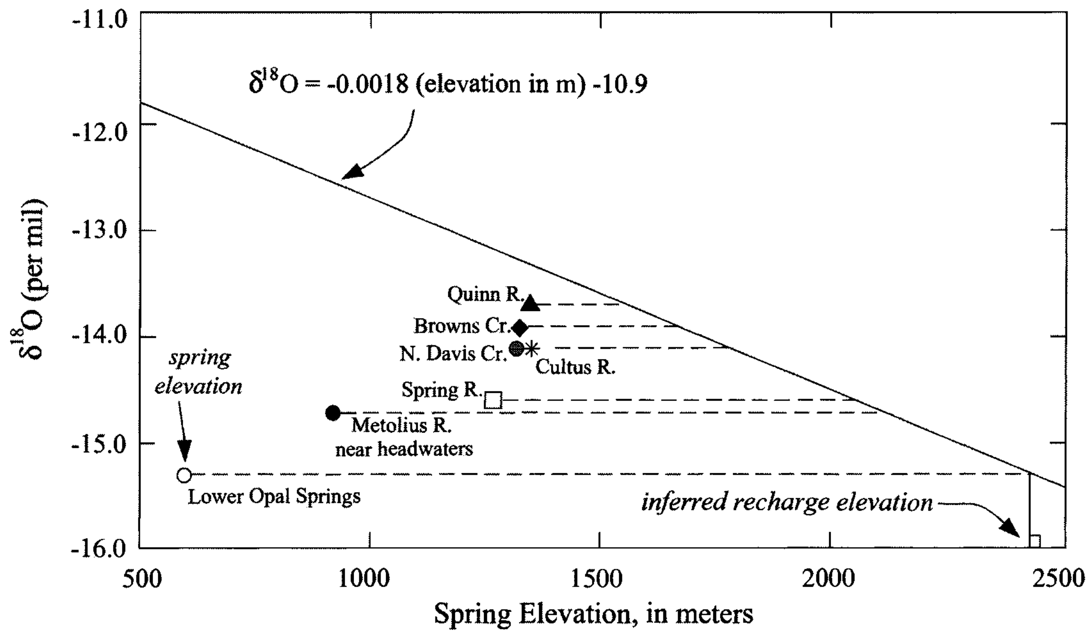

Figure 8. Relationship between spring elevation and oxygen isotope composition (symbols). The solid line shows the relationship between elevation and $\delta^{18}O$ of precipitation as defined by snow core samples. All data are reported in the conventional delta-notation as per mil (parts per thousand) deviations from Standard Mean Ocean Water (SMOW). The mean recharge elevation of the spring water can be estimated by tracing horizontal lines from the points representing spring samples to the elevations at which precipitation is comparable. Modified from *James et al.* [2000]. The data used for the linear regression are not shown; there is, however, significant scatter in the data (correlation coefficient 0.47), as shown in Figure 4 in *James et al.* [2000], that reflects a combination of variability between precipitation events and kinetic effects in the snowpack [e.g., *Friedman et al.*, 1992].

water is young enough to be comparable to modern precipitation. S. Hinkle (U.S. Geological Survey, written communication, 2001) has suggested, however, that the discharged water at Lower Opal Springs may be old enough that it was recharged during the Little Ice Age (circa A.D. 1500-1900) and would have been isotopically lighter than modern precipitation [*Naftz et al.*, 1996].

The data shown in Figure 8 are consistent with the water discharged at large springs being recharged at high elevations, along the crest of the Cascade Range and on the large volcanoes in the region. For example, Lower Opal Springs, near the confluence of the Crooked and Deschutes River, discharges water that is isotopically similar to precipitation that falls at high elevations on the Three Sisters and Newberry volcanoes, more than 50 km from the discharge location. That most of the recharge occurs at high elevations is not surprising because this is where precipitation rates are greatest. Indeed, the estimated precipitation-weighted recharge elevations calculated in *Manga* [1997] are consistent with those inferred isotopically in Figure 8. *Ingebritsen et al.* [1994] similarly found that hot springs at low elevation in the Western Cascades also discharge water that is recharged along the crest of the Cascade Range.

Leaking irrigation canals are the second largest source of present-day recharge in the basin [*Gannett et al.*, 2001]. Approximately 1150 km of canals and laterals carry water diverted from the Deschutes and Crooked Rivers to more than 650 km^2 of irrigated land in the area roughly bounded by Bend, Sisters, Prineville, and Gateway. Many of the canals are constructed in highly fractured basaltic lava and are unlined, and consequently have substantial transmission losses. Of the 30 m^3/s (average annual rate) diverted into canals in the upper Deschutes River basin during 1994, 14 m^3/s leaked through canal bottoms to become groundwater recharge [*Gannett et al.*, 2001]. Most of this loss occurs between Bend and the Crooked River north of Redmond. A comparison of estimated canal loses from the early 1900s to the present with baseflow to the Crooked River, as inferred from late-season streamflow, shows that most of the water lost through leaking canals returns as spring flow to the lower Crooked River [*Gannett et al.*, 2001]. *Caldwell* [1998] showed that canal water and shallow groundwater in the vicinity of the canals are isotopically similar.

Stream leakage is a substantial source of recharge in the upper Deschutes River basin along the Deschutes River between Benham Falls and Bend, where the river loses an average of 3.2 m^3/s (Figure 4). Several of the lakes and reservoirs in the southern part of the basin along the margin of the Cascade Range are known to lose water, but leakage rates are unknown. Crane Prairie Reservoir is the exception, where the average leakage rate, estimated from stream-gage data, is 2.3 m^3/s [*U.S. Geological Survey*, 1958].

Groundwater Flow Paths

Groundwater flow directions can be estimated from the distribution of hydraulic head, as measured in wells and as inferred from the elevations of major springs and gaining streams. On a basin-wide scale, groundwater generally moves from recharge areas high in the Cascade Range to discharge areas along the margin of the Cascade Range and near the confluence of the Deschutes and Crooked Rivers. Shallow flow directions are controlled primarily by surface topography and the stream network. Deeper flow directions are controlled by the regional distribution of recharge and discharge areas, and geologic boundaries. At any single location, therefore, groundwater flow directions may vary with depth. The distribution of hydraulic head in the upper Deschutes River basin is summarized in Figure 9. This generalized map depicts the overall regional head distribution and does not show small-scale variations in head such as might be caused by leaking canals or irrigation.

The general pattern of regional groundwater flow in the upper Deschutes River basin is from the Cascade Range toward the confluence of the Deschutes and Crooked Rivers. Little deviation from this pattern is apparent in the northern and central part of the upper basin. In the southern basin, however, shallow groundwater flows from the Cascade Range southward toward Crane Prairie and Wickiup Reservoirs before moving toward the La Pine subbasin. This is due to the presence of a topographic ridge formed by Mount Bachelor and the chain of associated volcanoes to the south.

Sparse head data and geologic information suggests that groundwater flows radially outward from Newberry Volcano. Groundwater that enters the La Pine subbasin from Newberry Volcano and the Cascade Range continues northeastward toward the Bend area and then northward toward the Deschutes-Crooked River confluence. Sparse head data in the eastern part of the mapped area suggest that groundwater flows generally westward, away from the contact between the late Tertiary rocks and the John Day Formation, but with a northward component of flow. This is consistent with inferences based on specific conductance measurements [*Caldwell*, 1998]. In the northern part of the mapped area, groundwater converges toward spring complexes in the canyons of the Deschutes and Crooked Rivers.

There is a large vertical component of groundwater flow in much of the upper Deschutes River basin. Vertical groundwater flow directions can be inferred from vertical

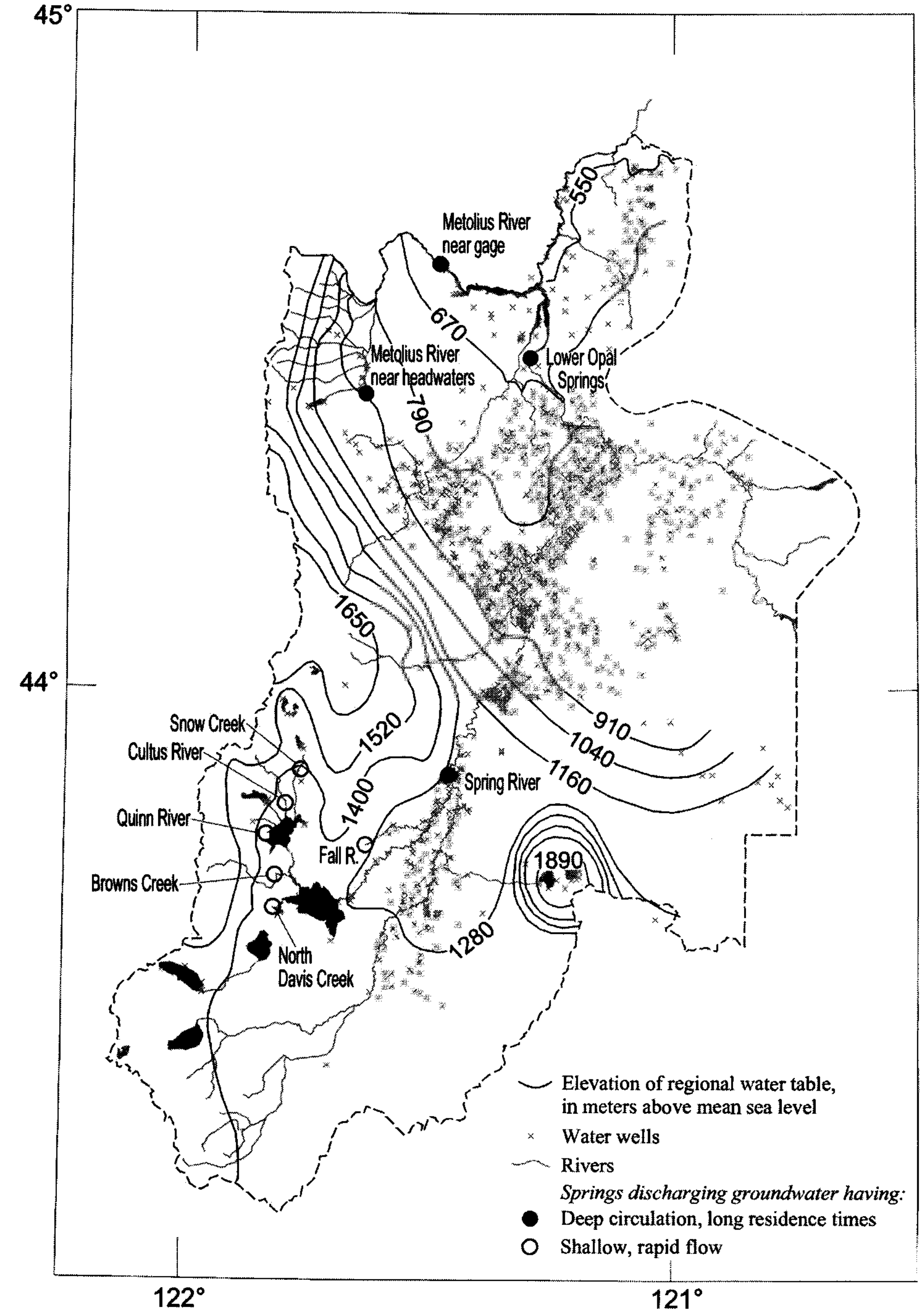

Figure 9. Generalized lines of equal elevation of the regional water table (in meters above mean sea level) and groundwater sampling locations in the upper Deschutes River basin. The water-table elevation is constrained by measurements in water wells and by elevations of major springs and gaining stream reaches. Deeply circulating water with long residence times contains magmatic volatiles and geothermal heat; shallow rapidly flowing groundwater contains no magmatic volatiles, and little or no geothermal heat.

head gradients measured in sets of wells and from temperature gradient data from wells in the Cascade Range. Vertical groundwater movement follows expected patterns in recharge and discharge areas (Figure 10). Downward flow and downward head gradients are to be expected in major recharge areas such as the Cascade Range. Data from *Robison et al.* [1981] show a dramatic drop in the static water level elevation with increasing depth in a 1,220-m well drilled on the flank of Mt. Hood and indicate a downward gradient approaching 0.6 m/m. Large downward head gradients, sometimes close to unity, are also observed locally in the area between Bend and Redmond, where leaking irrigation canals provide substantial local recharge.

Upward head gradients are not commonly observed in the upper Deschutes River basin. There are a number of possible reasons for this, related to both the distribution of available data and the geometry of the flow system. Recharge from leaking canals and irrigation cause generally downward gradients in the areas and at depths where most well data exist. The presence of deep canyons in the principal discharge area is another reason for the rarity of observed upward gradients. Because the canyons intersect the regional water table, water from the saturated zone discharges laterally to springs in canyon walls without upward flow. Finally, few wells penetrate to depths below the elevations of streams in the principal discharge area, where upward vertical gradients would normally be expected. Three such wells ranging in depth from 156 to 225 meters drilled in the bottom of the Crooked River canyon just upstream of Lake Billy Chinook encountered artesian pressures over 35 m above land surface (and river level).

Additional details of the pattern of groundwater flow can be obtained by considering the temperature of spring water and other "tracers" of deep groundwater flow [*Manga*, 2001]. Figure 11 shows the relationship between spring temperature and the mean recharge elevations inferred from the analysis of oxygen isotopes in the discharged water (from Figure 8). Temperatures of the individual springs vary by less than 0.3 °C over a period of several years [*Manga*, 1998]. For comparison, Figure 11 shows the mean annual surface temperature as a function of elevation, based on several climate stations in the basin. Assuming the recharge temperature is similar to the mean annual surface temperature [*Forster and Smith*, 1989; *Taniguchi*, 1993], the temperature difference ΔT shown in Figure 11 can be attributed to geothermal warming.

Figure 11 indicates that some springs in the lower reaches of the basin discharge water that is several degrees warmer than the mean recharge temperature. We can use this change in temperature along with measurements of groundwater discharge to estimate the amount of heat transported advectively and discharged at springs. For example,

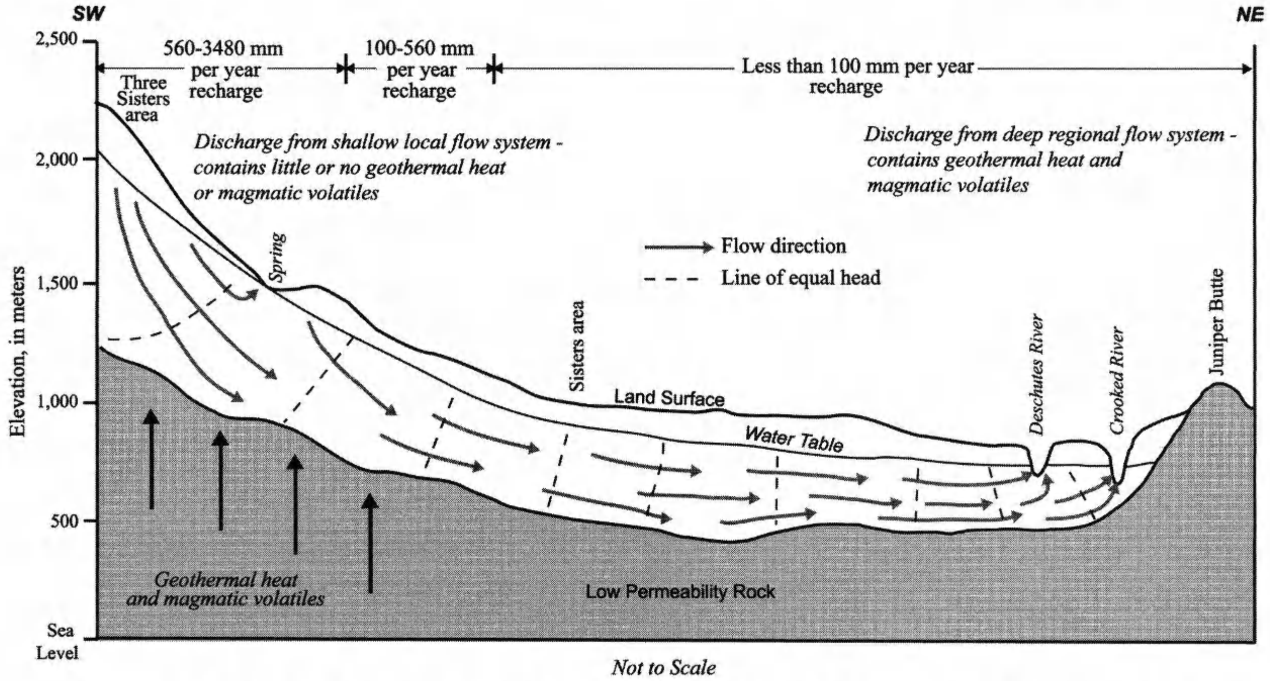

Figure 10. Schematic east-west section across the upper Deschutes River basin showing the generalized hydrogeologic setting, head distribution, and flow directions.

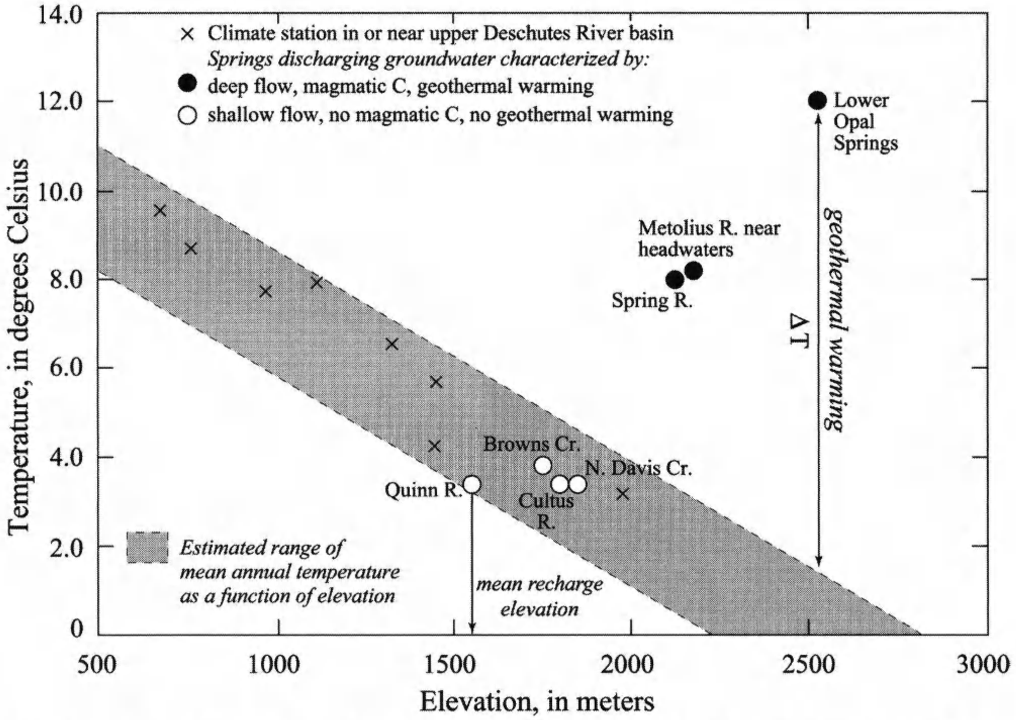

Figure 11. Relationships between elevation and temperature. Crosses are for Oregon climate stations in or near the upper basin. Circles show temperature of the spring water as a function of the recharge elevation inferred from the analysis of oxygen isotopes (see Figure 7).

at the Metolius headwaters spring, a temperature increase of 4.0 °C and discharge of 3.1 m^3/s imply a geothermal heat discharge of 50 megawatts (MW). Assuming that the aquifers are sufficiently thick and groundwater flows fast enough, we can assume that this 50 MW is the total heat flow into the contributing area for the Metolius headwaters spring. This approximation is consistent with the near-zero near-surface heat flow and isothermal shallow temperature gradients high in the Cascade Range [e.g., *Ingebritsen et al.*, 1989]. The background geothermal heat flux in the central high Cascades is about 130 mW/m^2 [e.g., *Blackwell et al.*, 1982], implying that the Metolius headwater spring discharges the total heat flow/geothermal heat flux from an area of approximately 400 km^2. There is no independent constraint on this estimate, though a 400 km^2 area is consistent with the topography and surface drainage patterns.

In contrast to springs such as the Metolius headwaters that discharge water with several degrees of geothermal warming, several other springs discharge water that shows no evidence of geothermal warming, even though the background heat flux in the basin varies by less than a factor of two [e.g., *Blackwell et al.*, 1990; *Ingebritsen et al.*, 1994]. Not only does this imply that these springs discharge groundwater that has followed shallow flow paths, the absence of geothermal warming also requires that deeper flow paths exist along which groundwater flow is rapid enough to advectively remove all the geothermal heat [*Manga*, 1998].

Another potentially sensitive means of identifying deeply circulating groundwater in volcanically active regions is to measure the carbon isotope content of groundwater [e.g., *Rose et al.*, 1996]. Carbon isotopes are useful for this purpose because the various sources of dissolved inorganic carbon (DIC) in groundwater (e.g., soil gases, the atmosphere, dissolution of carbonates, magmatically-derived gases) have distinct and identifiable relative abundances of carbon isotopes. In particular, there are three isotopes of carbon, of which ^{12}C and ^{13}C are stable, and ^{14}C is radioactive with a half-life of 5,730 years. Because magmatically-derived carbon has been sequestered for millions of years, it will not contain ^{14}C. Figure 12 shows the isotopic composition of the sources of DIC in groundwater in the Oregon Cascades [based on *Rose and Davisson*, 1996] assuming there are only three end members: magmatically-derived carbon, DIC equilibrated with the atmosphere, and DIC equilibrated with soil CO_2. Figure 12 also shows the carbon isotope content of spring waters measured by *James et al.* [1999]. The carbon

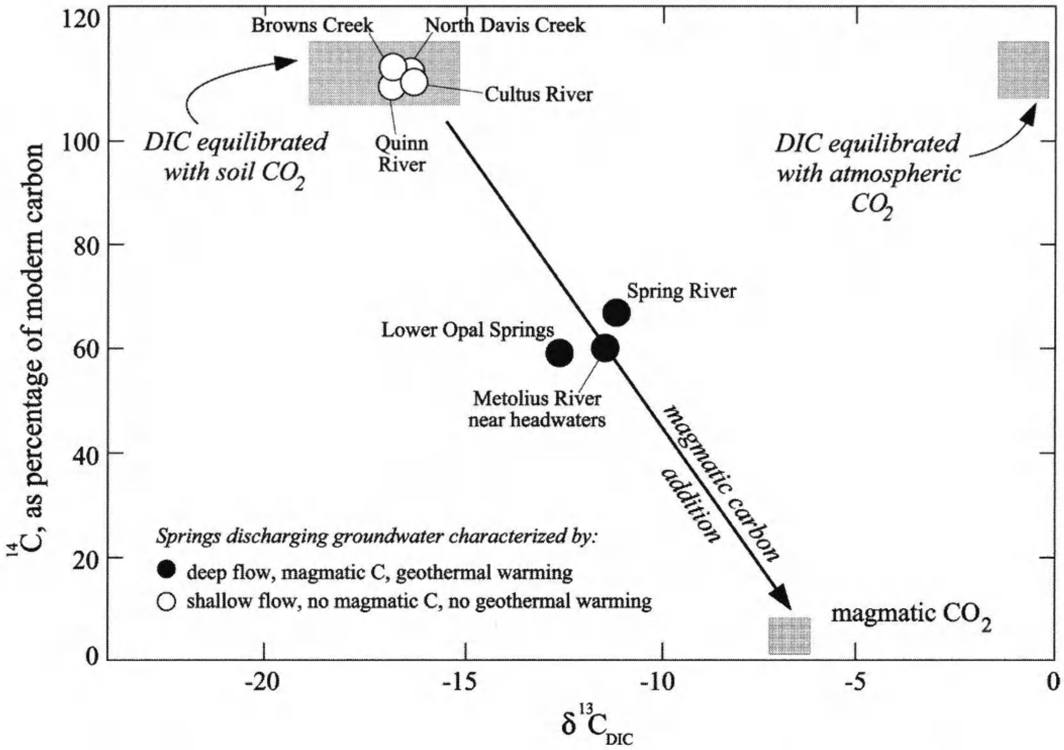

Figure 12. Plot of ^{14}C (as a percentage of modern carbon - pmc) versus $\delta^{13}C$ for spring waters. The three shaded boxes indicate three end-member isotopic compositions: dissolved inorganic carbon (DIC) equilibrated with soil CO_2, DIC equilibrated with the atmosphere, and carbon derived from a magmatic source. The magmatic source is based on *Rose and Davisson* [1996] and is similar to the magmatic source inferred elsewhere in the western U.S. [e.g., *Shevenell and Goff*, 1993; *Sorey et al.*, 1998] and in volcanic arcs [*Sano and Marty*, 1995].

isotope content of springs that show no evidence of geothermal warming is identical to groundwater equilibrated with soil CO_2. In contrast, the springs that show evidence of significant geothermal warming also have low ^{14}C abundances, implying that magmatically-derived carbon has been added to the water. Additionally, the intrusion rate of magmas required to produce the heat flow anomaly in the Oregon Cascades [*Ingebritsen et al.*, 1989] is consistent with the intrusion rate required to produce the measured magmatic carbon flux [*James et al.*, 1999].

Aging of the groundwater (to several thousand years) to produce low measured ^{14}C abundances is unlikely given the short mean residence times of the water, which probably range from years to hundreds of years (see next subsection). There are, however, other possible explanations for the low ^{14}C measurements, including dissolution of carbonates at depth (hundreds of meters) and methanogenesis of organic carbon in sedimentary interbeds. A direct magmatic origin is further supported, however, by the presence of magmatically-derived helium-3 (^3He) in the Metolius River headwaters, which also has a low ^{14}C abundance (see following subsection). Moreover, the ratio of magmatic CO_2 to magmatic ^3He in the Metolius River is within the range, but also near the upper limit of the range, of $CO_2/^3He$ ratios in fumarole gases from volcanic arcs [e.g., *Sano and Williams*, 1996; *Yamamoto et al.*, 2001].

Groundwater Flow Rates

The local rate of groundwater flow can be estimated from measured transmissivities, head gradients, and geometric information (e.g., aquifer thickness). A regional estimate can be obtained from mass balance considerations; that is, the mean residence time can be defined as the volume of water in the aquifer divided by the volume discharged per unit time. As an example, we again consider the groundwater system that discharges at the head of the Metolius River. Assuming a mean aquifer thickness of 300 m, a porosity of 10%, a discharge of 3.1 m^3/s, and a contributing area of 400 km^2 (see previous section), we obtain a mean residence time of 120 years.

Whereas the discharge rate (equivalent to the total recharge rate when the change in storage can be neglected) may be known, few data are available with which to reliably estimate aquifer volumes. For water ages in the range of years to several decades, such as we might expect in parts of the Deschutes River basin based on mass balance considerations, the isotopic tracer tritium (radiogenic hydrogen with a half life of 12.4 years) is often used to estimate residence times. At the Metolius River headwaters, *James et al.* [2000] measured a tritium concentration of 4.0 tritium units (TU). Assuming an exponential distribution of transit times for the water flowing through the groundwater system, a concentration of 4 TU is compatible with the mean residence time of 120 years estimated from mass balance considerations [see Figure 10 in *Manga*, 1999]. The lower tritium concentration of 0.8 TU at Lower Opal Springs [*Caldwell*, 1998] implies even longer mean residence times, possibly a few hundred years. It must be emphasized, however, that the interpretation of tracer measurements is complicated by the mixing and dispersion of water recharged at different times, and inferred ages are model dependent [*Maloszewski and Zuber*, 1982].

A better estimate of mean residence times can be made by also measuring the decay product of tritium, helium-3 [e.g., *Poreda et al.*, 1988]. The measured concentration of other noble gases must first be used to determine the amount of ^{3}He in the water that originated from the atmosphere. Unfortunately, in some springs, such as the Metolius River headwaters, there is also excess ^{4}He (after subtracting the atmospheric contribution) in the spring water, implying a contribution of magmatically-derived He (which contains both ^{3}He and ^{4}He) and also possibly a crustal source of He (^{4}He produced from the decay of uranium and thorium). The presence of magmatic He is expected where there appears to be magmatic carbon and geothermal heat in the spring water (Figures 11 and 12). Because we cannot reliably quantify the amount of added ^{3}He, we cannot determine the amount of ^{3}He in the groundwater produced by the decay of tritium. For some of the springs at the margin of the Cascade Range, however, the groundwater contains only atmospherically derived ^{4}He, implying that all the excess ^{3}He is produced by the decay of tritium. The mean residence times for these springs can thus be estimated, with values of 2.1 and 2.5 years for the Quinn River and Cultus River, respectively [*James et al.*, 2000]. Because of the mixing of water recharged at different times and places, these residence times are best thought of as "apparent ^{3}He/^{3}H ages." For reasonable mixing models, such as one with an exponential distribution of residence times, apparent ^{3}He/^{3}H ages will be similar to the apparent ages for residence times of a few years [e.g., *Aeschbach-Hertig et al.*, 1998; *Manga*, 1999]. Residence times of a couple of years are much lower than those for the springs at lower elevation such as the Metolius headwaters and Lower Opal Springs, springs that we have shown involve deeply circulating groundwater and long flow paths. Short residence times of two years require a small mean aquifer thickness—about 20 meters—and rapid flow rates. The length of the groundwater system feeding these springs is approximately 10 km (from the source of the springs to the crest of the Cascade Range), implying interstitial velocities of kilometers/year!

Summary

The distribution of hydraulic heads is consistent with groundwater being recharged primarily at high elevations in the Cascade Range and then discharged along the margin of the Cascade Range and near the confluence of the Deschutes, Crooked, and Metolius Rivers. The regional groundwater system involves deep circulation, thick aquifers (hundreds of meters), and long flow paths (tens of kilometers).

We can also draw several additional conclusions about the groundwater system from measurements made at large springs, in particular from estimates of residence times, the amount of geothermal warming, and the amount of magmatically-derived carbon and helium in the water. The springs at the margin of the Cascade Range discharge rapidly flowing groundwater from shallow groundwater flow paths. In contrast, the water from large springs at lower elevations, and the groundwater discharged near the confluence of the Crooked and Deschutes Rivers, travels through much thicker aquifers and has much longer mean residence times. Groundwater following these deeper flow paths is also recharged primarily at high elevation in the Cascade Range and circulates deeply and rapidly enough to remove most of the geothermal heat and magmatically-derived volatiles.

KEY FACTORS INFLUENCING THE REGIONAL HYDROLOGY AND STABILITY OF STREAMFLOW

The unusually stable flow of the Deschutes River is due to the large proportion of flow supplied by groundwater, estimated to be approximately 80% of the mean annual flow at the mouth. This generality is not sufficient, however, to explain its distinctive behavior. For example, why is it that groundwater discharge to the Deschutes River shows so little variation as compared to recharge, which is highly seasonal and can vary by an order of magnitude from year to year? To understand the remarkable character of the Deschutes River, we need to understand certain key aspects of the regional groundwater system that supports its flow.

First, groundwater flow paths exist at a variety of scales in the upper Deschutes River basin. Groundwater feeding high mountain springs follows short, relatively shallow flow paths. Such systems are likely to exhibit substantial temporal variations in discharge. Groundwater discharging to spring-fed streams on the margin of the Cascade Range follows intermediate length flow paths. Seasonal and interannual variations of such systems are smaller than for more local systems, and have been shown to be inversely proportional to the length of the flow paths [*Manga*, 1997]. A substantial part of the groundwater flow in the basin follows deep regional flow paths, often exceeding several tens of kilometers in length. Spring systems fed by these regional flow paths, such as Opal Springs, have very stable flows and are critical to the stability of the flow of the river. The two aspects of the regional groundwater flow system that allow the long flow paths are its large thickness (several hundred meters) and lateral extent. A single regional aquifer system extends from the principal recharge area in the Cascade Range to regional discharge areas near the confluence of the Deschutes, Crooked, and Metolius Rivers. Without these long, regional-scale groundwater flow paths, groundwater discharge would exhibit larger temporal variations.

Second, the high permeability of the young volcanic rocks and soils and the lack of an integrated drainage system over much of the basin promote groundwater recharge. The high near-surface permeability allows a large proportion of the annual snowmelt in the Cascade Range to percolate to the saturated zone. This greatly reduces the annual peak discharge related to the runoff of snowmelt commonly observed in other basins. This aspect of the basin also influences partitioning between runoff and groundwater recharge at the time scales of individual storms. Precipitation from individual storms will rapidly infiltrate and will not run off in most of the upper Deschutes River basin underlain by Pliocene and younger rocks.

A third factor contributing to the stable flow of the river is the ability of the regional groundwater system to accommodate large changes in groundwater storage without large and immediate variations in groundwater discharge. The heterogeneous assemblage of young volcanic deposits in the upper Deschutes River basin behave collectively as an unconfined or poorly confined aquifer system. Seasonal and interannual variations in recharge cause changes in storage in the aquifer system that are accommodated by changes in water-level elevations. Decadal fluctuations in the elevation of the water table exceed 7 m in and near the Cascade Range and are close to 3 m near Redmond [*Gannett et al.*, 2001]. Changes in groundwater discharge due to these variations in groundwater-level elevations are small because the groundwater and surface water systems are effectively uncoupled in most of the upper Deschutes River basin, from south of Bend to the major groundwater discharge area near the confluence of the Deschutes and Crooked Rivers. Groundwater lies tens to hundreds of meters below river level over most of the area between the city of Sisters and the confluence area. Similar conditions exist on the flanks of Newberry Volcano and in the High Lava Plains east of Bend. This large unsaturated zone between the groundwater system and streams allows groundwater elevation to change without causing large immediate changes in groundwater discharge. This is in contrast to areas, such as the Willamette Valley, where groundwater elevations are close to land surface. In these areas, as the water table rises in response to increased groundwater recharge, it quickly intersects a network of intermittent and perennial streams resulting in rapid increases in discharge.

It is not surprising, then, that the rain-on-snow events in 1964 and 1996 that produced widespread and catastrophic flooding in the lower Deschutes River basin and Willamette River Basin, had modest effects on streamflow in the upper Deschutes River basin. The large infiltration capacity and size of the groundwater system effectively damp discharge variations, making large meteorologically-induced floods uncommon.

Acknowledgments. Studies in the Deschutes River basin by M. Gannett and K. Lite were funded by the U.S. Geological Survey, the Oregon Water Resources Department, the Cities of Bend, Redmond, and Sisters, Deschutes and Jefferson Counties, and the Confederated Tribes of the Warm Springs Reservation of Oregon. M. Manga's studies were supported by the National Science Foundation. The authors thank Bob Main, Kyle Gorman, Larry Chitwood, Rod Caldwell, Tim Rose, Bryant Hudson, John Southon, Steve Hinkle, Martha Scholl, Steve Ingebritsen, and Liz James for reviews, discussions, ideas, field assistance, and sample analysis.

REFERENCES

Aeschbach-Hertig, W., P. Schlosser, M. Stute, et al., A ^{3}H/^{3}He study of ground water flow in a fractured bedrock aquifer, *Ground Water, 34*, 661-670, 1998.

Bauer, H. H., and J. J. Vaccaro, Documentation of a deep percolation model for estimating ground-water recharge, *U.S. Geol. Surv. Open-File Rep. 86-536*, 180 pp., 1987.

Blackwell, D. D., Thermal results of the Santiam Pass 77-24 drill hole, in *Geology and geothermal resources of the Santiam Pass area of the Oregon Cascade Range, Deschutes, Jefferson, and Linn Counties, Oregon, Oregon Dept. Geol. Min. Ind. Open-File Rep. O-92-3*, edited by B. E. Hill, pp. 37-52, 1992.

Blackwell, D. D., R. G. Bowen, D. A. Hull, J. Riccio, and J. L. Steele, Heat flow, arc volcanism, and subduction in northern Oregon, *J. Geophys. Res.*, *87*, 8735-8754,1982.

Blackwell, D. D., J. L. Steele, M. K. Frohme, et al., Heat flow in the Oregon Cascade Range and its correlation with regional gravity, Curie point depths, and geology, *J. Geophys. Res.*, *95*, 19,475-19,493, 1990.

Bolke, E. L., and A. Laenen, Ground-water inflow to the Deschutes River near the Warm Springs Indian Reservation, Oregon, August 1985, *U.S. Geol. Surv. Water Resour. Inv. Rep. 88-4184*, 18 pp., 1989.

Boyd, T.G., Groundwater recharge of the middle Deschutes Basin, Oregon, M.Sc. thesis, Portland State University, Portland, OR, 86 pp., 1996.

Caldwell, R. R., Chemical study of regional groundwater flow and groundwater/surface-water interaction in the upper Deschutes Basin, Oregon, *U.S. Geol. Surv. Water Resour. Inv. Rep. 97-4233*, 49 pp., 1998.

Forster, C., and L. Smith, The influence of groundwater on thermal regimes in mountainous terrain: A model study, *J. Geophys. Res.*, *94*, 9439-9451, 1989.

Friedman, I., G. I. Smith, J. D. Gleason, A. Warden, and J. M. Harris, Stable isotope composition of waters in southeastern California. 1. Modern precipitation, *J. Geophys. Res.*, *97*, 5795-5812, 1992.

Gannett, M. W., and K. E. Barger, Volcanic stratigraphy and secondary mineralization of USGS Pucci geothermal test well, Mount Hood, Oregon, *U.S. Geol. Surv. Open-File Rep. 81-1330*, 26 pp., 1981.

Gannett, M. W., K. E. Lite, Jr., D. S. Morgan, and C. A. Collins, Ground-water hydrology of the upper Deschutes Basin, Oregon, *U.S. Geol. Surv. Water Resour. Inv. Rep. 00-4162*, 77 pp., 2001.

Henshaw, F. F., J. H. Lewis, and E. J. McCaustland, Deschutes River, Oregon and its utilization, *U.S. Geol. Surv. Water-Supp. Pap. 344*, 200 pp., 1914.

Ingebritsen, S. E., D. R. Sherrod, and R. H. Mariner, Heat flow and hydrothermal circulation in Cascade Range, north-central Oregon, *Science*, *243*, 1458-1462,1989.

Ingebritsen, S. E., D. R. Sherrod, and R. H. Mariner, Rates and patterns of groundwater flow in the Cascade Range volcanic arc, and the effect on subsurface temperatures, *J. Geophys. Res.*, *97*, 4,599-4,627, 1992.

Ingebritsen, S. E., R. H. Mariner, and D. R. Sherrod, Hydrothermal systems of the Cascade Range, North-Central Oregon, *U.S. Geol. Surv. Prof. Pap. 1044-L*, 86 pp., 1994.

James, E. R., Isotope tracers and regional-scale groundwater flow: Application to the Oregon Cascades, M.Sc. thesis, University of Oregon, Eugene, OR. 150 pp., 1999.

James, E. R., M. Manga, T. P. Rose, and G. B. Hudson, The use of temperature and the isotopes of O, H, C and noble gases to determine the pattern and spatial extent of groundwater flow, *J. Hydrol.*, *237*, 100-112, 2000.

James, E. R., M. Manga, and T. P. Rose, CO_2 degassing in the Oregon Cascades, *Geology*, *27*, 823-826, 1999.

Keith, T. E. C., and K. E. Barger, Petrology and hydrothermal mineralogy of U.S. Geological Survey Newberry 2 drill core from Newberry Caldera, Oregon, *J. Geophys. Res.*, *93*, 10,174-10,190, 1988.

Keith, T. E. C., and K. E. Barger, Hydrothermal mineralogy of core from geothermal drill holes at Newberry Volcano, Oregon, *U.S. Geol. Surv. Prof. Pap. 1578*, 92 pp., 1999.

MacLeod, N. S., D. R. Sherrod, L. A. Chitwood, and R. A. Jensen, Geologic map of Newberry Volcano, Deschutes, Klamath, and Lake Counties, Oregon, *U.S. Geol. Surv. Misc. Inv. Ser. Map I-2455*, 23 pp., 2 sheets, 1995.

Maloszewski, P., and A. Zuber, Determining the turnover time of groundwater systems with the aid of environmental tracers. 1. Models and their applicability, *J. Hydrol.*, *57*, 207-231, 1982.

Manga, M., Hydrology of spring-dominated streams in the Oregon Cascades, *Water Resour. Res.*, *32*, 2,435-2,439, 1996.

Manga, M., A model for discharge in spring-dominated streams and implications for the transmissivity and recharge of Quaternary volcanics in the Oregon Cascades, *Water Resour. Res.*, *33*, 1813-1822, 1997.

Manga, M., Advective heat transport by low-temperature discharge in the Oregon Cascades. *Geology*, *26*, 799-802, 1998.

Manga, M., On the timescales characterizing groundwater discharge at springs, *J. Hydrol.*, *219*, 56-69, 1999.

Manga, M., Using springs to study groundwater flow and active geologic processes, *Ann. Rev. Earth Planet. Sci.*, *29*, 203-230, 2001.

Manning, J. C., *Applied principles of hydrology (3rd ed.)*, 276 pp., Prentice Hall, New Jersey, 1992.

Meinzer, O. E., Large springs in the United States, *U.S. Geol. Surv. Water-Supp. Pap. 557*, 94 pp., 1927.

Moffatt, R. L., R. E. Wellman, and J. M. Gordon, Statistical summaries of streamflow data in Oregon: Vol. 1. Monthly and annual streamflow, and flow-duration values, *U.S. Geol. Surv. Open-File Rep. 90-118*, 413 pp., 1990.

Naftz, D. L., R. W. Klusman, R. L. Michel, et al., Little Ice Age evidence from a south-central North American ice core, USA, *Arctic Alp. Res.*, *28*, 35-41, 1996.

Orr, E. L., W. N. Orr, and E. M. Baldwin, *Geology of Oregon (4th ed.)*, 254 pp., Kendall/Hunt, Dubuque, Iowa, 1992.

Poreda, R. J., T. E. Cerling, and D. K. Solomon, Tritium and helium isotopes as hydrologic tracers in a shallow unconfined aquifer, *J. Hydrol.*, *103*, 1-9, 1988.

Robinson, P. T., G. F. Brem, and E. H. McKee, The John Day Formation of Oregon: a distal record of early Cascade volcanism, *Geology*, *12*, 229-232, 1984.

Robison, J. H., L. S. Forcella, and M. W. Gannett, Data from geothermal test wells near Mt. Hood, Oregon, *U.S. Geol. Surv. Open-File Rep. 81-1002*, 24 pp., 1981.

Rose, T. P., and M. L. Davisson, Radiocarbon in hydrologic systems containing dissolved magmatic carbon dioxide, *Science*, *273*, 1367-1370, 1996.

Rose, T. P., M. L. Davisson, and R. E. Criss, Isotope hydrology of voluminous cold springs in fractured rock from an active volcanic region, *J. Hydrol.*, *179*, 207-236, 1996.

Russell, I. C., Geology and water resources of central Oregon, *U.S. Geol. Surv. Bull. 252*, 138 pp., 1905.

Sano, Y., and B. Marty, Origin of carbon in fumarolic gas from island arcs, *Chem. Geol.*, *119*, 265-274, 1995.

Sano, Y., and S. N. Williams, Fluxes of mantle and subducted carbon along convergent plate boundaries, *Geophys. Res. Lett.*, *23*, 2749-2752, 1996.

Sherrod, D. R., and J. G. Smith, Geologic map of upper Eocene to Holocene volcanic and related rocks of the Cascade Range, Oregon, *U.S. Geol. Surv. Misc. Inv. Ser. Map I-2569*, 17 pp., 2 sheets, 2000.

Sherrod, D. R., E. M. Taylor, M. L. Ferns, et al., Geologic map of the Bend 30- by 60-minute quadrangle, Deschutes, Jefferson, Lane, Linn, and Crook Counties, central Oregon, *U.S. Geol. Surv. Misc. Inv. Ser. Map I-2683*, in press.

Shevenell, L., and F. Goff, Addition of magmatic volatiles into the hot spring waters of Loowit Canyon, Mount St. Helens, Washington, USA, *Bull. Volcanol.*, *55*, 489-503, 1993.

Smith, G. A., Stratigraphy, sedimentology, and petrology of the Neogene rocks in the Deschutes basin, central Oregon — A record of continental-margin volcanism and its influence on fluvial sedimentation in an arc-adjacent basin, Ph.D. dissertation, Oregon State University, Corvallis, OR, 464 pp., 1986a.

Smith, G. A., Simtustus Formation: Paleogeographic and stratigraphic significance of a newly defined Miocene unit in the Deschutes basin, central Oregon, *Oregon Geol. 48*, 63-72, 1986b.

Smith, G. A., Geologic map of the Seekseequa Junction and a portion of the Metolius Bench Quadrangles, Jefferson County, Oregon, *Oregon Dept. Geol. Min. Ind. Geol. Map Ser. GMS-44*, 1 sheet, 1987a.

Smith, G. A., Geologic map of the Madras West and Madras East Quadrangles, Jefferson County, Oregon, *Oregon Dept. Geol. Min. Ind. Geol. Map Ser. GMS-45*, 1 sheet, 1987b.

Sorey, M. L., W. C. Evans, B. M. Kennedy, C. D. Farra, L. J. Hainsworth, and B. Hausback, Carbon dioxide and helium emissions from a reservoir of magmatic gas beneath Mammoth Mountain, California, *J. Geophys. Res.*, *103*, 15,303-15,323, 1998.

Swanberg, C. A., W. C. Walkey, and J. Combs, Core hole drilling and the "rain curtain" phenomenon at Newberry Volcano, Oregon, *J. Geophys. Res.*, *93*, 10,163-10,173, 1988.

Taniguchi, M., Evaluation of vertical groundwater fluxes and thermal properties of aquifers based on transient temperature-depth profiles, *Water Resour. Res.*, *29*, 2021-2026, 1993.

Taylor, G. H., *Normal annual precipitation, State of Oregon*, Oregon Climate Service, Oregon State University, Corvallis, OR, 1 sheet, 1993.

U. S. Geological Survey, Compilation of records of surface waters of the United States through September 1950, *U.S. Geol. Surv. Water-Supp. Pap. 1318*, 550 pp., 1958.

Walker, G. W., and N. S. MacLeod, *Geologic map of Oregon*, U.S. Geol. Surv., 2 sheets, 1991.

Yamamoto, J., M. Watanabe, Y. Nozaki, and Y. Sano, Helium and carbon isotopes in fluorites: Implications for mantle carbon contribution in an ancient subduction zone, *J. Volcanol. Geotherm. Res.*, *107*, 19-26, 2001.

Marshall W. Gannett, U.S. Geological Survey, 10615 SE Cherry Blossom Drive, Portland, OR 97216

Kenneth E. Lite, Jr., Oregon Water Resources Department, 158 12th Street NE, Salem, OR 97310

Michael Manga, Department of Earth and Planetary Science, University of California, Berkeley, CA 94720

Controls on the Distribution and Life History of Fish Populations in the Deschutes River: Geology, Hydrology, and Dams

Christian E. Zimmerman

U.S. Geological Survey, Western Fisheries Research Center, Seattle, Washington

Donald E. Ratliff

Portland General Electric, Madras, Oregon

In the Deschutes River basin, geology and hydrology exert first-order controls on salmonid fish populations through two broad mechanisms. As studies of the distribution of chinook salmon (*Oncorhynchus tshawytscha*), rainbow trout/steelhead (*O. mykiss*), and bull trout (*Salvelinus confluentus*) illustrate, the geologic history of the Deschutes River basin controls the hydrologic, sediment transport, and temperature regimes of the watershed, establishing the environmental niches and gradients to which fish species have adapted. Geological disturbances, such as floods, volcanism, and tectonism, have generated landforms that define habitat areas and constrain the interactions among fish species and populations. Specific events, such as an exceptionally large flood about 4400 years ago, may have created persistent habitat conditions partly responsible for the robust rainbow trout/steelhead fishery in the lower Deschutes River. Existing blockages to anadromy resulting from specific geologic events are clearly defined for sea-going salmonid species such as chinook salmon, steelhead, and sockeye salmon (*O. nerka*). Evidence for prehistoric blockages by ancient lava flows and landslides is more speculative but consistent with the present distribution of certain life history forms and genetic groups. Dams influence fish populations in manners similar to both types of broad geologic controls. Although changes to environmental gradients, such as temperature, substrate, and flow, often result downstream of impoundments, these habitat characteristics have apparently been little affected by the Pelton-Round Butte dam complex. The major effect of the dams on native fish populations has been to block fish passage, thus limiting anadromy and isolating fish populations above and below the dam complex.

INTRODUCTION

Fish have long been a significant focus of interest and research in the Deschutes River watershed. As early as 1824, explorers with the Hudson's Bay Company reported the presence of Native American salmon weirs on the Crooked River and, in 1855, described abundant salmon in the Metolius River [*Nehlsen*, 1995]. By the late 1800's, the mouth of the Deschutes River was the site of intensive commercial fisheries [*Nehlsen*, 1995], and today, significant recreational and Native American fisheries exist throughout the watershed. Indeed, much of the research reported in this volume was prompted by concerns regarding the effects of the Pelton-Round Butte dam complex on downstream fish

A Peculiar River
Water Science and Application 7

10.1029/007WS05

habitat. In addition, proposals to reinstate fish passage around these facilities have propelled fishery scientists and managers into renewed efforts to understand life histories and interactions among the various fish species in the Deschutes River basin [*Lichatowich,* 1998].

The aim of this paper is to relate aspects of the historic and present distribution of fishes in the Deschutes River basin to geologic and physiographic conditions in the watershed, thus linking a key aspect of the basin's ecology to the geologic and hydrologic understanding described in the other papers in this volume. Furthermore, this perspective is relevant to current issues surrounding human disturbance of fishes in the basin, such as dam construction, which have parallels with geologic events and processes. We first propose a framework for understanding relations between geologic conditions and fish distribution, then support that framework with examples from our research and that of others on fish distribution, community structure, and population dynamics in the basin. We conclude by discussing the similarities and differences between geologic controls on fish distribution and human influences on fishes in the basin, such as dam construction and management, and how this understanding might be pertinent for future management of fish resources in the Deschutes River basin. Our examples derive from studies of fish of the family Salmonidae, by far the best studied species in the basin due to their regional economic and cultural importance.

SALMONIDS OF THE DESCHUTES RIVER BASIN

Available literature, interviews with biologists, and a survey of cataloged specimens show that at least twenty-six species of fish inhabit the Deschutes River basin (Table 1), seven of which are of the family Salmonidae, collectively referred to as "salmonids". These include native salmon and trout: chinook salmon (*Oncorhynchus tshawytscha*), sockeye salmon/kokanee (*O. nerka*), rainbow trout/steelhead (*O. mykiss*), and bull trout (*Salvelinus confluentus*). Salmonid species introduced to the basin from other regions include: brown trout (*Salmo trutta*), Atlantic salmon (*S. salar*), and brook trout (*Salvelinus fontinalis*). Many species of salmonids in the Deschutes River can be further subdivided into distinct stocks or life-history forms based on differences in genetic, morphologic, and ecological characteristics.

Salmonids have a variety of life history characteristics reflecting diverse adaptations to landscape conditions. One characteristic that varies among and within fish species in the Deschutes River basin is migratory behavior. Life history forms include anadromous, fluvial, adfluvial, and resident fish. Anadromous species include chinook salmon, steelhead (a form of rainbow trout), and sockeye salmon. Anadromous species spawn in freshwater, and the juveniles migrate to the ocean before returning to freshwater as mature adults (Figure 1). Fluvial migration, typical of some rainbow trout and bull trout in the Deschutes River, is between larger rivers (such as the mainstem) and smaller tributaries. Migration to lakes for rearing is referred to as adfluvial migration and is observed in bull trout, kokanee (a freshwater form of sockeye salmon), and rainbow trout. Residency is observed in rainbow trout and describes fish that do not migrate between habitat types. Although resident fish do not migrate between habitat types, they often make long-distance movements within the same habitat [*Gowan et al.,* 1994].

All salmonids are substrate spawners. As a result, salmonid spawning and survival is directly related to substrate characteristics and the timing and frequency of bed-mobilizing flows and deposition. The female constructs a nest (or redd) in the gravel substrate by turning on her side and directing flow downward by arching her body. This action dislodges particles into the current and excavates a depression containing larger rocks. She then releases eggs into this depression as the male simultaneously releases sperm. The female then moves slightly upstream and digs another depression, displacing substrate material downstream that covers the previous depression and eggs. Each redd can contain several such egg pockets; the ultimate shape of the redd and its location serve to maximize downwelling and current through the egg pocket [*Chapman,* 1988; *Bjornn and Reiser,* 1991], which serves to bring oxygen to the eggs and remove metabolic wastes (Figure 2). Reduction in permeability following construction of the redd, due to the deposition of fine sediments, leads to decreased downwelling and can lead to lower survival of incubating eggs and embryos [*Chapman,* 1988].

Three species of salmonids, chinook, rainbow trout, and bull trout, have been particularly well studied in the Deschutes River basin because of their cultural significance, historic and modern importance as a food and recreational resource, and regional concerns regarding species preservation.

Chinook Salmon (Oncorhynchus tshawytscha)

Chinook salmon in the Deschutes River basin were and continue to be a mainstay of the cultural identity of Native Americans residing near the Deschutes River, especially in the northern part of the basin. In addition, management of wild chinook salmon in the Deschutes River basin is an important component of regional strategies to maintain viable populations in the Columbia River basin [*Lichatowich,* 1998]. Two separate populations of chinook

Table 1. Fish species present in the Deschutes River Basin.

Common Name	Scientific Name	Origin
Pacific lamprey	*Entosphenus tridentatus*	Native
Steehead/Rainbow trout	*Oncorhynchus mykiss*	Native
Chinook salmon	*Oncorhynchus tshawytscha*	Native
Sockeye salmon/ Kokanee	*Oncorhynchus nerka*	Native
Bull trout	*Salvelinus confluentus*	Native
Mountain whitefish	*Prosopium williamsoni*	Native
Shorthead sculpin	*Cottus confusus*	Native
Torrent sculpin	*Cottus rhotheus*	Native
Slimy sculpin	*Cottus cognatus*	Native
Mottled sculpin	*Cottus bairdi*	Native
Prickly sculpin	*Cottus asper*	Native
Longnose dace	*Rhinichthys cataractae*	Native
Speckled dace	*Rhinichthys osculus*	Native
Chiselmouth	*Acrocheilus alutaceus*	Native
Largescale sucker	*Catostomus macrocheilus*	Native
Bridgelip sucker	*Catostomus columbianus*	Native
Northern pikeminnow	*Ptychocheilus oregonensis*	Native
Redside shiner	*Richardsonius balteatus*	Native
Threespine stickleback	*Gasterosteus aculeatus*	Unknown
Brook trout	*Salvelinus fontinalis*	Introduced
Brown trout	*Salmo trutta*	Introduced
Atlantic salmon	*Salmo salar*	Introduced
Largemouth bass	*Micropterus salmoides*	Introduced
Smallmouth bass	*Micropterus dolomieu*	Introduced
Yellow perch	*Perca flavescens*	Introduced
Brown bullhead	*Ameiurus nebulosis*	Introduced

salmon have been defined in the Deschutes River basin on the basis of timing of adult migration from the ocean, age at out-migration of juveniles, and location of spawning [*Jonasson and Lindsay,* 1988; *Lindsay et al.,* 1989]. Fall chinook salmon (also known as "ocean-type" chinook salmon) typically spawn in mainstem reaches and the resulting progeny migrate to the ocean within a few months after emergence from the gravel [*Jonasson and Lindsay*, 1988; *Healey*, 1991]. Spring chinook salmon (or "stream-type" chinook salmon) spawn in headwater tributaries, and the juveniles remain in these streams for over a year before migrating to the ocean [*Lindsay et al.*, 1989; *Healey*, 1991]. Returning to their natal streams after about two or three years in the ocean, adult spring chinook salmon enter freshwater during the late spring and hold in cold pool habitats until the fall when they spawn. Fall chinook return to freshwater during the late summer or fall and spawn in October or November.

Spring chinook salmon historically spawned in the west side tributaries to the Deschutes River including the Warm Springs River, Shitike Creek, and the Metolius River (Figure 3). In the Deschutes River, Big Falls at River Mile (RM)[1] 132.2 was the upstream extent of spring chinook salmon [*Nehlsen*, 1995] (Figure 4). Anecdotal reports suggest that spring chinook salmon might have spawned in the Crooked River [*Nehlsen*, 1995]. At maturity, spring chinook are typically 60 to 90 cm long and attain weights of approximately 7 kg.

Fall chinook salmon are the largest salmonids in the Deschutes River basin, attaining lengths of 70 to 110 cm and

[1] Units given are metric except for locations, which are given as river miles (RM), or miles upstream from the river mouth as marked on USGS topographic maps. These values are close to, but not necessarily the same as, actual distances along the present channel. Fractional river miles given herein are based on interpolations between these published river miles.

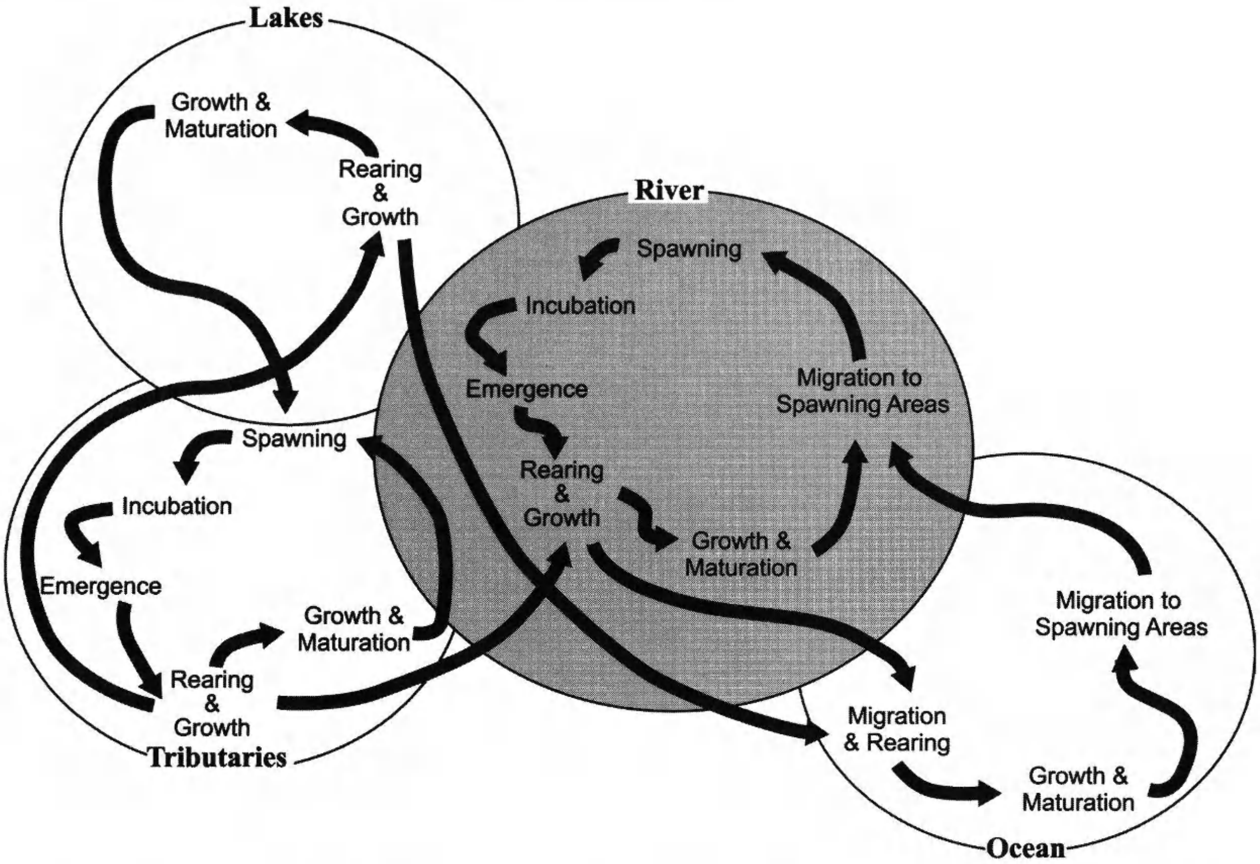

Figure 1. Conceptual model of life history events and migration across habitats by salmonids in the Deschutes River basin.

weights up to 14 kg. Fall chinook were historically found only downstream of Sherars Falls at RM 44 (Figure 5). A fish ladder was constructed at Sherars Falls in the 1920s and improved in the 1940s that allowed passage of fall chinook salmon at the relatively lower autumn flows [*Jonasson and Lindsay*, 1988; *Nehlsen*, 1995], which expanded the distribution of fall chinook salmon throughout the lower mainstem river to near the confluence of the Crooked, Deschutes, and Metolius Rivers [*Jonasson and Lindsay*, 1988; *Nehlsen*, 1995]. The Reregulating Dam at RM 100.1 is now the upstream boundary for both types of chinook salmon.

Rainbow Trout / Steelhead (Oncorhynchus mykiss)

Rainbow trout in the Deschutes River have two distinct life history forms. Anadromous rainbow trout, referred to as steelhead, spawn in the lower Deschutes River, and migrate as juveniles to the ocean, returning to natal streams after one to two years. At maturity, they are typically 60 to 70 cm long and attain weights of approximately 7 kg. Steelhead historically occupied the Deschutes River mainstem and tributaries upstream to Big Falls, and much of the Crooked River and its principal tributaries (Figure 6). Presently, upstream passage is blocked by the Pelton-Round Butte dam complex and steelhead are only found in the mainstem and tributaries downstream of the Reregulating Dam. Resident and fluvial rainbow trout spend their life in fresh water and are present throughout the Deschutes River basin in forty-six separate wild populations divided into three "gene conservation groups" [*ODFW*, 1995]. Resident rainbow trout are typically smaller than steelhead, attaining lengths of 20 to 40 cm and weights typically between 0.7 and 3 kg. Presently, resident and fluvial rainbow trout are sympatric with steelhead throughout the lower river, meaning that they spawn and rear in close proximity. Populations of resident rainbow trout are particularly strong in the lower mainstem Deschutes River, below the Pelton-Round Butte dam complex, where they are the basis of a robust recreational fishery [*Lichatowich,* 1998]

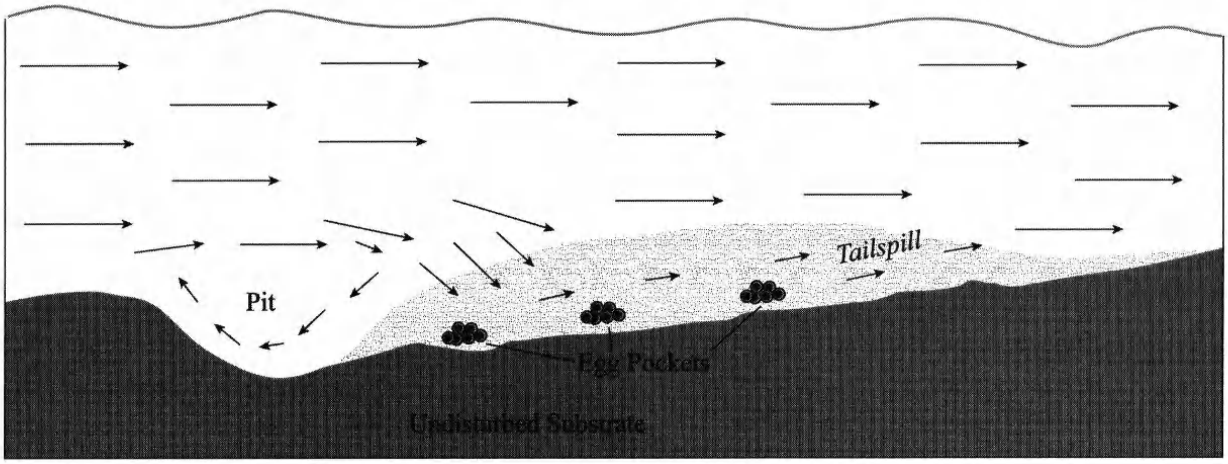

Figure 2. Longitudinal section of an idealized salmonid redd. Arrows indicate direction of water flow (after figures in *Chapman* [1988] and *Bjornn and Reiser* [1991]).

Bull Trout (Salvelinus confluentus)

Bull trout spend their lives in fresh water, migrating between small cold-water streams and larger rivers. At maturity, they are typically 40 to 70 cm long and attain weights of up to 14 kg. Bull trout were historically distributed along much of the mainstem Deschutes River, Metolius River, and lower Crooked River as well as in several high elevation tributaries to the lower Deschutes River in the Cascade Range (Figure 7). Their current distribution is restricted to the western portion of the basin. Formerly considered a "trash" fish and subject to bounties in the early part of the 20th century, the marked contraction of their distribution throughout their historic range has triggered significant concern regarding bull trout viability and has resulted in an "threatened" designation under the Endangered Species Act for much of the species' range in the intermountain west and Pacific Northwest.

GEOLOGIC CONTROLS ON FISH DISTRIBUTION AND POPULATION DYNAMICS

Geologic processes and conditions affect fish distribution and population dynamics in two distinct manners. Geologic events, the sequence of which constitutes the geologic history of a basin, affect fish by producing connections or barriers between watercourses and landscapes, shaping channel- and valley-bottom morphology, and by directly disturbing fish populations. In the Pacific Northwest, tectonic activity, volcanism, glaciation, and floods have likely played an important role in structuring fish communities throughout the Cenozoic Era [*McPhail and Lindsey*, 1986; *Reeves et al.*, 1998]. In addition to discrete geologic events, the present-day physical environment or "regime" of a watershed, which is ultimately a product of geologic history and climate, also controls the distribution, composition, and structure of fish communities and populations by forming environmental gradients of habitat conditions [*Li et al.*, 1987; *Mathews*, 1998]. Aspects of the physical regime important to fish include conditions of water flow (discharge, velocity, and daily, seasonal, annual, and longer-time-scale discharge fluctuations), water temperature, water chemistry, and the size distribution of the channel-bottom sediment and frequency of sediment transport. Understanding the present-day structure of fish communities, therefore, requires an appreciation of both the geologic history of a basin and the current conditions and geologic processes affecting the aquatic environment.

In the Deschutes River basin, as elsewhere, there are clear relations between fish and current habitat conditions such as flow, temperature and substrate composition. These relations can be readily analyzed in controlled field and laboratory experiments, and involve timescales conducive to human observation. Less apparent are relations between geologic history and modern fish distribution and behavior (aside from the role of modern and historic channel blockages), which are site specific, involve long timescales, and commonly depend on incomplete knowledge of regional and local geologic history. However, increased understanding of the role of geologic history in controlling fish distribution has emerged in recent years, as a result of the increased ability to track fish groups with genetic methods as well as from increased communication between geoscientists and biologists. The remainder of this paper describes

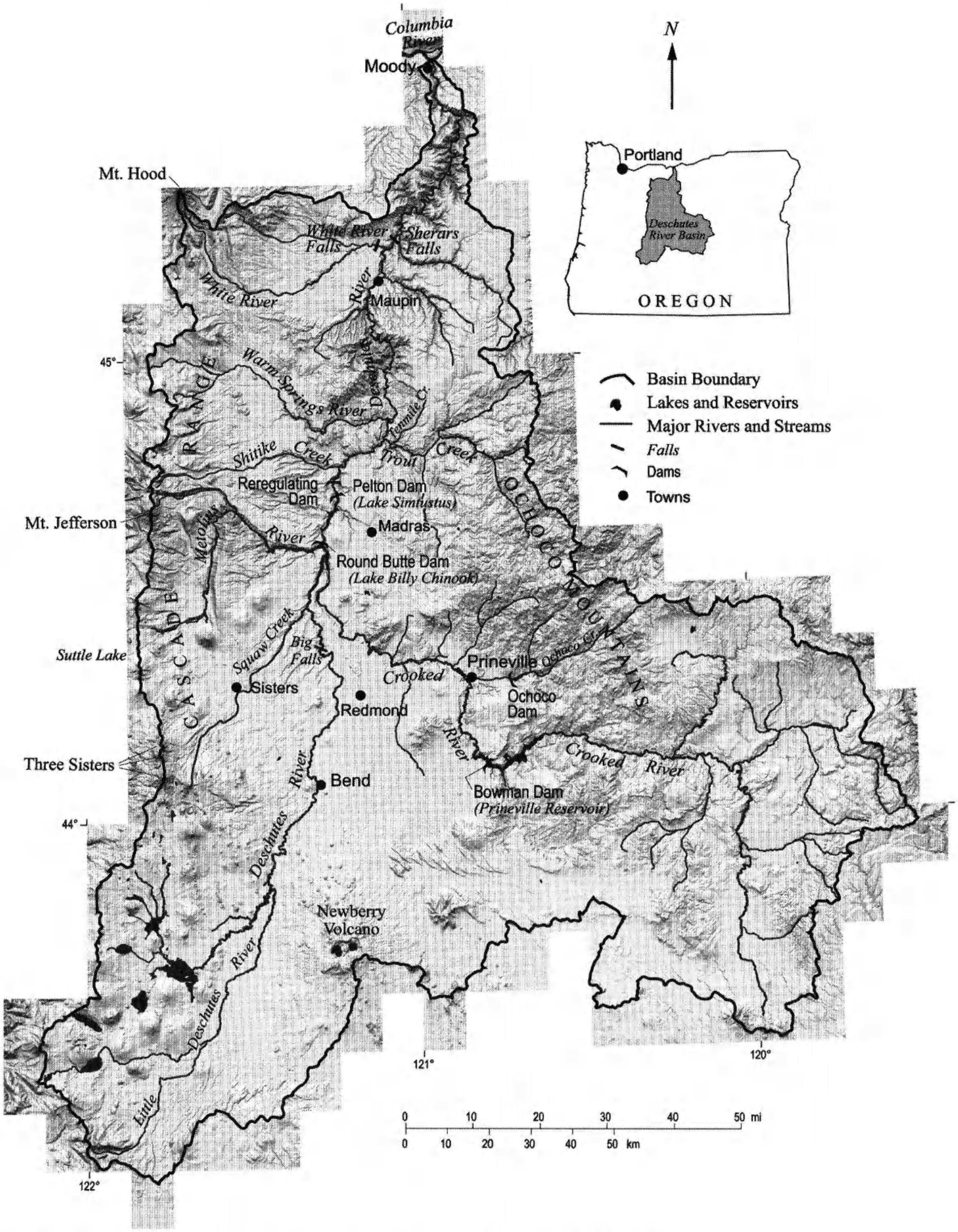

Figure 3. Map of Deschutes River basin, Oregon, with locations mentioned in the text.

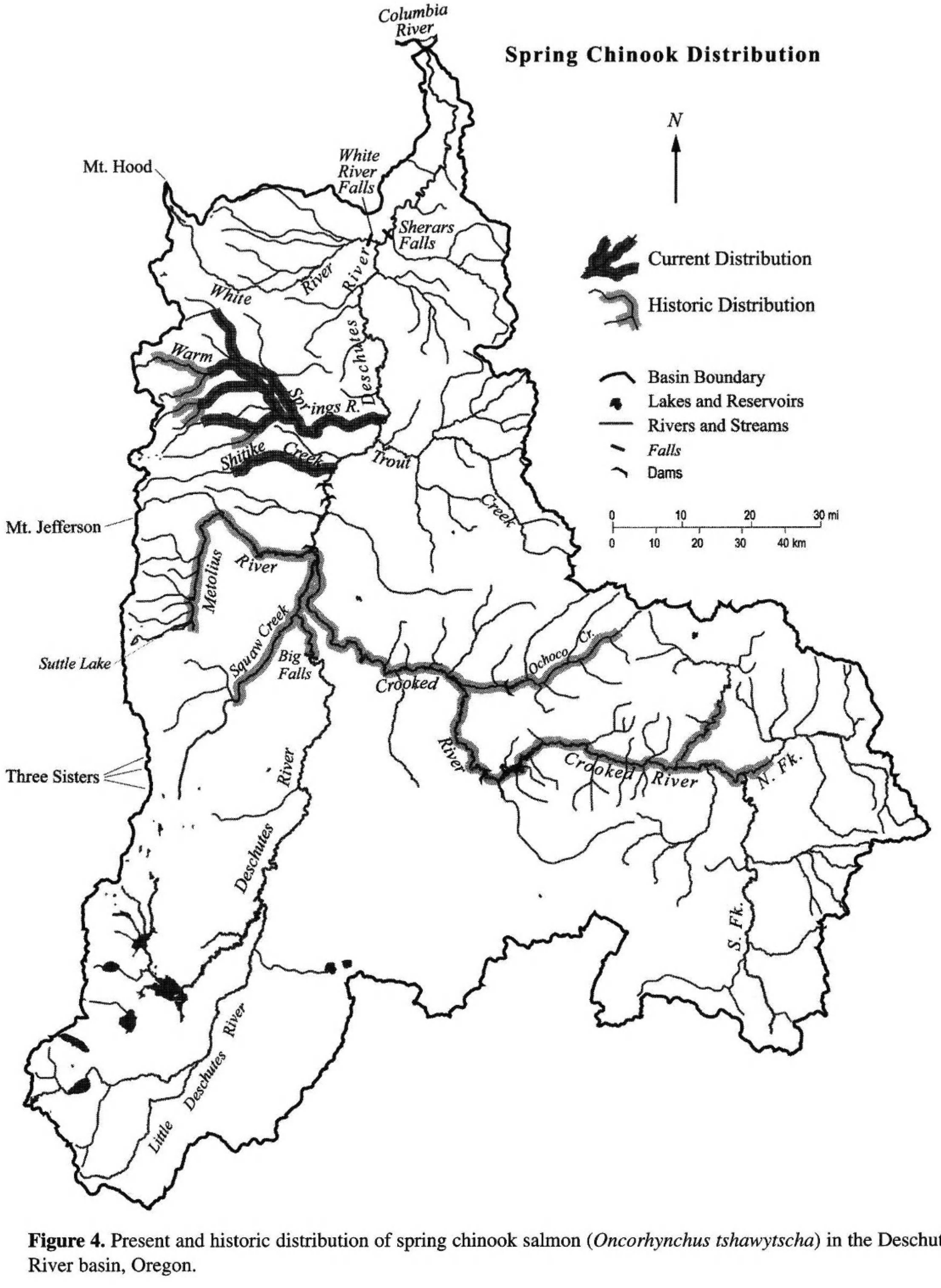

Figure 4. Present and historic distribution of spring chinook salmon (*Oncorhynchus tshawytscha*) in the Deschutes River basin, Oregon.

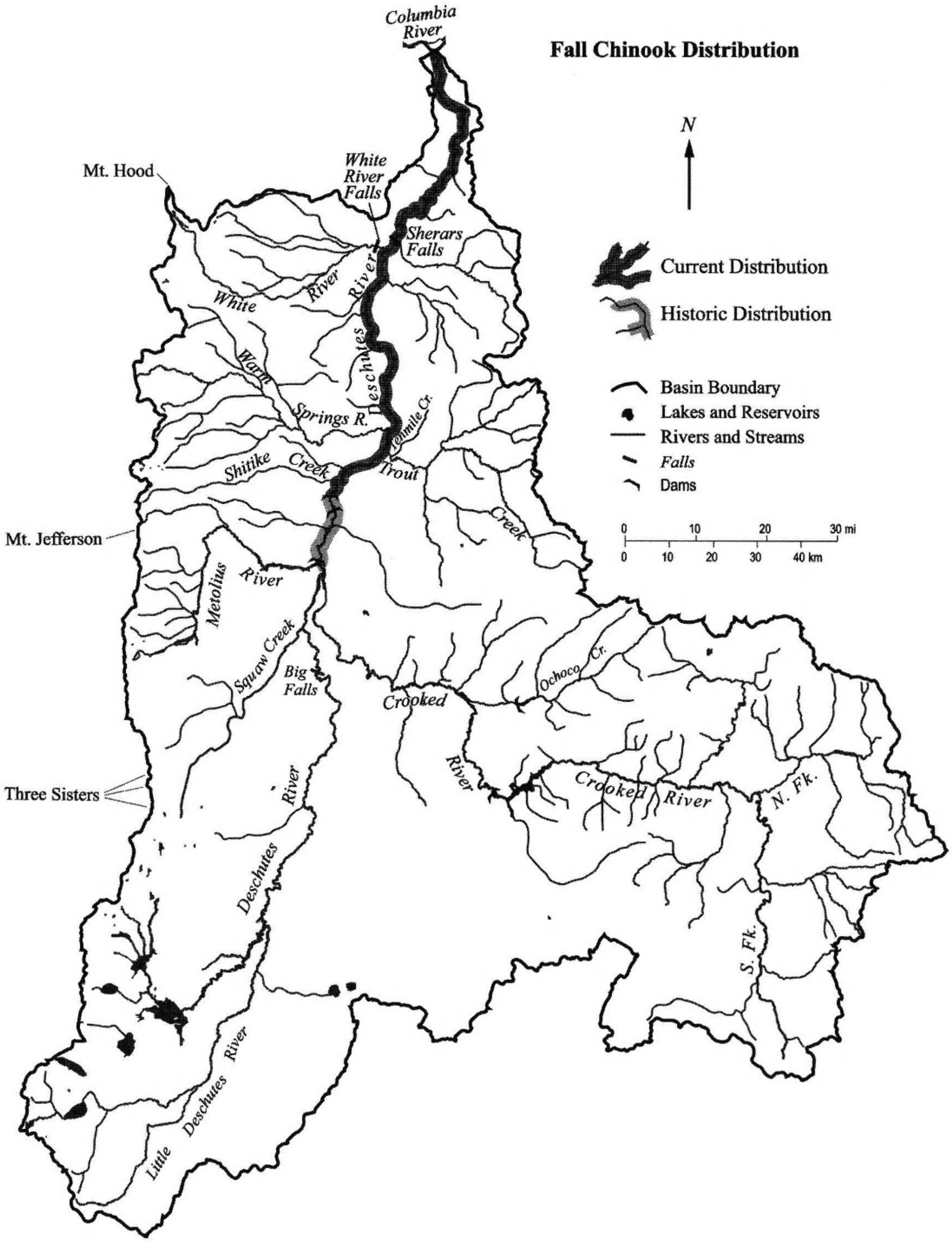

Figure 5. Present and historic distribution of fall chinook salmon (*Oncorhynchus tshawytscha*) in the Deschutes River basin, Oregon.

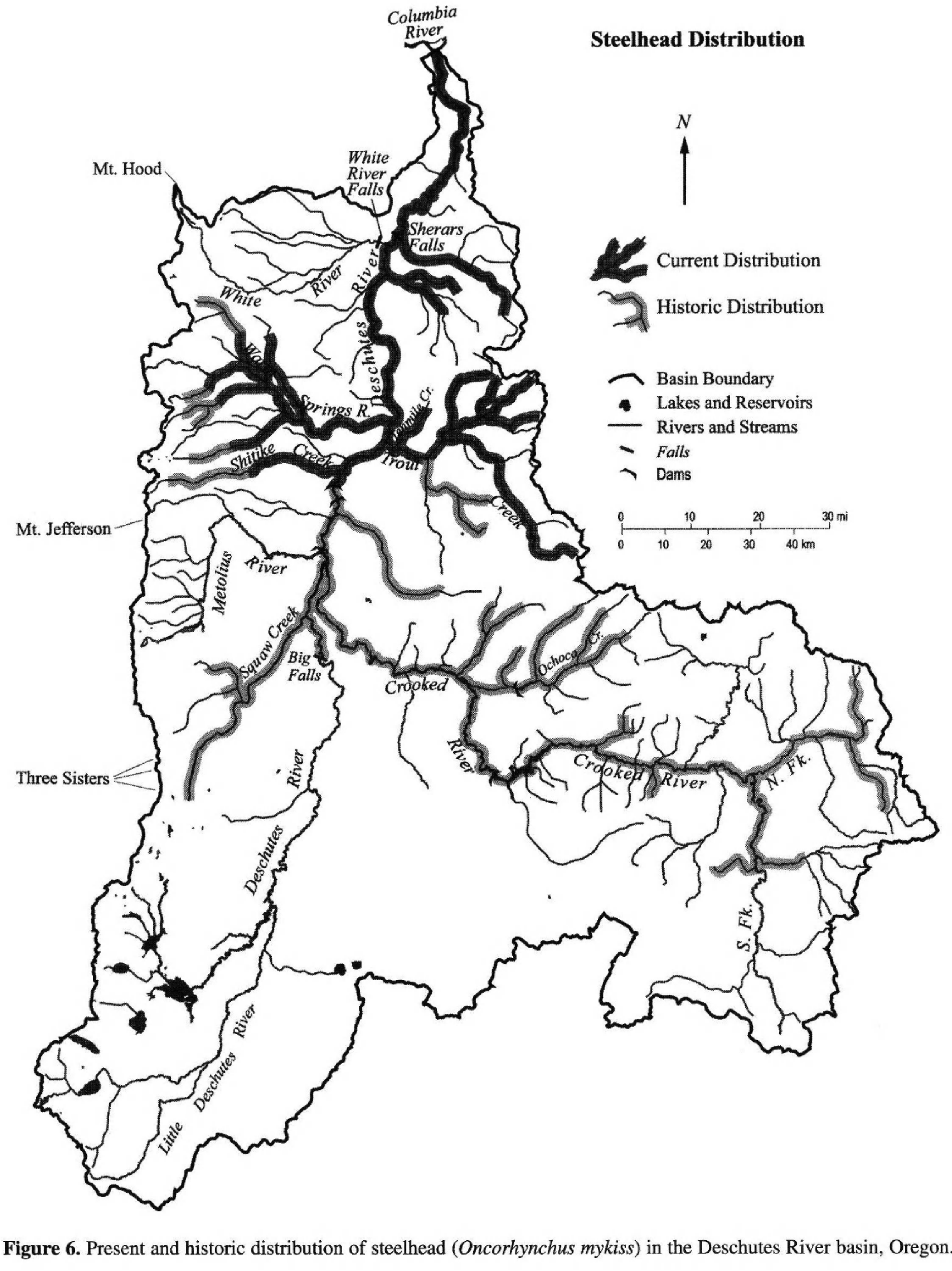

Figure 6. Present and historic distribution of steelhead (*Oncorhynchus mykiss*) in the Deschutes River basin, Oregon.

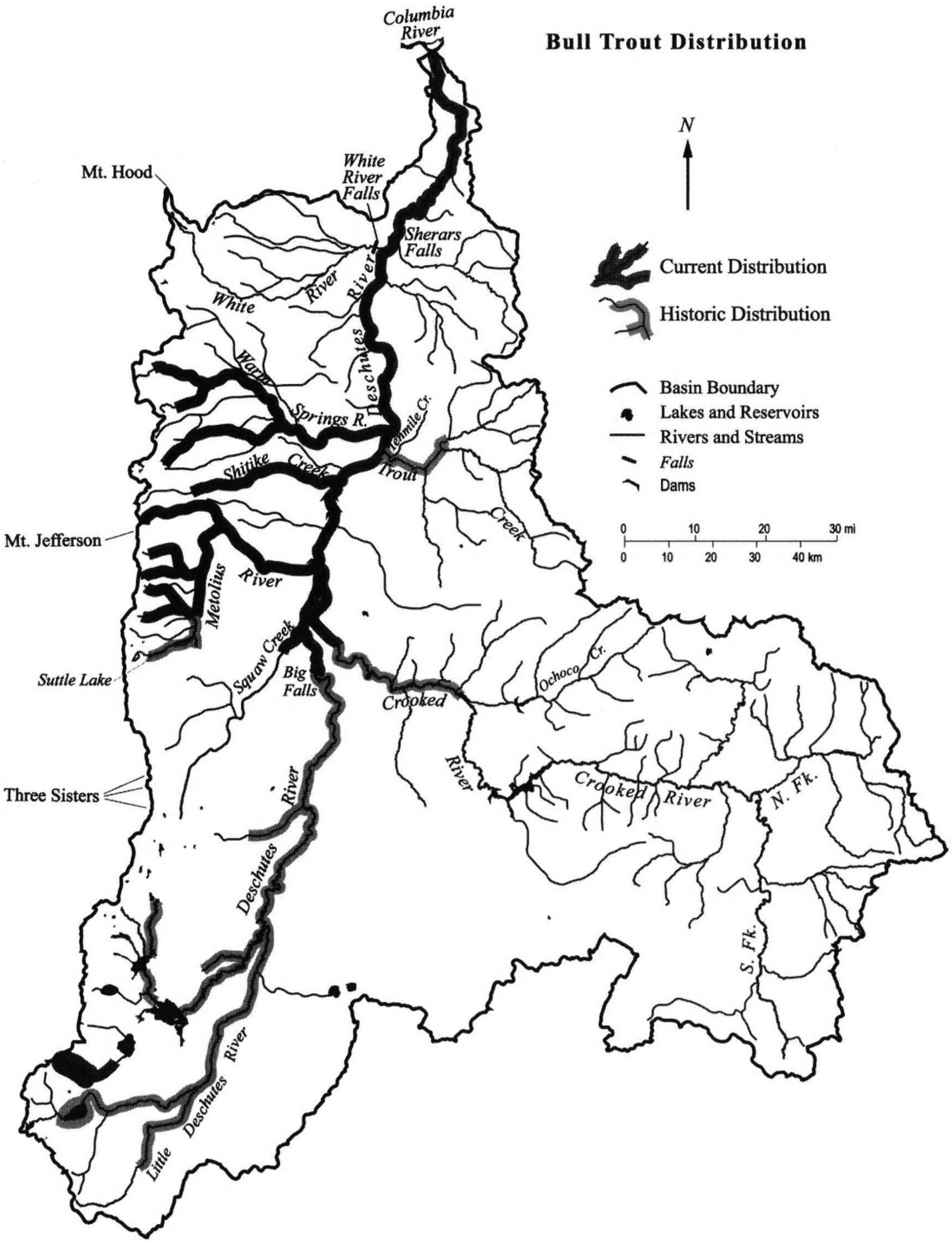

Figure 7. Present and historic distribution of bull trout (*Salvelinus confluentus*) in the Deschutes River basin, Oregon.

examples of geologic influences on Deschutes River basin fish distribution and population dynamics, illustrated with cases of both "regime" and "history" controls. For the reasons noted above, the geologic history aspects are more speculative than are the factors relating to modern conditions. Nevertheless, such speculation is relevant because it increasingly pertains to issues confronting modern fish management, in which modern human perturbations to the river system, such as dam construction and subsequent reconnecting of habitats, mimic geologic events as well as alter environmental gradients.

Watershed Regime Controls

Climate, physiography, and geology exert "regime-type" controls on fish distribution in the Deschutes River basin through their effects on environmental variables such as water temperature, flow conditions, and sediment transport and substrate conditions. Water temperature is a critical factor in structuring fish communities, and changes in temperature regime can cause changes in fish community structure and distribution [*Li et al.,* 1987]. For example, *Reeves et al.* [1987] found that behavioral interactions between competing juvenile steelhead and redside shiner (*Richardsonius balteatus*) were mediated by temperature. When water temperature was >15°C, the production of steelhead decreased by up to 54% when redside shiner were present. *Ebersole et al.* [2001] found that warm stream temperatures effectively limited the distribution and abundance of salmonids in streams due to mortality associated with higher water temperatures.

Bull trout distribution. The effects of water temperature are most evident in the distribution of bull trout. The present day (and presumably historic) distribution of spawning and rearing locations used by bull trout is highly related to water temperature. In the Metolius River, bull trout spawning and initial rearing of juveniles is limited to tributaries with water temperatures below 5°C [*Ratliff,* 1992]. This relationship is driven by physiological requirements of bull trout. Intergravel survival of the eggs and alevins is temperature dependent with egg to fry survival of 0-20% at 8-10°C, 60-90% at 6°C, and 80-95% at 2-4°C [*McPhail and Murray,* 1979]. An additional but related aspect is flow stability. For bull trout, which spawn during summer and early fall, the eggs and resulting embryos incubate and remain in the redd for approximately 160 to 190 days before they emerge from the gravel as free-swimming fry [*Pratt,* 1992], thus requiring that the redds are neither scoured nor dewatered for nearly half a year. In contrast, rainbow trout that spawn during late spring and early summer in water temperatures of 12°C may emerge in less than 60 days [*Zimmerman,* 2000]. The narrow range of temperatures selected by spawning adults and the temperature-dependent survival of emerging juveniles form the primary constraints on bull trout distribution within the Deschutes River basin. Therefore, the cold-water habitats preferred by bull trout correspond to spring-fed streams and rivers, most of which emerge from the High Cascade geologic province of young volcanic rocks.

Similarly, spring chinook require cool pools for refuges during the holding period between entering freshwater in the spring and spawning in the fall [*Torgersen et al.,* 1999]. Consequently, historic spring chinook habitat in the Deschutes River basin was primarily in the tributaries draining the High Cascade geologic province and in the spring-fed Deschutes River. It is unlikely that the anecdotal observations of spring chinook in the warmer Crooked River reflect large populations of spring chinook salmon, although it cannot be completely ruled out. Spring chinook in the Yakima River, Washington and John Day River, Oregon behaviorally thermoregulate to maintain internal temperatures by seeking patches of cooler water [*Berman and Quinn,* 1991; *Torgersen et al.,* 1999], and such behavior might have allowed spring chinook salmon to exist in the Crooked River.

Local species composition in relation to environmental gradients. In addition to controlling distributions of individual species, environmental gradients controlled by overall geologic, hydrologic, and climatologic conditions likely influence fish community structure. Although a detailed analysis of fish community structure has not been conducted in the Deschutes Basin, our surveys provide an anecdotal demonstration of large variations in fish assemblage composition among five locations in the Deschutes River basin downstream of the Pelton-Round Butte dam complex. At each of these sites, all fish present were identified to species and counted by electrofishing. The area sampled at each site ranged from 239 m^2 to 346 m^2. The mainstem Deschutes River sites included side-channels associated with islands on the east bank of the river at RM 9.9, RM 82.6, and RM 98.8 (Figure 8). Mainstem sites were sampled in August 1997 with the exception of the site at RM 82.6, which was sampled in July 1996. The study site on Shitike Creek was located approximately 3.5 km upstream from the Deschutes River (Figure 8), and was sampled by dive counting rather than electrofishing in August 1997. Tenmile Creek was sampled by electrofishing in July 1998, and the sampled area included approximately 600 m of stream beginning approximately 200 m upstream of the confluence with Trout Creek (Figure 8).

These surveys identified twelve species of fish during tabulation of 1,059 individuals. Rainbow trout (resident and

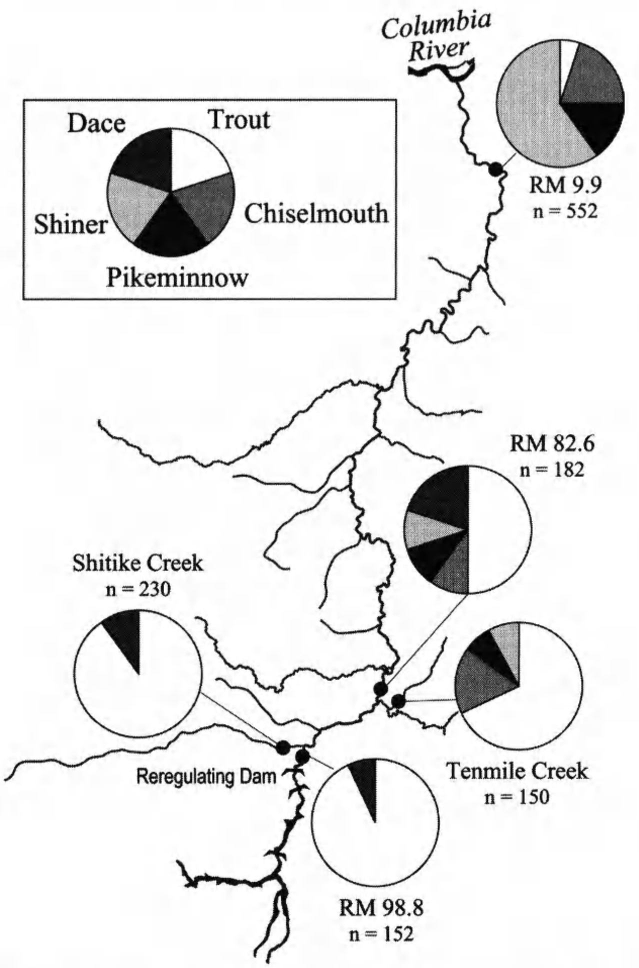

Figure 8. Percent composition of the dominant fish species at five locations in the lower Deschutes River, Oregon.

steelhead combined), speckled dace (*Rhinichthys osculus*), longnose dace (*R. cataractae*), redside shiner, northern pikeminnow (*Ptychocheilus oregonensis*), and chiselmouth (*Acrocheilus alutaceus*) were the dominant species, but bull trout, chinook salmon, mountain whitefish (*Prosopium williamsoni*), threespine stickleback (*Gasterosteus aculeatus*), and sculpins (*Cottus* spp.) were also encountered. Bull trout, chinook salmon, whitefish, and sculpins were excluded from this analysis because, in most cases, only one or two individuals were encountered. Sculpins were present in much greater numbers, but because they are benthic and live within the gravel substrate, they are difficult to count accurately.

Rigorous statistical comparisons among the survey sites are inappropriate because the sampling was conducted by different methods and at different times, but the results show distinct differences in fish assemblages among locations within the lower Deschutes River (Figure 8). The various proportions of fish species are similar to the longitudinal distribution of fish species presented by *Li et al.* [1987], which they attributed to longitudinal variation in temperature. Other studies have demonstrated temperature dependent variation in fish community structure or distribution [*Reeves et al.*, 1987; *Ebersole et al.*, 2001]. For example, *Rosenfeld et al.* [2001] found that chiselmouth in British Columbia rivers were typically absent from sites with maximum temperatures below 20°C. This is consistent with the variation in abundance of chiselmouth in the lower Deschutes River sites (Figure 8). Chiselmouth are more abundant at Tenmile Creek and the island side-channel sites at RM 82.6 and RM 9.9, which are characterized by warmer water temperatures, than they are at the cooler sites in Shitike Creek and the island side-channel site at RM 98.8.

Geologic Events and Fish Distribution

Individual geologic events and geologic processes also control patterns of fish distribution and community structure by establishing the physical template for modern habitats and environmental gradients, including features such as migration barriers, channel and valley-bottom morphology and substrate, and channel network geometry. Geologic events have also caused substantial changes to watershed and habitat conditions (such as ancient blockages and inter-basin connections) that have a continuing legacy for fish distribution and population dynamics. The understanding of the geologic history for the Deschutes River basin, summarized in the other contributions to this volume, allows us to hypothesize about how the history of geologic processes and events contributed to the control of certain aspects of fish distribution within the basin.

Lower Deschutes River valley-bottom morphology. Within the lower Deschutes River, downstream of the Pelton-Round Butte dam complex, side channels associated with islands provide important spawning and rearing habitats for salmonids and other species. For example, in 1995, 68% of all steelhead spawning between the Reregulating Dam and the mouth of Trout Creek occurred in side channels between islands and channel margins, despite the fact that such side channels comprise less than 10% of the channel length within that reach [*Zimmerman*, 2000]. The remaining steelhead spawning occurred in areas associated with edge habitats (along river margins) not associated with islands.

Systematic snorkeling counts on the lower Deschutes River also indicate the importance of edge habitats as rearing sites for juvenile fishes. We identified and counted fish distribution within 3-m lanes in 100 line transects snorkeled from the bank to middle of the river. Juvenile salmonids were observed from the bank to a maximum of 30 m from the bank, but their distribution was highly influenced by stream depth and velocity. In some transects, juvenile salmonids were not observed beyond 1 m from the bank, especially where water depth exceed one meter.

The islands and channel margins in the lower Deschutes River reflect specific geologic events that may make the Deschutes River channel environment unique among Pacific Northwest rivers. Downstream of the Pelton-Round Butte dam complex, the Deschutes River flows in a channel averaging about 71 m wide within a valley bottom averaging about 165 m wide [*Curran and O'Connor*, this volume]. This channel has been exceptionally stable compared to typical alluvial channels: nowhere has the channel migrated more than a few tens of meters since the first historic surveys of the late 1800s and early 1900s [*Curran and O'Connor*, this volume]. Of the 153 existing and historic (since 1911) islands within the lower Deschutes River, 75% percent are alluvial and the remainder are formed of bedrock, reflecting long term incision of the Deschutes River into basalt flows of the Columbia River Basalt Group [*Curran and O'Connor*, this volume]. Historically, the bedrock islands have changed little, but the alluvial islands have been more dynamic, with a very general pattern of growth between large floods and erosion during the largest historic floods, such as those in 1964 and 1996. Nevertheless, most alluvial islands (and associated side channels) have maintained very similar areas and locations for the past century [*Curran and O'Connor*, this volume]. All islands between the Reregulating Dam and Trout Creek, the reach sampled in the spawning surveys, are alluvial.

The stability of the side channels and channel margins, key fish habitat features, may be attributed to a large flood that affected the lower Deschutes River about 4400 years ago. Termed the "Outhouse flood" [*Curran and O'Connor*, this volume; *Beebee and O'Connor*, this volume], this event probably exceeded the magnitude of the largest historic floods by a factor of at least two, and left boulder bars that now form many of the channel margins and islands of the lower Deschutes River [*Curran and O'Connor*, this volume]. Large landslides are another process contributing to the stability of the Deschutes River channel, as debris from the landslides themselves or coarse flood deposits from the breaching of landslide dams forms the channel margins between RM 60 and 85. We suspect that the stability of the channel and islands of the lower Deschutes River, which is attributable to specific geologic events, is an important factor (along with the stable flow regime) in maintaining the relatively strong populations of resident rainbow trout in the lower mainstem. This channel and flow stability is also likely a factor in the survival of a fall chinook population, which spawns in the lower Deschutes River and is the single remaining population of a gene conservation group of chinook salmon that probably once included now-extinct populations in the John Day, Umatilla, and Walla Walla Rivers [*Lichatowich*, 1998].

Existing geologic barriers. Barriers to fish migration, such as waterfalls and rapids, basin divides, and reaches of insufficient flow, are geologic and hydrologic factors that strongly control fish distribution and migration patterns. These patterns are most evident in the historic distributions of anadromous fish such as chinook salmon, steelhead, and sockeye salmon, which navigate from the ocean to accessible spawning grounds within the basin. Blockages at the upstream limits of anadromy, including falls and reaches of insufficient flow, likely influence the distribution of resident, fluvial, and adfluvial populations, as well as the gene flow of bull trout and resident rainbow trout, although these latter effects are more difficult to document.

Historic chinook salmon distribution on the mainstem Deschutes River basin was controlled by geologic barriers to upstream migration. Big Falls at RM 132.2 was the upstream limit for all anadromous fish on the Deschutes River, including spring chinook and steelhead [*Nehlsen*, 1995] (Figure 3). Big Falls likely formed sometime between 700,000 and 300,000 years ago when lava flows from the vicinity of Newberry Volcano repeatedly filled the Deschutes River canyon from near Bend to as far downstream as Round Butte Dam at RM 110.1 [*Sherrod et al.*, in press]. Near the vicinity of Big Falls, the Deschutes River was apparently diverted about 5 km westward from a channel near Redmond [*Sherrod et al.*, 2002], resulting in incision of a younger canyon along the present course of the Deschutes River. This incision is recent enough that the river has not yet attained a graded profile, resulting in rapids and falls where it intercepts more resistant strata, such as the basalt flow that composes Big Falls. An important hydrologic factor enhancing the blockage at Big Falls is that the Deschutes River descends below the level of the regional water table near this location, and discharge increases substantially downstream of Big Falls [*Gannett et al.*, this volume]. The rapidly diminishing flow encountered by fish migrating upstream likely compounded the difficulty in navigating Big Falls.

The larger fall chinook salmon may have been blocked most years by the 4.7-m-high Sherars Falls at RM 44 [*Jonasson and Lindsay*, 1988; *Nehlsen*, 1995] (Figure 3), where the Deschutes River intercepts resistant basalt flows of the Columbia River Basalt Group [*O'Connor et al.*, this volume]. Sherars Falls is probably at least partly the result of incision during the last 10,000-100,000 years, judging from the distribution of Quaternary deposits within the Deschutes River canyon [*O'Connor et al.*, this volume] and, thus, may not be as old as the upstream blockage at Big Falls. In addition, during periods of increased flow and sediment transport, such as during the Pleistocene ice ages, channel aggradation may have decreased the severity of the blockage, allowing passage of fall chinook. Recently, passage facilities constructed and improved between the 1920s and 1940s at Sherars Falls allowed annual migration of fall chinook as far upstream as the location of Pelton Dam at RM 102.6. At present, anadromous fish are prevented from upstream passage at the downstream end of the Pelton-Round Butte dam complex at RM 100.1.

Ancient geologic barriers. The effects of ancient geologic barriers that have since been removed are more speculative than those of existing barriers. Ancient barriers are presumably reflected in the present distribution of distinct populations of genetic subgroups and life history types. Within the Deschutes River basin, several recent studies evaluating genetic variation within individual salmonid species indicate patterns of genetic variation potentially attributable to geologic events and conditions.

The coexistence of alternate life-history forms of rainbow trout in the lower Deschutes River likely reflects past formation and removal of geologic barriers. *Zimmerman and Reeves* [2000] examined the relationship between steelhead and resident rainbow trout in the lower Deschutes River through analysis of the timing and location of spawning, and by investigating population structure using the analysis of otolith microchemistry. The timing studies showed that steelhead and resident rainbow trout spawning was spatially and temporally isolated, with only a small amount of temporal overlap, suggesting that significant interbreeding was not likely.

The otolith microchemistry studies were used to identify the maternal origin of adult steelhead and rainbow trout from the Deschutes River, in order to determine if interbreeding occurred between the two life history forms. Comparison of strontium to calcium ratios (Sr/Ca) in the primordia (the part of the otolith that forms first) with those from the region of the otolith formed during the period of time the fish was rearing as a juvenile can be used to identify whether the mother of that fish was a steelhead or a resident rainbow trout (Figure 9). Based on these analyses, the adult populations of steelhead and resident rainbow trout in the Deschutes River did not include progeny of the alternate life history form. That is, there was no evidence of steelhead of resident rainbow trout maternal origin, or of resident rainbow trout of steelhead maternal origin. Both the timing of spawning and otolith results allowed *Zimmerman and Reeves* [2000] to surmise that steelhead and resident rainbow trout in the Deschutes River were reproductively isolated, and hence constituted potentially distinct populations.

To explain the presence of both life history forms using the same reach of river, *Zimmerman* [2000] suggested that this population structure could be the result of allopatric (during separation) divergence caused by the large Pleistocene landslide dams between RM 60 and RM 85 described by *O'Connor et al.* [this volume]. One or more of these landslide dams may have created a physical blockage of the river, forcing divergence of a downstream group of anadromous steelhead from an upstream group of resident rainbow trout for a sufficient duration to allow the behavioral characteristic of spawning timing to become distinct enough to persist even after breaching of the landslide dam(s). A similar case was reported by *Morita et al.* [2000] in conjunction with a constructed dam, for which they demonstrated that anadromous white spotted char (*Salvelinus leucomaenis*) populations separated from the sea showed substantial changes in behavioral characteristics within thirty years. Above the dam, there was a decrease in the production of smolts and an increase in the rate of residency. Likewise, *Kurenkov* (1978) described a similar scenario leading to the development of reproductively isolated populations of kokanee in Kamchatka, Russia. Consistent with these rapid changes in life history strategy, *Hendry et al.* [2000] demonstrated that genetic divergence and reproductive isolation in salmonids can occur within thirteen generations.

The genetic variation of resident rainbow trout within the Deschutes River basin provides evidence of longer-term blockages and exchanges of genetic material. *Currens et al.* [1990] determined the genetic structure of resident rainbow trout in the Deschutes River basin by analysis of genetic and morphologic variation among several distinct populations. A primary finding was that resident rainbow trout above White River Falls (Figure 3) shared similar genetic characteristics with rainbow trout populations in now-isolated drainages of the northern Great Basin, including the Fort Rock Basin and Catlow Valley, but were distinctly different from other populations in the Deschutes River basin. *Currens et al.* [1990] concluded that a common ancestral rainbow trout was present in the northern Great Basin and Deschutes River, thus indicating connections between these now-separate basins. The Fort Rock population was probably separated by late Pleistocene lava flows from the vicinity of Newberry Volcano that separated the Deschutes River

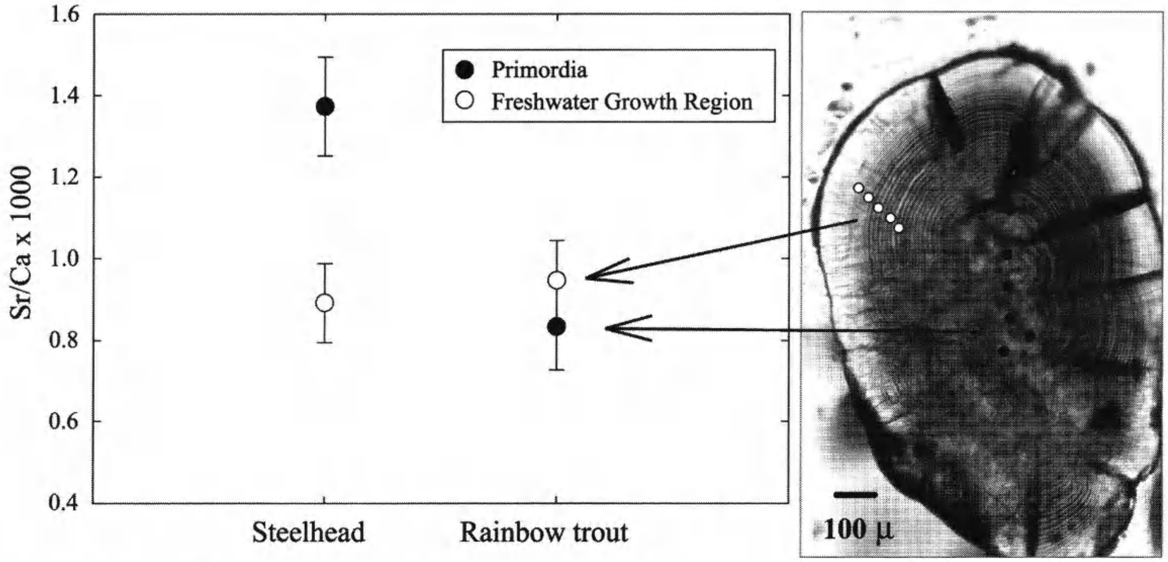

Figure 9. Determination of maternal origin in steelhead and resident rainbow trout (*Oncorhynchus mykiss*) progeny based on otolith microchemistry. Strontium to calcium ratios (Sr/Ca) are determined in points sampled within the primordia and freshwater growth region of sectioned otoliths. This otolith is from a young-of-year steelhead.

basin and the Fort Rock basin. Subsequent divergence or colonization of resident rainbow trout in the Deschutes River led to the present genetic differences between the rainbow trout above White River Falls and those in the rest of the Deschutes River basin.

Genetically distinct populations of bull trout in the Deschutes River basin may also be the legacy of former geologic blockages. *Spruell and Allendorf* [1997] examined the genetic structure of bull trout throughout Oregon, including samples from the Warm Springs River, Shitike Creek, and the Metolius River. Their results indicated that populations from the lower Deschutes River tributaries Shitike Creek and the Warm Springs River were markedly different from the population in the Metolius River, and that the Metolius River bull trout were more similar to bull trout in the Klamath River basin in southern Oregon. *Spruell and Allendorf* [1997] suggested geologic changes in connectivity within and adjacent to the Deschutes River basin as one explanation for this difference. To explain the observed genetic correlations, there would need to be connections between the upper Klamath River and the Metolius River, coincident with a blockage of gene flow between the lower Deschutes River and the Metolius River. While there is no specific evidence of a connection between the Deschutes and Klamath River basins, abundant basin-and-range faulting during the Quaternary may have locally shifted the drainage divide, thus making connections between the basins plausible (David Sherrod, U.S. Geological Survey, personal communication, 2002). However, a persistent late Quaternary blockage between the Metolius and lower Deschutes River is quite likely. Repeated basalt flows from Newberry Volcano and nearby vents between 1.2 and <0.4 million years ago flowed into and partly filled the Deschutes River, Crooked River and lower Metolius River [*Bishop and Smith,* 1990; *Sherrod et al.,* in press]. Such flows filled the Deschutes River canyon to a depth of more than 200 m near the present location of Round Butte Dam at RM 110.1, at the confluence of the Deschutes and Metolius Rivers. The falls formed at that time would undoubtedly have blocked migration from the lower Deschutes River to the Metolius River, probably for several tens of thousand of years, until incision around and through the basalt flows returned the Deschutes and Metolius Rivers to near their previous grades.

MODERN IMPOUNDMENTS AND EFFECTS ON FISH

Just as geologic events and conditions have profoundly affected fish populations, humans have also exerted a profound influence on fish distribution and population dynamics in the Deschutes River basin. Human influences on fish species in the Deschutes River basin have taken many forms, ranging from activities focused on fish management (harvest, hatchery programs, fish planting, and construction of fish ladders to improve passage over natural barriers) to reasoned tradeoffs aimed at other societal objectives (dam construction and water diversions), to actions that inadvertently affect fish (upland landuse actions that adversely affect fish habitat). Most of the human actions that have affected salmonids in the Deschutes River basin are summarized in *Nehlsen* [1995] and *Lichatowich* [1998].

The human actions most similar to geologic controls on fish distribution and population dynamics are dam construction and water diversion; these are also the human activities that have arguably had the greatest impact on aquatic ecosystems and habitat [*Stanford and Ward*, 1979; *Li et al.*, 1987]. In the Deschutes River basin, seven large dams, many small reservoirs, and numerous diversion structures have been constructed over the past 100 years, starting with construction of an irrigation diversion on Squaw Creek in 1871 [*Nehlsen*, 1995] (Figure 3). These projects were built for various purposes and objectives, and have had varying impacts on fish communities.

In this section, we consider how these modern impoundments may have affected the distribution and composition of fish communities, using a framework similar to that developed for analyzing geological controls and focusing on the effects of the Pelton-Round Butte dam complex. Like geological controls, dams can influence the physical environment of rivers by directly changing the water flow regime, sediment flux, and temperature regime throughout the system, with potentially serious consequences for aquatic habitat. In much the same way as natural blockages, dams can also be viewed as physical barriers limiting fish migration or interbreeding of populations. In this way, dam construction could be viewed as a singular type of anthropogenic "event" or disturbance. But dams also introduce new processes into a river system, and here we examine the complex relationship between fish and the temperature, blockage, and circulation patterns of water in the reservoir created by Round Butte Dam that have created problems for restoring fish runs in the Deschutes River basin.

Regime Effects of Dams

To assess the ecological effects of changes in streamflow and sediment transport downstream from dams, *Ligon et al.* [1995] proposed a five-step procedure: (1) Characterize the stream and watershed using quantitative measures such as stream type, bar morphology, degree of confinement, and vegetation; (2) Monitor water and sediment discharge; (3) Estimate pre- and post-dam sediment budgets and hydrology; (4) Model dam effects on streambed elevation and grain size; and (5) Predict channel response to the dam. Following this approach, little impact in the lower Deschutes River from the Pelton-Round Butte dam complex might be expected, since geomorphic studies reported in this volume show little change in flow frequency or hydrograph characteristics, bedload transport, channel morphology, and channel bed texture [*Fassnacht et al.*, this volume], or in sediment budgets [*O'Connor, Grant and Haluska*, this volume] attributable to the dam. All of these physical measures directly affect habitat variables that influence biotic communities [*Ligon et al.*, 1995].

The physical variables that were studied do not represent an exhaustive list of all potentially ecologically relevant physical changes introduced by the dams, however, nor are all dam effects necessarily negative. Changes in suspended sediment flux due to reservoir trapping of fine sediment, for example, were not directly evaluated, but may have biological implications. As has occurred with other dams, reduced suspended sediment loads following dam construction on the Deschutes River may have lowered turbidity below the dams. Biological consequences of increased water clarity can include enhanced primary production, decreased impacts of fine sediment on incubating salmonid eggs and embryos, and improved foraging efficiency [*Barrett et al.*, 1992; *Kinoshita et al.*, 2001].

Water temperature is critical to biological communities, because reproduction and growth is frequently temperature dependent [*Bjornn and Reiser*, 1991]. Changes in temperature have been documented downstream of many dams, and frequently lead to dramatic changes in fish communities and their reproductive success [*Stanford and Ward*, 1979]. These changes typically result from withdrawal of water from deep stratified reservoirs, resulting in colder water temperatures and a low-amplitude thermal regime downstream [*Hagen and Roberts*, 1973], as has occurred in the Colorado and Green Rivers in Utah [*Stanford and Ward*, 1979; *Tyus and Saunders*, 2000]. Corresponding shifts from warmwater to coldwater fish communities have been observed in many of these cases.

Huntington et al. [1999] conducted a detailed analysis of pre- and post-dam temperature profiles in the Deschutes River and addressed four primary questions: (1) Are changes in temperature evident; (2) What is the magnitude of change; (3) How far downstream are changes evident; and (4) What effects have those changes had on the biota downstream of the dam? Changes in annual maximum and minimum temperatures downstream of the dams on the Deschutes River are small and not significant [*Huntington et al.*, 1999]. There are shifts in the timing of temperature cycles just downstream of the dam, but these impacts are dampened further downstream. *Huntington et al.* [1999] suggested that shifts in temperature are likely to have delayed the emergence of incubating steelhead embryos by about ten to fourteen days immediately below the dam, but have had no significant impact on the emergence timing of fall chinook salmon. In summary, although there has been some alteration in temperature regime below the Pelton-Round Butte dam complex, these changes are small compared to those below other dams elsewhere.

Migration Barrier Effects

Construction of the Pelton-Round Butte dam complex altered distributions of spring chinook salmon and steelhead (Figures 4 and 6), because these dams form a physical barrier to their former migration. Fish passage facilities initially included a fish ladder from the Reregulating Dam to Pelton Dam, a fish lift over Round Butte Dam, and juvenile collection facilities at both Pelton and Round Butte Dams, which were operated from 1956 to 1968. During this period, a total of 6,933 adult chinook salmon and 6,248 adult steelhead were passed upstream and over Round Butte Dam [*Ratliff and Schulz*, 1999]. Downstream passage of juvenile chinook and steelhead was less successful, and in 1968 upstream and downstream passage of fish was abandoned in favor of hatchery mitigation. Spring chinook salmon and steelhead are produced at the Round Butte Hatchery to replace production in the area of the watershed blocked by dams. In addition to loss of chinook salmon and steelhead production upstream of Round Butte Dam, population dynamics of other migratory species including rainbow trout and bull trout were altered. As a result, blockage of fish passage is probably one of the greatest impacts of the modern dams constructed in the mainstem of the Deschutes River.

Complex Interactions Due to Dams and Management Response

The decision to cease fish passage in 1968 was primarily due to the perceived failure of juvenile fish production and lack of downstream passage of juvenile steelhead and chinook salmon [*Ratliff and Schulz*, 1999]. This failure was likely due to temperature and current conditions in the reservoir at Round Butte Dam, Lake Billy Chinook (Figure 3). In contrast with natural barriers where *upstream* passage is blocked, this large reservoir with its three major tributaries and a deep outlet (73 m below full pool) for hydropower generation created a *downstream* passage barrier. Because of the hydraulic stability (low variation in discharge) at this location [*Gannett et al.*, this volume], Round Butte Dam only spills water from the surface during extremely rare flood events. Thus, essentially all flow exits the reservoir through the power intake at depth. Of the three tributaries, the Crooked River has the warmest inflow and tends to fill the upper portion of the reservoir, whereas the Metolius River is significantly colder and its denser water tends to fill the bottom of the reservoir up to the intake level. The temperature of the Deschutes River is intermediate between the other two tributaries. Downstream migration of juvenile salmonids occurs during spring with peak numbers in April and May. Typically, juvenile steelhead and chinook salmon are surface oriented when passing through deep waters and travel with the prevailing currents [*Smith*, 1974]. Because of the deep intake of Round Butte Dam, surface currents are very slight and variable, and the combination of deep intake and temperature variation between the arms results in an unusual surface circulation pattern. During spring, surface currents used by fish as directional cues tend to be oriented downstream for the Crooked and Deschutes River arms of the reservoir, and upstream for the Metolius River arm [*Yang et al.*, 2000], because at the interface between the Metolius River and the reservoir, the plunging cold water tends to entrain the surface reservoir water [*Yang et al.*, 2000]. These countercurrents do not guide downstream-migrating salmonids to the dam where the juvenile fish collection facilities were located. Juvenile salmon attempting to emigrate from Lake Billy Chinook tended to concentrate in the upper Metolius River arm [*Korn et al.*, 1967]. Given these difficulties, passage was terminated in favor of a fish hatchery mitigation program.

In 1994, research and planning was initiated to reestablish passage of salmonids at the Pelton-Round Butte dam complex. This effort includes altering Round Butte Dam to allow withdrawal of water from the surface during most of the year [*Ratliff et al.*, 2001]. The alteration will include a facility designed to withdraw generation water from either the top or the bottom or a mix of the two. Fish will be excluded from the generation water, and those attempting to emigrate will be diverted into a capture and bypass facility. Key to the success of this facility will be the ability to mix warm surface and deep cold water to allow for management of the temperature of the water entering the lower Deschutes River. It is anticipated that only surface water will be discharged from autumn (after the reservoir surface cools) through June of the following year. During this period, waters of the warmer Crooked and Deschutes Rivers will be discharged off the surface while the reservoir fills from the bottom with cold Metolius River water. Mean reservoir temperatures approaching summer will be several degrees cooler than under present conditions [*DeGasperi et al.*, 2000]. After June, when few juvenile salmon are emigrating and the surface of Lake Billy Chinook warms, an increasing percentage of cold hypolimnetic water will be discharged, in an effort to mimic the natural pre-dam temperature cycle of the lower Deschutes River [*Huntington et al.*, 1999].

The goal of this program will be to reestablish spring chinook salmon runs in the Metolius River, and steelhead runs in the upper Deschutes River (to Big Falls) including Squaw Creek (Figure 3). Steelhead will also be reestablished in tributaries to the Crooked River system. However, it is anticipated that the species that will benefit the most with successful fish passage will be sockeye salmon. When Lake Billy Chinook was formed in 1964, kokanee (resident sockeye salmon) from Suttle Lake in the Metolius River basin naturally seeded this reservoir, and by the early 1970s were the most abundant fish present [*Thiesfeld et al.*, 1999]. With downstream passage of juvenile salmonids, it is likely that sockeye salmon, the anadromous form of kokanee, will reestablish in Suttle Lake and in the reservoirs of the Pelton Round Butte hydroelectric complex.

Reestablishing fish passage at the Pelton-Round Butte dam complex is not an easy proposition. There are questions concerning selection of fish for transport upstream, with a goal of limiting disease transmission yet allowing migration of fish in as natural a manner as if the dams were not present. There is also the question of how success of passage will be measured. Do we measure the number of juvenile fish migrating downstream, or the number of fish returning to migrate upstream past the dams? If those metrics are chosen, how do we distinguish the effects of passage from a host of other influences? These questions need to be addressed, but should not limit opportunities for restoration of migratory fishes in the Upper Deschutes, Crooked, and Metolius rivers.

CONCLUSIONS

Although the geomorphology of a watershed is often invoked as a primary template for understanding the organization of biological systems [*Swanson*, 1980; *Montgomery*, 1999], the interaction among geology, geomorphology and ecosystems has many different facets. As illustrated by the Deschutes River, geology exerts a first-order control on fish populations through two broad mechanisms. First, geology determines the hydrologic, sediment transport, and temperature regimes of the watershed that define the environmental niches and gradients to which organisms are adapted. Second, the history of geological disturbances and events in the basin generates landforms that define critical habitat, and also constrain or define the extent to which species and populations of aquatic organisms can interact with each other. The history of geological blockages and their impacts on ecosystems is still poorly understood, but genetic composition of fish populations in the Deschutes River and elsewhere suggests that ecosystems may retain a long "memory" of geological events in the past. In some cases, the genetics of organisms may even provide clues as to the direction of geomorphic evolution, as in cases where similarities between currently separated populations may show where past drainage network changes have isolated formerly connected river systems. Modern dams affect ecosystems in a similar manner to geological blockages, and the Deschutes River dams have made their greatest impact on fish by isolating lower river from upper river populations. Dams may also influence water, sediment, and temperature regimes, although this impact is modest on the Deschutes River. Because of their sheer size and engineering characteristics, dams may introduce new processes into the landscape to which fish are poorly adapted, often requiring heroic and expensive human efforts and interventions to restore fish runs. The jury is still out on the success of these restoration ventures in the Deschutes River basin and elsewhere.

Acknowledgments. We thank Ian Waite, Bill Trush, and an anonymous reviewer for comments that improved this manuscript. Gordon Grant and Jim O'Connor, as editors of this volume, invited us to produce this paper and offered important advice and guidance in its production. Eric Schulz of Portland General Electric provided much needed assistance gathering information. Gordon Reeves and the U.S. Forest Service provided office space and logistic support for Zimmerman during the initial production of this manuscript. Thor Tingey assisted with creation of figures. Kathryn Ronnenberg provided invaluable editorial and graphic support.

REFERENCES

Barrett, J. C., G. D. Grossman, and J. Rosenfeld, Turbidity-induced changes in reactive distance of rainbow trout, *Trans. Amer. Fish. Soc.*, *121*, 437-443, 1992.

Berman, C. H., and T. P. Quinn, Behavioral thermoregulation and homing by spring chinook salmon, *Oncorhynchus tshawytscha* (Walbaum), in the Yakima River, *J. Fish Biol.*, *39*, 301-312, 1991.

Bishop, E. M., and G. A. Smith, A field guide to the geology of Cove Palisades State Park and the Deschutes Basin in central Oregon, *Oregon Geology*, *52*, 3-16, 1990.

Bjornn, T. C., and D. W. Reiser, Habitat requirements of salmonids in streams, *Amer. Fish. Soc. Spec. Pub. 19*, 83-138, 1991.

Chapman, D. W., Critical review of variables used to define effects of fines in redds of large salmonids, *Trans. Amer. Fish. Soc.*, *117*, 1-21, 1988.

Currens, K. P., C. B. Schreck, and H. W. Li, Allozyme and morphological divergence of rainbow trout (*Oncorhynchus mykiss*) above and below waterfalls in the Deschutes River, Oregon, *Copeia*, 730-746, 1990.

DeGasperi, C. T., T. Khangaonkar, S. Breithaupt, and K. Marshall, Design of optimum selective withdrawal operation for temperature management at Round Butte Dam, Lake Billy Chinook, Oregon, *Proceedings of the Water Environment Federation (WEF) 73rd Annual Conference and Exposition on Water Quality and Wastewater Treatment (CD-ROM)*, October 18, 2000, Anaheim, California, 2000.

Ebersole, J. L., W. J. Liss, and C. A. Frissell, Relationship between stream temperature, thermal refugia and rainbow trout *Oncorhynchus mykiss* abundance in arid-land streams in the northwestern United States, *Ecology of Freshwater Fish, 10*, 1-10, 2001.

Gowan, C., M. K. Young, K. D. Fausch, and S. C. Riley, Restricted movement in resident stream salmonids: a paradigm lost?, *Can. J. Fish. Aquat. Sci., 51*, 2626-2637, 1994.

Hagen, R. M., and E. B. Roberts, Ecological impacts of water storage and diversion projects, in *Environmental Quality and Water Development*, edited by C. R. Goldman, J. McEvoy, and P. J. Richardson, W. H. Freeman, San Francisco, California, 1973.

Healey, M. C., Life history of chinook salmon (*Oncorhynchus tshawytscha*), in *Pacific Salmon Life Histories,* edited by C. Groot and L. Margolis, UBC Press, Vancouver, British Columbia, pp. 313 – 393, 1991.

Hendry, A. P., J. K. Wenburg, P. Bentzen, E. C. Volk, and T. P. Quinn, Rapid evolution of reproductive isolation in the wild: evidence from introduced salmon, *Science, 290*, 516-518, 2000.

Huntington, C., T. Hardin, and R. Raymond, Water temperatures in the Lower Deschutes River, Oregon, Portland General Electric Company, Portland, Oregon, 1999.

Jonasson, B. C., and R. B. Lindsay, Fall chinook salmon in the Deschutes River, Oregon, Oregon Department of Fish and Wildlife, *Inf. Rep. 88-6*, Portland, Oregon, 1988.

Kinoshita, A., T. Mizuyama, M. Fujita, T. Sawada, and M. Yoshikiyo. An impact of sediment flushing from a sabo dam on char in Hiru-Dani River. *River Technical Papers, 7*, 363-368, 2001.

Korn, L., L. H. Hreha, R. G. Montagne, W. G. Mullarkey, and E. J. Wagner, The effect of small impoundments on the behavior of juvenile anadromous salmonids, Fish Commission of Oregon Research Division (now Oregon Department of Fish and Wildlife), Clackamas, Oregon, 1967.

Kurenkov, S. I., Two reproductively isolated groups of kokanee salmon, *Oncorhynchus nerka kennerlyi*, from Lake Kronotskiy, *J. Ichthyology, 17*, 526-534, 1978.

Li, H. W., C. B. Schreck, C. E. Bond, and E. Rexstad, Factors influencing changes in fish assemblages of Pacific Northwest streams, in *Community and Evolutionary Ecology of North American Stream Fishes*, edited by W. J. Mathews and D. C. Heins, pp. 193-202, University of Oklahoma Press, Norman, Oklahoma, 1987.

Lichatowich, J., A conceptual foundation for the management of native salmonids in the Deschutes River, Portland General Electric Company, Portland, Oregon, 1998.

Ligon, F. K., W. E. Dietrich, and W. J. Trush, Downstream ecological effects of dams: a geomorphic perspective, *Bioscience, 45,* 183-192, 1995.

Lindsay, R. B., B. C. Jonasson and R. K. Schroeder, Spring chinook salmon in the Deschutes River, Oregon, *Inf. Rep. 89-4*, April 1989, Fish Division, Oregon Dept of Fish and Wildlife, Portland, Oregon, 1989.

Mathews, W. J., Patterns in Freshwater Fish Ecology, Chapman and Hall, New York, 1998.

McPhail, J. D., and C. C. Lindsey, Zoogeography of the freshwater fishes of Cascadia (the Columbia System and rivers north to the Stikine), in *The Zoogeography of North American Freshwater Fishes*, edited by C. H. Hocutt and E. O. Wiley, pp. 615-637, John Wiley and Sons, New York, 1986.

McPhail, J. D., and C. B. Murray, The early life-history and ecology of Dolly Varden (*Salvelinus malma*) in the Upper Arrow Lakes, Vancouver, B. C., University of British Columbia, Department of Zoology and Institute of Animal Resources, 1979.

Morita, K., S. Yamamoto, and N. Hoshino, Extreme life history change of white-spotted char (*Salvelinus leucomaenis*) after damming, *Can. J. Fish. Aquat. Sci., 57*, 1300-1306, 2000.

Montgomery, D. R., Process domains and the river continuum, *J. Amer. Water Resour. Assoc., 35*, 397-410, 1999.

Nehlsen, W., Historical salmon and steelhead runs of the upper Deschutes River and their environments, Portland General Electric Company, Portland, Oregon, 1995.

Oregon Department of Fish and Wildlife (ODFW), Biennial report on the status of wild fish in Oregon Portland, Oregon, 1995.

Pratt, K. L., A review of bull trout life history, in *Proceedings of the Gearheart Mountain Bull Trout Workshop*, edited by P. J. Howell and D. V. Buchanan, pp. 5-9, Oregon Chapter American Fisheries Society, Corvallis, Oregon, 1992.

Ratliff, D. E., Bull trout investigations in the Metolius River–Lake Billy Chinook system, in *Proceedings of the Gearheart Mountain Bull Trout Workshop*, edited by P. J. Howell and D. V. Buchanan, pp. 37 – 44, Oregon Chapter of the American Fisheries Society, Corvallis, Oregon, 1992.

Ratliff, D. E., and E. E. Schulz, Fisheries program at the Pelton-Round Butte Hydroelectric Project (Oregon) 1956-1995, Portland General Electric Company, Portland, Oregon, 1999.

Ratliff, D. E., E. E. Schulz, and S. D. Padula, Pelton-Round Butte Project, Fish Passage Plan, Second Edition, Portland General Electric, Portland, Oregon, The Confederated Tribes of the Warm Springs Reservation of Oregon, Warm Springs, Oregon, 2001.

Reeves, G. H., F. H. Everest, and J. D. Hall, Interactions between redside shiner (*Richardsonius balteatus*) and the steelhead trout (*Salmo gairdneri*) in western Oregon: the influence of water temperature, *Can. J. Fish. Aquat. Sci., 44*, 1603-1613, 1987.

Reeves, G. H., P. A. Bisson, and J. M. Dambacher, Fish communities, in *River Ecology and Management: Lessons from the Pacific Coastal Ecoregion*, edited by R. J. Naiman and R. E. Bilby, pp. 200-234, Springer-Verlag, New York, 1998.

Rosenfeld, J., M. Porter, M. Pearson, et al. The influence of temperature and habitat on the distribution of chiselmouth, *Acrocheilus alutaceus*, in British Columbia, *Environmental Biology of Fishes, 62*, 401-413, 2001.

Sherrod, D. R., M. W. Gannett, and K. E. Lite Jr., Hydrogeology of the upper Deschutes Basin, Central Oregon: A young basin adjacent to the Cascade Volcanic Arc, in *Field Guide to Geologic Processes in Cascadia*, edited by G. W. Moore, *Oregon Dept. Geol. Min. Ind. Spec. Pap. 36*, pp. 109-144, 2002.

Sherrod, D. R., E. M. Taylor, M. L. Ferns et al., Geologic map of the Bend 30′ X 60′ Quadrangle, central Oregon, *U. S. Geol. Surv. Geol. Inv. Map I-2683*, scale 1:100,000, in press.

Smith, J. R., Distribution of seaward-migrating chinook salmon and steelhead trout in the Snake River above Lower Monumental Dam, *Marine Fish. Rev., 36*, 42-45, 1974.

Spruell, P., and F. W. Allendorf, Nuclear DNA analysis of Oregon bull trout, Final Report to the Oregon Department of Fish and Wildlife, University of Montana, Wild Trout and Salmon Genetics Laboratory Report 97/5, 1997.

Stanford, J. A., and J. V. Ward. Stream regulation in North America, in *The Ecology of Regulated Streams*, edited by J. V. Ward and J. A. Stanford, pp. 215-236, Plenum Press, New York, 1979.

Swanson, F. J., Geomorphology and ecosystems, in *Forests: Fresh Perspectives from Ecosystem Analysis: Proceedings of the 40th Annual Biology Colloquium*, edited by R. W. Waring, pp. 159-170, Oregon State University, Corvallis, Oregon, 1980.

Thiesfeld, S. L., J. C. Kern, A. R. Dale, M. W. Chilcote, and M. A. Buckman. Lake Billy Chinook sockeye salmon and kokanee research study, 1996-1998, Contract Completion Report. Oregon Department of Fish and Wildlife, Portland, Portland General Electric Company, Portland, Oregon, 1999.

Torgersen, C. E., D. M. Price, H. W. Li, and B. A. McIntosh, Multiscale thermal refugia and stream habitat associations of chinook salmon in northeastern Oregon, *Ecol. Appl., 9*, 301-319, 1999.

Tyus, H. M., and J. F. Saunders III, Nonnative fish control and endangered fish recovery: lessons from the Colorado River, *Fisheries, 25*(9), 17-24, 2000.

Yang, Z., T. Khangaonkar, C. DeGasperi, and K. Marshall, Three-dimensional modeling of temperature stratification and density-driven circulation in Lake Billy Chinook, Oregon, in *Proceedings of the 6th International Conference on Estuarine and Coastal Modeling*, edited by M. L. Spaulding and H. L. Butler, pp. 411-425, American Society of Civil Engineers, New Orleans, 2000.

Zimmerman, C. E., Ecological relation of sympatric steelhead and resident rainbow trout in the Deschutes River, Oregon, PhD Dissertation, Oregon State University, Corvallis, Oregon, 2000.

Zimmerman, C. E. and G. H. Reeves, Population structure of sympatric anadromous and nonanadromous *Oncorhynchus mykiss*: evidence from spawning surveys and otolith microchemistry, *Can. J. Fish. Aquat. Sci., 57*, 2152-2162, 2000.

Christian E. Zimmerman, U.S. Geological Survey, Alaska Science Center, 1011 E. Tudor Rd., Anchorage, Alaska, 99503

Donald E. Ratliff, Portland General Electric, 726 Lower Bend Rd., Madras, Oregon, 97741

Section II

The Geomorphology and Flood History of the Lower Deschutes River

Despite its unusually stable and subdued modern flow regime, the history of the Deschutes River has been punctuated by a series of floods of gargantuan size and widely varying origins. Ironically, it may be because of the stability of the modern flow regime that the record of these floods is preserved in the stratigraphy and deposits that fill the valley floor. Because modern floods occur rarely, and even those of historic magnitude, such as the flood of February 1996, are largely ineffective in sculpting valley landforms or erasing the ancient flood record, we may know more about the history of paleofloods on the Deschutes River than for any other river in the Pacific Northwest.

Even so, the record is frustratingly incomplete and ambiguous. But as revealed in the papers in this section, understanding the history of floods, including flood mechanisms, magnitudes, frequencies, and legacies, is essential to interpreting the modern channel and valley floor morphology of the river, and understanding the impact of human interventions, such as dams. *O'Connor et al.* provide an overarching framework for this history in their description of the Quaternary geology and geomorphology of the lower Deschutes River—that portion of the river below the Pelton-Round Butte dam complex. Again emphasizing the theme of geological control, they explore how the width of the valley bottom, the prevalence of alluvial and bedrock surfaces, the distribution of mass movements, and the planform of the river all vary systematically in relation to the underlying geology and structure. At a finer scale, they describe how large landslides have episodically dammed the river, leading to breakout floods with their distinctive legacies of boulder bars and rapids. A wide range of other flood-generating processes have occurred throughout the Quaternary, including volcanic lahars, glacial outbreaks, backwater floods from the Missoula floods on the Columbia River, and recent meteorological floods and debris flows, each leaving a distinctive stratigraphy or mark on the valley bottom. The result is that the Deschutes River is a veritable museum of fluvial catastrophe.

This overprinting of floods of different ages, origins, and magnitudes results in a complex valley floor and channel morphology of islands, rapids, and boulder bars—the focus of the paper by *Curran and O'Connor*. They demonstrate that a disproportionate number of these features owe their origin to outsized floods larger than any observed in the historical past. In particular, most of the islands in the Deschutes River are cored by large flood deposits. Modern floods, such as that of 1996, modify islands and transport gravel, but the valley and channel margins are largely fixed by the larger, more competent events.

In the final two papers of this section, authors examine the late Holocene record of floods in more detail. *Hosman et al.* combine stratigraphic evidence with modern gage records to interpret the history of Holocene floods, as preserved in fine-grained alluvial deposits. They develop a paleoflood chronology of over twenty floods during the last ~6000 years that is broadly consistent among sites. The largest flood by far was the mid-Holocene "Outhouse flood," the subject of the final paper by *Beebee and O'Connor*, who use sedimentologic evidence and hydraulic modeling to constrain the magnitude of this event and interpret its origin. The evidence points to a meteorological source, raising the prospect that climatic events more than twice the size of the historic flood of 1996 can occur in the Deschutes River.

A Peculiar River
Water Science and Application 7
10.1029/007WS06

Quaternary Geology and Geomorphology of the Lower Deschutes River Canyon, Oregon

Jim E. O'Connor[1], Janet H. Curran[2], Robin A. Beebee[3], Gordon E. Grant[4], and Andrei Sarna-Wojcicki[5]

The morphology of the Deschutes River canyon downstream of the Pelton-Round Butte dam complex is the product of the regional geologic history, the composition of the geologic units that compose the valley walls, and Quaternary processes and events. Geologic units within the valley walls and regional deformation patterns control overall valley morphology. Valley bottom morphology is mostly the result of Quaternary events. These include several large landslides, which have caused retreat of the canyon rims but have also constricted the valley bottom with immense volumes of debris. In at least two instances (as at Whitehorse Rapids), landslides blocked the channel, resulting in ponding, breaching of landslide dams, and downstream floods. Large floods from other mechanisms have also formed many valley-bottom features along the lower Deschutes River. A large Pleistocene lahar resulting from a circa 0.07 Ma eruption of Mount Jefferson left bouldery deposits along the valley margins for most of the canyon length. The 15,000-12,700 ^{14}C yr BP Missoula floods backflooded *up* the Deschutes River from the Columbia River and mantled the downstream-most 60 km of Deschutes River valley with bedded silt and clay. A large, possibly meteorologic flood between 6,500 and 3,000 ^{14}C yr BP left abundant boulder bars and high sand and silt deposits that flank the channel in wider valley-bottom locations. In contrast, large historic main-stem floods, such as December 1964 and February 1996, had few effects on channel geomorphology due to the volume and coarseness of valley bottom deposits left by the earlier and larger floods and landslides.

INTRODUCTION

The overall valley morphology of the 160 km of the Deschutes River downstream of the Pelton-Round Butte dam complex reflects the regional geologic history and local processes and events of the past million years. The purpose of this paper is to give a brief description of the morphologic development of the present canyon and valley bottom, bridging the temporal and spatial scales spanned by previous papers in this volume describing the overall geologic and hydrologic setting of the Deschutes River basin [*Gannett et al.*, this volume; *O'Connor, Grant, and Haluska.*, this volume] and later papers that provide more detailed information on Holocene processes and events that formed and affected the channel and valley bottom downstream of the Pelton-Round Butte dam complex [*Beebee and O'Connor*, this volume; *Curran and O'Connor*, this volume; *Fassnacht et al.*, this volume; *Hosman et al.*, this volume]. Specific locations are referred to by River Mile (RM) as shown on USGS topographic quadrangles and Oregon State Water Resource Board maps; RM 0 is at the Deschutes River confluence with the Columbia River, and values increase upstream to RM 100.1 at the Reregulating Dam, the downstream-most structure within the Pelton-Round Butte dam complex (Figure 1).

[1]U.S. Geological Survey, Portland, Oregon
[2]U.S. Geological Survey, Anchorage, Alaska
[3]University of Oregon, Eugene, Oregon
[4]U.S. Forest Service, Corvallis, Oregon
[5]U.S. Geological Survey, Menlo Park, California

A Peculiar River
Water Science and Application 7

10.1029/007WS07

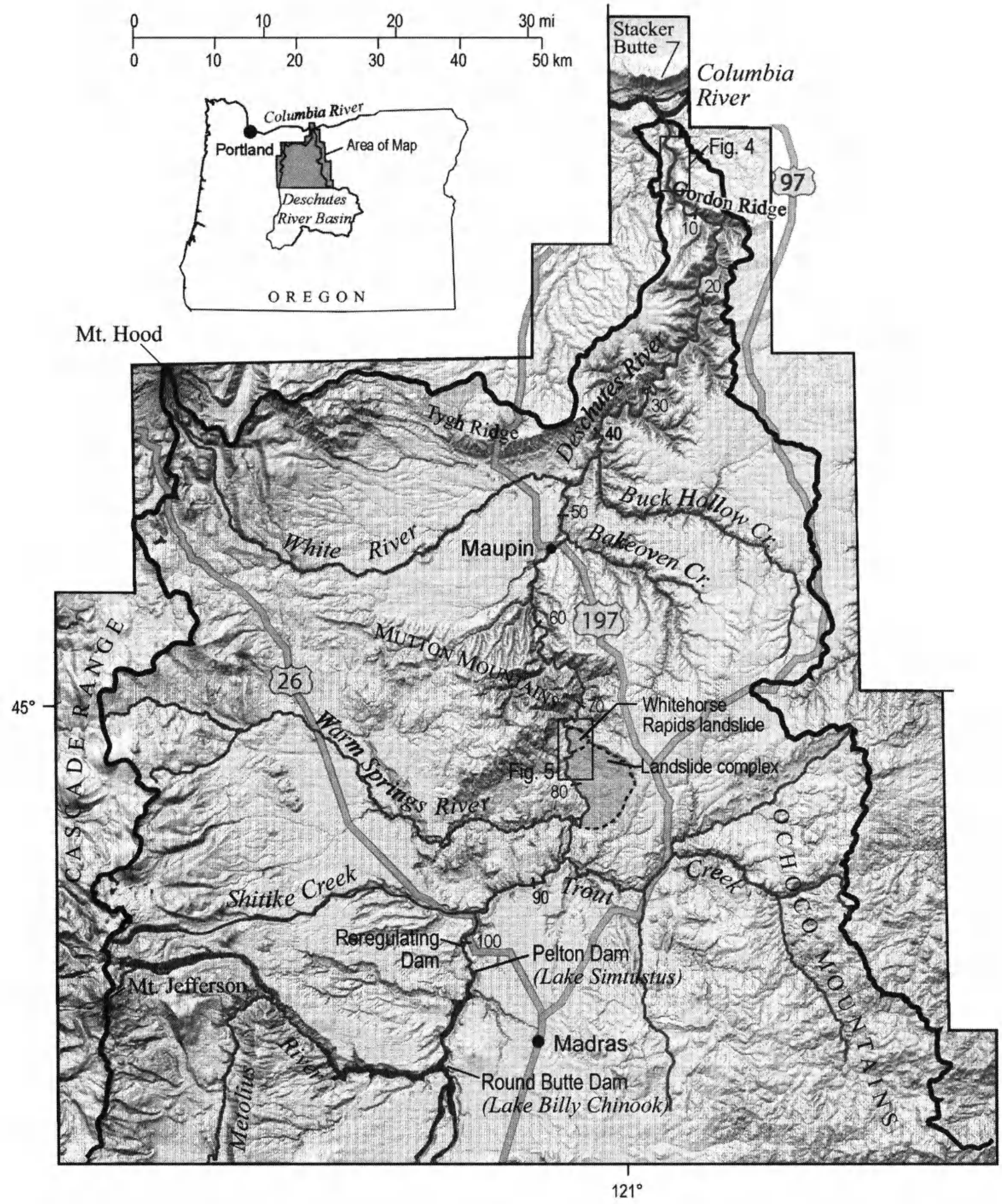

Figure 1. Shaded relief map of the lower Deschutes River basin, showing key locations, highways, and River Miles (in 10-mile increments) along the Deschutes River between the confluence with the Columbia River and the Reregulating Dam at River Mile 100.1. Topography from 30-m resolution digital elevation models produced by the U.S. Geological Survey. River Mile locations from the 1973 map of the Deschutes River drainage basin (map no. 5.6) produced by the State Water Resources Board, Oregon.

GEOLOGIC CONTROLS ON THE GEOMORPHOLOGY OF THE LOWER DESCHUTES RIVER

Canyon Morphology

Downstream of the Pelton-Round Butte dam complex, the Deschutes River flows within a canyon incised up to 600 m into the adjacent terrain (Figures 1, 2, and 3). Canyon depth corresponds to regional tectonic deformation of the once-planar top of the Miocene Columbia River Basalt Group (Figure 3). The deepest portions of the canyon occur where the Deschutes River crosses the trends of the uplifted Mutton Mountains (~RM 70) and the Tygh Ridge anticline (~RM 40). The canyon rims are lowest downstream of the Pelton-Round Butte dam complex between RM 100 and 85, near the town of Maupin (RM 50), and at the Columbia River confluence—all locations where the Deschutes River flows through post-Columbia River Basalt Group basins that have been partly filled with the Miocene-Pliocene Deschutes and Dalles Formations.

Canyon rims are formed of flows of the Columbia River Basalt Group, except where younger basalt flows cap structural basins. Upstream of RM 60, outcrops of lava flows and tuffs in the John Day and Clarno Formations form prominent ledges below the canyon rims (Figure 2a). Canyon walls are bare or talus-covered bedrock, landslide debris, and locally, thick colluvial aprons that descend in long sweeping slopes. Alluvial terraces up to 40 m above river level are preserved in wider portions of the canyon, notably near the Shitike Creek, Trout Creek, and Warm Springs River confluences. A blanket of fine sand, silt, and clay laid down by the late-Pleistocene Missoula floods mantles the lower portions of gentler slopes downstream of RM 40 (Figure 3).

The bedrock forming the canyon margins varies downstream in degree of internal deformation and weathering, susceptibility to landsliding, and grain size of weathering products, and these differences influence canyon and valley bottom morphology. From the Pelton-Round Butte dam complex downstream to about RM 85, the Deschutes River flows within a canyon with exposures of John Day Formation near water level, overlain by up to 150 m of Columbia River Basalt Group, which in turn is covered by as much as 150 m of Deschutes Formation capped by younger basalt flows. Downstream of RM 85, the Deschutes River approaches the uplifted Mutton Mountains and much of the canyon wall is formed of the Eocene-to-Miocene John Day Formation and underlying Clarno Formation. High and distant rims are capped by flows of the Columbia River Basalt Group. By RM 60, the Deschutes River has passed the Mutton Mountains and enters the tectonic basin near Maupin, where the top of the John Day Formation descends to near river level, and the northward-thickening Columbia River Basalt Group composes much of the valley walls. In the structural trough between RM 60 and 40, Dalles Formation and capping basalt flows overlie the Columbia River Basalt Group. Downstream of RM 50, the entire canyon is formed in Columbia River Basalt Group except for less than 100 m of Dalles Formation capping the tablelands downstream of RM 10.

From the Pelton-Round Butte dam complex downstream to about RM 60, the John Day and Clarno Formations are exposed at river level. These formations are susceptible to landsliding, and the canyon margins within this reach have been affected by an almost continuous series of landslide complexes. Landslides are largest where the John Day Formation has been uplifted the highest, such as along the axis of the Mutton Mountains anticline between RM 85 and 65. The largest landslides cover areas as great as 50 km^2, and extend as far as 6 km from canyon rim to river. As described in greater detail in later sections, some of these landslides temporarily blocked the Deschutes River. The overall result in this reach is that the Deschutes River winds tortuously through an irregular, landslide-dominated topography underlain by the alternating soft tuffaceous sediment and much harder volcanic rocks of the John Day and Clarno Formations, as well as by volcanic rocks displaced from canyon walls by slides, and remnant landslide dams of various ages.

Downstream of RM 60, the Deschutes River flows within a canyon largely composed of layered basalts of the Columbia River Basalt Group. The general canyon trend follows regional structures, especially where it parallels the Tygh Ridge anticline between RM 40 and 12, and the Gordon Ridge anticline between RM 12 and 8 (Figure 1). The somewhat regular meandering pattern (Figures 1 and 2b) within these general trends must reflect the course of a low-gradient and wandering proto-Deschutes River, before incision into the Columbia River Basalt Group sometime between 4 and 1 million years ago [*O'Connor, Grant, and Haluska*, this volume]. At present, the river flows within a consistently narrow canyon deeply incised in the resistant Columbia River Basalt Group (Figure 3b), between precipitous valley walls drained by short, steep tributaries.

Valley-Bottom Morphology

The influence of underlying geology on morphology of the valley walls and bottom of the Deschutes River below

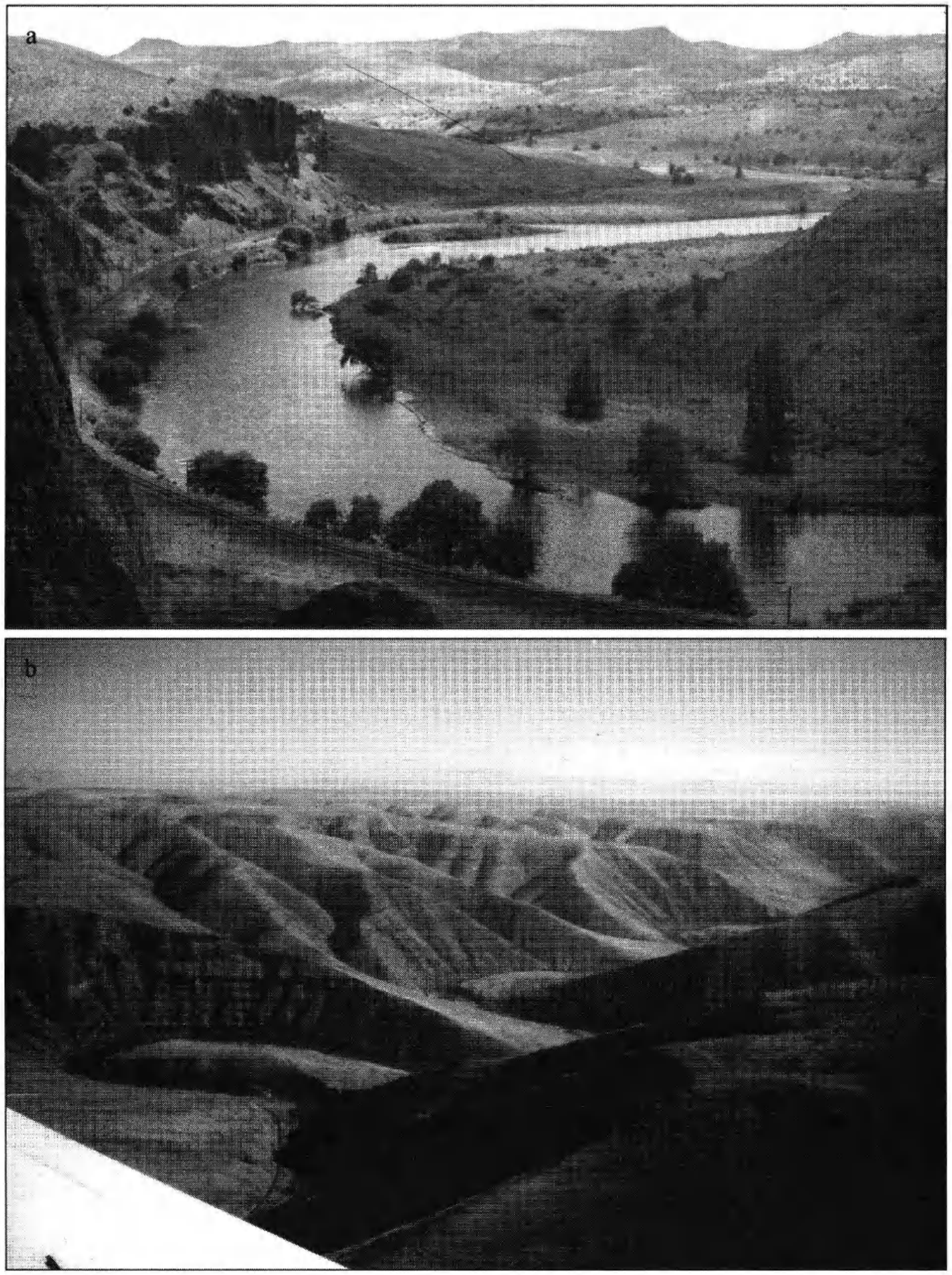

Figure 2. Photographs of the Deschutes River canyon. (a) June 24, 1998, view upstream (southwest) from RM 76.5. Cliffs in left foreground are rhyolite lava flows in the John Day Formation. Photograph by J.E. O'Connor. (b) Oblique aerial view downstream (northeast) from about RM 35, showing meanders incised into the layered flows of the Columbia River Basalt Group. Meander loop in the foreground is known as Beavertail, and the exposure shown in Figure 12 was excavated during construction of a railroad alignment across the inside of the meander loop. July 28, 1998, photograph by J. E. O'Connor.

the Pelton-Round Butte dam complex is illustrated by the transition in canyon morphology that takes place near RM 60, where the river leaves the Mutton Mountains anticline (Figure 3). Upstream of RM 60, the river flows on the soft and landslide-prone John Day and Clarno Formations, whereas the downstream 100 km of valley is mostly within the more resistant Columbia River Basalt Group. This distinction is most clearly shown by the pattern of valley width

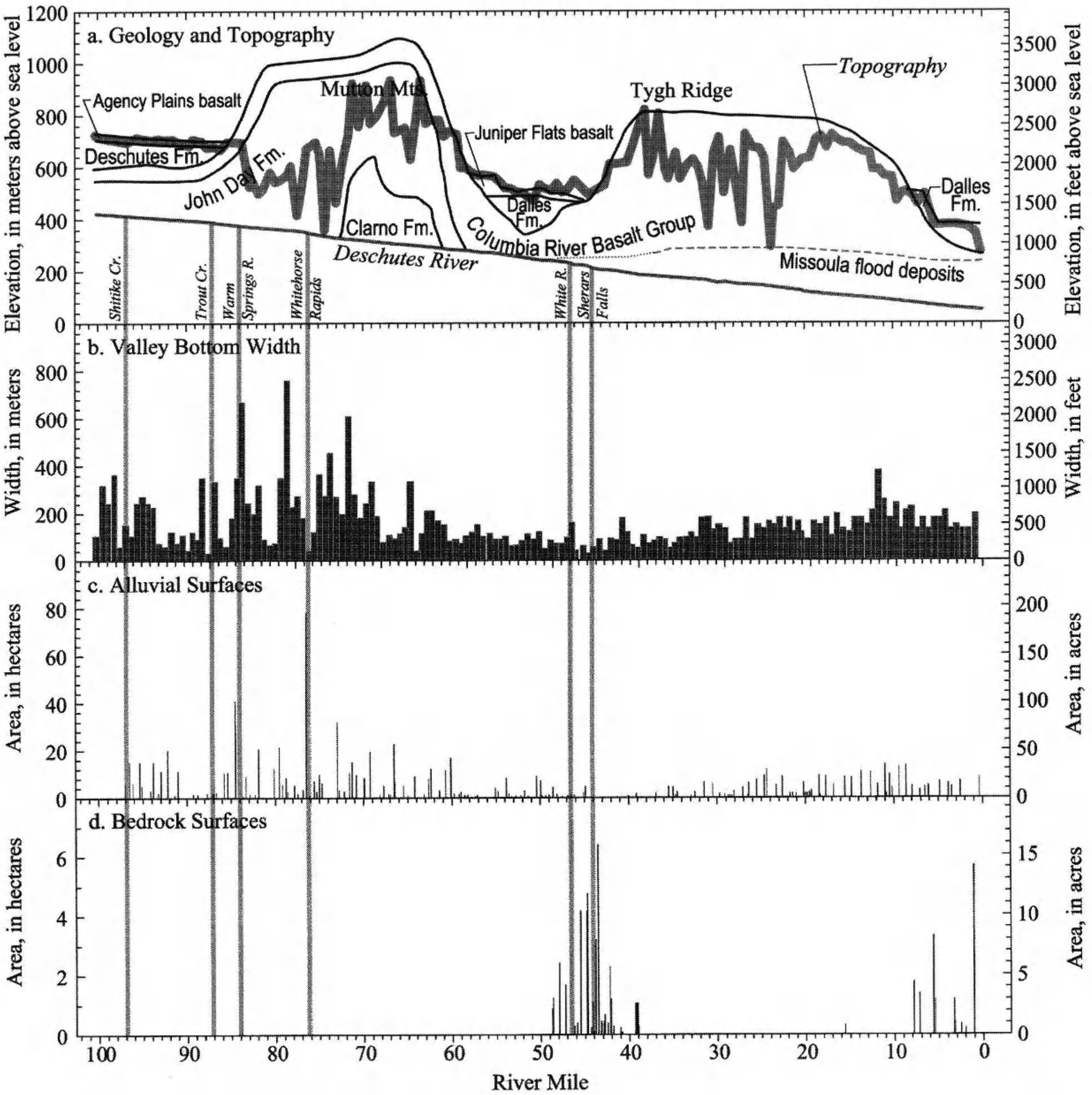

Figure 3. Canyon and valley-bottom characteristics of the lower Deschutes River. (a) Deschutes River profile and generalized geology and topography. River profile from elevation data on USGS 7.5-minute topographic maps. Topography is represented by the highest point within 2 km of the Deschutes River channel, measured from transects placed orthogonal to the channel and spaced at 1 km increments on USGS 7.5-minute topographic maps. Pre-Quaternary geology of the valley walls along the river generalized from position of contacts on 1-km spaced transects oriented perpendicular to the channel. Contact positions, in downstream order, after *Smith* [1987], *Smith and Hayman* [1987], *Waters* [1968a, b], *Bela* [1982], *Sherrod and Scott* [1995], and *Newcomb* [1969]. The distribution of Missoula flood deposits blanketing older rocks was mapped from aerial photographs and field reconnaissance. (b) Width of the valley bottom, as measured from transects oriented perpendicular to the channel and spaced at 1-km increments. (c) Distribution and size of alluvial surfaces within the valley bottom. (d) Distribution and size of bedrock surfaces within the valley bottom.

along the canyon bottom (Figure 3b). Upstream of RM 60, valley width varies greatly, ranging from 35 to 750 m. Most of the narrow reaches occur where relatively recent landslides or mass movements have encroached upon the valley bottom. There is no clear trend in downstream variation of valley width within this reach. Downstream of RM 60, valley width is almost everywhere less than 200 m, has much less spatial variation, and systematically increases downstream. Variation in valley width has in turn affected the sizes and distribution of valley bottom features such as alluvial surfaces (relatively flat surfaces underlain by fluvial deposits; Figure 3c), because there is additional space within the valley bottom upstream of RM 60 to accommodate their formation and preservation. *Curran and O'Connor* [this volume] present more information on the distribution of valley-bottom surfaces and their relation to channel and valley processes.

Another effect of overall canyon geology is the distribution of bedrock in the channel bottom and along channel margins. Between RM 50 and RM 40, bedrock crops out along much of the channel bottom and flanking valley-bottom surfaces (Figure 3d). In this reach, channel and valley width are at their overall minima. This section of the Deschutes River is a bedrock reach [e.g., *Tinkler and Wohl*, 1998], and it corresponds to the canyon entering the rising limb of the Tygh Ridge anticline (Figure 2). This reach is almost completely erosional, with little stored alluvium, due to either ongoing uplift or a more pronounced resistance of the slightly upturned Columbia River Basalt Group flows [e.g., *Bretz*, 1924]. A similar reach of abundant bedrock surfaces occurs in the final 13 km of the river above its confluence with the Columbia River. All of the large bedrock rapids and falls on the lower Deschutes River are within these two reaches [*Curran and O'Connor*, this volume].

QUATERNARY HISTORY OF THE LOWER DESCHUTES RIVER

Within the context of general geologic controls on valley morphology, several processes and events have further shaped the lower Deschutes River. Here we describe evidence and features left by several specific events, including volcanic eruptions (lava flows, lahars and pyroclastic fallout), landslides, and floods of various sources and magnitudes. This overview is not complete, especially for the Pleistocene history of the canyon, for which we have conducted only reconnaissance-level field studies. Description of Holocene and modern events and processes is brief here—further information may be found in the cited companion papers that appear later in this volume.

Volcanic Events

In the last million years, the Deschutes River canyon has been inundated by basalt flows, pyroclastic flows, and lahars that have locally altered canyon morphology and introduced immense quantities of sediment to the channel and valley bottom.

Lava flows. Just upstream of the study area, extensive flows from the Newberry Volcano and nearby vents flowed into and partly filled the Crooked and Deschutes River canyons between <0.4 and 1.2 Ma [Figure 2 of *O'Connor, Grant, and Haluska*, this volume; *Russell*, 1905; *Stearns*, 1931; *Smith*, 1986, 1991; *Sherrod and others*, in press]. The vestige of these flows farthest downstream is the bench near RM 109, just upstream of Round Butte Dam. After partial filling of the canyons with lava flows, the Deschutes and Crooked Rivers re-incised through the lava flows and less resistant rocks at the margins of the flows. This incision was likely rapid at first, but slowed as the overall gradient declined and the downcutting river intersected more resistant strata. The pronounced increase in the general gradient of the Deschutes River upstream of the Crooked River confluence (now inundated by Lake Billy Chinook) indicates that the river has not yet completely re-incised to pre-lava flow levels. While these lava flows did not have a direct effect on the Deschutes River valley downstream of the Pelton-Round Butte dam complex, early stages of incision of new canyons likely generated tremendous volumes of sediment that would have been rapidly transported downstream.

Within the study area and close to the Columbia River confluence, a small basaltic lava flow from Gordon Butte entered the Deschutes River canyon from the east at RM 4.5 and flowed down the canyon for at least 2 km (Figure 4). Two remnants are preserved on valley margins on the east side of the river: one where the flow entered between RM 4.5 and 4.0, and another between RM 2.6 and 2.2 [*Newcomb*, 1969]. At both locations, the river apparently incised new canyons and channels west of the previous river corridor, resulting in locally narrower valley bottoms, flanked on the east by basalt cliffs formed from the lava flow remnants. Exposures at the base of the lava flow at RM 2.5 show basalt directly on top of unweathered gravel, indicating that the flow invaded the Deschutes River at an elevation about 17.2 m above the elevation of present low-flow water surface. An adit excavated 30 m into the gravel along the base of the basalt flow shows that the bottom of the basalt flow dips slightly eastward, suggesting that the thalweg of the river at the time of the flow was likely under the present extent of basalt. The basalt flow has not been dated, but a similar flow from Stacker Butte, 21 km to the NNW

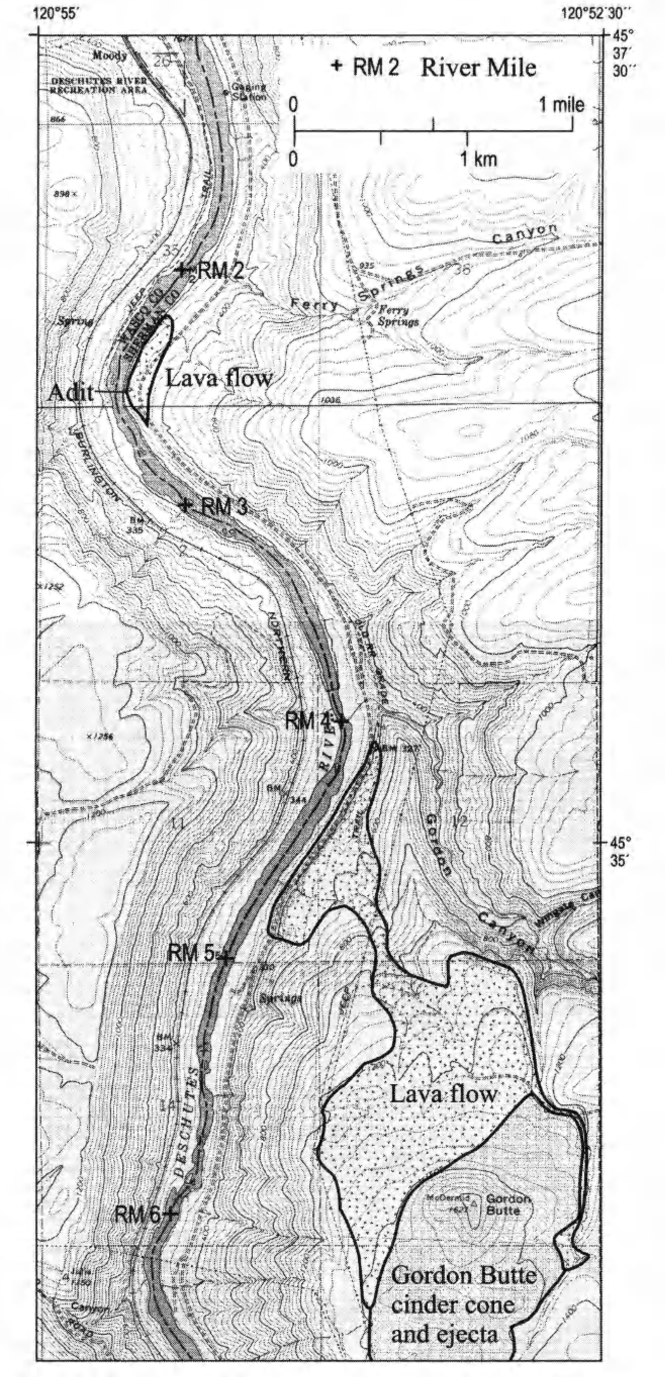

Figure 4. Quaternary cinder cone and lava flow from Gordon Butte. Topographic base from Emerson USGS 7.5-minute topographic quadrangle [contour interval 40 ft (12 m)]. Geology modified from *Newcomb* [1969].

(Figure 1), which flowed into the Columbia River at a similar elevation relative to the historic (pre-impoundment) river elevation, has been dated at 0.9±0.1 million years (Ma) [*Shannon and Wilson Inc.*, 1973, cited in *Bela*, 1982].

Lahars, pyroclastic flows, and tephra falls. Lahars (debris flows of volcanic origin) and other eruptive processes have episodically transported large quantities of sediment to the lower Deschutes River canyon. Concentrations of pumice granules and pebbles geochemically matching the 0.40-0.46 Ma Bend Pumice have been found in fluvial deposits exposed at RM 64 and RM 31 (Tables 1 and 2). Quaternary terraces between Pelton Dam (RM 104) and the Shitike Creek confluence (RM 96.6) contain a white pyroclastic-flow deposit, probably from Mount Jefferson [*Smith and Hayman*, 1987; G.A. Smith, 1998, written communication]. The elevation above the river and degree of soil development on the terrace surfaces suggest that the pyroclastic flow probably occurred at least 100,000 years ago.

Two outcrops along the lower Deschutes River contain deposits of a large lahar from Mount Jefferson that flowed most of the length of the canyon downstream of RM 84 (Figure 5). A 35-m-exposure at a railroad-cut into a terrace along the right side of the river at RM 84.0 shows round-cobble gravel capped by several pumice- and ash-rich beds of sand and gravel, including a 10-m-thick bed of poorly sorted bouldery gravel (Figure 5a). Glass in pumice clasts collected from a 20-cm-thick zone of pumice fragments at the bottom of the basal sandy bed (unit D of Figure 5a) geochemically matches a thick pumice fall from the last major explosive eruption of Mount Jefferson (Tables 1 and 2). At this exposure, the lahar deposits overlie about 5 m of unweathered fluvial gravel exposed to an elevation about 25 m above present river level, indicating that the channel was substantially higher at the time of the Mount Jefferson eruption than at present.

Another outcrop of a Mount Jefferson lahar from the same eruptive episode is exposed in a railroad cut at RM 14 (Figures 5b, 5c). The bottom of the exposure at this site consists of white silt-sized tephra conformably overlying grayish-tan silt, presumed to be loess (Figure 5c). This tephra, which also geochemically matches Mount Jefferson tephra and pumice (Tables 1 and 2), is capped by 50 to 75 cm of coarsening-up pumiceous sand and angular gravel, with diameters of isolated pumice clasts exceeding 5 cm. These pumice clasts also match Mount Jefferson tephra and pumice sampled from dispersed sites in Oregon and Idaho (Tables 1 and 2). Conformably overlying the angular gravel is 3 m of poorly sorted bouldery gravel. The contact between the two gravel units is gradational over about 30 cm, leading to the inference that both units were deposited contemporaneously

Table 1. Lower Deschutes River tephra and pumice correlations.

Site	Sample ID	Location (latitude and longitude, in degrees W and N)	Stratigraphic context	Correlation	Comments regarding stratigraphic relations, age and sources of age information
South Junction terrace RM 84.0	5/14/99-1(1)	44.8582 121.0708	1-5 cm diameter pumice clasts in lahar deposit	Mount Jefferson	Correlative tephra exposed in south-central Idaho underlies a Yellowstone tephra that has been dated by fission-track on glass at 76±34 ka [*Pierce,* 1985].
Whitehorse landslide ARM 75.6	6/24/98-2(1)	44.9400 121.0653	Silt-sized fallout tephra within closed depression on land-slide	Mount Mazama	6730±40 ^{14}C yr B.P. [*Hallett et al.*, 1997]
Dant debris flow RM 64.2	7/16/98-2(2)	45.0403 121.0006	Pumice granules in fluvial and lacustrine deposits	Bend Pumice	Correlative pumice fall near Bend, OR, dated at 400 to 460 ka [*Sarna-Wojcicki et al.*, 1989; *Lanphere et al.*, 1999]
Caretaker Flat RM 61.7	7/16/98 1(17)	45.0670 121.1125	Silt-sized fallout tephra interbedded with Holocene fluvial overbank deposits	Mount Mazama	(see above)
Beavertail RM 31.0	9/29/98-1(1)	45.3325 120.9422	Pumice granules in Pleistocene fluvial deposit, 25.4 m above present river level	Bend Pumice	(see above)
Lockit siding RM 14.0	10/1/98-2(1)	45.4962 120.8345	Silt-size fallout tephra on Pleistocene loess	Mount Jefferson	(see above)
Lockit siding RM 14.0	10/1/98-2(2)	45.4962 120.8345	1-2 cm diameter pumice clasts at base (lowermost 5 cm) of lahar deposit overlying fallout tephra	Mount Jefferson	(see above)
Lockit siding RM 14.0	10/1/98-2(3)	45.4962 120.8345	2-5 cm pumice clasts from lower 1.0 m of lahar deposit	Mount Jefferson	(see above)

or in close succession by a large lahar or lahars from Mount Jefferson. The lahar deposits are capped by 1.5 m of tan silt, probably Missoula flood deposits and loess. The base of the lahar is 13 m above the present water surface. Although the channel elevation at the time of the lahar at this location is not known, the presence of at least a meter of loess beneath the lahar deposit indicates that the river was several meters lower than the bottom of the lahar deposits.

The lahar-producing Mount Jefferson eruption was large and explosive, generating thick tephra falls in the 20 km surrounding the volcano, and lighter falls detectable as far away as southeast Idaho [*Beget*, 1981; *Conrey*, 1991; *Walder et al.*, 1999]. Pyroclastic flows entered drainages on the east and west sides of the volcano [*Conrey*, 1991]. Judging from the distribution of eruptive products, the eruption was likely concurrent with advanced glaciers (Gary Smith, University of New Mexico, written communication, 2001). Consequently, tremendous meltwater volumes were likely generated during major eruptions, significantly contributing to the size and travel distance of the lahars. The thickness and coarseness of deposits and >225 km travel distance, as well as the superposition of lahar deposits on >5 m of unweathered coarse gravel fill at RM 84 (Figure 5a) and loess that was apparently actively accumulating at RM 14 (Figure 5c), suggest that an eruption occurred during a time of substantial ice volume. Poorly exposed boulder

Table 2. Volcanic glass compositions of tephra in outcrops along the lower Deschutes River and inferred correlative and dated tephra (shaded). Composition values given as oxides, in weight-percent, recalculated to 100 percent on a fluid-free basis. Details of analytical methods provided in Appendix 2 of O'Connor et al., 2001.

Sample[a]	SiO_2	Al_2O_3	Fe_2O_3	MgO	MnO	CaO	TiO_2	Na_2O	K_2O	ΣWt%
					Bend Pumice Correlatives					
7/16/98-2(2)	74.69	13.70	1.85	0.11	0.07	0.80	0.14	5.11	3.55	100.02
9/29/98-1(1)	74.82	13.58	1.81	0.10	0.06	0.76	0.14	4.95	3.78	100.00
BPT-1 (Bend Pumice, near Bend, OR)	74.85	13.72	1.94	0.11	0.07	0.74	0.14	5.09	3.34	100.00
					Mount Jefferson Correlatives					
5/14/99-1(1)	74.58	14.36	1.77	0.34	0.04	1.60	0.25	4.80	2.27	100.01
10/1/98-2(1)	74.87	13.85	1.76	0.31	0.05	1.54	0.24	4.87	2.50	99.99
10/1/98-2(2)	74.56	13.93	1.81	0.31	0.05	1.55	0.26	5.01	2.53	100.01
10/1/98-2(3)	74.60	13.89	1.77	0.32	0.06	1.57	0.27	5.02	2.50	100.00
SD 1490-1 (Pumice at Mount Jefferson)	74.85	14.08	1.79	0.32	0.05	1.54	0.24	4.68	2.44	99.99
ARCO A2-8 (>0.40 Ma tephra in south-central Idaho)	74.98	13.78	1.79	0.31	0.05	1.54	0.26	4.77	2.52	100.00
					Mount Mazama Correlatives					
7/16/98 1(17)	72.54	14.52	2.20	0.47	0.06	1.58	0.43	5.40	2.79	99.99
6/24/98-2(1)	72.55	14.54	2.25	0.48	0.05	1.58	0.44	5.35	2.76	100.00
Mazama Ash average (n=100)	72.79	14.65	2.12	0.46	0.05	1.61	0.42	5.19	2.71	100.00
					Homogenous Glass Standard (18 electron microprobe analyses)[b]					
RLS 132 (±1σ)	75.4±0.1	11.3±0.2	22±0.04	0.06±0.01	0.16±0.01	0.11±0.01	0.19±0.01	4.9±0.01	4.4±0.1	100.00

[a]Sample location and stratigraphic context provided in Table 1.

[b]Replicates of a natural glass standard (RLS 132) provide indication of analytical precision.

deposits flanking the Deschutes River valley bottom at many other locations may also date from this Mount Jefferson lahar. A lahar from the same eruptive period also traveled far enough to enter the Willamette Valley from the east [*O'Connor et al.*, 2001]

The only quantitative age information for this Mount Jefferson eruption is from a trench in eastern Idaho, where stratigraphic relations show that the eruption closely predates a Yellowstone tephra that has a 76±34 ka[1] fission track date [*Pierce*, 1985], thus indicating that the eruption and associated lahars are probably 42-110 ka. A plausible time for the eruptive period is the penultimate ice age of 74-59 ka during marine oxygen isotope stage 4 [*Martinson et al.*, 1987].

A much more recent lahar from Mount Hood flowed down the White River and perhaps into the Deschutes River at the White River confluence at RM 46.4. Downstream of the confluence, deposits of coarse lithic-rich sand flank both sides of the Deschutes River for several kilometers downstream on surfaces just above the limits of historic flooding.

[1] ka = kilo-annum, or thousand years ago

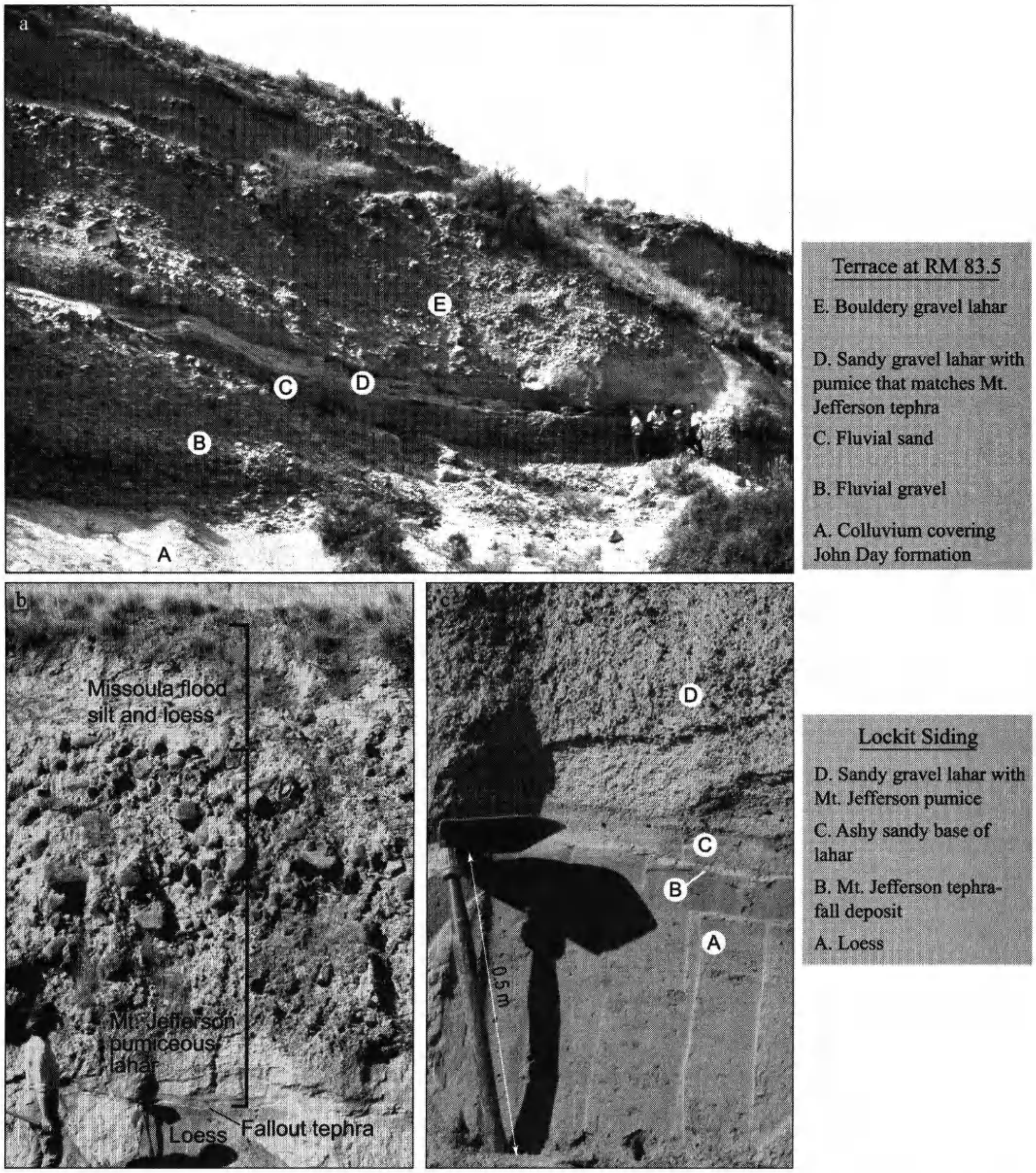

Figure 5. Exposures of lahar deposits from the circa 70 ka eruption of Mount Jefferson. (a) Part of 35-m-high terrace exposure at RM 83.5. The terrace surface is about 50 m above river level. A. colluvium covering tilted strata of the John Day Formation; B. fluvial gravel; C. fluvial sand; D. sandy gravel lahar with abundant pumice and volcanic glass fragments, including pumice clasts (collected near people in photo) that geochemically match Mount Jefferson tephra (Tables 1 and 2); E. poorly sorted bouldery gravel lahar containing abundant pumice clasts. May, 14, 1999, photograph by J.E. O'Connor. (b) Exposure of deposits at Lockit siding on the left valley margin, 12 to 17 m above the level of the Deschutes River and 22.5 km upstream of the Columbia River confluence (R.M. 14.0). The volcanogenic units overlie unweathered micaceous loess and are overlain by 15-12 ka Missoula flood deposits and loess. The fallout tephra at the base of the lahar and pumice clasts within the lahar match the composition of pumice and tephra from a large, circa 70 ka, Mount Jefferson eruption (Tables 1 and 2). Shovel handle is 0.5 m long. Photograph by J.E. O'Connor, Oct. 1, 1998. (c) Close-up of b (shovel is in the same location), showing: A. loess; B. Mount Jefferson tephra-fall deposit; C. ashy sandy base of lahar; and D. poorly-sorted sandy gravel lahar, containing abundant pumice clasts from Mount Jefferson. Photograph by J. E. O'Connor, Oct. 1, 1998.

These sands are similar to sandy lahar deposits farther up the White River that were deposited during the Old Maid eruptive period at Mount Hood, tentatively dated at AD 1781 (Patrick Pringle, Washington Dept. Natural Resources, and Thomas Pierson, U.S. Geological Survey, oral communication, 2002). The White River is continuing to entrain these sandy lahar deposits from eroding terraces, bringing much sandier sediment to the lower Deschutes River than the other Cascade Range tributaries [*McClure*, 1998; *Fassnacht et al.*, this volume].

Landslides

Between the Reregulating Dam (at RM 100) and RM 60, the valley margins are an almost continuous series of landslides composed of large and jumbled blocks of John Day and Clarno Formations [*Smith and Hayman*, 1987]. In addition, there have been large landslides within the Columbia River Basalt Group between RM 55 and 53, and smaller mass movements within Missoula flood deposits downstream of RM 8. Some of the largest landslide complexes involved up to 50 km² of terrain. Judging from the morphology of the landslides, these mass movements have a wide variety of ages, probably ranging from several hundred thousand years old to perhaps less than 10,000 years old. These large landslides have had several direct and indirect effects on the valley bottom and channel that persist today. Foremost, many have rafted large volumes of debris to the bottom of the canyon and significantly narrowed the valley bottom and channel. The mass movements at Whitehorse Rapids (Figures 6 and 7; RM 76) and near Dant (Figure 8; RM 64) completely blocked the channel, resulting in temporary impoundment of the Deschutes River. Such landslide dams are intrinsically unstable [*Costa and Schuster*, 1988], and boulder deposits downstream of Whitehorse Rapids and Dant suggest that both landslide dams breached rapidly enough to cause large floods. Additional evidence for such flooding is discussed in a later section.

Whitehorse Rapids landslide. The Whitehorse Rapids landslide (Figures 6 and 7) is probably the youngest and best documented of the major mass movements to affect the valley bottom. This landslide, shown on the 1968 geologic map by Waters, covers a semicircular-shaped area of 7 km² on the eastern valley slope. The slope slid or flowed westward, completely blocking the valley for a channel-wise distance of about 1 km. The entire landslide is within the John Day Formation, locally composed of rhyolite lava domes and flows, as well as tuffs and tuffaceous claystones [*Waters*, 1968a, 1968b; *Robinson et al.*, 1984]. The surface of the landslide is a chaotic landscape of knobs and closed depressions, bounded to the east by an arcuate scarp 60 to 100 m high. Whitehorse Rapids landslide is a morphologically younger part of an even larger landslide complex involving 50 km² of terrain that has moved westward into the Deschutes River Canyon between RM 85 and 74 (Figure 1).

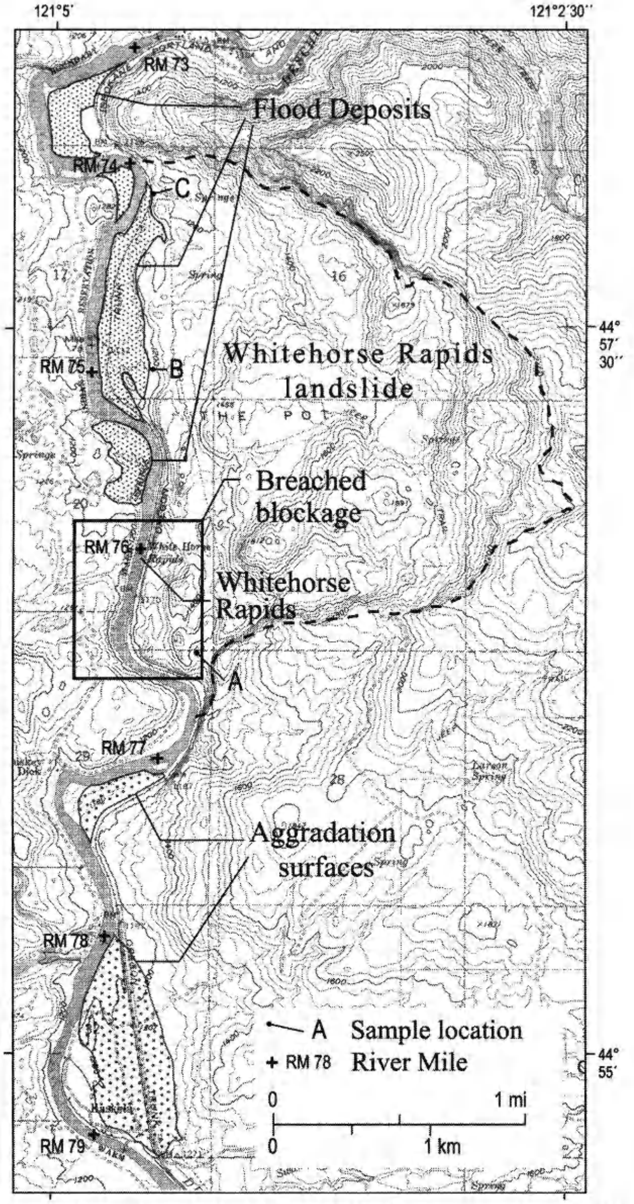

Figure 6. Portion of the Kaskela USGS 7.5-minute topographic quadrangle [contour interval 40 ft (12 m)] showing the Whitehorse Rapids landslide and associated features. Labeled stratigraphic sites are described in text and show locations where radiocarbon and tephra samples were collected and analyzed (Tables 1 and 2).

The present topography near the blockage indicates that the maximum impoundment could have been as high as 35-

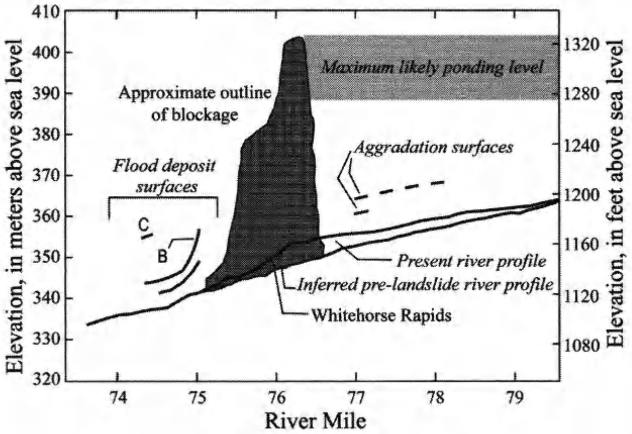

Figure 7. Profile of Deschutes River, and landslide and flood features near Whitehorse Rapids landslide. Deschutes River profile from the 1.5-m-contour (5 ft) river survey of *Henshaw et al.* [1914], conducted in 1911. The river mile locations in that survey are about 0.2 mi downstream of river mile locations shown on current maps. The pre-landslide river profile was based on extrapolation of the surveyed gradient of the Deschutes River from downstream of Whitehorse Rapids. Elevations of flood deposits and aggradation surfaces from site surveys and USGS 7.5-minute topographic quadrangles. 'C' and 'B' indicate locations of stratigraphic sites shown in Figure 6 and discussed in text.

50 m (Figure 7), which would have caused a temporary lake to back up nearly 30 km upstream to the Trout Creek confluence, although there is no evidence that ponding attained that level. Two gravel terraces, 5 m and 10 m above present river level, 1.4 km upstream from the blockage, are inferred to have resulted from aggradation behind the landslide dam. These terraces may indicate that the landslide dam lasted long enough to allow more than 10 m of sand and gravel to accumulate in the valley bottom (relative to the inferred pre-landslide channel profile shown in Figure 7); and that there were at least two periods when the channel was stable at different elevations significantly higher than the present channel elevation. The latter inference suggests that the landslide dam did not fail completely in one breaching episode, but with multiple episodes of incision, and that the time between incision episodes was sufficient for development of distinct aggradation surfaces. The landslide has not yet been completely breached—Whitehorse Rapids, which drops about 12 m in 1 km, is the remains of the landslide dam, and is composed of blocks too large to have been moved during incision. A comparison of the present river profile with the overall channel profile trend indicates that the present channel is as much as 7.5 m higher than the pre-landslide channel elevation (Figure 7).

There is no precise information on the age of the landslide and resulting flood(s). An excavation into the floor of a small closed depression on the landslide exposed Mazama ash 1.1 m below the surface (site A in Figure 6; Tables 1 and 2), indicating that the landslide formed before the 6730±40 ^{14}C yr BP [*Hallet et al.*, 1997] climactic eruption of Mount Mazama. A small charcoal clast in a high flood deposit exposed in a railroad cut at RM 74.4 (site C in Figure 6) had an age of 38,740±540 ^{14}C yr BP (Table 3), providing a maximum bracketing age on both the landslide and the flood that apparently resulted from breaching of the landslide dam (discussed in a subsequent section). A piece of charcoal sampled from sediment that accumulated on top of flood deposits (site B in Figure 6) indicates that the high flood deposits predate 3840 ^{14}C yr BP (Table 3). In summary, these dated samples suggest that the landslide occurred between 38,740±540 ^{14}C yr BP and 6730±40 ^{14}C yr BP, and the resulting flood(s) took place between 38,740 ^{14}C yr BP and 3840±40 ^{14}C yr BP. The thick and coarse accumulation of gravel upstream of the blockage may indicate that the landslide and resulting aggradation occurred during a period of enhanced sediment production in the basin, perhaps coincident with aggradation of the Willamette River (the adjacent basin to the west) during the last glacial maximum of 30,000 to 22,000 years ago [*O'Connor et al.*, 2001].

Dant debris flow. Another mass movement blocked the Deschutes River channel near the present-day vacation community of Dant at RM 64 (Figure 8). This mass movement has a flow-like morphology, with 5- to 10-m-high subparallel ridges aligned with the apparent flow direction for the lowermost kilometer of the deposit. The flow deposit is not traceable to a distinct mass movement or head scarp, but emerges from 1 km^2 of terrain that presumably partly collapsed. Like the Whitehorse Rapids landslide, the source area of the Dant debris flow is entirely within the John Day Formation.

The Dant debris flow apparently blocked the Deschutes River for a length of about 0.5 km. Bedded silt, sand, and gravel exposed in a road cut and underlying a colluvial slope at the upstream margin of the blockage (Figure 8) is inferred to have been deposited in the lake dammed by the deposit, and indicates that the blockage was at least 30 to 40 m high. Fluvially transported pumice granules deposited within these lacustrine deposits are chemically similar to the Bend Pumice [*Taylor*, 1981; Tables 1 and 2], and may indicate that the landslide occurred close to the 0.40-0.46 Ma age [*Sarna-Wojcicki et al.*, 1989; *Lanphere, et al.*, 1999] of the pumice.

Boxcar landslide complex. Three contiguous landslides, all smaller than the Whitehorse and Dant mass movements,

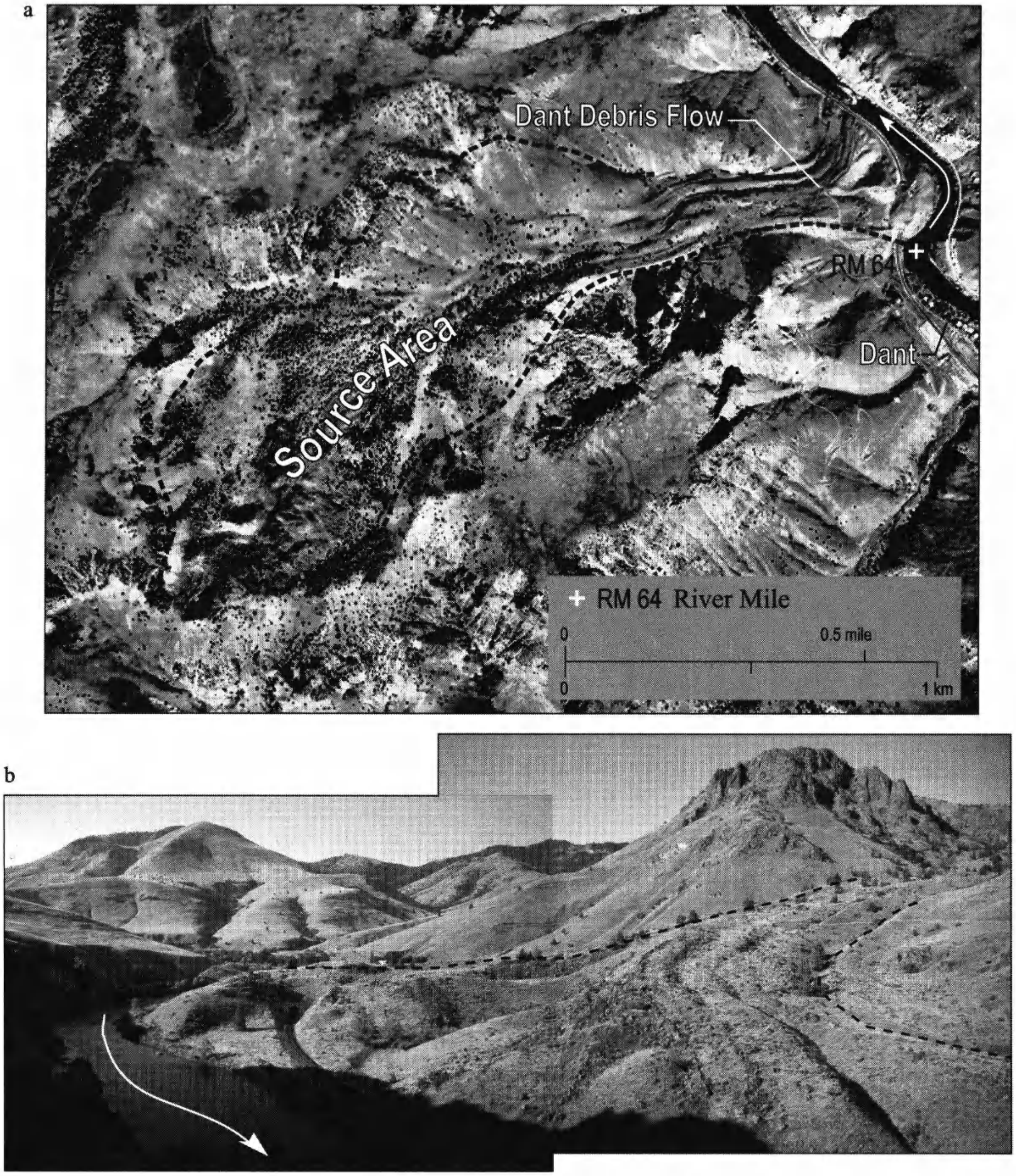

Figure 8. Dant debris flow. (a) Vertical aerial photograph (1995, Portland General Electric) showing flow deposit and inferred source area. (b) Two-photograph panorama directed upstream (south) showing terminus of flow deposit. Railroad and tunnel indicate scale. July 17, 1998, photographs by J. H. Curran.

Table 3. Radiocarbon ages.

Site	Sample ID (field label and laboratory no.)	Location (latitude and longitude, in degrees W and N)	Material	Corrected conventional ^{14}C age BP ±1 sigma[a]	$^{13}C/^{12}C$ ratio (%)
Whitehorse Landslide B	6/25/98-2(1) Beta 122390	44.9559 121.0825	charcoal	3840±140	-23.6
Whitehorse Landslide C	6/25/98-3(3) Beta 121597	44.9666 121.0750	organic fragments	38,740±540	-26.6

[a] Radiocarbon ages (in ^{14}C yr B.P.) are calculated on basis of Libby half-life for ^{14}C (5568 years). The error stated is $\pm 1\sigma$ on basis of combined measurements of the sample, background, and modern reference standards. Age referenced to AD 1950.

have partly blocked the lower Deschutes River between RM 55 and RM 53 near Boxcar Rapids (Figure 9). These landslides moved northwestward, and each involved 0.5 to 1.0 km^2 of eastern valley margin, which is formed entirely of Columbia River Basalt Group and overlying loess. A head scarp, up to 20 m high and extending 150 m above the present river level, bounds each of the landslides. Cross-cutting relations among the bounding scarps and distinct differences in the morphology of the landslide surfaces indicate that the middle landslide is the youngest, and the landslide to the northeast is the oldest. The landslides presently constrict the channel and valley bottom between a steep, 150-m-high, canyon slope formed in the Columbia River Basalt Group on the left, and 60-to-70-m-high bouldery slopes along the landslide toes. Some or all of these landslides may have blocked the river, although we have found no evidence of ponding upstream. Coarse bouldery deposits at Boxcar Rapids (Figure 9) and downstream may have resulted from breach of one or more landslide dams at this site.

Other hillslope processes. These previously discussed mass movements are the most dramatic hillslope processes modifying the valley bottom, but not the only ones that have affected valley-bottom and channel morphology [*Curran and O'Connor*, this volume]. Rockfall and talus aprons reach the valley bottom in places, contributing coarse sediment to the valley and channel, especially where Columbia River Basalt Group is exposed at river level. Rills and gullies have locally contributed fine sediment to the valley bottom. Mecca Flat, at RM 95, appears to be composed of three coalescing alluvial fans that emanate from unvegetated gullies in the east canyon walls (Figure 10a). These gullies and several others nearby are incised into the fine sediment of the John Day Formation, possibly triggered by breaching of the protective cover of rubble derived from basaltic lava flows higher in the canyon walls. Rills and gullies have also dissected hillslopes flanking the lower 60 km of the Deschutes River valley, where late Pleistocene Missoula flood deposits and loess have mantled the valley with up to several meters of silt and clay (Figure 10b). Rill and gully formation triggered by local convective storms has likely always occurred, but the frequency and volume of rill and gully erosion have probably increased during the last two centuries due to domestic grazing, rerouting of drainage by rail and road construction, and field runoff.

Floods and Fluvial Processes

Large floods and debris flows generated by a variety of mechanisms have coursed down and into the Deschutes River canyon during the Quaternary. These floods and their transported materials are mainly responsible for the present morphology of the river channel and floodplain features. Mainstem Deschutes River floods of different sizes and sources have formed nearly all of the alluvial surfaces that flank the channel and have carved the bedrock channels in the bedrock reaches [Curran and O'Connor, *this volume*]. Tributary floods and debris flows have built up alluvial fans at tributary junctions. Backflooding of the Deschutes River by the late Pleistocene Missoula floods flowing down the Columbia River also left deposits on the Deschutes River valley bottom and margins.

Landslide breach floods. Large bars of coarse bouldery gravel downstream from landslides are evidence that breaching of temporary landslide dams has been an important mechanism producing large floods on the lower Deschutes River. These gravel bars locally contain subrounded boulders with diameters exceeding 5 m. Immediately downstream from breached landslide dams, flood bars are far above stages achieved by more recent floods. Flood deposits are lower and finer farther down-

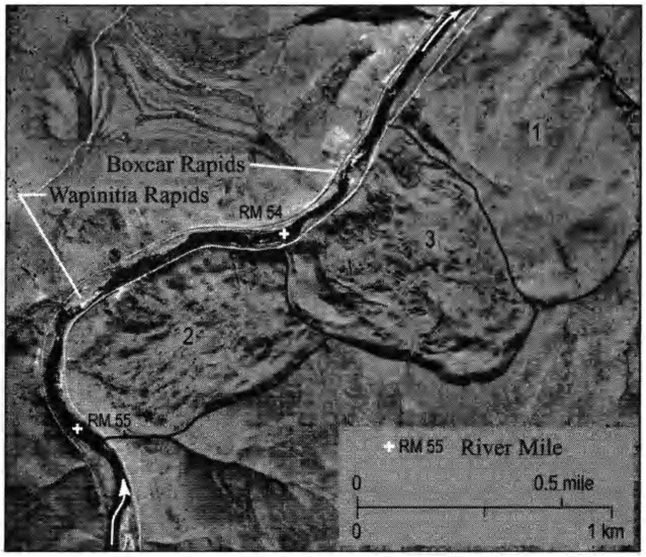

Figure 9. Vertical aerial photograph (1995, Portland General Electric) of landslides near Boxcar Rapids.

stream of breaches, and indistinguishable from flood deposits left by other types of floods. Between RM 100 and RM 50, bouldery gravel deposits can be traced up to 5 km downstream from the landslide breaches at Whitehorse Rapids, Dant, and Boxcar Rapids. The evidence is most compelling for the Whitehorse Rapids landslide, where the landslide, upstream aggradation features, and downstream flood features are all logically linked (Figures 6, 7, and 11). Nevertheless, bouldery deposits downstream of the Dant debris flow and the complex of landslides near Boxcar Rapids are strong evidence that such breaches have been a repeated process.

Based on limited information on the age of the landslides and resulting floods, most of these deposits are likely of Pleistocene age. Nevertheless, the clasts left in deposits by landslide-breach floods are exceptionally large and have been very resistant to subsequent modification. Consequently, landslide-related flood deposits form persistent elements of the Deschutes River valley bottom. These features include flood bars adjacent to the channel downstream of all the identified landslide breaches, and in-channel boulder accumulations that now form rapids or riffles downstream of breaches, such as Trout Creek Rapids (RM 87), the bouldery riffles downstream of Whitehorse Rapids landslide, and the Four Chutes Rapid 0.8 km downstream from the Dant debris flow. Boxcar Rapids may also be part of an accumulation of huge, 5-to-10-m diameter boulders, deposited during the breach of one of the nearby landslides [Figure 9; *Curran and O'Connor*, this volume].

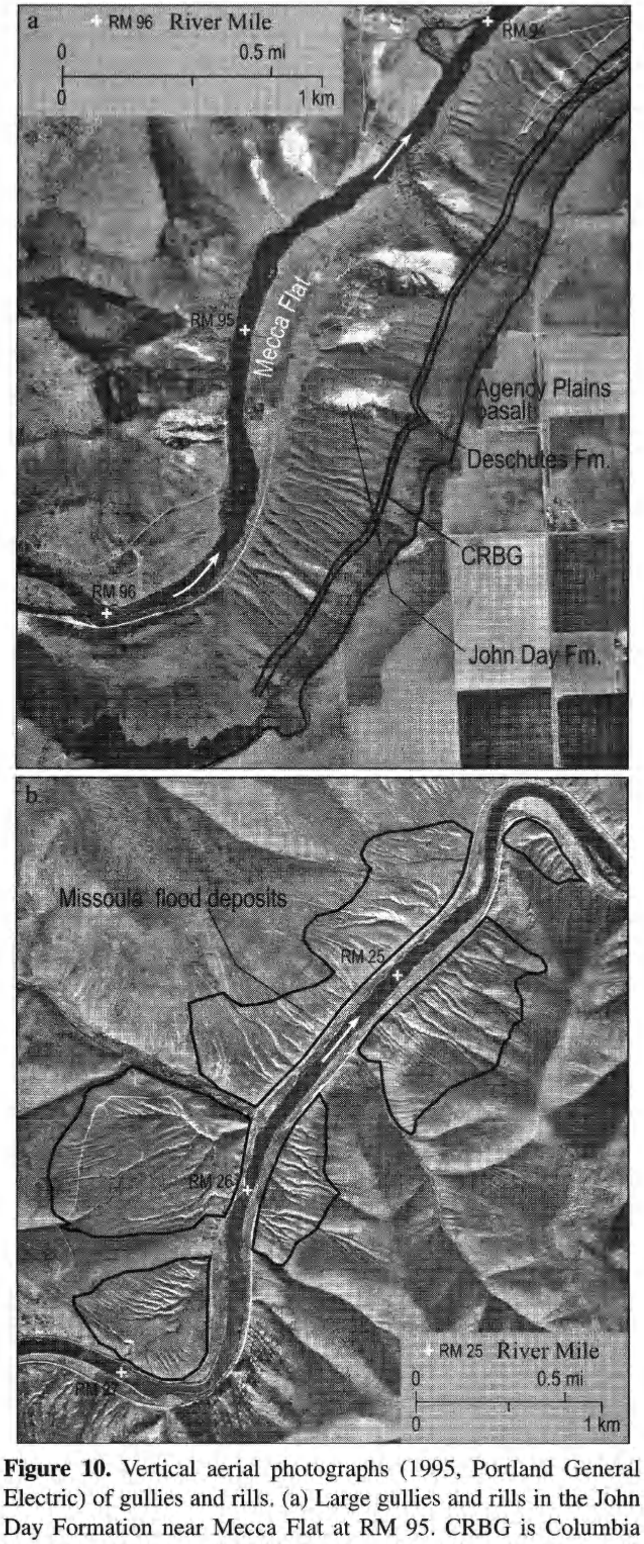

Figure 10. Vertical aerial photographs (1995, Portland General Electric) of gullies and rills. (a) Large gullies and rills in the John Day Formation near Mecca Flat at RM 95. CRBG is Columbia River Basalt Group. (b) Rills developed in Missoula flood sediment near RM 25. Missoula flood sediment mantles valley slopes developed in Columbia River Basalt Group.

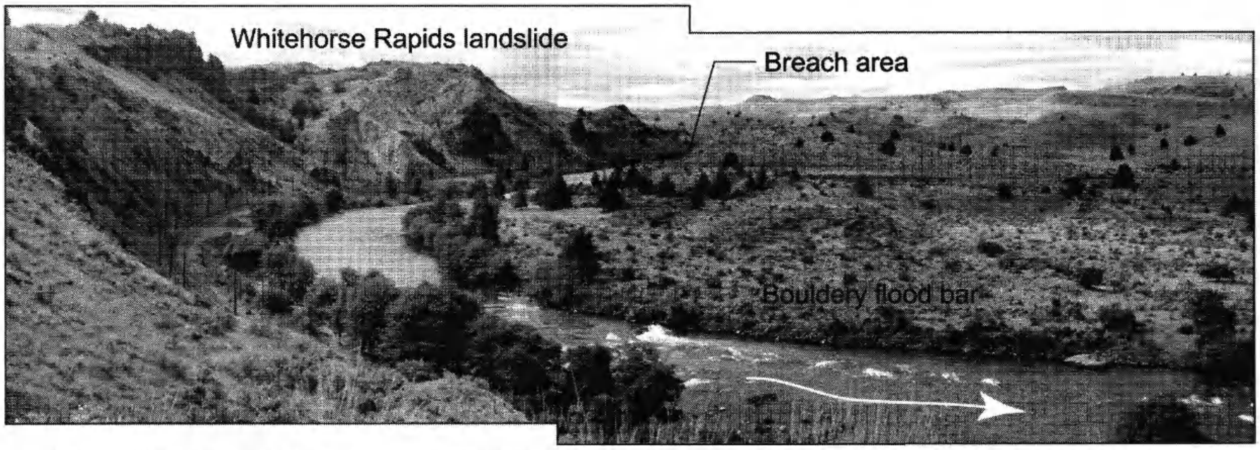

Figure 11. Two-photograph panorama of boulder flood bar downstream from the breach of Whitehorse Rapids landslide. View upstream (south) from right valley slope near RM 75.0. June 25, 1998, photographs by J. E. O'Connor.

Missoula floods. The late Pleistocene Missoula floods resulted from cataclysmic releases of ice-dammed Glacial Lake Missoula [*Bretz*, 1969], sending 60 to 90 large floods [*Atwater*, 1986] down the Columbia River between 15 and 12.7 ka [*Waitt* 1980, 1985; *Atwater*, 1986]. In the Columbia River valley at the confluence of the Deschutes River, the maximum stage of the largest Missoula flood was about 300 m above sea level or about 250 m deep [*O'Connor and Waitt*, 1995]. If maintained at steady state, this water would have back-flooded the Deschutes River valley as far upstream as RM 60. Silt, clay, and sand carried in suspension by these floods mantles the valley slopes adjacent to the Deschutes River to an elevation of 275 m above sea level and as far upstream as RM 45 (Figures 3 and 12). Erosion of these fine-grained deposits has been a continuing source of sediment to the lowermost 60 km of the lower Deschutes River (Figure 10b).

The Outhouse flood. At several locations along the Deschutes River canyon downstream of the Pelton-Round Butte dam complex, high cobble and boulder bars are evidence of a Holocene flood much larger than the largest historic floods of 1964 and 1996 (Figure 13). We have termed this flood the "Outhouse flood," because of the apparent preference of the Bureau of Land Management for placing outhouses on bouldery bars deposited by this flood. Features, deposits, and the timing of this flood are discussed in more detail by *Beebee et al.* [this volume], *Curran and O'Connor* [this volume], and *Hosman et al.* [this volume]. In summary, many valley bottom features, including large boulder-gravel point bars and islands that stand several meters above maximum historic flood stages, similarly high stripped bedrock surfaces and adjacent boulder deposits, and large accumulations of sand and silt in backwater areas, are inferred to have been produced by this flood. Hydraulic modeling indicates that the peak discharge of the Outhouse flood was about twice that of the largest historic floods. Evidence for increasing peak discharge in the downstream direction indicates that this flood was likely generated by a meteorological mechanism rather than by some sort of natural dam failure [*Beebee and O'Connor*, this volume]. Radiocarbon and tephra relations constrain the age of the flood to between 7.6 and 3.0 ka.

Like the deposits resulting from the landslide dam failure floods, the cobbly and bouldery Outhouse flood bars are extremely resistant to subsequent erosion. The clasts composing these bars are larger than clasts entrained by modern floods, and large portions of these bars stand above stages achieved by the largest historic floods of 1964 and 1996. Only locally are these large bars eroded where high velocity flows of modern floods attack bar edges, but nowhere does it appear that cumulative erosion has exceeded more than a few percent of their original extent. It is far more common for these Outhouse flood bars to have been mantled by silt and sand by more recent flooding, especially on upstream apices.

Recent mainstem floods. Large floods have historically affected the mainstem of the Deschutes River downstream of the Pelton-Round Butte dam complex. Notable floods include the December 1964 and February 1996 floods, both of which had discharges of about 2000 m^3/s at the mouth and were the largest recorded in nearly 100 years of systematic streamflow measurements. Both of these floods, as well as the large historic flood of December 1861, were regional "rain-on-snow" events caused by rapid melting of heavy mountain snowpacks by warm and wet storms from the south Pacific. The Willamette River also flooded during

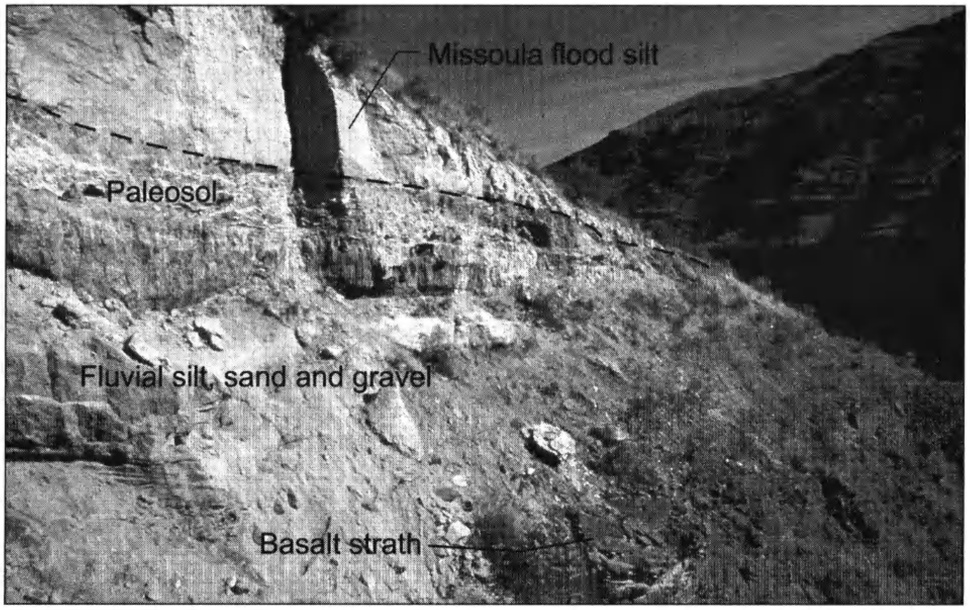

Figure 12. Exposure of 3 m of Missoula flood silt capping a paleosol developed in terrace gravel on right valley margin near Beavertail Campground at RM 31.0. The upper 2 m of terrace sand and gravel contains local concentrations of pumice grains that are geochemically similar to the circa 0.4 Ma Bend Pumice (Tables 1 and 2). September 29, 1998, photograph by J. E. O'Connor.

Figure 13. Boulder gravel of an Outhouse flood bar on the left bank at RM 4.2. Intermediate diameters of most boulders between 30 and 50 cm, but some intermediate diameters exceed 1 m. Sand between boulders deposited by the February 1996 flood, which inundated the bar to the elevation at which the person is standing, approximately 4 m lower than the prominent trim-line inferred to have been formed by the Outhouse flood. October 2, 1998 photograph by J. H. Curran.

each of these storms, as did the John Day River in 1964. On the Deschutes River, the 1861 flow was reported to be "higher than was ever known to white man or aboriginal" (Salem Statesman, December 23, 1861). Early settlers in the Willamette Valley vaguely recorded a large flood in the fall of 1813 that achieved stages close to, but probably slightly less than the 1861 flood [*Brands*, 1947]. Given the correspondence between the two basins, there was likely also an exceptionally large flow in the Deschutes River Basin in 1813. Flood frequency analysis of large main-stem floods, based on the historic record of flooding augmented by a 6000-yr stratigraphic record of Deschutes River floods is reported in *Hosman et al.* [this volume].

The February 1996 flood eroded some islands and margins of alluvial surfaces flanking the Deschutes River channel, and deposited gravel, sand, and silt in some overbank areas and island margins [Figure 14; *Curran and O'Connor*, this volume]. But compared to the consequences of large floods on most other alluvial rivers, there were few major or persistent geomorphic effects of the February 1996 flood in terms of bank erosion and deposition, channel scour and fill, and changes in substrate conditions [*McClure*, 1998; *Curran and O'Connor*, this volume, *Fassnacht et al.*, this volume]. The major broad-scale effects on the valley bottom due to flooding of this magnitude are the episodic accumulation and erosion of silt and sand overbank deposits on alluvial surfaces away from the main channel. A common depositional location is on the upstream ends of Outhouse flood bars (Figure 13). In these settings, high flows ramp up and slacken against the ascending bar surface. During the February 1996 flood, silt, sand, gravel, and much of the large wood carried by the flood was stranded on the upstream ends of many of these large bars. Wood accumulations locally impeded or concentrated flow, controlling patterns of scour and deposition of these surfaces. These alluvial surfaces may serve as the major sediment storage sites for sand and silt transported into and down the Deschutes River canyon. The sporadic accumulation and release of fine sediment depends on the sequence of flows, flow duration, suspended sediment and wood abundance, vegetation conditions, and the local hydraulic environment. Only the rare floods of magnitude similar to that of February 1996 are large enough to inundate these surfaces and cause significant sediment mobilization.

Tributary floods and debris flows. U.S. Geological Survey 7.5-minute quadrangle maps show 272 tributaries entering the Deschutes River between the Reregulating Dam at RM 100.1 and the Columbia River confluence. These tributaries contribute 6,904 km^2 of the total 27,460 km^2 drainage area of the Deschutes River basin. Most of the drainage area below the dams belongs to three large western tributaries that drain the eastern slopes of the Cascade Range, and three

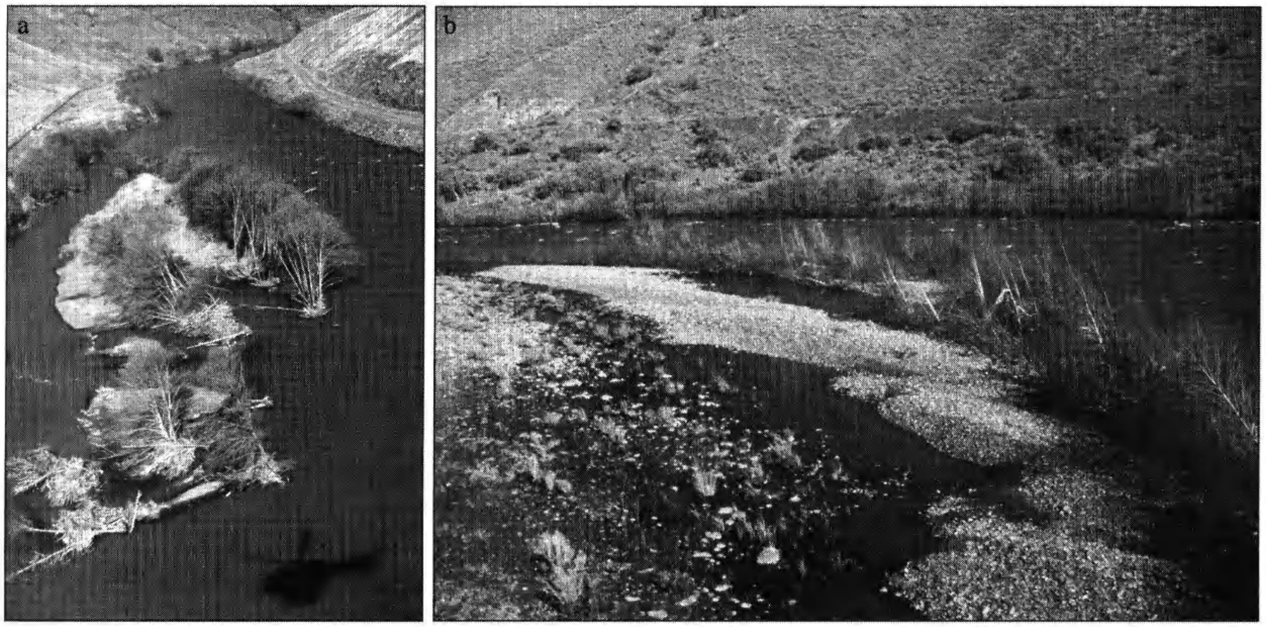

Figure 14. Photographs of effects of the February 1996 flood (February 14, 1996 photographs by H. Fassnacht). (a) View downstream of a partly eroded island with downstream gravel deposits at RM 7.1. (b) View downstream from left bank at RM 8.4 of gravel deposited on point bar in lee of riparian vegetation.

major eastern tributaries that capture flow from the dissected uplands and tablelands of the northern Ochoco Mountains and the Columbia Plain. Shitike Creek (269 km^2), the Warm Springs River (1403 km^2), and the White River (1041 km^2) together drain most of the eastern Cascade Range between Mount Jefferson and Mount Hood. From the east, Trout Creek drains 1789 km^2 of the northwestern Ochoco Mountains, and Buck Hollow (396 km^2) and Bakeoven Creeks (513 km^2) drain tablelands underlain by the Columbia River Basalt Group (Figure 1). These six tributaries account for 78% of the drainage area downstream of RM 100.1. The remaining tributaries are short and steep ephemeral channels that primarily drain the valley sides. Downstream of RM 35, there are no tributaries with drainage areas more than 50 km^2.

Even taken together, these tributaries and the few springs in the lower 60 km of the river contribute little to the mean annual flow. The average annual discharge at the Madras gage at RM 100.1 is 80 percent of the flow at the Moody gage near the Columbia confluence at RM 1.4 [*O'Connor, Grant, and Haluska*, this volume], and close to 90 percent of late summer flow is generated upstream of the Madras gage [*Gannett et al.*, this volume]. For large floods, however, the six large tributaries entering downstream of the dams are important contributors [*Beebee and O'Connor*, this volume]. The peak discharges of the 1964 and 1996 floods increased by factors of three to four between Madras and the Columbia River confluence. The major contributors to the February 1996 peak discharge were Shitike Creek (125 m^3/s), the Warm Springs River (640 m^3/s) and the White River (ungaged in 1996, but 375 m^3/s in December 1964). These three tributaries are connected by incised and steep channel networks to high Cascade Range source areas, and during regional rain-on-snow events they rapidly deliver runoff to the mainstem Deschutes. The smaller tributaries generally flow only seasonally and during runoff events. The largest flows on the short, steep tributaries are mostly due to localized storm cells.

In addition to producing high runoff, Shitike Creek, the Warm Springs River, and the White River are situated to deliver abundant coarse sediment to the Deschutes River valley: They generate peak discharges comparable to peak discharges in the mainstem Deschutes River, and they all flow in steep and confined valleys from high-relief source areas composed of unconsolidated volcanic and glacial deposits. Sediment transport by these large tributaries into the mainstem Deschutes River has not been measured, but active islands and gravel bars at the mouth of Shitike Creek, and the large gravel fan at the Warm Springs River confluence demonstrate that these tributaries do indeed contribute significant volumes of coarse sediment into the Deschutes River during large flows. Given the paucity of coarse sediment delivered from the upper Deschutes River basin during the present geologic and hydrologic regime, it is likely that these Cascade Range tributaries contributed as much or more sediment to the lower Deschutes River as did the entire upper Deschutes River basin prior to regulation [*O'Connor, Grant, and Haluska*, this volume].

The large eastern tributaries and the smaller tributaries that drain the valley sides also episodically contribute sediment to the valley bottom, although these events generally result from localized storm runoff rather than from regional flooding. Between RM 100 and RM 60, these tributaries primarily drain basins formed in the fine-grained sedimentary rocks of the Deschutes, John Day, and Clarno Formations, and their sediment contributions are likely to be primarily silt and clay, although lava-flow interbeds within these formations and Columbia River Basalt Group lavas contribute some gravel. This is consistent with *McClure's* [1998] observation that the surface grain size distribution of deposits at the confluence of Trout Creek was distinctly finer than most of the thirteen other sampled tributaries. Downstream of RM 60, the small tributaries are primarily formed in rocks of the Columbia River Basalt Group. These rocks produce cobble and pebble-sized clasts that are readily transported by floods and debris flows down channels draining the steep canyon slopes. In July 1995, a number of such flows brought a large volume of cobbly gravel to the valley bottom during an intense convective storm that affected the lower 30 km of the Deschutes River canyon (Steve Pribyl, Oregon Department of Fish and Wildlife, 1998 oral communication).

Tributary floods transport coarse sediment that either directly enters the Deschutes River channel, or is deposited in alluvial fans that build up at tributary mouths. There are 84 recognizable tributary fans between RM 100.1 and the Columbia River confluence, ranging in size from 0.1 hectares (ha) to the 68-ha fan at the Warm Springs River confluence [*Curran and O'Connor*, this volume]. These fans are generally composed of poorly sorted cobbly gravel deposited by debris flows and sediment-laden water flows. Some fans are built out onto alluvial surfaces that flank the Deschutes River and have little direct interaction with the channel, but several fans constrict the channel, narrowing flow and forming rapids or riffles. A recent example is the July 1995 tributary flood at Mud Springs Canyon (RM 8), which built a fan of bouldery debris out into the Deschutes River channel, constricting the channel and forming a new rapid, Washout Rapids [Figure 15; *Curran and O'Connor*, this volume]. The fans that encroach into the channel are commonly eroded by moderate Deschutes River flows, and

Figure 15. View north of the tributary fan at RM 7.8, where a July 1995 debris flow transported bouldery gravel into the Deschutes River channel, forming "Washout Rapids." Culverts under railroad have diameters of 4 m. June 2, 1998 photograph by J. E. O'Connor.

they are local sources of readily-mobilized coarse-grained sediment. According to Steve Pribyl (Oregon Dept. of Fish and Wildlife, oral communication, 1998), the fan emanating from the Harris Canyon tributary (RM 12) has repeatedly encroached into the Deschutes River channel over the last decade, only to be trimmed back several times by large mainstem flows. Just downstream, the apex of Harris Island has accumulated angular basalt gravel and cobbles that likely derive from the Harris Canyon fan. *Curran and O'Connor* [this volume] more fully discuss locations, sizes, and distribution of tributary fans.

SUMMARY

The present canyon and valley bottom of the lower Deschutes River reflect a long and complicated history of events and processes, encompassing temporal and spatial scales ranging from regional tectonic forces operating over millions of years to the effects of summer thunderstorms. Late Cenozoic incision of the lower Deschutes River basin, combined with stable discharges, a muted flood generation regime, and exceptionally low sediment production of the upper Deschutes River basin [*O'Connor, Grant and Haluska*, this volume] comprise a setting in which events and processes of long recurrence interval have strong influence on the valley and channel morphology of the lower Deschutes River. Moreover, many features of the present canyon and valley bottom can be attributed to individual events and circumstances. Some aspects of the processes and events that have affected the valley and valley bottom are:

1. Geologic units within canyon walls and regional deformation patterns partly control the overall morphology of the canyon and canyon bottom. The canyon is deeper where it passes through structural highs, and shallower where it crosses structural lows. Where bounded by the softer John Day and Clarno formations, extensive landsliding has widened the canyon, and the width of the valley bottom varies substantially. Where the valley is bounded by Columbia River Basalt Group, the canyon bottom is uniformly narrower and closely sheltered by steep valley walls. A distinct bedrock reach between RM 50 and RM 40 coincides with the Deschutes River flowing toward the rising limb of the Tygh Ridge anticline.
2. Regional volcanism and episodic incursion of lava flows and lahars into the Deschutes River canyon have had localized effects on valley geometry, and these events have probably resulted in rare but immense pulses of sediment into the lower Deschutes River. A large Pleistocene lahar from Mount Jefferson traveled much of the length of the canyon, leaving poorly sorted bouldery gravel deposits along the valley margins. In addition, eruptions of the Bend Pumice, Mount Mazama, and Mount Hood left localized sediment accumulations along the lower Deschutes River.
3. Between RM 100 and RM 60, Quaternary landslides have profoundly influenced valley morphology. Numerous large landslides rafted immense volumes of debris to the valley bottom, constricting the channel and forcing the river into tortuous routes through chaotically deformed terrain. Several landslides temporarily impounded the river, later to fail and send large floods downstream. The breached landslide dams and resulting flood deposits have left a persistent legacy of rapids, such as Whitehorse Rapids and Boxcar Rapids, and immobile flood bars that now constrain the channel.
4. In addition to floods from breached landslides, large floods from within and outside the Deschutes River basin have affected the valley and valley bottom of the lower Deschutes River. Between 15 and 12.7 ka, huge floods from ice-dammed glacial Lake Missoula came down the Columbia River valley and backflooded up the Deschutes River, depositing clay, silt, and sand to an elevation of 275 m on valley slopes 60 km upstream from the Columbia River confluence. Sometime during the late Holocene, probably between 7600 and 3000 yr BP, an exceptionally large flood surged through the Deschutes River canyon. This "Outhouse flood" likely had a discharge twice that of the 2000 m^3/s discharge of

the flood of February 1996. The cobble and boulder bars left by this flood have resisted erosion from subsequent floods, and in many locations, these features confine the Deschutes River channel to its present position.

5. The largest historic main-stem floods, in December 1861, December 1964, and February 1996, resulted from regional rain-on-snow events. These floods apparently had little effect on the overall morphology of the Deschutes River valley bottom. Their primary effects have been to deposit and erode fine sediment and wood on alluvial surfaces flanking the channel, and to erode edges of alluvial fans that episodically encroached into the Deschutes River channel between mainstem floods.
6. Within the present geologic and hydrologic regime, the major Cascade Range tributaries (Shitike Creek, Warm Springs River, White River) generate a substantial portion of the discharge of large flood flows. Moreover, these tributaries supply abundant coarse sediment, perhaps exceeding the gravel volume delivered from upstream. Smaller tributaries episodically deliver fine and coarse sediment to the Deschutes River and to alluvial fans that have formed on the valley bottom. In some locations, this material is a source of moderately coarse sediment that can be transported by moderate mainstem flows.

Acknowledgments. This research was funded by the U.S. Geological Survey, U.S.D.A. Forest Service, Portland General Electric and the University of Oregon. Discussions with Don Ratliff, Steve Pribyl, Heidi Fassnacht, Gary Smith and Dave Sherrod improved our understanding of the geology and geomorphology of the Deschutes River canyon. Michelle Brink, Heidi Fassnacht, John Green, Jasper Hardison, Toby Minear, Eric Schulz, and Walt Wolfe helped with fieldwork and river logistics. Previous versions of this paper were reviewed by William E. Scott and Thomas C. Pierson. John Williams, Kathryn Ronnenberg, and Tana Haluska provided assistance with editing and illustrations.

REFERENCES

Atwater, B. F., Pleistocene glacial-lake deposits of the Sanpoil River Valley, northeastern Washington, *U.S. Geol. Surv. Bull. 1661*, 39 pp., 1986.

Beget, J. E., Evidence of Pleistocene explosive eruptions of Mount Jefferson, Oregon, *EOS, Trans. AGU* (1981 Fall Meeting Supplement), *62*(45), 1089, 1981.

Bela, J. L., Geologic and neotectonic evaluation of north-central Oregon: The Dalles 1° x 2° quadrangle, *State of Oregon Dept. Geol. Min. Ind. Geol. Map Ser. GMS-27*, Portland, Oregon, scale 1:250,000, 1982.

Brands, M. D., 1947, Flood runoff in the Willamette Valley, Oregon, *U.S. Geol. Surv. Water-Supply Pap. 968-A*, 211 pp., 1947.

Bretz, J H., The Dalles type of river channel, *J. Geology*, *24*, 129-149, 1924.

Bretz, J H., 1969, The Lake Missoula floods and the Channeled Scabland, *J. Geology*, *77*, 505-543, 1969.

Conrey, R. M., Geology and petrology of the Mt. Jefferson area, High Cascade Range, Oregon, Ph.D. Dissertation, 357 pp., Washington State University, Pullman, Washington, 1991.

Costa, J. E., and R. L. Schuster, The formation and failure of natural dams, *Geol. Soc. Amer. Bull.*, *100*, 1054-1068, 1988.

Hallett, D. J., L. V. Hills and J. J. Clague, New accelerator mass spectrometry radiocarbon ages for Mazama tephra layer from Kootenay National Park, British Columbia, Canada, *Canadian J. Earth Sci.*, *34*, 1202-1209, 1997.

Henshaw, F. F., J. H. Lewis, and E. J. McCaustland, Deschutes River, Oregon, and its utilization, *U.S. Geol. Surv. Water-Supply Pap. 344*, 200 pp., 1914.

Lanphere, M. A., D. E. Champion, R. L. Christiansen et al., Evolution of tephra dating in the western United States, *Geol. Soc. Amer. Abstr. with Prog.*, *31*(6), A-73, 1999.

Martinson, D. G., N. J. Pisias, J. D. Hays et al., Age dating and the orbital theory of the ice ages: development of a high resolution 0 to 300,000-year chronostratigraphy, *Quaternary Res.*, *27*, 1-29, 1987.

McClure, E. M., 1998, Spatial and temporal trends in bed material and channel morphology below a hydroelectric dam complex, Deschutes River, Oregon, M.S. thesis, Oregon State University, Corvallis, Oregon. 1986.

Newcomb, R. C., Effect of tectonic structure on the occurrence of ground water in the basalt of the Columbia River Group of The Dalles area, Oregon and Washington, *U. S. Geol. Surv. Prof. Pap. 383-C*, 33 pp., 1969.

O'Connor, J. E., and R. B. Waitt, Beyond the Channeled Scabland—A field trip guide to Missoula flood features in the Columbia, Yakima, and Walla Walla Valleys of Washington and Oregon, *Oregon Geology*, Part I, *57*(3), 51-60, Part II, *57*(4), 75-86, Part III *57*(5), 99-115, 1995.

O'Connor, J. E., A. Sarna-Wojcicki, K. C. Wozniak, D. J. Polette, and R. J. Fleck, Origin, extent, and thickness of Quaternary geologic units in the Willamette Valley, Oregon, *U.S. Geol. Surv. Prof. Pap. 1620*, 52 pp., 2001.

Pierce, K. L., Quaternary history of faulting on the Arco segment of the Lost River fault, central Idaho, in *Proceedings of Workshop XXVIII on the Borah Peak, Idaho, Earthquake, U.S. Geol. Surv. Open-File Rep. 85-290*, edited by R. S. Stein and R. C. Buckman, pp. 195-206, 1985.

Robinson, P. T., G. F. Brem, and E. H. McKee, John Day Formation of Oregon–A distal record of early Cascade volcanism, *Geology*, *12*, 229-232, 1984.

Russell, I. C., Preliminary report on the geology and water resources of central Oregon, *U.S. Geol. Surv. Bull. 252*, 138 pp., 1905.

Sarna-Wojcicki, A. M., C. E. Meyer, J. K. Nakata et al., Age and correlation of mid-Quaternary ash beds and tuffs in the vicinity of Bend, Oregon, in *Guidebook for Field Trip to the Mount Bachelor-South Sister-Bend Area, Central Oregon High Cascades. U.S,* *Geol. Surv. Open-file Rep. 89-645*, edited by W. E. Scott, C. A. Gardner and A. M. Sarna-Wojcicki, pp. 55-66, 1989.

Shannon and Wilson Inc., Geologic studies of Columbia River basalt structures and age of deformation, The Dalles-Umatilla region, Washington and Oregon, Boardman Nuclear Project, report to Portland General Electric Company, Portland, Oregon, 52 pp. 1973.

Sherrod, D. R., and W. E. Scott, Preliminary geologic map of the Mount Hood 30- by 60-minute Quadrangle, northern Cascade Range, Oregon, *U.S. Geol. Surv. Open-File Rep. 95-219*, 28 pp., scale 1: 100,000, 1995.

Sherrod, D. R., E. M. Taylor, M. L. Ferns et al., Geologic map of the Bend 30′ X 60′ Quadrangle, central Oregon, *U. S. Geol. Surv. Geol. Inv. Map I-2683*, scale 1:100,000, in press.

Smith, G. A., Stratigraphy, sedimentology, and petrology of Neogene rocks in the Deschutes basin, central Oregon: A record of continental-margin volcanism and its influence on fluvial sedimentation in an arc-adjacent basin, Ph.D. Dissertation, 464 pp., Oregon State University, Corvallis, Oregon, 1986.

Smith, G. A., Geologic map of the Madras West and Madras East quadrangles, Jefferson County, Oregon, *Oregon Dept. Geol. Min. Ind. Geol. Map Ser. GMS-45*, Portland, Oregon, scale 1:24,000, 1987.

Smith, G. A., A field guide to depositional processes and facies geometry of Neogene continental volcaniclastic rocks, Deschutes basin, central Oregon, *Oregon Geology*, *53*(1), 3-20, 1991.

Smith, G. A., and G. A. Hayman, Geologic map of the Eagle Butte and Gateway quadrangles, Jefferson and Wasco Counties, Oregon, *Oregon Dept. Geol. Min. Ind. Geol. Map Ser. GMS-43*, Portland, Oregon, scale 1:24,000, 1987.

Stearns, H. T., Geology and water resources of the middle Deschutes River basin, Oregon, *U.S. Geol. Surv. Water-Supply Pap. 637-D*, pp. 125-220, 1931.

Taylor, E. M., Central High Cascade roadside geology, Bend, Sisters, McKenzie Pass, and Santiam Pass, Oregon, in *Guides to Some Volcanic Terranes in Washington, Idaho, Oregon, and Northern California: U.S. Geol Surv. Circ. 838*, edited by D. A. Johnston and J. Donnelly-Nolan, pp. 55-58, 1981.

Tinkler, K. and E. Wohl, A primer on bedrock channels, in *Rivers Over Rock: Fluvial Processes in Bedrock Channels, Amer. Geophys. Union Mono. 107*, edited by K. J. Tinkler and E E. Wohl, pp. 1-18, 1998.

Walder, J. S., C. A. Gardner, R. M. Conrey, B. J. Fisher, and S. P. Schilling, Volcano hazards in the Mount Jefferson Region, Oregon, *U.S. Geol. Surv. Open-File Rep. 99-24*, 14 pp., 1999.

Waitt, R. B., About forty last-glacial Lake Missoula jökulhlaups through southern Washington, *J. Geology*, *88*, 653-679, 1980.

Waitt, R. B., Case for periodic, colossal jökulhlaups from Pleistocene glacial Lake Missoula, *Geol. Soc. Amer. Bull. 96*, 1271-1286, 1985

Waters, A. C., Reconnaissance geologic map of the Madras quadrangle Jefferson and Wasco Counties, Oregon, *U.S. Geol. Survey Misc. Geol. Inv. Map I-555*, scale 1:62,500, 1968a.

Waters, A. C., Reconnaissance geologic map of the Dufur quadrangle Hood River, Sherman, and Wasco Counties, Oregon, *U.S. Geol. Survey Misc. Geol. Inv. Map I-556*, scale 1:62,500, 1968b.

Jim E. O'Connor, U.S. Geological Survey, 10615 SE Cherry Blossom Drive, Portland, OR 97216

Janet H. Curran, U.S. Geological Survey, 4230 University Drive, Suite 201, Anchorage, AK 99508

Robin A. Beebee, Department of Geological Sciences, University of Oregon, 2410 Cherry Grove Street, Eugene, OR 97403-1272

Gordon E. Grant, U.S. Forest Service, 3200 SW Jefferson Way Corvallis, OR 97331

Andrei Sarna-Wojcicki, U.S. Geological Survey, Menlo Park, CA

Formation and Evolution of Valley-Bottom and Channel Features, Lower Deschutes River, Oregon

Janet H. Curran

U.S. Geological Survey, Anchorage, Alaska

Jim E. O'Connor

U.S. Geological Survey, Portland, Oregon

Primary geologic and geomorphic processes that formed valley-bottom and channel features downstream from the Pelton-Round Butte dam complex are inferred from a canyon-long analysis of feature morphology, composition, location, and spatial distribution. Major controls on valley-bottom morphology are regional tectonics, large landslides, and outsized floods (floods with return periods greater than 1000 yrs), which include the late Holocene Outhouse Flood and several Quaternary landslide dam failures. Floods with a return period on the order of 100 yrs, including historical floods in 1996, 1964, and 1861, contribute to fan building and flood plain formation only within the resistant framework established by the major controls. Key processes in the formation of channel features, in particular the 153 islands and 23 large rapids, include long-term bedrock erosion, outsized floods, and century-scale floods. Historical analysis of channel conditions since 1911 indicates that the largest islands, which are cored by outsized-flood deposits, locally control channel location, although their margins are substantially modified during annual- to century-scale floods. Islands cored by bedrock have changed little. Islands formed by annual- to century-scale floods are more susceptible to dynamic interactions between tributary sediment inputs, mainstem flow hydraulics, and perhaps riparian vegetation. Temporal patterns of island change in response to the sequence of 20th century flooding indicate that many islands accreted sediment during annual- to decadal-scale floods, but eroded during larger century-scale floods. There is, however, no clear trend of long-term changes in patterns of island growth, movement, or erosion either spatially or temporally within the lower Deschutes River.

INTRODUCTION

The Deschutes River drains 27,000 km^2 in north-central Oregon before joining the Columbia River 160 km east of Portland, Oregon (Figure 1). The lowermost 160 km of the river, below the Pelton-Round Butte dam complex, is in a narrow valley or canyon. The channel alternates between alluvial and bedrock substrates and is flanked by alluvial and bedrock surfaces, tributary fans, and minor amounts of landslide deposits, colluvium, and railroad ballast. Surveyors for the General Land Office, scouting the area in the late 1800s for future homesteading, described their map area by noting, "The Western half is in the Deschutes River Cañon, which is 2000 feet in depth, and in many places has almost precipitous rock bluffs, and is unfit for anything and not surveyed" [General Land Office map, 1885]. In 1957,

A Peculiar River
Water Science and Application 7

Published in 2003 by the American Geophysical Union
10.1029/007WS08

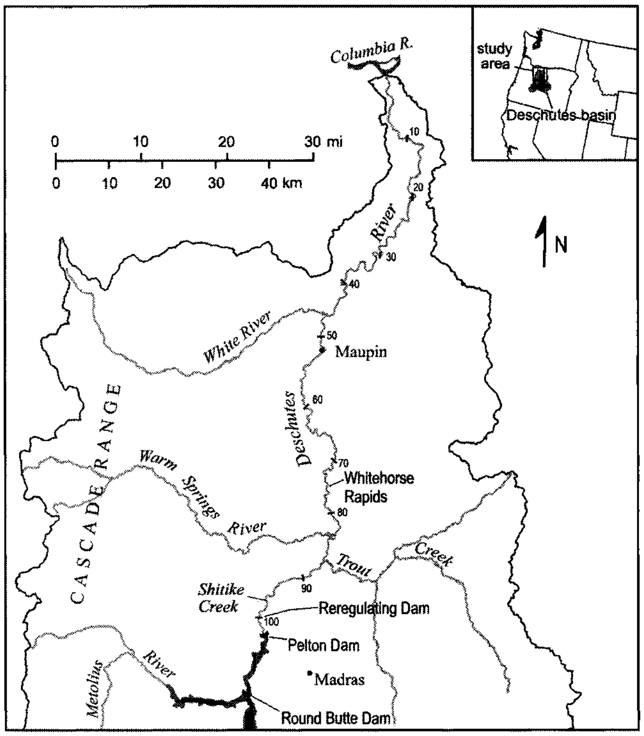

Figure 1. Location map of lower Deschutes River, Oregon. Markers denote river miles at 10-mile increments.

less than 70 years later, construction of the Pelton-Round Butte dam complex had begun, and by 1964, this 427-megawatt capacity hydroelectric project consisting of the Round Butte, Pelton, and Reregulating Dams (Figure 1) was in operation by Portland General Electric.

Beginning in 1996, the Federal Energy Regulatory Commission license renewal process for the Pelton-Round Butte dam complex resulted in the initiation of several studies to determine past and potential future effects of the dam complex on downstream channel and valley-bottom morphology and processes. The objective of this study was to contribute to this understanding by (1) mapping geomorphic features along the channel and valley bottom for the 160 km of river downstream of the dam complex and (2) relating these features to formative geologic and hydrologic processes on the basis of feature morphology, field observations, and historical information. These proposed relations to formative processes led to hypotheses regarding which valley-bottom and channel features may be sensitive to changes in flow and sediment flux caused by impoundment.

Previous work on channel and valley-bottom features along the lower Deschutes River included a mid-1960s investigation of salmon spawning conditions that documented 302 gravel bars [*Aney et al.*, 1967] and an update in the mid-1980s that suggested that gravel had been eroded from bars and islands near the dam [*Huntington*, 1985]. More recently, investigations of bedload transport and changes to channel morphology and bed texture have shown that bedload-transporting events are infrequent [*Fassnacht*, 1998; *Fassnacht et al.*, this volume], that channel morphology is largely stable within the lower Deschutes River [*McClure*, 1998; *Fassnacht et al.*, this volume], and that bed texture has not changed substantially as a result of dam-related alterations of water and sediment input [*McClure*, 1998; *Fassnacht et al.*, this volume]. These studies examined various channel processes at specific locations but did not place observations of channel features and processes into an overall framework of valley-bottom geomorphology. The need for such a context was demonstrated by observations immediately after the large flood of February 1996, which showed that the largest flow in the last 135 yrs had few effects on channel and valley-bottom morphology [*Fassnacht*, 1998; *McClure*, 1998], thus raising the question, "What types and frequencies of processes do form and modify channel and valley-bottom features of the Deschutes River?"

STUDY AREA

Physical and Geological Setting

The lower Deschutes River extends from the Pelton Reregulation Dam at river mile (RM) 100.1 to the confluence with the Columbia River (Figure 1)[1]. Between the Pelton-Round Butte dam complex and RM 60, the river flows through a canyon incised into soft volcaniclastic units, primarily the John Day and Clarno Formations. Extensive landslide complexes affect one or both valley sides between RM 90 and 74. In contrast, the more resistant basalts of the Columbia River Basalt Group (CRBG) are present near river level from about RM 60 to the Columbia River confluence and form a deep, narrow bedrock canyon with largely stable slopes [*O'Connor et al.*, this volume].

Hydrologic Setting

Flow in the lower Deschutes River is dominated by significant groundwater contributions from above the dam

[1] Units are given are in metric except for locations, which are given in as river miles (RM), or miles upstream from the river mouth as marked on USGS topographic maps. These values are close to, but not necessarily the same as, actual distances along the present channel. Fractional river miles given herein are based on interpolations between these published river miles.

Table 1. Sources of information

Period	Source	Date	Scale	Coverage
Pre-dam	General Land Office Survey maps	1860-1895	1:48,000	limited sections
	USGS topographic maps	surveyed 1911 published 1914	1:31,680	complete
	Black and white aerial photographs, 4M series, U.S. Army Corps of Engineers	1944	1:21,000	complete
Post-dam	USGS topographic maps	1957-1977	1:24,000	complete
	Color infrared aerial photographs, Portland General Electric; selected images in *Huntington* [1985]	1981	1:2000	limited sections
	Black and white aerial photographs, Portland General Electric	1995	1:24,000	complete
	Color infrared aerial photographs, Portland General Electric	June 24, 29, 30, 1995	1:2000	nearly complete
Post-1996 flood	Color infrared digital aerial images, Bureau of Land Management	June 24, 1996	1:2000[1]	nearly complete
	Video, photographs	1996	scale varies	selected areas
	Field observations	1998-1999	not applicable	complete

[1] Scale varies with method of viewing, but altitude of flight is comparable to that for 1:2000 aerial photographs.

complex, resulting in flow having little seasonal or daily fluctuation [*Gannett et al.*, this volume; *O'Connor, Grant, and Haluska*, this volume]. Mean annual flows are 128 m^3/s near the dam complex (Madras gage at RM 100) and 163 m^3/s near the river mouth (Moody gage at RM 1.4). Large floods in December 1861, December 1964, and February 1996 are recorded in both historical documents and Deschutes River streambank sediments [*Hosman et al.*, this volume]. Peak flows for the floods of December 1964 and February 1996 were about 500 m^3/s and 1,950 m^3/s at the two gages, respectively, and were the largest flows in a gaged record that began in 1897 and has been continuous since 1906. Return periods calculated for these floods solely on the basis of gaged records are about 500 yrs, but diminish to about 75 yrs if the longer geologic record of late Holocene floods is considered [*Hosman et al.*, this volume]. *Hosman et al.* estimate that the peak 1861 flood discharge was about 50 percent larger than the peaks of the 1964 and 1996 floods. Collectively, we refer to the 1861, 1964, and 1996 floods—floods that have return periods on the order of 100 yrs—as century-scale floods and smaller floods as annual- to decadal-scale floods.

Human Use of the Lower Deschutes River

Anthropogenic modifications to the lower Deschutes River aside from river impoundment at the Pelton-Round Butte dam complex include minor channel encroachment from turn-of-the-century construction of railroad lines up both banks of the river from the Columbia River to Trout Creek (RM 87.3). Land use of the lower Deschutes River valley bottom has included agriculture and grazing, but these activities have diminished during the last two decades, and the river and adjacent banks are now used primarily by

Table 2. Surficial processes active in forming the Deschutes River valley-bottom and channel features and defining characteristics of the resulting landforms.

Formative Process	Description	Defining Characteristics of Landforms Created
Outsized flood (> 1000 year flood)	Deschutes River flood with recurrence interval on the order of 1000 years; includes the Outhouse Flood [*Beebee and O'Connor,* this volume] and breaches of channel-damming landslides [*O'Connor et al.*, this volume]	Deposits include rounded, imbricated boulders; top elevation of deposit is above the 1996 flood level; features are convex in cross section; features are lenticular in planform or have a bar shape
Annual- to century-scale flood	Deschutes River flood with recurrence interval less than 1000 years, more typically 10 to 100 yrs; includes historical floods of 1996, 1964, and 1861. The 1996 flood is used as a model for this category of flooding because the flood was well documented and high water marks were still evident at the time of field studies.	Deposits do not include boulders; top elevation of deposit is near or below the 1996 flood level
Undifferentiated flood	Deschutes River flood of undetermined magnitude	Lacks characteristics sufficient to categorize as result of outsized flood or annual- to century-scale flood but includes rounded clasts and other fluvial features
Tributary flood	Floods and debris flows emanating from a tributary into the Deschutes River	Fan-shaped deposits at tributary mouths; deposits may include angular and sub-angular clasts
Bedrock erosion	Slow removal of bedrock by fluvial erosion	Exposed bedrock straths at or near river level; zones of bedrock channel bed with small bedrock islands
Colluvial processes	Distributed transport of hillslope material onto valley bottom by gravity; includes rockfall and talus slopes	Angular, coarse clasts with few fines
Mass movements	Discrete transport of hillslope material onto valley bottom by roughly simultaneous movement of a large mass of earth; includes landslides and debris flows not at tributaries	Coherent blocks of landslide material; coarse remnants of landslide dams
Undetermined	Process not clearly identifiable	Characteristics not unique enough to categorize under a single process

recreationists attracted to the river's remote and scenic setting as well as its coldwater fishery. The entire Deschutes River between the Pelton-Round Butte dam complex and the Columbia River is a congressionally designated Wild and Scenic River.

DISTRIBUTION AND FORMATION OF VALLEY-BOTTOM AND CHANNEL FEATURES

The valley bottom of the Deschutes River downstream from the Pelton-Round Butte dam complex is composed of a suite of landforms that have developed from Quaternary hillslope and fluvial processes. To better develop understanding of the relation between current valley-bottom and channel morphology and formative processes downstream of the dam complex, we have systematically inventoried landforms from maps, aerial photographs and field observations (Table 1). On the basis of feature morphology and reconnaissance observations of composition and stratigraphy, we have inferred the primary formative processes responsible for each valley and channel feature (Table 2).

The lower Deschutes River valley bottom, defined as the relatively flat area between canyon walls or colluvial slopes, has a total area of about 2600 hectares (ha) (Table 3). The val-

Table 3. Surface area of lower Deschutes River valley-bottom and channel features.

Feature	Area (ha)	Area (% of total)
Islands	56	2
Channel (excluding islands)	1100[1]	43
Alluvial surfaces	960	38
Fluvially stripped bedrock surfaces	55	2
Tributary fans	240	9
Other surfaces[2]	140[3]	5

[1] Channel area calculated from measured channel widths (Figure 2) applied over 1 km intervals.

[2] Landslide debris, colluvial surfaces, bedrock not modified by fluvial processes, and railroad ballast.

[3] Area obtained by subtracting area of all measured features from area of valley bottom.

ley bottom has an average width of 165 m (Figure 2), and is occupied primarily by the channel and flanking alluvial surfaces (Table 3). Fluvially modified (stripped or eroded) bedrock surfaces are in and adjacent to the channel in discrete reaches. Tributary fans locally protrude into the river and constrict the channel (Figure 3c). Alluvial and bedrock islands (Figure 3a) are a small part of the valley but are ecologically important because of the aquatic habitat provided by their flanking side channels. Rapids are found throughout most of the study reach and are an important element of the river's recreational value. The remainder of the valley bottom is composed of landslide debris, colluvial surfaces, bedrock outcrops not clearly modified by fluvial processes, and railroad ballast. The distribution of these features along the river corridor, their prominent characteristics, and their implications for surficial processes are discussed in the following sections.

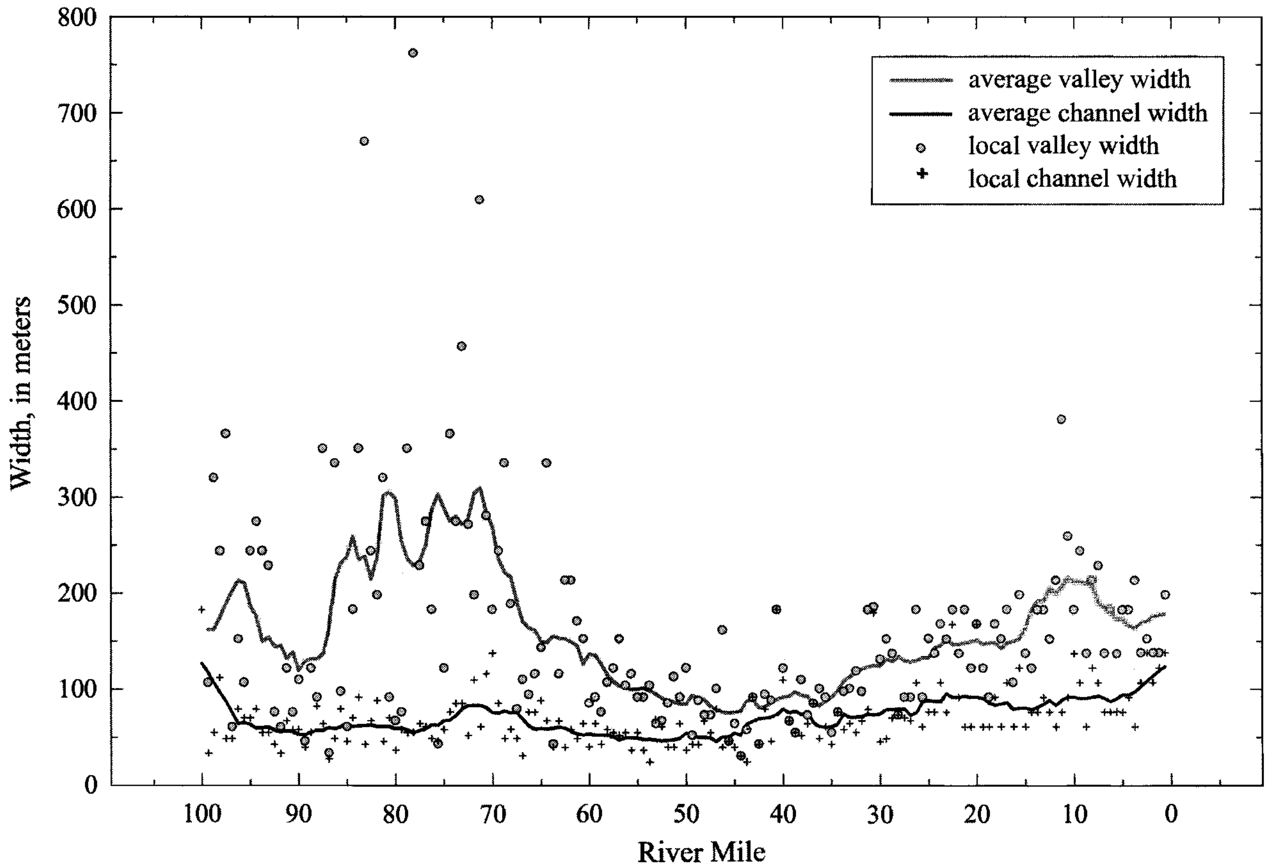

Figure 2. Lower Deschutes River valley width and channel width. Extensive landsliding in the less resistant upper canyon has resulted in a wider valley, on average. Average channel width does not parallel the valley width trends of the upper canyon, but increases gradually over the length of the lower canyon. Local widths shown are from USGS 1:24,000-scale topographic maps. Averages shown are 11-value running averages of local widths.

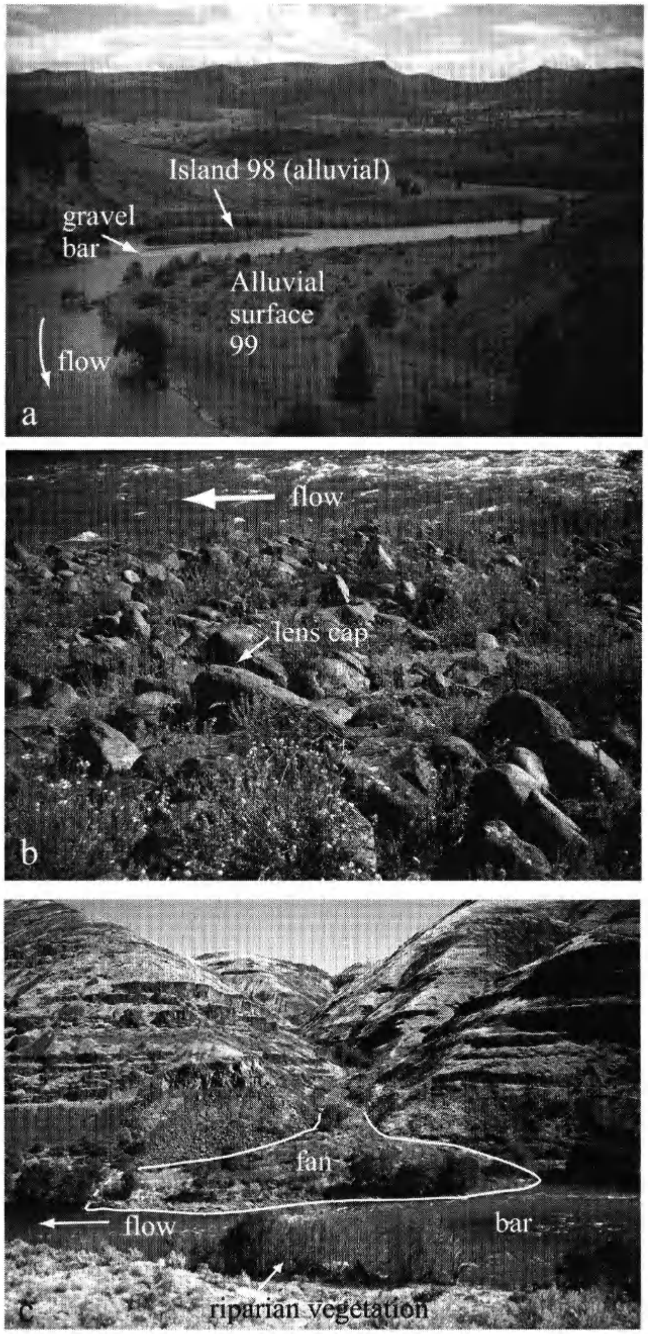

Figure 3. Typical lower Deschutes River valley-bottom and channel features. (a) View upstream at RM 77, showing an alluvial surface formed by an outsized flood, an alluvial island, and a gravel bar. (b) Imbricated boulders on an alluvial surface in the lower canyon that was formed by an outsized flood. (c) Fan constructed by debris flows from low-order tributary is presently constricting channel. Dark area is a barely exposed bar. Fringe of riparian vegetation is typical of lower Deschutes River banks.

Alluvial Surfaces

Alluvial surfaces flanking the lower Deschutes River are formed of gravel (clast diameter greater than 2 mm) deposits with convex or planar sloping surfaces (in cross section across the valley) and, less commonly, silty deposits with planar level or planar sloping surfaces. Well-sorted sandy (0.062 to 2 mm) deposits are rare. Alluvial surfaces are sparsely vegetated with grasses and desert shrubs except for a dense riparian fringe of white alder (*Alnus rhombifolia*) that discontinuously flanks the channel (Figure 3c).

Alluvial-surface distribution and geometry correlates strongly to valley morphology. Alluvial surfaces are most common in wider reaches of the canyon (upstream of RM 60) where they are generally wider than the more continuous strips that flank the channel in the lower reaches of the canyon (Figure 4). Alluvial surfaces are shorter upstream of RM 40, where features that truncate them, including bedrock outcrops, landslide blocks, fluvially modified bedrock surfaces (e.g., RM 50 to 40), and tributary fans (e.g., RM 94 to 90), are more common.

Outsized Flood Bars. Most alluvial surfaces flanking the lower Deschutes River are underlain by coarse-grained alluvial deposits that rise 2 to 6 m above typical summer flow stage. The deposits are typically composed of cobbly gravel with surfaces studded or armored with large, imbricated, and rounded boulders with intermediate diameters commonly exceeding 500 mm (Figure 3b). These surfaces have distinctive morphologies, with single or multiple barforms evident in their cross section and planform and with surfaces that commonly ramp upward in the downstream direction. These deposits are evidence of a large, late Holocene flood, known as the Outhouse Flood, described in more detail by *Beebee and O'Connor* [this volume]. The Outhouse Flood occurred likely about 4000 yrs ago and had a discharge 2 to 3 times larger than any subsequent flow indicated by historical or stratigraphic records [*Hosman et al.*, this volume; *Beebee and O'Connor*, this volume].

Additional coarse-grained alluvial surfaces at elevations up to several meters above the typical summer water levels are mantled with subrounded boulders with diameters up to 6 m in diameter. In-channel boulder deposits associated with these surfaces locally form large rapids. These deposits are invariably downstream of landslides or large landslide complexes and are inferred to have formed from brief, local, and large-magnitude floods resulting from breached landslide dams [*O'Connor et al.*, this volume]. Most of these deposits appear to be Pleistocene.

We refer to the Outhouse Flood and floods from landslide breaches, collectively, as "outsized floods" because their magnitudes are substantially greater than historical meteorologic floods and their return periods are on the order of 1000 yrs or more. The alluvial surfaces that appear to have been formed by outsized floods account for at least 35 percent of the total area of alluvial surfaces that flank the lower Deschutes River (Figure 5).

Other Coarse-Grained Surfaces. Other cobbly gravel surfaces flanking the Deschutes River are lower or do not have the large distinct barform morphology or boulder-covered surfaces of typical coarse-grained Outhouse Flood deposits. Most of these surfaces were overtopped and modified by the February 1996 flood, indicating that their present morphology is at least partly due to floods of century-scale return periods. However, because many such deposits may be derived by or cored by features from other processes, such as the Outhouse Flood or tributary flooding, we classify these features as formed by Deschutes River floods of undetermined magnitude and frequency (Figure 5).

There are no apparent late Pleistocene terrace surfaces flanking the lower Deschutes River, despite abundant late Pleistocene outwash flanking headwater drainages in the Cascade Range [*Scott*, 1977] and extensive late Pleistocene surfaces flanking the Willamette River to the west [*O'Connor et al.*, 2001] and many other western U.S. rivers. Nevertheless, remnants of much older Quaternary terraces stand about 50 m above river level in isolated wider portions of the valley bottom such as near the Shitike and Trout Creek confluences, [*O'Connor et al.*, this volume]. These much-higher surfaces were not considered part of the valley bottom and are not included in the analyses. Local coarse-grained surfaces 5-15 m above river level near Kaskela (RM 77) and Whiskey Dick (RM 79, background of Figure 3a) probably resulted from aggradation behind the Whitehorse Landslide dam [*O'Connor et al.*, this volume].

Fine-grained Alluvial Surfaces. Several surfaces flanking the lower Deschutes River are underlain by subhorizontally bedded silt and sand with isolated gravel lenses. These surfaces typically stand 1 to 7 m above summer water levels with planar and level surfaces. Sediment accumulated on most of these surfaces during the February 1996 flood, but the highest of these surfaces have perhaps been stable since the Outhouse Flood [*Beebee and O'Connor*, this volume]. Fine-grained deposits at Caretaker Flat (RM 62) and near Dant contain airfall and fluvially transported Mazama tephra, indicating that they have been forming for at least the last 7700 years [*Hosman et al.*, this volume]. In general, the stratigraphy and chronology of these deposits indicates that they form primarily by vertical accretion of silt and sand during century-scale floods [*Hosman et al.*, this volume].

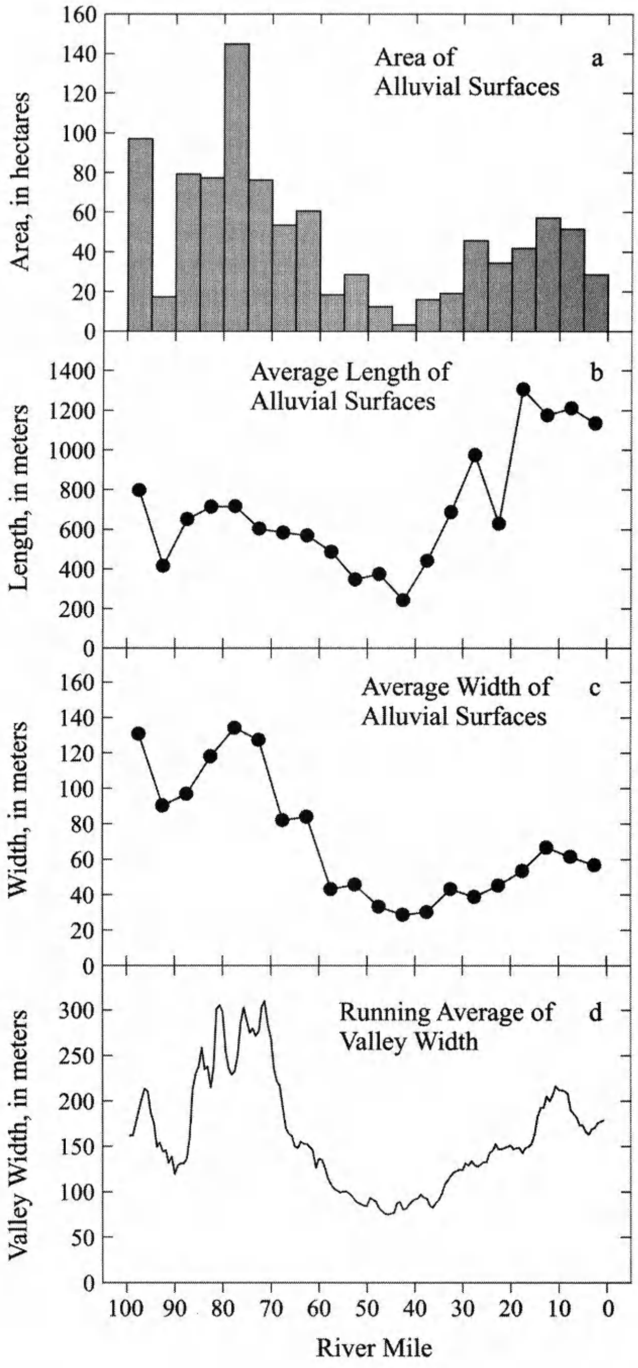

Figure 4. Geometric characteristics of alluvial surfaces and correlation with valley width. (a) Sum of area of alluvial surfaces in 5-mile increments. (b) Average length of alluvial surfaces within 5-mile increments. (c) Average width of alluvial surfaces within 5-mile increments. (d) Running average of valley width. Alluvial surface width and length and valley width were obtained by scaling from 1:24,000 scale USGS topographic maps.

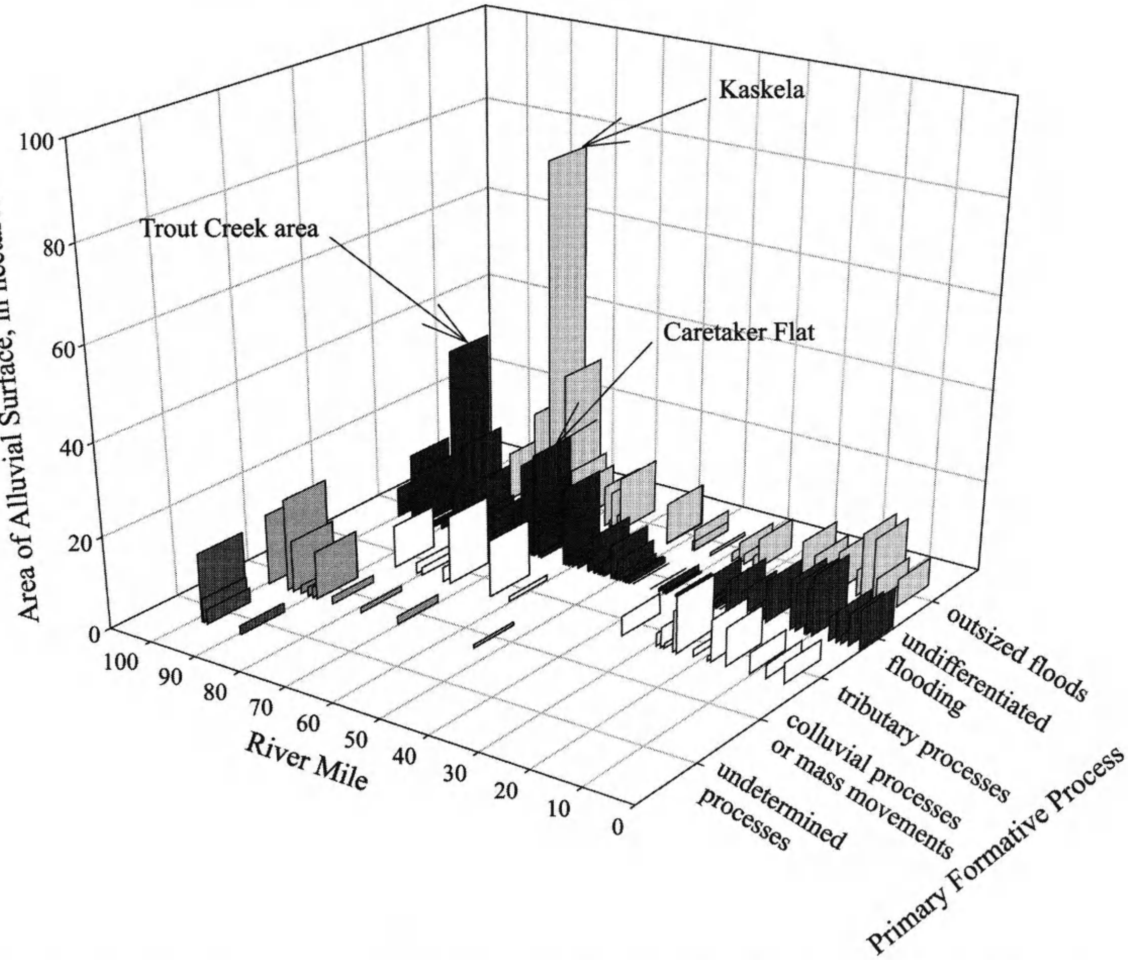

Figure 5. Area and distribution of alluvial surfaces in the lower Deschutes River, categorized by formative process. Features in the tributary processes, colluvial processes, and mass movements categories appear to have been strongly influenced by these processes but were modified by mainstem fluvial processes.

Bedrock Surfaces

Fluvially stripped and eroded bedrock occurs in two zones along the lower 160 km of the Deschutes River (Figure 6a). A narrow and nearly continuous stretch of bedrock channel between RM 50 and 40 corresponds to where the canyon enters the rising limb of the Tygh Ridge anticline [*O'Connor et al.*, this volume]. A second reach between RM 10 and 0 consists of a less continuous bedrock channel with adjacent fluvially stripped bedrock surfaces interspersed with channel and floodplain alluvium. This reach partly corresponds to the *circa* 1 Ma diversion of the Deschutes River channel by lava flows from Gordon Butte [*O'Connor et al.*, this volume]. All channel bedrock in both bedrock reaches consists of basalt from the Columbia River Basalt Group.

Bedrock surfaces in these reaches (Figure 7) include irregular but roughly planar benches near water level to planar or knobby straths as high as 20 m above summer water levels that enclose the low-flow channel within narrow slots and chasms. Planar surfaces generally correspond to contacts between individual basalt flows. Where bedrock occurs in the channel, it forms knobby islands, fin-shaped islands elongated in the downstream direction, or shallowly submerged shelves and ridges. Although typically bare, some bedrock islands have collected sandy or gravelly alluvial deposits, especially along their downstream margins. Immediately downstream from Sherars Falls, a 4.7-m bedrock knickpoint at RM 44, joint-controlled erosion has generated alternating channel constrictions and expansions. Bedrock surfaces in the lower Deschutes River are discontinuous and are at a variety of elevations with respect to the present river level indicating that they do not

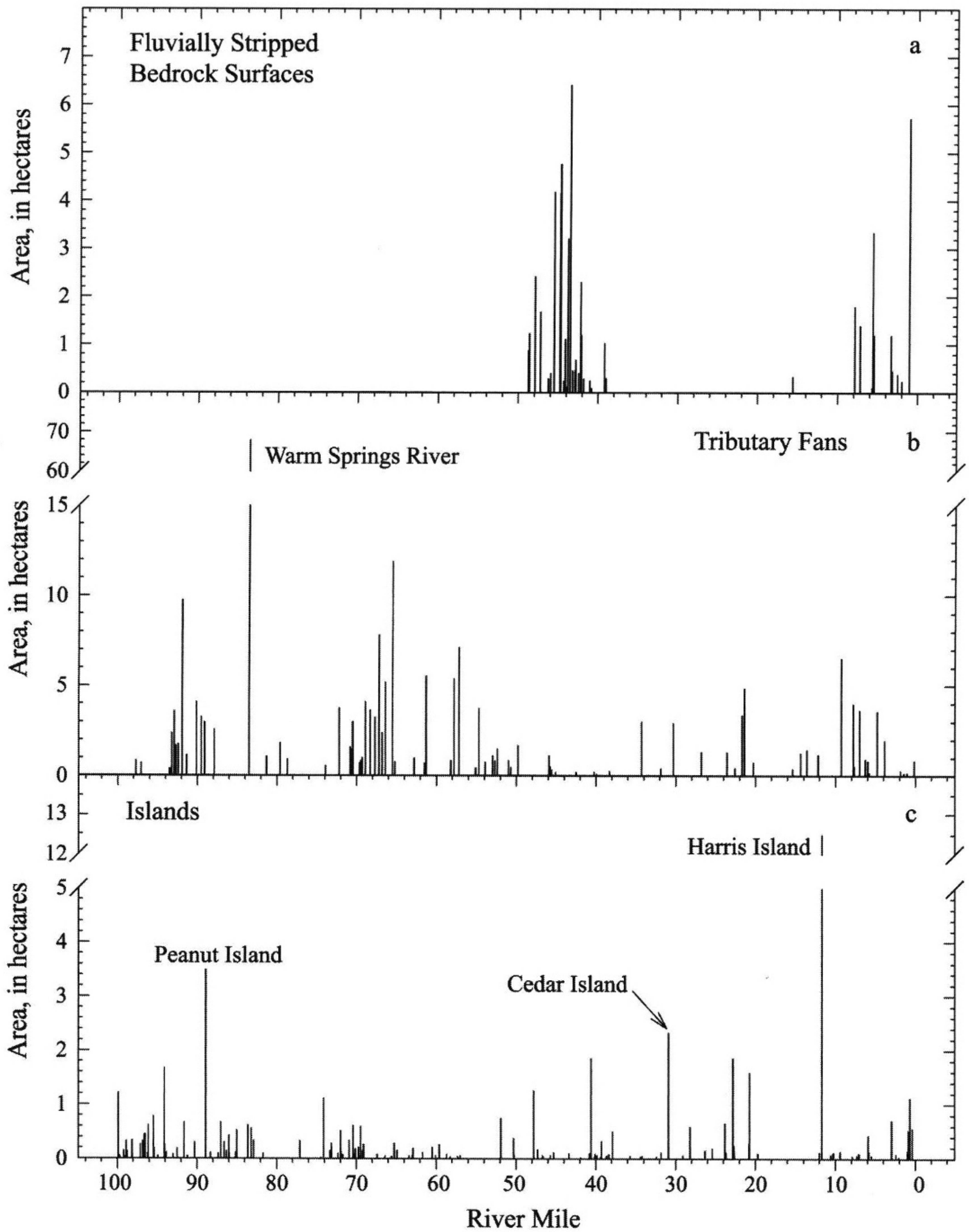

Figure 6. Locations and areas of (a) fluvially stripped bedrock surfaces, (b) tributary fans, and (c) islands in the lower Deschutes River.

comprise a continuous strath surface eroded by a singular and relatively higher river position.

Some bedrock surfaces show extensive evidence of fluvial modification well above the elevation of the February 1996 flood [*Beebee and O'Connor*, this volume]. Such evidence includes fluted surfaces, trimlines in flanking colluvium, and small bars of rounded cobbles and boulders. This evidence leads us to infer that the morphology and distribu-

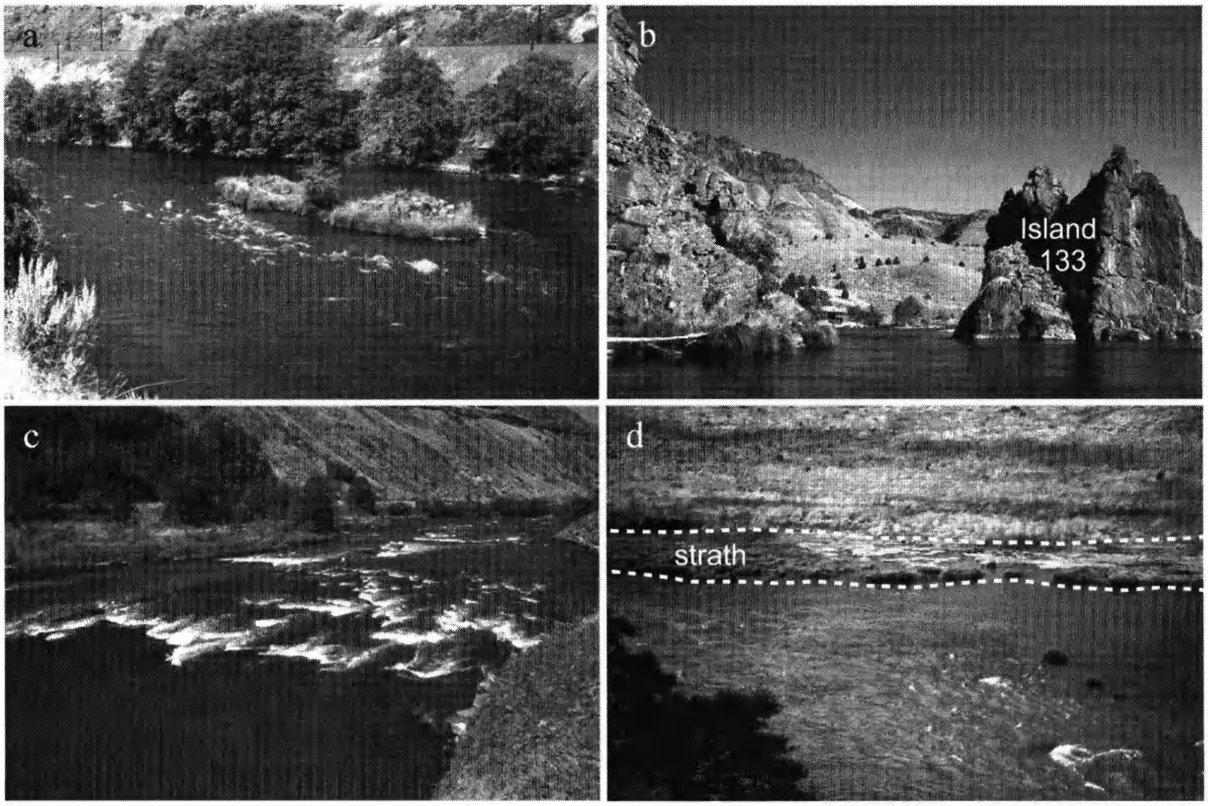

Figure 7. Bedrock features in the lower Deschutes River. (a) Island 257. (b) Upstream part of Island 133 (view upstream). Alluvial deposits formerly linked this island fragment, which extends a short distance to the right of the photo, to other nearby island fragments. (c) Shallow underwater shelves at Oak Springs Rapid. (d) Strath near water level.

tion of valley-bottom bedrock surfaces at least partly resulted from outsized floods, although the overall distribution of channel and valley-bottom bedrock is due to the regional geologic environment and history.

Tributary Fans

Almost 275 tributaries enter the lower Deschutes River, ranging from short steep gullies that drain the canyon walls to large drainages such as White River and Warm Springs River that drain the eastern slope of the Cascade Range (Figure 1). Many tributaries, particularly those upstream of RM 50, have formed fans at their confluence with the Deschutes River (Figure 6b). Although there is a slight, statistically significant, positive correlation between fan area and tributary order (t-test, $p < 0.05$), fan area varies widely, indicating that factors other than tributary size influence fan area. Tributary valley geomorphology, geological variations that affect sediment size and supply, and the sequence of tributary runoff events all likely influence fan morphology and interactions with the main Deschutes River channel.

Several of the 36 third-order [based on *Strahler*, 1952] or larger streams joining the lower Deschutes River, including Shitike Creek, Trout Creek, and Warm Springs River, have produced expansive, low-angle fans composed of silt and sand with varying amounts of gravel. These large fans from higher-order tributaries, which are concentrated in the upper half of the study reach, have affected the gross morphology of the valley bottom by directing the Deschutes River channel toward the opposite valley margin, but generally do not constrict the present-day channel.

The 236 tributary fans formed by low-order (1 and 2) drainages joining the lower Deschutes River can be categorized by their effects on the river as (1) debris-flow prone, cone-shaped or lobate tributary fans that protrude into the Deschutes River, narrowing the low-flow channel and affecting in-channel depositional patterns (Figure 3c), (2) similar fans that do not protrude substantially into the channel but which provide sediment directly to the Deschutes River, and (3) fans that are situated entirely upon other alluvial surfaces, and therefore do not constrict the channel or directly contribute substantial amounts of sediment to the

Deschutes River (e.g., fans at Two Springs Ranch, RM 68). Sediment forming these fans is typically angular cobbly and bouldery gravel, deposited by debris flows and sediment-rich water flows. Deposits in and adjacent to the Deschutes River are entrained by large main-stem flows, commonly forming downstream bars of angular gravel.

Tributary fans that encroach into the Deschutes River also affect local main-stem hydraulic conditions, thus affecting patterns of erosion and deposition similarly to that described by *Schmidt and Rubin* [1995] for the Colorado and Green Rivers. Such fans are concentrated between RM 90 and 94 but also occur at more isolated locations throughout the length of the lower Deschutes River. During high flows at these locations, a recirculation zone or eddy commonly forms as flow separates into downstream-directed and recirculating components where flow exits the constricted channel in the lee of the fan. Suspended silt and sand is commonly deposited on the submerged downstream margins of the constricting fans within these recirculation zones because of the lower flow velocities, forming what have been termed "separation deposits." Locally, "reattachment" bars also build at the downstream end of the recirculation zones where diminished velocity at the downstream point of flow separation promotes deposition [*Schmidt*, 1990; *Schmidt and Graf*, 1990]. Upstream of flow-constricting fans, gravel bars are commonly deposited where flow velocities decrease as a result of hydraulic ponding caused by the constriction. Although the local flow conditions adjacent to fans in the Deschutes River are similar to those of other rivers, the resulting deposits on the Deschutes River are generally much smaller. Unlike the sediment-laden rivers of the Colorado Plateau, there are few extensive and high subaerial beaches formed of sandy separation or reattachment deposits along the Deschutes River. Instead, most separation and reattachment bars on the Deschutes River are subaqueous or barely emergent at low flow, reflecting the small range of flow stages and low volume of sand transport [*O'Connor, Grant, and Haluska*, this volume]. There are, however, several gravelly mid-channel islands and bars upstream of constrictions formed by tributary fans (Figure 3c).

The Channel

Over the 160 km between the Pelton-Round Butte dam complex and the confluence with the Columbia River, the Deschutes River descends from 425 m to 50 m above sea level with an average gradient of 0.0023. Channel width averages 71 m, but ranges from about 8 m in bedrock constrictions near Sherars Falls (RM 44) to a maximum of 180 m. The channel bed is composed primarily of gravel, except for the two reaches of extensive bedrock substrate, and isolated silty- and sandy-bottom areas in recirculation zones. *McClure* [1998] measured grain-size distributions at 23 island and bar heads and found the median clast size to range from 30 to 120 mm, with an overall median diameter of about 90 mm.

For more than 90 percent of its length below the dam complex, the river flows within a single channel; for the remaining length, islands up to 1000 m long divide the channel. The river is bounded by banks of variable height and composition and there is no readily identifiable morphological feature that we can consistently relate to bankfull, or the stage at which the channel overflows its banks.

Islands

Islands within the lower Deschutes River are important ecological features because their corresponding side channels provide a substantial portion of the spawning and rearing habitat for several indigenous salmonid species [*Zimmerman and Ratliff*, this volume]. To determine the important processes responsible for formation and maintenance of these islands, we systematically mapped the positions and evolution of islands from historical maps and photographs as well as inspected their form and composition from field reconnaissance and interpretation of aerial photographs. In total, we identified 153 islands downstream of the Pelton-Round Butte dam complex that appeared at least once in the 1911, 1944, 1995, and 1996 sources we reviewed (Figure 6c, Table 1). An average of 119 islands appeared in any one of these years.

Island areas, as measured from U.S. Geological Survey 7.5 minute topographic maps, range from 0.01 to 12 ha with a median value of 0.11 ha. Island lengths, measured in the streamwise direction, range from 9.1 to 980 m with a median value of 61 m. In general, the abundance and total area of islands are greatest in the upper 50 km of the study reach, especially between RM 100-95, where there are 2.4 islands per kilometer. Otherwise, islands are distributed along the entire length of the lower Deschutes River except for three 8 km-long reaches centered at RM 79, 54, and 15 (Figure 6c).

About 75 percent of the islands present in the lower Deschutes River during this period are alluvial; the remainder are formed of bedrock, of which nearly all are within the two bedrock reaches between RM 50-40 and RM 10-0. Inspection of the overall distribution of alluvial islands with respect to channel width, valley width or tributary locations reveals no clear relation. Nevertheless, the overall greater abundance of islands between RM 100 and RM 60 does cor-

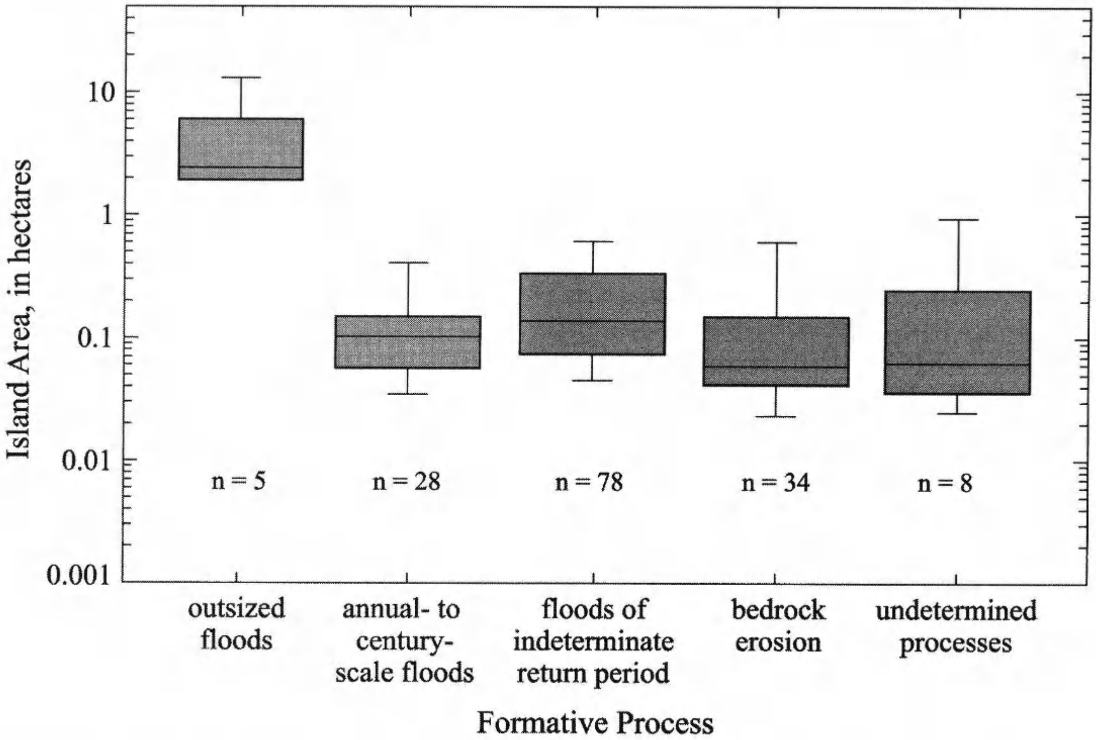

Figure 8. Island areas, stratified by formative process. The median outsized island is an order of magnitude larger than the median of islands formed by any other process. Bars represent 95th, 75th, 50th, 25th, and 5th percentiles. The 5th percentile for the outsized floods category nearly equals the 25th percentile.

respond to river-level outcropping of the relatively softer John Day and Clarno Formations compared to the Columbia River Basalt Group, which forms the river-level bedrock farther downstream [*O'Connor et al.*, this volume]. There are only two small islands between RM 83 and 74 where the channel is confined on both sides by extensive landslide complexes.

Alluvial islands were categorized on the basis of our interpretation of primary formative processes. The categories include islands formed by (1) outsized floods (floods with a return period greater than 1000 yrs), including Pleistocene dam-break floods and the Outhouse Flood, (2) century-scale floods, such as those in 1861, 1964, and 1996, and smaller, annual- to decadal-scale floods, (3) floods and channel processes of uncertain origin and magnitude, and (4) unknown processes. We identified no islands directly formed by landslides, hillslope processes, or volcanic events.

Islands formed by these different processes have similar size distributions except five much larger islands clearly formed by outsized floods (Figure 8). These include the largest islands in the lower Deschutes River: Harris Island at RM 11.7; Cedar Island at RM 30.9; and islands at RM 22.8, 40.6, and 88.9, informally named Airstrip Island, Doe Island, and Peanut Island, respectively (Figure 9). These large islands are composed of coarse gravel and have bouldery surfaces that are up to 2 m above the maximum stage of the February 1996 flood. All of these islands are inferred to have been deposited by the Outhouse Flood [*Beebee and O'Connor*, this volume]. The average size of the five Outhouse Flood islands is 4.6 ha, more than 10 times greater than the average size of islands formed by other processes. Islands formed of Outhouse Flood deposits have a combined area of 22 ha, equivalent to 39 percent of the total island area.

Most islands in the lower Deschutes River appear to be associated with relatively fixed valley-bottom and channel features that generate hydraulic conditions favorable for deposition. For example, the Outhouse Flood islands appear to have been deposited as transverse bars at valley and channel inflections (e.g., Cedar Island, Figure 9c) or valley expansions (e.g. Harris Island). In some cases, these islands were apparently modified subsequently by waning or smaller flows (e.g., Airstrip Island and Islands 343-346, Figure 10). Smaller islands apparently more related to century-scale and smaller return-period floods have formed at geometric irregularities along the river such as at bank protru-

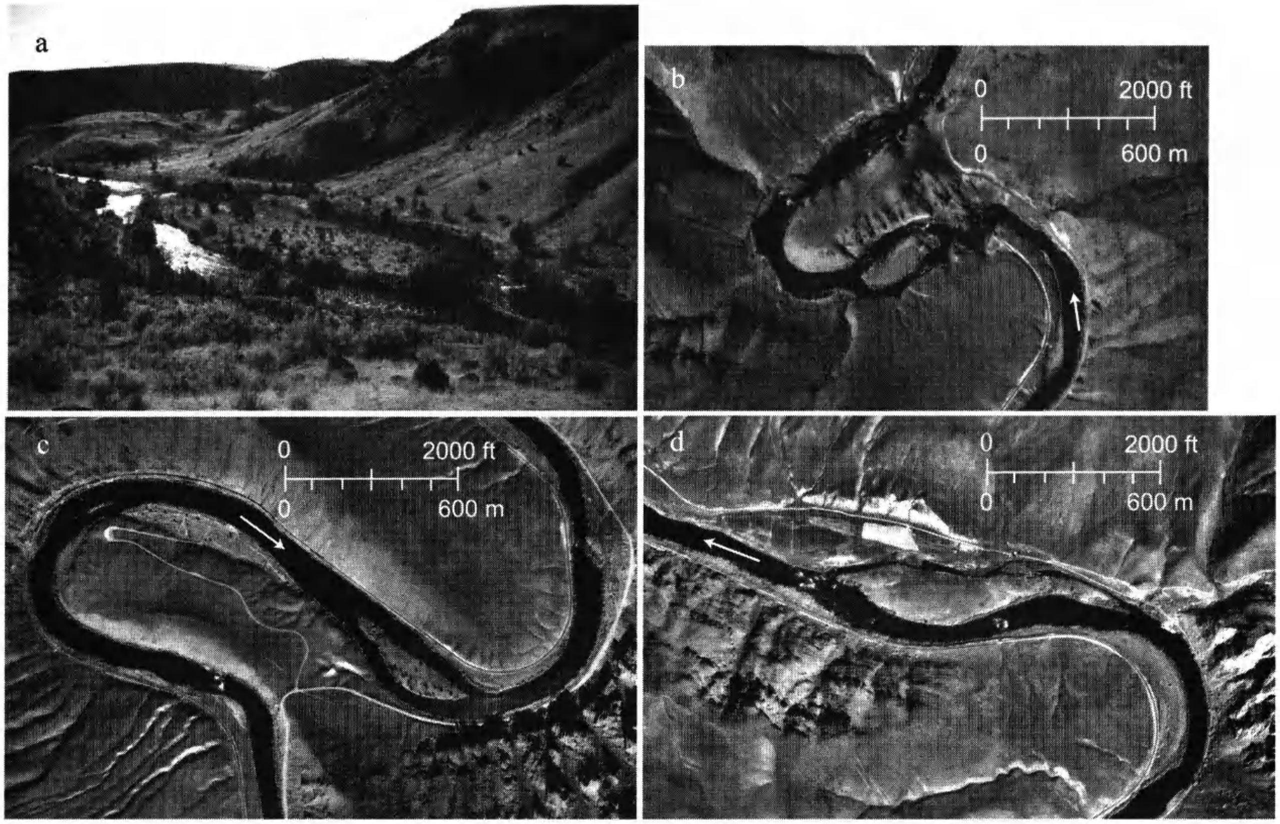

Figure 9. Islands formed by outsized floods. (a) Peanut Island (380 m long). Photograph by Robin Beebee. (b) Doe Island. (c) Cedar Island. (d) Harris Island. Aerial photographs in b, c, and d are dated 1995, Portland General Electric.

sions [e.g., *Lisle*, 1986] or channel contractions and expansions, where locally reduced flow velocity has promoted in-channel deposition. Although islands in other river systems have been described as moving progressively downstream or attaching to the floodplain in association with bank erosion and accompanying changes in channel width [e.g., *Hooke*, 1986; *Church and McLean*, 1994], Deschutes River islands do not migrate freely in conjunction with evolving channel geometries.

Rapids

The lower Deschutes River presently drops over 23 named rapids larger than Class 2 (Table 4), a recreational rating based on difficulty of navigation. Impoundment of the Columbia River by The Dalles Dam in 1956 inundated one additional steep fall near the mouth of the Deschutes River. Together, these rapids account for about 20 percent of the total elevation drop from the Pelton-Round Butte dam complex to the Deschutes River confluence with the Columbia River. The steepest rapids include the 4.7 m drop at Sherars Falls (Figure 11b) and Whitehorse Rapids, where the river descends 8 m in 0.5 km. Numerous unnamed minor rapids and riffles also contribute substantially to the total river descent.

Thirteen of the 23 major rapids are clustered within the two bedrock zones between RM 50-40 and RM 10-0 (Table 4). There are no large rapids between RM 40 and RM 20. The 10 remaining named rapids are distributed between RM 87-53 and RM 19-11. The formation, distribution, and stability of major rapids along the lower Deschutes River are strongly controlled by geologic conditions of the valley and by hillslope processes. Twelve of the major rapids occur where flow drops over ledges of basaltic bedrock, reflecting the interplay over the last several million years between the downcutting Deschutes River, regional tectonic structures, and diversions by lava flows and landslides. The remaining 11 major rapids were formed by outsized flood deposits, mass movements from valley sides, and coarse-grained tributary flood or debris-flow deposits (Table 4).

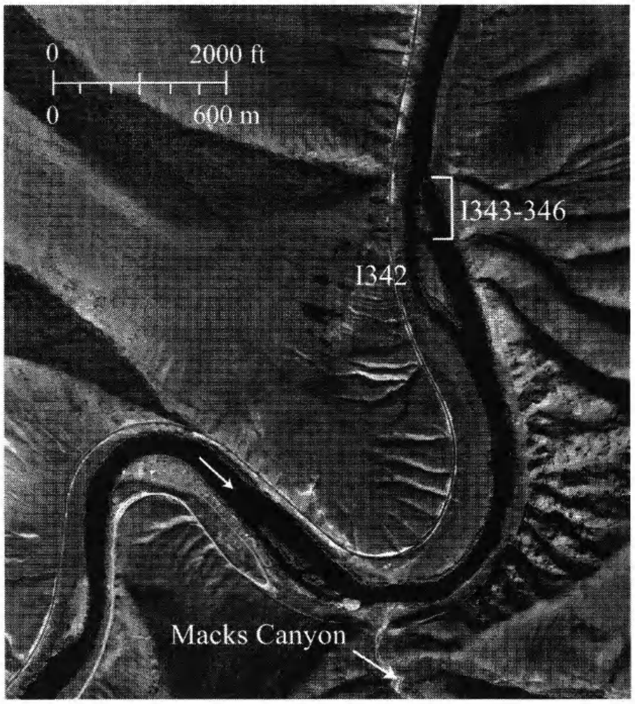

Figure 10. Airstrip Island (Island 342) is cored by gravel, cobbles, and boulders up to 0.5 m in diameter and was not overtopped in the February 1996 flood, evidence that it was formed by outsized flooding. Islands 343 through 346 are inferred to have been deposited at the same time, such that the entire group of five islands is an erosively modified transverse bar. Aerial photograph dated 1995, Portland General Electric.

Large Quaternary mass movements directly or indirectly account for the six named rapids between RM 100 and 50 [*O'Connor et al.*, this volume]. Trout Creek Rapids is composed of 2- to 3-m-diameter boulders deposited during a flood that apparently resulted from a landslide-dam breach. Whitehorse Rapids is the remnant of a landslide dam formed by a large, late Pleistocene mass movement at RM 76 (Figure 11c). Similarly, mass movement from the left valley slope near Dant temporarily dammed the Deschutes River at RM 64 and left a lag of large boulders that now form Buckskin Mary Rapids (Figure 11a). Four Chutes Rapids, 1 km downstream, is composed of remnants of coarse debris brought to the valley bottom and redistributed by floodwaters escaping the breached dam at Buckskin Mary Rapids. Wapinitia and Boxcar Rapids (Figure 11d) formed where large landslides moved onto the valley bottom and have either blocked or partially diverted the channel.

White River Rapids, Bull Run Rapids, Harris Rapids (Figure 9d), and Colorado Rapids are all reaches where the Deschutes River flows over and through accumulations of large boulders. In each instance, these boulder fields are near termini of Outhouse Flood bars, leading us to infer that the rapids developed in lags of coarse deposits of the Outhouse Flood (Table 4).

Coarse debris delivered by tributaries has formed just one major rapid on the lower Deschutes River. Washout Rapids

Table 4. Name, location, rating, and formative process for major Deschutes River rapids

Rapid	Location (RM)[1]	Class[2]	Formative Process
Upper Trout Creek	87.0	3	outsized flood
Lower Trout Creek	86.9	3	outsized flood
Whitehorse	76.1	4	mass movement
Buckskin Mary	63.8	3	mass movement
Four Chutes	63.4	3	mass movement
Wapinitia	54.7	3	bedrock
Boxcar	53.7	3	mass movement
Oak Springs	47.3	4	bedrock
White River	46.3	3	outsized flood
Upper Rollercoaster	45.7	3	bedrock
Lower Rollercoaster	45.4	3	bedrock
Osborne	45.0	3	bedrock
Sherars Falls	44.0	6	bedrock
Bridge	43.6	3	bedrock
Wreck	40.0	3	bedrock
Bull Run	18.4	3	outsized flood
Jet Pump	15.5	3	bedrock
Harris	11.4	3	outsized flood
Washout	7.8	4	tributary
Gordon Ridge	5.9	3	bedrock
Colorado	4.2	4	outsized flood
Rattlesnake	2.7	4	bedrock
Moody	0.8	3	bedrock

[1] River mile

[2] Rating obtained from BLM brochure "Welcome to the Lower Deschutes River," undated. Scale varies from Class 1, beginner, to Class 6, unrunnable. Only rapids Class 3 or greater are included.

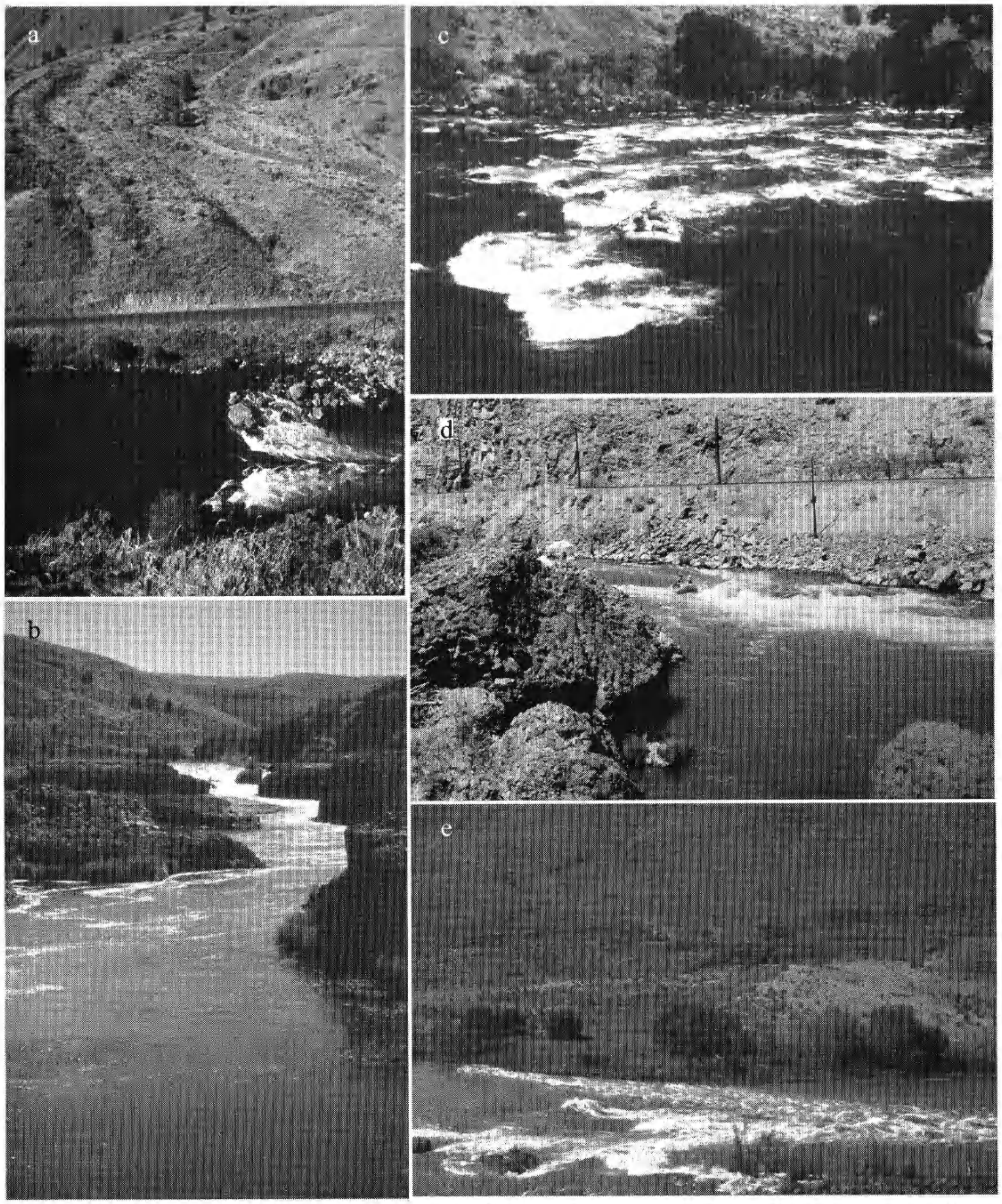

Figure 11. Rapids in the lower Deschutes River. (a) Buckskin Mary Rapids, formed by a debris flow visible directly behind the rapid. (b) Bedrock Sherars Falls and surrounding irregular bedrock surfaces. (c) Whitehorse Rapids, formed from the remnants of a massive landslide dam. (d) Boxcar Rapids, formed by bedrock landslide debris. (e) Washout Rapids, formed by debris and constriction from tributary flooding in a July 1995 thunderstorm.

at RM 8 (Figure 11e) was created in 1995 when an intense rainstorm caused significant flooding and debris flow activity in tributaries entering the lowermost 20 km of the Deschutes River [Steve Pribyl, oral commun., 1998]. In a manner similar to that described for the Colorado River in the Grand Canyon [*Webb et al.*, 1999], two of these debris flows delivered a large volume of mostly cobble- and small boulder-sized material to a small fan at the mouth of Stecker

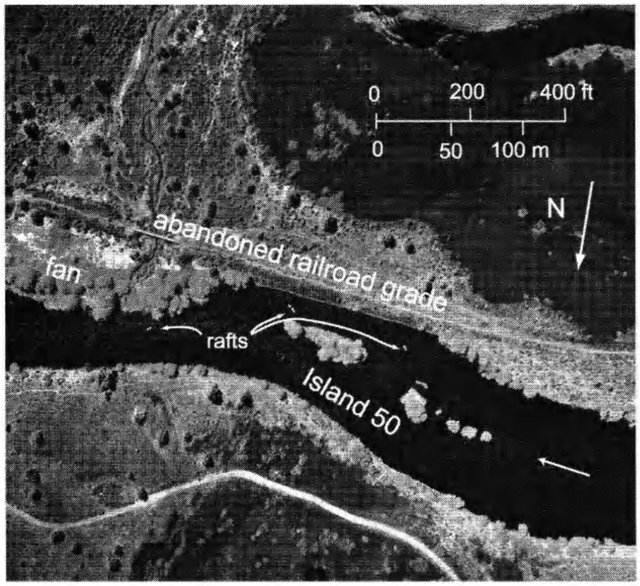

Figure 12. Influences on channel morphology. The tributary fan at RM 90.2 is typical of a 5-mile-long zone of frequent fan constrictions between RM 90 and 94. Islands within this zone appear to be largely associated with hydraulic conditions generated by the alternating constrictions and expansions. The linear and unvegetated nature of the right bank upstream of the tributary fan suggests that railroad ballast has retarded erosion at this location. Island 50 was a single island in 1911, eroded from one island to two between 1911-1944, and eroded into the present seven-island cluster between 1944-1995. Minor erosion occurred at the two largest islands in the February 1996 flood.

Canyon, constricting the Deschutes River channel between the enlarged tributary fan and bedrock outcrops on the opposite bank.

Other Landforms

Landslides and colluvial deposits, bedrock not modified by fluvial processes, and railroad ballast and roads occupy the remainder of the valley bottom. Mass movements onto the valley bottom have directly influenced channel morphology by locally constricting the valley bottom and channel and, indirectly, by forming dams that have subsequently been breached, resulting in large floods. Rock-fall and talus aprons locally reach the valley bottom and contribute coarse sediment to the valley and channel, especially where the Columbia River Basalt Group is exposed near river level.

Railroad construction and maintenance has been the most pervasive human disturbance to the valley bottom, including two separate railroad right-of-ways that were constructed up portions of both sides of the river between 1910 and 1912. Only one line is presently operational; the other line has been abandoned and partially converted to roadway. Railroad and road construction has not resulted in relocation of the Deschutes River channel or substantial cut and fill of channel banks. In isolated locations riprap has been placed where erosion has threatened the railway. At some locations where active and abandoned railroad routes flank the channel, slopes formed of railroad ballast form the channel margin, perhaps stabilizing channel banks (Figure 12).

HISTORICAL ANALYSIS OF VALLEY-BOTTOM AND CHANNEL EVOLUTION

We further develop inferences of key processes affecting the lower Deschutes River by evaluating historical changes to the channel and valley bottom. This approach was partly inspired by previous reports of landform stability within the lower Deschutes River valley [*Aney et al.*, 1967; *McClure*, 1998], which concluded that changes to the channel position and most channel and valley-bottom features have been small. These studies, however, have only evaluated short reaches or isolated features in the channel. For this reason, we systematically identified changes in the entire 160 km reach over the historical record (Table 1).

The Channel

The position of the Deschutes River channel has changed little over the 20th century despite being flanked by alluvial deposits for about 80 percent of its length downstream of the Pelton-Round Butte dam complex. Comparisons between maps from a 1911 U.S. Geological Survey topographic survey of the channel, isolated General Land Office surveys of varying detail dating back to 1865, 1996 aerial photographs, and 1995-2000 field mapping show that most banks and islands have remained in identical locations for the last 100 years (Figure 13). This finding is consistent with *Klingeman et al.'s* [1990] observation of less than a kilometer of what they term "severe" bank erosion between RM 73.6 and the Columbia River confluence during a 1989 inspection. At isolated locations, such as near North Junction (Figure 14) and the mouth of Shitike Creek (Figure 15), channel widening or local deposition has resulted in as much as 90 m of lateral bank migration, but nowhere has there been unidirectional channel or meander migration of more than a few tens of meters.

Islands

Islands have been the most historically dynamic component of the lower Deschutes River valley bottom. Historical

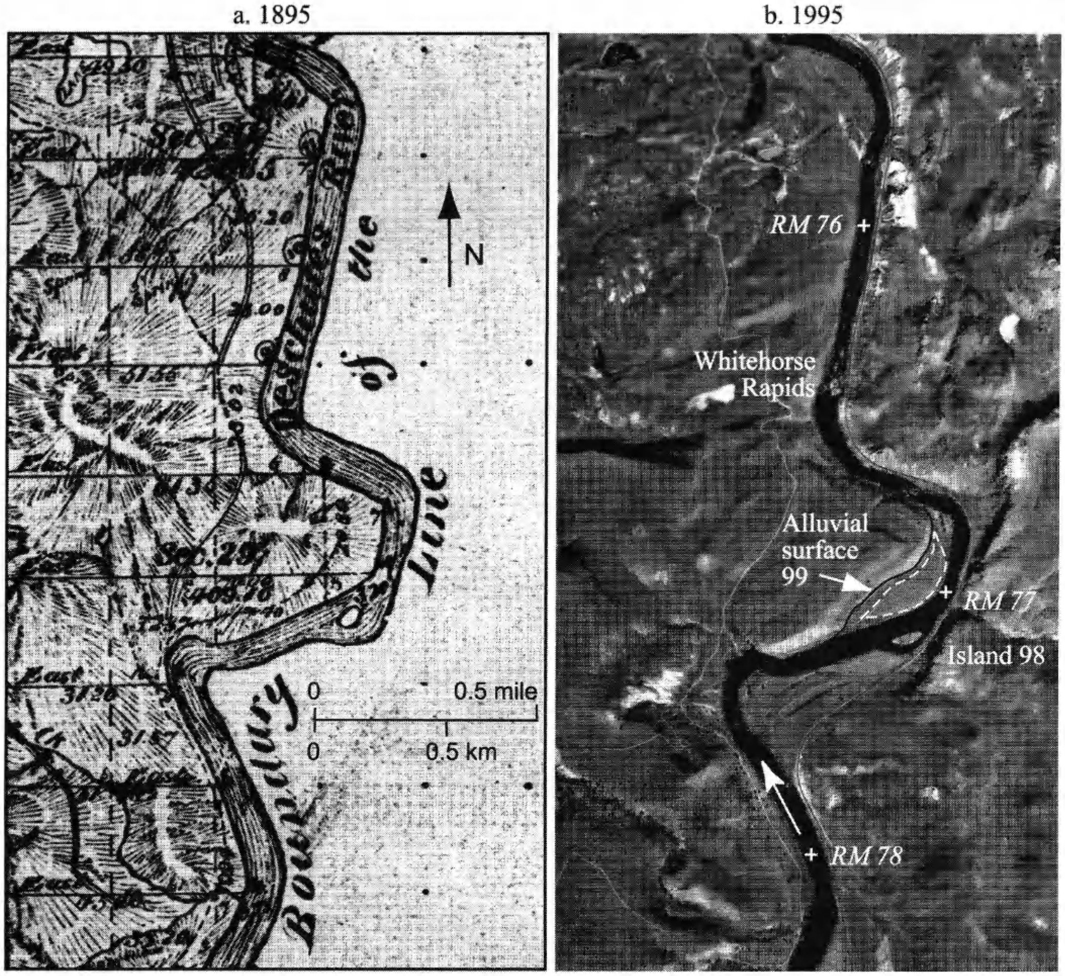

Figure 13. Comparison of channel conditions at RM 75.5 to RM 78.5 in 1895 and 1995. (a) Map from a General Land Office Survey conducted in the mid to late 1800s. (b) Aerial photograph of same area, showing that Island 98 has remained in the same position for 100 years. Scale varies across the photograph but is approximately similar to map scale. Figure 3 shows an oblique view of a portion of this area.

maps and aerial photographs (Table 1) provided a basis for assessment of changes to each of the 153 islands that we have identified in the lower Deschutes River for three distinct periods between 1911 and 1996: (1) a 1911-1944 predam period in which no floods with a return period on the order of a century or more occurred, (2) the 1944-1995 period, which includes the completion of the Pelton-Round Butte dam complex and the century-scale 1964 flood, and (3) a 1995-1996 period defined by sets of aerial photographs made before and after the century-scale February 1996 flood.

For each island and for each time period, changes were categorically defined on the basis of the type (growth or shrinkage) and magnitude (in terms of percent area). Changes generally were categorized as erosion or growth affecting (1) less than 10 percent, (2) 10 to 50 percent, or (3) 50 to 100 percent of the island area. We also defined a fourth category for new islands formed or existing islands completely eroded away; in those cases, change was by definition 100 percent. For islands that had both growth and erosion during a time period, such as would result from erosion at the upstream end and coincident deposition at the downstream end, we recorded both changes. To calculate absolute magnitudes of areas of erosion and deposition for islands with detectable change, we multiplied island area by values 0.07, 0.30, 0.75, or 1.0, respectively, corresponding with midpoint of the first three classifications of change (except at the exceptionally large Harris Island, where the change was estimated to the nearest percent). The value of 0.07 for the "less than 10 percent" category reflects our observation

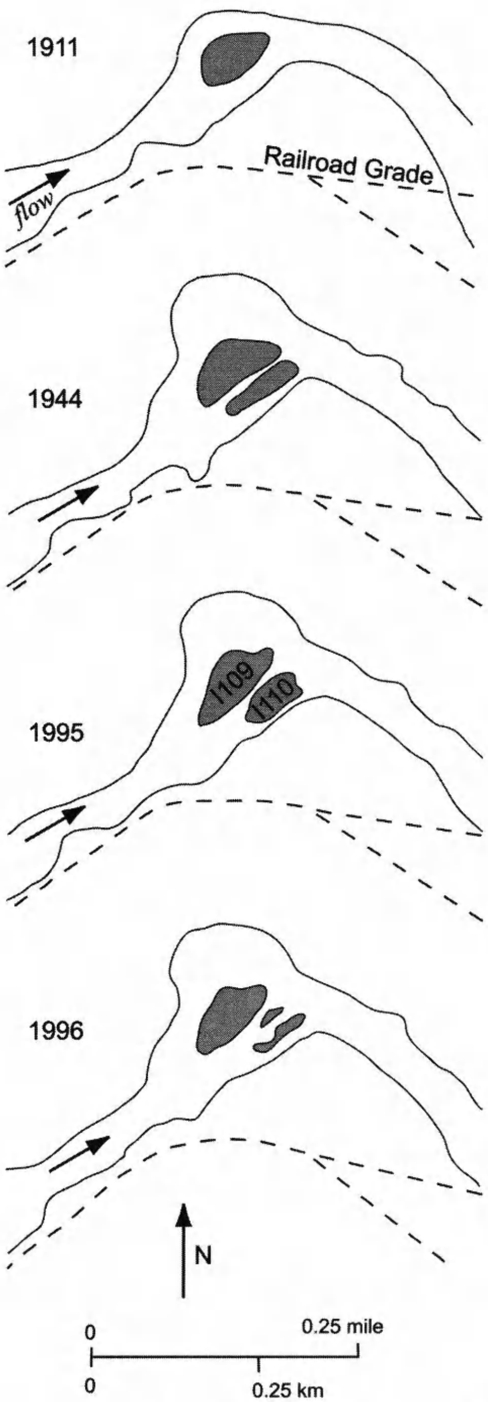

Figure 14. Bank erosion and island conditions at RM 73.1. A large scoop was eroded into the tall, fine-grained, left bank between 1911 and 1944. The combined area of Islands 109 and 110 increased between 1911 and 1944, then progressively decreased, but island position remained constant. Sketches are from the 1911 map, 1944 photos, 1995 1:24,000 photos, and 1996 digital images.

that changes of less than about 4 percent of island area were not detectable with confidence given the accuracy of the historical maps and slightly different flow stages on the photograph dates. Island numbers used in the text refer to Island ID numbers assigned for the analysis.

Island Changes. Only 21 of the 153 islands have apparently not changed over the entire 1911-1996 time period. Of these, 17 are formed of bedrock. Most individual islands did have detectable change at some point, but most changes were small—either being categorized as less than 10 percent or 10 to 50 percent of the island area for a given time period. For each of the three time periods, the total area of erosion and deposition ranged between 7.4 and 11 ha, equivalent to 13 to 20 percent of the total island area (Table 5).

Island changes during all periods examined typically consisted of local erosion, growth, or a combination of both along island margins. Our observations of fresh deposits in the 1981, 1995, and 1996 photos and during field reconnaissance indicate that island growth is typically by lateral accretion of gravelly deposits along one or two of an island's margins. Erosion and growth also occurred on upstream and downstream tips and on both flanks of individual islands, but without apparent consistency within reaches or among groups of islands. Upstream and downstream island migration, where erosion at one end coincided with growth at the other end, occurred at some locations but was no more common than any other documented pattern of change.

Erosion or growth affected more than the island margins at only a few locations. Examples include sites where single islands divided into multiple smaller islands (Figures 12, 14), complete erosion of islands, and formation of new islands. The largest island completely removed was the 0.3-ha Island 17 at the mouth of Shitike Creek (Figure 15). Through analysis of a sequence of aerial photographs, *McClure* [1998] determined that this island was eroded by the 1964 flood. The 43 new islands that formed during the three analysis periods all resulted from deposition of alluvium during floods; nowhere did we observe new islands generated by channel avulsion or similar processes that would result in detachment of a portion of flanking alluvial surfaces. Some new alluvial islands were formed where shallow subaqueous bars existed in previous years.

The relationship between islands and channel banks is an important factor in aquatic habitat generation and stability. Side channels between islands and banks are typically shallow and are an important element for aquatic habitat [*Aney et al.*, 1967]. Fifty of the non-bedrock islands in the lower Deschutes River are in mid-channel positions, dividing the river into two roughly equal channels; the remaining 69 are significantly closer to one bank than the other, separating

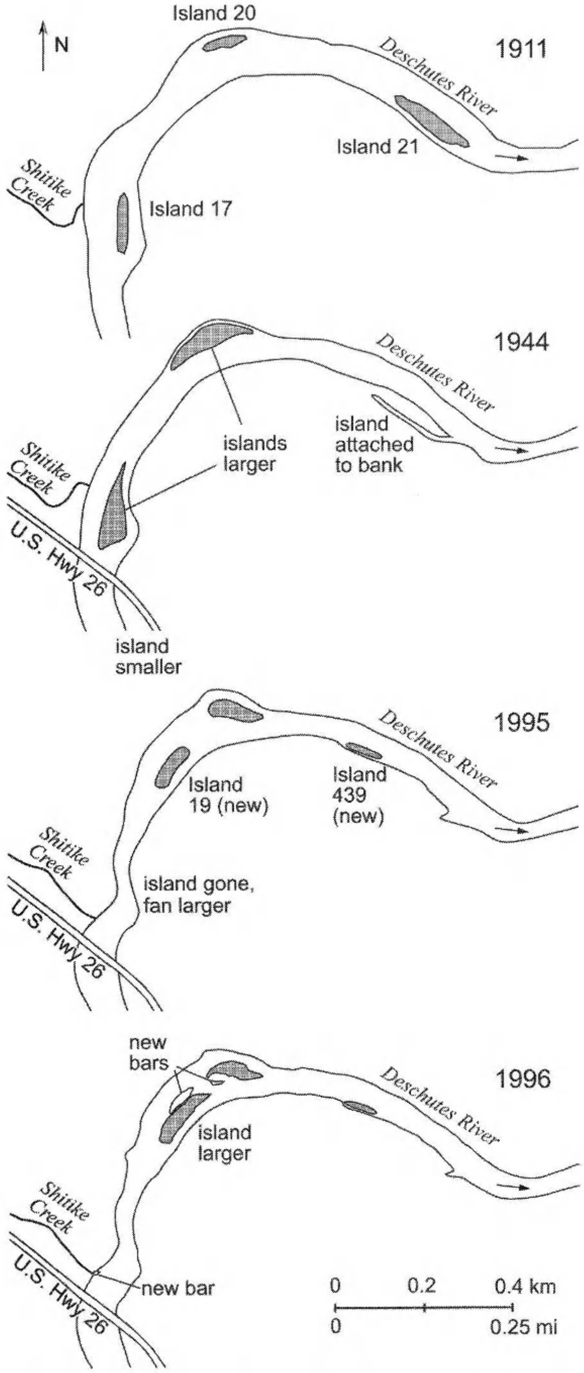

Figure 15. Changes to islands and banks near Shitike Creek between 1911 and 1996. Sketches are from the 1911 map, 1944 photos, 1995 1:24,000 photos, and 1996 digital images.

flow into unequal channels. Although most islands in close proximity to banks remained separate from the bank even when affected by erosion or growth, six islands clearly isolated from the bank in the 1911 maps subsequently became attached. In all six cases, the islands became completely or partially attached to the bank by 1944, were completely attached by 1995, and did not change substantially in the 1996 flood. Five of these – Islands 444, 21, 445, 450, and 451 – were situated along the downstream edge of a point bar (e.g., Island 451 in Figure 16). The remaining island, Island 80, was on the outside of a bend just downstream of the confluence with the Warm Springs River. The accreted islands remain distinguishable as densely vegetated low

Table 5. Type and magnitude of island change for three periods from 1911 to 1996

Type of change	No. of islands	Total Area Affected (ha)	Net Area Affected (ha)
1911 to 1944			
not available[1]	22		
no change	44		
erosion	8	0.43	-0.43
growth	70	9.1	9.1
erosion & growth	9	1.9	-0.79
total for period		11	7.8
1944 to 1995			
no change	68		
erosion	42	2.0	-2.0
growth	31	2.7	2.7
erosion & growth	12	3.2	-0.026
total for period		7.8	0.68
1995 to 1996			
not available[2]	4		
no change	64		
erosion	52	3.3	-3.3
growth	27	1.8	1.8
erosion & growth	6	2.4	-0.20
total for period		7.4	-1.7

[1] Islands not evaluated because historical source judged inaccurate, primarily bedrock islands not mapped in 1911 that were likely present.
[2] Islands not evaluated because historical source missing.

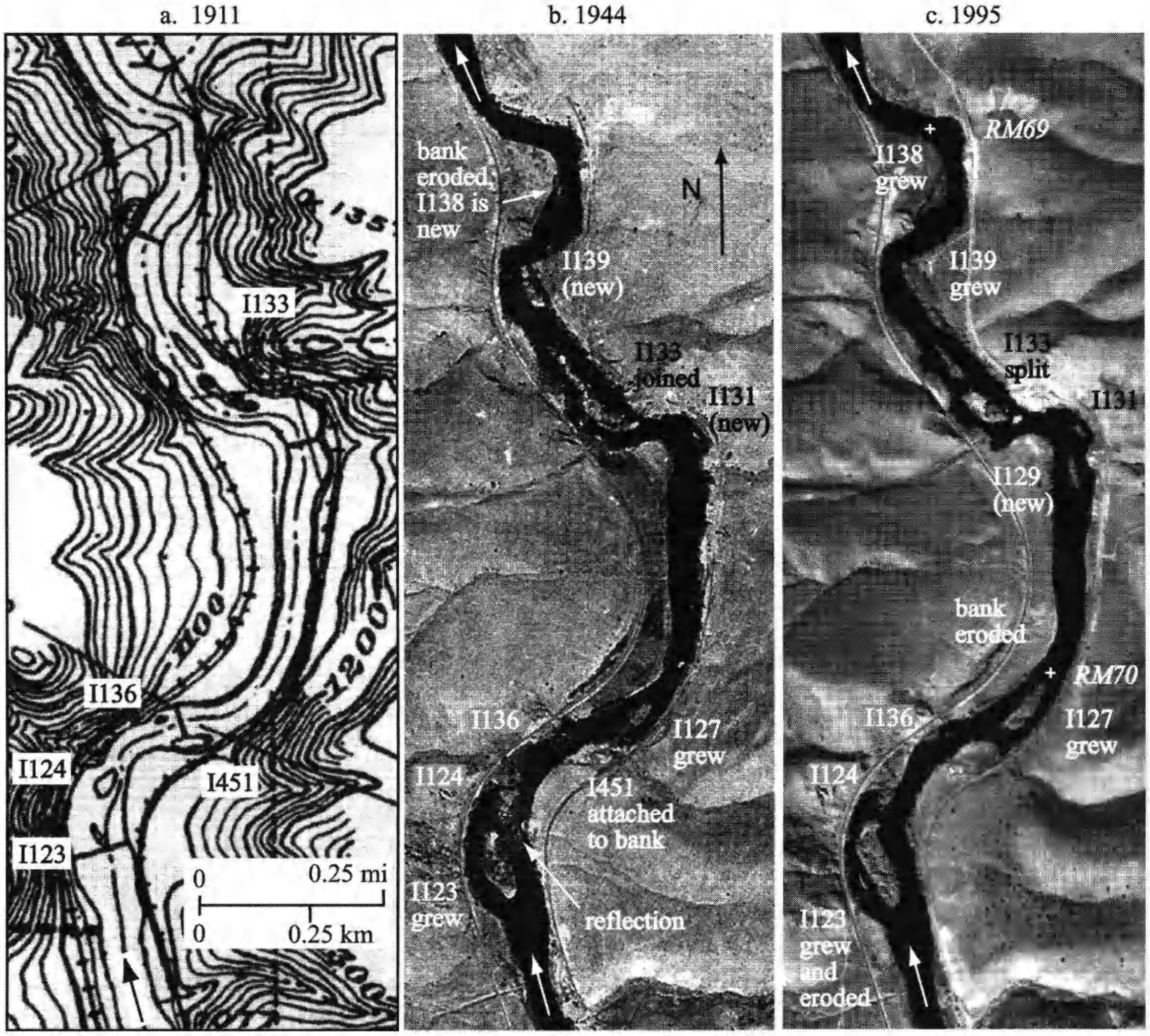

Figure 16. Changes to an active reach near Two Springs Ranch, RM 69-70.5, between 1911 and 1995. Changes in 1996 were almost entirely erosional, with substantial erosion to Island (I) 138 and moderate erosion to I129, I133, and I139. There are no nearby sources of sediment, and changes cannot be characterized as spatially or temporally progressive, nor are they clearly related to large floods. Scale varies across the photographs but is approximately similar to map scale.

areas attached to the main bank. We did not observe any locations where attached islands were separated by reopening of side channels.

Longitudinal Distribution of Island Changes. No longitudinal pattern of island growth or erosion was evident during any of the three time periods analyzed, unlike in other alluvial rivers, where erosional and depositional zones may persist and migrate downstream on decadal timescales [e.g., *McLean and Church*, 1999]. However, three discrete reaches had groups of islands that changed substantially during each time period. These reaches of island instability were near the Shitike Creek confluence (RM 96-97, Figure 15), upstream of Two Springs Ranch (RM 69-70.5, Figure 16), and near Macks Canyon (RM 23.5 - 24, Figure 17). Although compared to those in most western rivers, the changes within these reaches were small, they do represent the only locations along the lower Deschutes River of substantial changes to island and side channel conditions during the last 100 years.

Shitike Creek is the only large tributary confluence where islands have actively evolved. Frequent changes at this site can probably be attributed to the influx of sediment and water from Shitike Creek during large floods. Between 1911 and 1944, the islands nearest the confluence, Islands 17 and 20, roughly doubled in size, but the number and position of

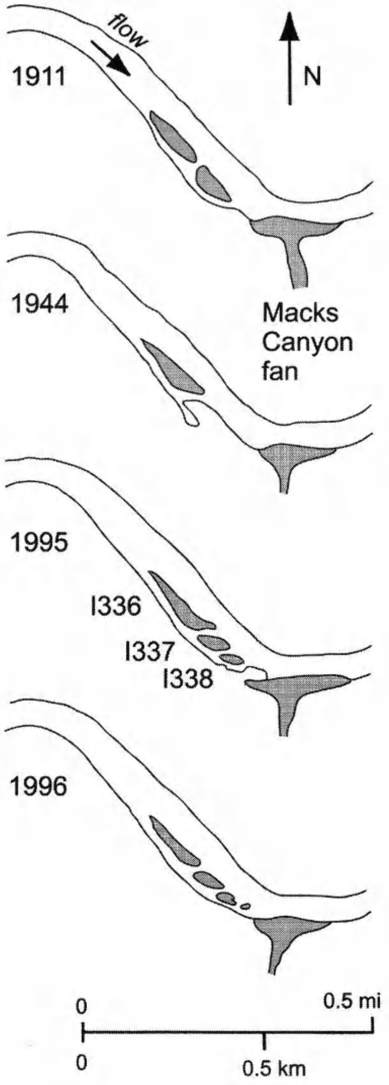

Figure 17. Changes to active islands at Macks Canyon, RM 23.5-24.1, between 1911 and 1996. Sketches are from the 1911 map, 1944 photos, 1995 1:24,000 photos, and 1996 digital images. The 1995 photograph is shown in Figure 10.

islands in the reach was constant (Figure 15). *McClure* [1998] documented changes to islands and banks at and downstream of the confluence of Shitike Creek between 1944 and 1996 from a series of aerial photos and concluded that the most significant changes at this site, which included complete erosion of Island 17, emergence of Islands 19 and 439, downstream movement of Island 20, and bank attachment of Island 21, occurred as the result of the 1964 and 1996 floods.

Islands within the reach upstream of Two Springs Ranch evolved during every period we examined (Figure 16). Individual islands grew and eroded between 1911 and 1996, new islands emerged, and an existing island attached to the bank at the same time that banks farther downstream eroded. The 1996 flood eroded Islands 129, 133, 139, and the tip and surface of Island 138, which became attached to the bank when the narrow side channel closed off.

Of the small tributaries in the lower canyon that constrict the channel with their fans (e.g., Figure 3c), only Macks Canyon has actively influenced island evolution since 1911. A series of islands and ephemeral bars has formed upstream of the constriction imposed by the Macks Canyon fan (Figure 17). These islands and bars grew and partly merged with the channel bank near the fan by 1944, but then were eroded and mostly separated from the bank by 1995. The 1996 flood further eroded the islands and the channel bank.

Temporal Changes to Islands. In contrast to the absence of clear longitudinal (spatial) trends in island evolution, temporal trends associated with the three distinct analysis periods are more evident (Table 5, Figure 18).

1911-1944: Pre-dam Period With Annual- to Decadal-Scale Floods. Seventy of the 153 islands grew by detectable amounts during this pre-dam period, during which net growth totaled 7.8 ha (Table 5). Twenty-nine small new islands appeared, and only three islands were completely eroded. The average annual area affected by erosion or growth was less than 1 percent of the total island area.

Islands grew throughout the lower Deschutes River, but island growth was particularly noticeable between RM 100 and 60 (Figure 18a). Eroded islands were also almost exclusively in the upper canyon. The absence of erosion and growth between RM 50 and 40 corresponds to the reach of bedrock islands, where few islands changed during any of the periods studied. The largest individual changes were at Peanut Island, where more than 1 ha of the island flank was eroded, forming its present peanut shape, and at Harris Island, where nearly 1 ha of gravel accreted to the upstream tip of the island.

1944-1995: Pre/Post-Dam Period With A Century-Scale Flood. Slightly more islands eroded than grew during the 1944-1995 period, although the net change was about 1 ha of growth (Table 5). Similar to the pre-dam period, the number and total area of new islands exceeded the number and area of completely eroded islands. The average annual island area affected by erosion and growth amounted to <1 percent of the total island area.

Island erosion and growth during the period 1944-1995 were more evenly distributed throughout the canyon than during the period 1911-1944. However, islands near Shitike

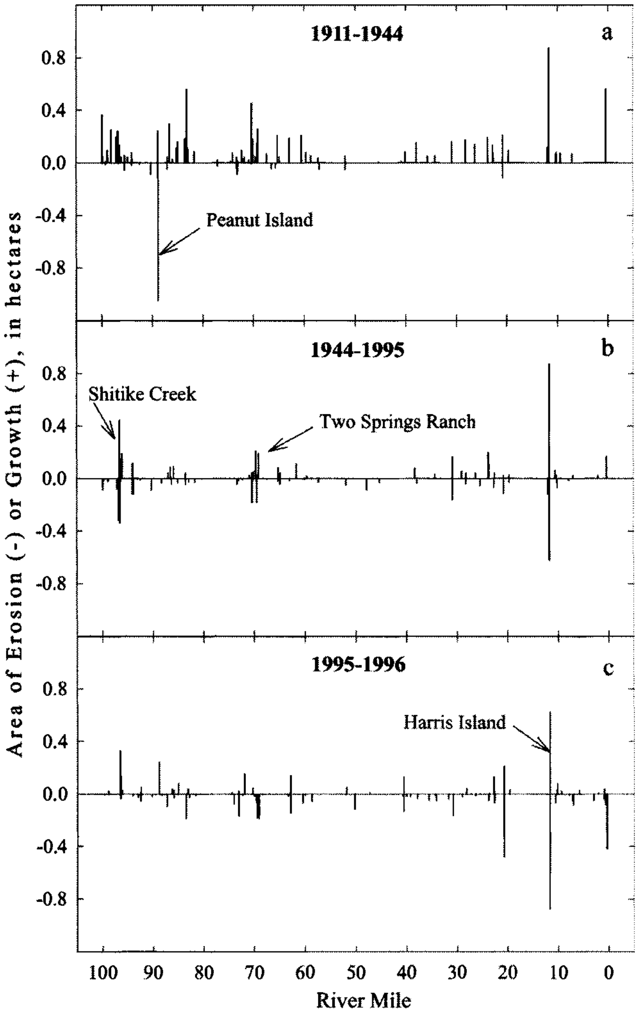

Figure 18. Surface area affected by erosion and growth at islands during three periods from 1911 to 1996. (a) Pre-dam period with no major floods, 1911 to 1944. (b) Pre/post dam period with a century-scale flood, 1944 to 1995. (c) Effects of a century-scale flood, 1995 to 1996. Islands that grew are shown as positive values and eroded islands are shown as negative values.

Creek and Two Springs Ranch, as well as Harris Island, were particularly dynamic (Figure 18b).

1995-1996: Effects of a Century-Scale Flood. Photographs taken during the summers of 1995 and 1996 (supplemented by reconnaissance immediately after the flood) show that the February 1996 flood resulted primarily in island erosion (Table 5). About twice as many islands eroded as grew, and net island area decreased by nearly 2 ha. This single flood affected 13 percent of the total island area, which significantly exceeds the annual rates of island change for the periods 1911-1944 and 1944-1995.

Island erosion and growth were evenly distributed throughout the canyon during 1995-1996 (Figure 18c). As was the case for the other two time periods, changes at Harris Island accounted for a substantial portion of the total island change.

Rapids

There has been little discernible evolution of most of the major rapids on the Deschutes River below the Pelton-Round Butte dam complex during historic time. Many individual boulders within major rapids such as Boxcar and Whitehorse have been in place since the earliest historic navigation. Isolated movement of a few boulders during the February 1996 flood occurred at some of the named rapids, but caused no fundamental change in rapid geometry [Walt Wolfe, Portland General Electric, oral comm., 1997]. The only major historic change in rapids on the Deschutes River occurred in July 1995 when Washout Rapids formed as a result of a debris flow or flood. This rapid was modified only slightly by subsequent annual- to century-scale flows.

DISCUSSION

The distribution and evolution of valley-bottom and channel features summarized in the previous sections allows for some general remarks on the overall geomorphic regime of the Deschutes River below the Pelton-Round Butte dam complex as well as on specific hypotheses regarding the potential effect of natural and human disturbance on channel and valley-bottom features.

Valley-Bottom Features, Processes, and Dynamics

The primary valley-bottom features that flank the lower Deschutes River channel are bouldery bars of outsized floods, gravel bars formed or reworked by century-scale floods, isolated fine-grained flood plains that accumulate drapes of overbank silt and sand during century-scale floods, coarse-grained tributary fans, and fluvially eroded bedrock surfaces. For most of the length of the canyon, the overall geometry of the valley bottom is largely established by the locations of the outsized flood deposits, and between RM 100.1 and RM 60 by large landslide complexes that have slid onto the valley bottom [*O'Connor et al.*, this volume]. Bedrock locally confines the channel between RM 60-40 and RM 10-0. Thus, the major controls on the valley-bottom morphology result from processes such as regional tectonics, large landslides, and dam-break floods that operate on timescales or return periods of thousands to millions of years. Processes such as flood plain formation and fan building that are associated with historic events such as the July 1995 convective storm and the regional floods of 1861, 1964, and 1996 can only generate persistent landforms where the dominant longer-term valley-bottom processes have left space for such features to form away from the channel.

The timescales of these dominant valley-bottom processes restrict the physical legacy of human perturbations such as upstream impoundment to the relatively small proportion of the valley bottom (beyond the channel) that is affected by century-scale or smaller processes. For the lower Deschutes River, where the primary historic alteration to the overall system consists of reduced downstream delivery of fine-grained sediment from the upper Deschutes and Crooked River basins [*O'Connor, Grant, and Haluska*, this volume; *Fassnacht et al.*, this volume], the most likely long-term effect of impoundment will be reduced long-term vertical accretion rates on the isolated fine-grained flood plains as well as reduced overbank sedimentation on the coarse-grained alluvial surfaces that are inundated by century-scale or smaller flood flows.

Channel and Island Features, Processes, and Dynamics

The major channel features of the Deschutes River include islands, rapids, and submerged gravel bars. In contrast to other valley-bottom features, certain geomorphic elements of the channel environment, such as islands, are dynamic, and change over timescales of a century or less despite being within a channel geometry that has been relatively fixed by processes that operate at longer timescales. The following discussion focuses on processes that affect islands and rapids; *Fassnacht et al.* [this volume] describe processes that affect gravel bar formation and evolution.

Islands. Key island formation processes include long-term bedrock erosion and floods. The largest islands, such as Harris and Peanut Islands, resulted from the Outhouse Flood [*Beebee and O'Connor*, this volume] and now control overall channel location. Similarly, some of the large bedrock islands dictate channel position within the valley bottom. Thus, the largest islands are formed by exceptionally rare floods or by long-term tectonic processes. In contrast, many of the smaller islands are formed either by floods with a return period of a century or less, or by recurring inputs of tributary sediment. These smaller islands reflect ongoing dynamic interactions between the channel and gravel movement in the Deschutes River. Consequently, evolution of smaller islands could be expected to be more sensitive to changes in modern conditions, such as alterations of stream flow and sediment flux imposed by the Pelton-Round Butte dam complex.

We can attempt to detect changes to island conditions that may relate to changes in stream and sediment conditions on the basis of the observations of historical changes to islands coupled with our interpretations of primary formative processes.

Classifying the islands by their dominant formative process and then analyzing their historical evolution as individual groups (Figure 19) shows that all alluvial islands have been susceptible to growth and erosion during the last century. As expected, islands cored by bedrock changed the least, and those changes invariably reflect erosion and deposition of pendant gravel bars. Islands composed of outsized-flood deposits remained in relatively fixed positions within the channel, but local hydraulic conditions promoted accretion or erosion of large areas (although small relative to island size) along their margins during each of the three analyzed time periods (Figure 19). Small islands formed by century-scale floods were most susceptible to relatively large changes, including complete erosion or formation of new islands. Thus, formative flood magnitude is strongly correlated to overall island stability, but is less important than local hydraulic conditions to the canyon-long total area of island erosion and growth. Future response to altered sediment or flow regimes may indeed affect the overall stability of small islands formed by annual- to century-scale floods, but the cumulative area of erosion and deposition at small islands may remain comparable to areas eroded and accreted to islands formed by outsized floods.

Canyon-scale spatial trends in island evolution are not evident in the lower Deschutes River valley for any of the three analyzed time periods (Figure 18). There are no reaches of persistent erosion or deposition, nor is there evidence of downstream propagation of island erosion or deposition. Because effects of the Pelton-Round Butte dam complex would be expected to affect reaches immediately downstream faster and with greater magnitude (e.g., *Williams and Wolman* [1984]; *Andrews* [1986]; *Schmidt and Graf* [1990]; *Schmidt et al.* [1995]), the lack of spatial trends indicates that the impacts of sediment and flow impoundment by the Pelton-Round Butte dam complex have not yet substantially affected island formation or erosion. This result is apparently at least partly due to the substantial sediment input by Shitike Creek, just 3 km downstream from the dam complex.

Temporal trends in island changes are detectable, however. Islands of all origins generally grew from 1911 to 1944, a predam period during which no century-scale floods occurred. Islands changed little between 1944 and 1995, a period that included dam closure and the century-scale 1964 flood. Islands of all origins except those formed by Outhouse Flood deposits were eroded between 1995 and 1996 as a result of the century-scale February 1996 flood. These results indicate that

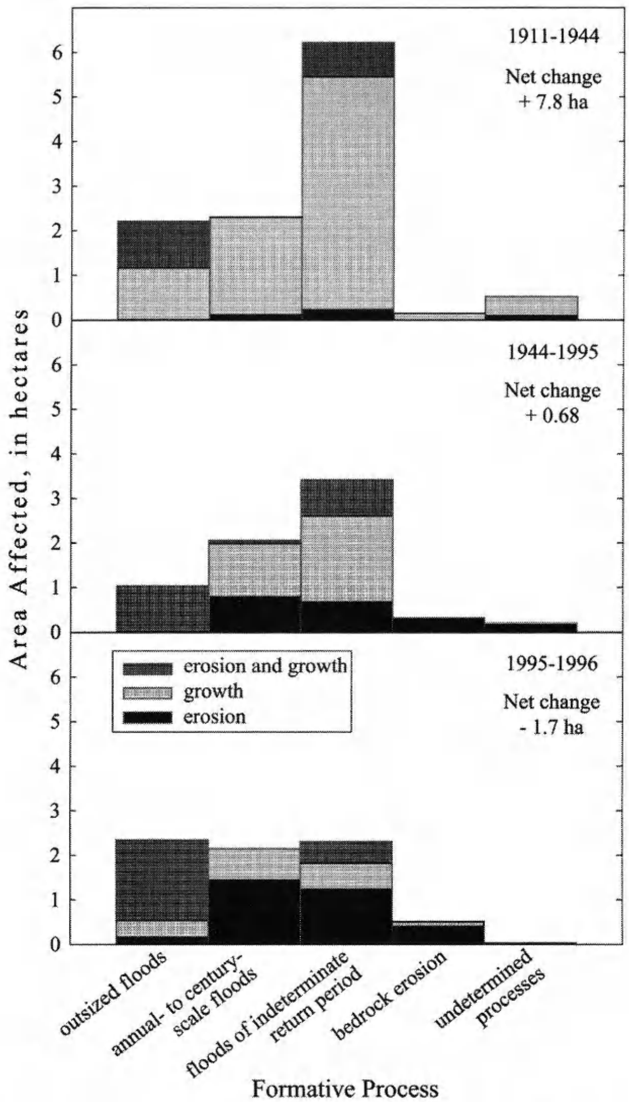

Figure 19. Island area affected by change, stratified by formative process, for three periods between 1911 and 1996. The total number and a summary of the size of islands formed by each process is shown in Figure 8.

islands mainly erode during the *circa* 500-m^3/s (at Madras) century-scale floods, but preferentially form and grow during smaller flows. However, because gravel transport in the Deschutes River requires flows greater than about 250-300 m^3/s [*Fassnacht et al.*, this volume], island growth is restricted to the approximately 1 percent of the time that such discharges are exceeded.

Rapids. Rapids on the lower Deschutes River have been formed by a variety of processes, including long-term bedrock incision, Quaternary landslides, large Quaternary floods, and Holocene tributary floods and debris flows. Similar to observations of rapids in canyon rivers of the Colorado Plateau [*Graf*, 1979], there are no evident overarching controls on the location or stability of rapids. Most Deschutes River rapids were formed by events or processes of exceptional timeframes or magnitude, such as bedrock incision, Quaternary landslides, and floods. As a result, most rapids have been relatively stable in historic time and are likely to remain so in the absence of cataclysmic processes that affect the entire Deschutes River valley bottom. Such conditions differ from those of many canyon rivers such as the Colorado River in the Grand Canyon, where a dynamic balance develops over decades or centuries between rapids-building processes and eroding mainstem flows [*Graf*, 1980; *Kieffer*, 1985]. Only Washout Rapids on the Deschutes River, which formed by debris deposited by a 1995 tributary flood and was subsequently modified by the February 1996 flood, fits the Colorado River model.

SUMMARY AND CONCLUSIONS

Systematic inventory of lower Deschutes River valley-bottom and channel features, interpretation of their origins, and analysis of island erosion and growth during three periods between 1911 and 1996 allow us to assess the relative influence of geologic setting, formative process, and modern-day modifications to river sediment and water flux on the river's valley-bottom and channel evolution.

The overall geology and geomorphology of the Deschutes River basin [*O'Connor et al.*, this volume] has resulted in valley reaches dominated by bedrock (RM 50 – 40 and RM 10 – 0) and landslides (RM 100 – 60); other reaches are within a canyon formed primarily in the Columbia River Basalt Group. This framework largely explains variations such as channel substrate and the geometry of valley and channel features.

Rivers in canyons generally have relatively stable planform geometries. Nevertheless, the Deschutes River is remarkably stable compared to similar canyon rivers that flow through primarily alluvial bottomlands. This stability is largely imposed by high and coarse banks formed of coarse cataclysmic flood deposits from the Outhouse Flood [*Beebee and O'Connor*, this volume], landslides, and deposits from several local landslide-dam breach floods [*O'Connor et al.*, this volume]. The bouldery deposits of these outsized floods, present both as flood bars flanking the present-day channel and as large mid-channel islands, have largely fixed the modern channel into its present position.

Similarly, all but one of the major rapids on the lower Deschutes River are stable and relic features formed by landslides, by landslide breaches, by the Outhouse Flood, or by bedrock outcrops. Only Washout Rapids reflects interactions of decade-to-century timescale processes and is likely to be substantially modified by mainstem flood flows.

Within this context of long-term stability, floods having annual-to-century return periods only locally modify valley-bottom features, generally by minor local erosion of channel banks, deposition of sandy silt on top of isolated fine-grained flood plains, and deposition of gravel and sand on lower parts of coarse flood bars. Historical analysis of the 153 islands in the lower Deschutes River between 1911 and 1996 shows that the largest of these floods, specifically floods in 1964 and 1996, generally erode island margins, regardless of their origin. Islands generally grow in intervening periods. Individual islands formed entirely by century-scale or smaller floods are susceptible to large relative changes in their size, including complete erosion, but deposition and erosion at the margins of the fewer-but-larger islands formed by the Outhouse Flood accounts for comparable areas of island change. The absence of spatial patterns of historical island erosion or growth indicates that most island change reflects local dynamics of sediment inputs, flow hydraulics, and perhaps riparian vegetation characteristics, rather than more pervasive changes in flow or sediment regime.

Acknowledgments. Portland General Electric provided partial funding for this project. We gratefully acknowledge Gordon Grant, Heidi Fassnacht, Michelle Brink, Jasper Hardison, and Toby Minear for assistance in the field and for discussions of various aspects of this project. Eric Schultz and Walt Wolfe provided logistical support during field activities. Portland General Electric and University of Oregon provided access to their aerial photograph collections. Review comments by Jon Major and Patricia McDowell significantly improved this paper.

REFERENCES

Andrews, E. D., Downstream effects of Flaming Gorge Reservoir on the Green River, Colorado, *Geol. Soc. Am. Bull.*, *97*, 1012-1023, 1986.

Aney, W. W., M. L. Montgomery, and A. B. Lichens, Lower Deschutes River, Oregon: Discharge and the fish environment, Lower Deschutes Flow Study Final Report, Oregon State Game Commission, Portland, Oregon, USA, 1967.

Church, M. and D. G. McLean, Sedimentation in Lower Fraser River, British Columbia: Implications for Management, in *The Variability of Large Alluvial Rivers*, edited by S. A. Schumm and B. R. Winkley, pp. 221-241, ASCE, New York, 1994.

Fassnacht, H., Frequency and magnitude of bedload transport downstream of the Pelton-Round Butte Dam Complex, Lower Deschutes River, Oregon, M.S. thesis, Oregon State University, Corvallis, Oregon, 1998.

Graf, W. L., Rapids in canyon rivers, *J. Geol.*, *87*, 533-551, 1979.

Graf, W. L., The effect of dam closure on downstream rapids, *Water Resour. Res.*, 16(1), 129-136, 1980.

Hooke, J. M., The significance of mid-channel bars in an active meandering river, *Sedimentology*, *33*, 839-850, 1986.

Huntington, C. W., Deschutes River Spawning Gravel Study, Final Report, prepared by Buell & Associates for U.S. Department of Energy, Bonneville Power Administration, Division of Fish and Wildlife, Portland, Oregon, v. 1, 179 p. and v. 2, 671 p., 1985.

Kieffer, S. W., The 1983 hydraulic jump in Crystal Rapid – Implications for river-running and geomorphic evolution in the Grand Canyon, *J. of Geol.*, *93*, 385-406, 1985.

Klingeman, P. C., H. Matin, and C.-C. Huang, Investigation of motorboat-induced streambank erosion of the lower Deschutes River, *Water Resources Research Institute WRRI-104*, Corvallis, Oregon, 67 p., 4 appendices, 1990.

Lisle, T. E., Stabilization of a gravel channel by large streamside obstructions and bedrock bends, Jacoby Creek, northwestern California, *Geol. Soc. of Am. Bull.*, *97*, 999-1011, 1986.

McClure, E. M., Spatial and temporal trends in bed material and channel morphology below a hydroelectric dam complex, Deschutes River, Oregon, M.S. thesis, Oregon State University, Corvallis, Oregon, 1998.

McLean, D. G. and M. Church, Sediment transport along lower Fraser River, 2, Estimates based on the long-term gravel budget, *Water Resour. Res.*, *35*(8), 2549-2559, 1999.

O'Connor, J. E., A. Sarna-Wojcicki, K. C. Woxniak, D. J. Polette, and R. J. Fleck, Origin, extent, and thickness of Quaternary geologic units in the Willamette Valley, Oregon, *U.S. Geological Survey Prof. Pap. 1620*, 51 p., 2001.

Schmidt, J. C., Recirculating flow and sedimentation in the Colorado River in Grand Canyon, Arizona, *J. of Geol.*, *98*, 709-724, 1990.

Schmidt, J. C., and J. B. Graf, Aggradation and degradation of alluvial sand deposits, 1965 to 1986, Colorado River, Grand Canyon National Park, Arizona, *U.S. Geological Survey Prof. Pap.* 1493, 48 p., 1990.

Schmidt, J. C. and D. M. Rubin, Regulated streamflow, fine-grained deposits, and effective discharge in canyons with abundant debris fans, in *Natural and Anthropogenic Influences in Fluvial Geomorphology*, edited by J. E. Costa, A. J. Miller, K. W. Potter, and P. R. Wilcock, pp. 177-196, AGU, Washington, D. C., 1995.

Schmidt, J. C., R. H. Webb, and P. E. Grams, Comparison of the magnitude of erosion of alluvial bars along two large regulated rivers, *Wat. Res. Bull.*, *31*, 617-631, 1995.

Scott, W. E., Quaternary glaciation and volcanism, Metolius River area, Oregon, *Geol. Soc. of Am. Bull.*, *88*, 113-124, 1977.

Strahler, A. N., Hypsometric (area-altitude) analysis of erosional topography, *Bull. of the Geol. Soc. of Am.*, 63, 1117-1142, 1952.

Webb, R. H., T. S. Melis, P. G. Griffiths, J. G. Elliott, T. E. Cerling, R. J. Poreda, T. W. Wise, and J. E. Pizzuto, Lava Falls Rapid in Grand Canyon: Effects of late Holocene debris flows on the Colorado River, *U.S. Geological Survey Prof. Pap. 1591*, 90 p., 1999.

Williams, G. P., and M. G. Wolman , Downstream effects of dams on alluvial rivers, *U.S. Geological Survey Prof. Pap. 1286*, 83 p., 1984.

Janet H. Curran, U.S. Geological Survey, 4230 University Drive, Suite 201, Anchorage, AK 99508

Jim E. O'Connor, U.S. Geological Survey, 10615 SE Cherry Blossom Drive, Portland, OR 97216

Holocene Paleoflood Hydrology of the Lower Deschutes River, Oregon

Kurt J. Hosman and Lisa L. Ely

Central Washington University, Ellensburg, Washington

Jim E. O'Connor

U.S. Geological Survey, Portland, Oregon

Flood deposits at four sites along the lower Deschutes River, Oregon, were analyzed to determine magnitude and frequency of late Holocene flooding. Deposit stratigraphy was combined with hydraulic modeling at two sites to determine ranges of likely discharges for individual deposits. Combining these results with gaged flood data provides improved flood frequency estimates at the Axford site. The completeness and age spans of preserved flood chronologies differed among the four sites, but results were consistent for the largest floods of the last 5000 years. Single floods exceeded 2860-3800 m^3/s ~4600 cal yr BP, 1060-1810 m^3/s ~1300 cal yr BP, and 1210-2000 m^3/s <290 cal yr BP (corresponding to the historic flood of 1861). No floods have exceeded 2860-3770 m^3/s since the flood of ~4600 cal yr BP. Incorporating these results into a flood frequency analysis based on maximum likelihood estimators gives slightly higher flood quantile estimates and narrower confidence limits compared with analysis of gage data alone. Discharge and 2σ uncertainty for the 100-yr flood calculated using combined paleoflood and gaged records is 1120 +310/-240 m^3/s, compared with 930 +650/-250 m^3/s from analysis of only gaged floods. This revised estimate for the 100-yr flood is slightly greater than our estimate of 1060 m^3/s for the February 1996 flood at Axford, a finding consistent with historical records of two floods comparable to the 1996 flood in the last 140 years and with stratigraphic records of several like floods during the last ~1000 years.

INTRODUCTION

Flood-frequency analyses for rivers are commonly based on historical records of limited extent. In the western United States, these records go back a century at most, and are insufficient to determine with confidence the frequency distributions of flood discharges, especially for tail regions of distributions encompassing rare, large floods. To augment short or nonexistent historical records, various geologic methods have been developed and applied to determine the number, timing, and magnitude of past floods and effectively integrate this information into flood-frequency analyses [*Stedinger and Cohn*, 1986; *Stedinger and Baker*, 1987; *Blainey et al.*, 2002; *Jarrett and England*, 2002; *Levish*, 2002; *Webb et al.*, 2002]. Such studies, termed "paleoflood

A Peculiar River
Water Science and Application 7

10.1029/007WS09

has operated near the location of the Pelton-Round Butte dam complex since 1923 (Deschutes River near Madras). Two gaged floods stand out in the record at Moody, both of which occurred after completion of the Pelton-Round Butte dam complex. A flood in December 1964 was measured at 1910 m^3/s, and would have been larger if not for substantial flow storage by the recently-completed Pelton-Round Butte dam complex and other upstream reservoirs [*Waananen et al.*, 1971]. Another flood, the largest in the systematic record, occurred in February 1996 and measured 1990 m^3/s. Upstream reservoirs captured much less of this flow than for the 1964 flood [*Fassnacht*, 1998]. No other gaged floods have exceeded 1240 m^3/s at Moody. Prior to the gaged record, newspaper reports indicate that an exceptionally large flood occurred on the Deschutes River in December 1861, during widespread regional flooding [*Engstrom*, 1996; *Miller*, 1999]. The floods of 1861, 1964, and 1996 resulted from regional rain-on-snow events when warm and wet subtropical storms melted substantial low-elevation snowpacks.

Suitability for Paleoflood Studies

The lower Deschutes River is well suited for paleoflood studies based on slackwater deposits [*Kochel and Baker*, 1982]. It is confined along its entire length either by steep bedrock walls or by massive, stable blocks of landslide material. At certain sites, floods deposit silt and sand close to maximum flood stages, commonly in horizontally layered or laterally inset deposits that record several floods. Such sand and silt deposits provide reliable evidence for the maximum stage achieved by the depositing floods, providing a basis for calculating flood discharge. For example, during the February 1996 flood, sand and silt was deposited to within 10 to 20 cm of the maximum flood stage at several places along the lower Deschutes River, as indicated by local organic flotsam and eyewitness accounts.

The channel of the Deschutes River has been laterally and vertically stable for at least the last 100 years, thus increasing confidence in discharges estimated for paleoflood deposits based on present topography. Comparisons between aerial photographs taken prior to the February 1996 flood and current channel and overbank morphology show that there was little lateral channel movement during that flood [*Curran and O'Connor*, this volume]. Likewise, long-term trends in bed elevation at the Madras gaging station show little change [*Fassnacht et al.*, this volume]. The absence of channel gravel interbedded with the slackwater sediment at any of the sites further indicates that the channel bed elevation has probably remained relatively unchanged for at least the period of slackwater sediment accumulation.

Study Sites

Four sites of fine-grained flood deposits downstream of the Pelton-Round Butte dam complex were subjected to a detailed paleoflood analysis (Figure 1). Three sites, Axford, Dant, and Caretaker Flat, were located within a 32-km reach between River Mile (RM)[1] 81.6 and 62.0. A fourth site at Harris Island was much farther downstream at RM 11.6. No large tributaries enter the Deschutes River between the Axford, Dant, and Caretaker Flat sites. Consequently, there should be little difference in the frequency and magnitude of large mainstem floods at these three sites. The Harris Island site, in contrast, receives runoff from several large intervening tributaries. We measured stratigraphic sections and obtained chronological information at all four sites, but flow modeling and discharge estimation for this study were conducted only at Axford and Dant. Flood frequency analysis was conducted on the basis of the flood chronology and discharges determined at the Axford site. *Beebee and O'Connor* [this volume] report on hydraulic flow modeling for the Harris Island site.

STRATIGRAPHY AND PALEOFLOOD CHRONOLOGY

Stratigraphic analysis and geochronology of flood slackwater deposits formed the basis for our interpretations of the number, magnitude, and timing of large floods on the Deschutes River during the last several thousand years. From deposit elevation and thickness, especially in comparison with local evidence of the stages and deposits of the February 1996 flood, we inferred the relative magnitude of the floods associated with the different deposits.

Methods

Slackwater deposits were measured and described using standard field techniques [e.g., *Webb and Jarrett*, 2002]. We observed and recorded sediment characteristics, presence and type of fluvial structures, cohesiveness, color, moisture content, thickness, degree and type of bioturbation, and types of contacts between beds. Evidence of depositional hiatus between beds, such as soil formation, *in situ* traces of

[1] Units given are metric except for locations, which are given as river miles (RM), or miles upstream from the river mouth as marked on USGS topographic maps. These values are close to, but not necessarily the same as, actual distances along the present channel. Fractional river miles given herein are based on interpolations between these published river miles.

Table 1. Radiocarbon ages of samples from stratigraphic sections.

Site/ Section	Sample (field label)	Material	Corrected Conventional ^{14}C Age BP ±1sigma[a]	Dendrocalibrated 2σ Age Range(s), in calendar years B.P.[b]	$^{13}C/^{12}C$ Ratio (‰)	Laboratory ID#
Axford/1	D2-1b	charcoal	220±40	315-0	-25.8	Beta 131826
Axford /2	D2-1	shell	4420±60	5295-4850	-8.7	Beta 136513
Axford /2	D2-2	charcoal	1480±40	1420-1300	-25.8	Beta 131827
Axford /2	D2-3	charcoal	1490±45	1515-1295	-25.3	AA36673
Axford /2	D2-5	shell	4500±45	5310-4970	-9.48	AA36674
Axford /2	D2-7	charcoal	4530±70	5450-4960	-23.8	Beta 131829
Axford /2	D2-8	charcoal	1360±50	1335-1185	-27.7	Beta 131830
Axford /2	D2-10	charcoal	4080±50	4815-4425	-24.9	Beta 131831
Axford /2	D2-11	shell	4520±45	5315-4980	-9.6	AA36675
Axford /3	5/14/99-2(1)	charcoal	4090±40	4815-4440	-20.7	Beta 131835
Axford /3	5/14/99-2(3)	charcoal	5260±70	6200-5905	-24.1	Beta 131836
Axford /4	7/8/99-1(1)	charcoal	1060±40	1055-925	-26.4	Beta 136512
Dant/2	D5-8	charcoal	1310±50	1305-1155	-26.5	Beta 131833
Dant/2	D5-10	charcoal	140±40	290-5	-24.7	Beta 131834
Dant/2	3/17/00-1(3)	charcoal	1836±42	1875-1630	-25.3	AA37926
Dant/2	8/23/00-1(1)a	conifer charcoal[c]	2980±40	3310-3000	-22.3	Beta 152465
Dant/2	8/23/00-1(1)b	charcoal	2020±40	2060-1880	-26.9	Beta 152466
Dant/2	8/23/00-1(2)a	conifer charcoal[c]	2150±40	2310-2010	-24.6	Beta 152467
Dant/2	8/23/00-1(2)b	Rosaceae charcoal[c]	2000±40	2030-1870	-24.3	Beta 152468
Dant/2	8/23/00-1(2)c	charcoal	2530±40	2750-2470	-23.5	Beta 152469
Dant/2	8/23/00-1(3)a	Alnus charcoal[c]	2160±40	2320-2030	-26.9	Beta 152470
Dant/2	8/23/00-1(3)b	conifer charcoal[c]	1380±40	1330-1260	-23.7	Beta 152471
Caretaker/low	7/16/98-1(1)	charcoal	100±50	280-5	-26.8	Beta 121605
Caretaker/low	7/16/98-1(6)	charcoal	270±40	435-365 325-275 175-150 5-0	-26.3	Beta 121606
Caretaker/low	7/16/98-1(7)	charcoal	910±50	930-705	-26.4	Beta 121607
Caretaker/low	7/16/98-1(3)	charcoal	850±50	910-675	-23.4	Beta 121605
Caretaker/low	7/16/98-1(4)	charcoal	900±60	935-685	-24.6	Beta 124897
Caretaker/high	5/17/99-2(1)	charcoal	2850±50	3160-2825	-28.9	Beta 131837
Caretaker/high	7/16/98-1(18)	shell	7730±90[d]	7920-7570	--	Beta 121608
Caretaker/high	7/16/98-1(22)	shell	7730±60[d]	7895-7610	--	Beta 121609
Harris Island	7/1/98-1(17)	bone collagen	280±40	445-355 330-280 170-155 5-0	-20.3	Beta 121604
Harris Island	7/1/98-1(15)	charcoal	140±50	290-0	-24.8	Beta 124901
Harris Island	7/1/98-1(16)	charcoal	580±70	665-500	-25.6	Beta 121603
Harris Island	7/1/98-1(11)	charcoal	410±40	520-425 390-320	-25.7	Beta 121601
Harris Island	7/1/98-1(13)	charcoal	310±40	475-285	-27.7	Beta 121602
Harris Island	7/1/98-1(7)	charcoal	400±50	525-310	-26.1	Beta 124896
Harris Island	7/1/98-1(8)	charcoal	370±50	515-300	-27.7	Beta 121599
Harris Island	7/1/98-1(1)	charcoal	780±40	745-660	-25.1	Beta 124895
Harris Island	7/1/98-1(2)	bone collagen	300±40	465-285	-21.6	Beta 121598
Harris Island	7/1/98-1(6)	charcoal	300±40	465-285	-24.3	Beta 124900
Harris Island	7/1/98-1(10)	charcoal	520±40	555-500	-29.4	Beta 121600

[a] Radiocarbon ages (in ^{14}C yr BP) are calculated on basis of Libby half-life for ^{14}C (5568 years). The error stated is ±1σ on basis of combined measurements of the sample, background, and modern reference standards. Age referenced to AD 1950. Where no measurements of $^{13}C/^{12}C$, a value of -25‰ assumed for determining corrected conventional age.

[b] Calibration on basis of INTCAL98 [*Stuiver et al.,* 1998] and a laboratory error multiplier of 1, referenced to AD 1950. The 2σ range(s) encompass the intercept of the corrected conventional radiocarbon age ± 2σ with the calibrated calendar time-scale curve.

[c] Sample identification by Paleo Research, Golden, Colorado.

[d] Corrected conventional radiocarbon age includes a local reservoir correction of 390±25 yr.

ed charcoal along its length, indicating that the dated sample was from a surface burned prior to deposition and is a secure maximum limiting age. To the north (upstream) this bed descends, coarsens to silty sand, and thickens to more than 1 m, forming the lowermost unit of Section 1 (Figures 7 and 8). To the south (downstream), it rises and thins, pinching out in colluvium underlying railroad ballast where the river closely approaches the left valley slope. The stratigraphic position of this deposit, its elevation with respect to the highest flotsam of the February 1996 flood, and the young radiocarbon age lead us to infer that this deposit was left by the large historical flood of December 1861.

The winter of 1861-62 was one of exceptionally large floods in many western U.S. river basins [*Engstrom*, 1996; *Miller*, 1999]. On the Deschutes River, the December 1861 flood was reported to be "higher than was ever known to white man or aboriginal" (Salem Statesman, Dec. 23, 1861). On the Crooked River, a major upstream tributary to the Deschutes River, evidence of an exceptionally large flood was dated to the early 1860s by dendrochronological evidence of flood-damaged trees [*Levish and Ostenaa*, 1996]. At this Crooked River site, deposits from the 1861 flood buried an alluvial surface with an age of 3300-1900 cal yr BP This flood also eroded channels into parts of a higher surface with an age of ~5000 cal yr BP, indicating that the 1861 flood was one of the largest in the last 1900-5000 years on the Crooked River.

In Section 1, five flood beds overlie the 1-m-thick layer presumably deposited by the 1861 flood. These deposits all likely resulted from floods of the last 140 years. The uppermost unit of fine sand, ranging from 5 to 40 cm thick, has only very young surface vegetation and contains an aluminum soda can, indicating that this deposit resulted from the 1996 flood. Similarly, the December 1964 flood likely deposited the underlying unit. Identification of the three underlying units is more speculative, but two of them may have resulted from large gaged flows in January 1923 and February 1961 (Figure 2).

Section 3 was described in a 1.8 m deep pit excavated into the higher surface, away from the cut bank (Figures 6 and 8). Deposits in this section range from silty sand to coarse sand, including lenses of pumice grains and angular red and black volcanic fragments with diameters up to 2 mm. No primary sedimentary structures were visible. Samples retrieved by auger to a total depth of 2.5 m were of similar composition and texture. The uppermost 7 cm is silty very-fine sand, with abundant grass stems and rootlets. Aside from the contact beneath this uppermost 7-cm layer, contacts exposed in the pit consist of only gradual changes in grain size and color. There is no evidence of pedogenic alteration or depositional hiatus at any of these boundaries. Pumice grains collected from 95-100 cm from the top of the unit were identified as Mazama tephra (F.N. Foit, Washington State University, written communication, 2000), indicating that this deposit postdates the 7627±150 cal yr. BP age of the Mazama eruption [*Zdanowicz et al.*, 1999]. The position, thickness, coarse-grained texture, and post-Mazama age lead us to infer that this >2.5-m-thick deposit correlates to the Outhouse flood deposits at Axford and elsewhere along the lower Deschutes River [*Beebee and O'Connor*, this volume]. Sections 1 and 2 at Dant are apparently inset into this deposit, and probably entirely postdate the Outhouse flood.

In total, the stratigraphy at Dant records at least fifteen floods. These floods likely include the large Outhouse flood of about 4600 cal yr BP, up to five floods before 2060 cal yr BP, two floods ca. 2060-1880 cal yr BP, a flood dating to 1330-1260 cal yr BP, the exceptional historical flow of A.D.1861, and five post-1861 historical flows, probably including the floods of 1964 and 1996. The Outhouse flood and the floods ca. 1300 BP and A.D. 1861 all had maximum stages surpassing the flood of February 1996.

Caretaker Flat. "Caretaker Flat" is a 200-m wide, 500-m long alluvial surface on the right bank of the Deschutes River at RM 62, near the residence of the caretaker for a private fishing club. A vertical cutbank in this surface extends for nearly 100 m, exposing several beds of fine-grained flood deposits (Figure 9). A low surface, 2.7 m above the low-flow river stage, is inset into the higher and more extensive surface, which is about 5.0 m above the low-flow stage (Figure 10). The February 1996 flood did not inundate the upper surface, whereas the lower surface was flooded by about 1 m at peak stage (Floyd Patterson, Deschutes Club caretaker, oral communication, 1998).

The high surface consists of basal gravel, interpreted as a mid-channel bar or point bar, that is overlain by silt, sand, and gravel overbank flood deposits. A prominent layer in this exposure is fallout Mazama tephra (identified by Andrei Sarna-Wojcicki, USGS, written communication, 1999), which varies from 0 to 20 cm thick and ranges from 1.8 to 3.5 m below the surface. This ash layer defines the surface topography at the time of the eruption. Overlying the tephra and fine-grained flood deposits is a fining-upward gravel, sand and silt deposit that contains abundant 0-2 mm pumice clasts and lenses of broken and whole freshwater clamshells. This unit was probably left by a single large flood that overtopped a then-low floodplain near a channel that ran near the western end of the exposure. Primary sedimentary structures such as cross bedding and planar lamina are common in the sandy parts of the unit. The upper 70 cm

compared to the deposit left by the February 1996 flood, several of the earlier recorded floods likely exceeded it in magnitude.

Summary of stratigraphy and geochronology. All four study sites show broadly consistent stratigraphic and chronologic relations, especially for the largest floods, although there are differences in the number of floods preserved at each site and their ages. All sites contain evidence of an exceptionally large Holocene flood, known as the Outhouse flood [*Beebee and O'Connor*, this volume]. At Axford and Dant this flood left high, thick, fine-grained deposits in recirculation eddy zones downstream of gravel bars, where the geometry of the sites is most favorable for deposition of slackwater sediments at heights that approach the peak water surface. At Caretaker Flat, Outhouse flood deposits comprise overbank gravel and sand, whereas at Harris Island, the same flood left immense gravel bars. At both of these sites, fine-grained flood deposits from subsequent smaller floods mantle Outhouse flood deposits. Radiocarbon ages at Axford indicate that the Outhouse flood postdated (perhaps closely) 4815-4440 cal yr BP This is consistent with stratigraphic relations at Caretaker Flat, where inferred Outhouse flood deposits are bracketed by the 7775-7475 cal yr BP Mazama tephra and a 3160-2825 cal yr BP hearth.

At both the Axford and Dant sites, two comparatively thick and high deposits indicate at least two floods since the Outhouse flood that were significantly larger than the February 1996 flood. Radiocarbon dating indicates that one of these floods was ~1300 cal yr BP and the other within the last 290 cal yr BP, and may correspond to the large historic flood of 1861. Similarly, at Caretaker Flat there is evidence of at least one large flood subsequent to 3160-2850 cal yr BP Although these two floods were larger than most others in the stratigraphic record, their deposit elevations, thicknesses, and grain sizes show that they were not as large as the Outhouse flood.

All sites have deposits from several post-Outhouse floods: thirteen to fifteen at Axford and Dant, seven to eight at Caretaker flat and nine to eleven at Harris Island. Approximately half of the post-Outhouse flood deposits at Axford and Dant are older than 1300 cal yr BP The lowermost inset deposits at Axford, Dant and Caretaker Flat record up to nine floods, with one or two deposits between ~900 and 700 cal yr BP and the rest mainly in the last 400 years. There are eight or nine flood deposits from the last ~500 years preserved at Harris Island, slightly more than at the other sites. February 1996 flood deposits cap the stratigraphy on the low, inset sections at Dant and Caretaker flat, as well as the bar surface near the excavated section at Harris Island.

The paleoflood chronologies are broadly consistent among sites, particularly with respect to the highest and thickest flood deposits. However, every site preserves a slightly different record of lower magnitude floods. For example, Axford is the only site containing slackwater flood deposits older than the Outhouse flood, with five deposits between approximately 6200 and 5000 cal yr BP This site also records multiple floods from ~1300-1200 cal yr BP, whereas only one is distinguishable at Dant. At Dant, two or more of the flood deposits have ages ca. 2000 cal yr BP, a time of no apparent deposits at the other sites. The Harris Island site records more recent floods than the other sites.

The lack of precise correlation between study locations probably owes to the different depositional environments at each site [e.g., *Blainey et al.*, 2002; *House et al.*, 2002]. As deposits accrete vertically with layers of flood deposits, the flood stage required for subsequent deposition increases. At different sites, depending on the local hydraulic setting, the discharge required for formation of a new flood deposit will vary. Only the very largest floods will be preserved at all sites. Likewise, the development and erosion of inset deposits will vary between sites, depending on local conditions. Hence, the development and preservation of lower, inset sections will likely differ between sites. Nevertheless, evaluation of multiple sites allows for more confident assessment of the completeness of the record at any one site, as well as for firm conclusions regarding the number and timing of the largest floods that have affected the river system.

DISCHARGE ESTIMATION

Quantitative estimates of flood discharges associated with the deposits at the Axford and Dant sites were obtained by surveying the adjacent channel and floodplain reaches and relating results of step-backwater flow modeling to flood-deposit elevations.

Methods

The U.S. Army Corps of Engineers' Hydrologic Engineering Center River Analysis System, HEC-RAS [*Hydrologic Engineering Center*, 1998], was used to model discharges associated with individual paleoflood deposits. Input parameters for HEC-RAS include cross-sectional geometry, reach lengths, energy loss coefficients, starting water-surface elevations, flow regime and specified discharges. The two parameters having the greatest effect on the outcome are channel geometry and specified discharge value [*Feldman*, 1981; *O'Connor and Webb*, 1988; *Orth*, 1998; *Webb and Jarrett*, 2002].

Deschutes River (Figure 16). Like most paleoflood records of this type, the combined record of flood discharges and ages is almost certainly not complete [*House et al.*, 2002]. Both erosion of deposits and bioturbation of contacts may have resulted in lost or obscured records. Some floods are likely unrepresented by deposits, due to the progressively increasing stage necessary to overtop the vertically accreting deposits. Only a few deeply buried deposits predate the Outhouse flood. There were surely many large floods prior to ~4600 cal yr BP whose records were destroyed or covered by the Outhouse flood. The record of floods subsequent to the Outhouse flood is probably more complete, especially for floods large enough to emplace thick deposits on high, long-lived surfaces, such as Section 2 at Axford and Section 2 at Dant. However, bioturbation of deposits forming these sections may have reduced the number of recognizable flood beds. The lack of flood deposits with ages between ~4600 and 3300 cal yr BP might reflect lack of age data for parts of some sections or erosion of deposits. Nevertheless, the lack of thick deposits from that period at any site in our study, coupled with strong evidence that the 1861 flood was the largest of the last 5000 years on the tributary Crooked River [*Levish and Ostenaa*, 1996], makes it unlikely that there were any floods from ~4600 to 3300 cal yr BP with discharges as large as the two large ~2000 m^3/s discharges of the last ~1300 cal yr BP.

FLOOD FREQUENCY ANALYSIS

Appropriate consideration of paleoflood data like that obtained for the Deschutes River can improve estimates of flood frequency, especially for low frequency floods [*Stedinger and Cohn*, 1986; *Stedinger and Baker*, 1987; *Blainey et al.*, 2002; *O'Connell et al.*, 2002]. Recent techniques and applications have used paleohydrologic data and interpretations to establish "bounds" of flood occurrence—that is, statements of flood exceedence and non-exceedence over specified time periods [*Levish*, 2002]. These bounds are commonly combined with gaged records to produce estimates of flood frequency, resulting in narrower constraints on likely flood frequency distributions at long return periods than can be obtained from consideration of the gaged data alone [e.g., *O'Connor et al.*, 1994; *O'Connell et al.*, 2002].

Methods

For this study, we have calculated flood frequency with an algorithm developed by the Bureau of Reclamation for a model called FLDFRQ3 [*O'Connell*, 1998; *O'Connell et al.*, 2002] that is specifically designed to incorporate paleoflood data into flood frequency analysis for dam safety assessment [*Levish*, 2002]. This method employs a Bayesian approach [*Tarantola*, 1987] in conjunction with the maximum likelihood methods of *Stedinger and Cohn* [1986]. It combines gaged records and paleoflood data, and allows for specification of the uncertainty in the magnitude and timing of paleohydrologic bounds that inevitably results from uncertainties in stratigraphic interpretations, deposit chronology, and paleoflood discharge. In addition, uncertainty in the gaged measurements can also be specified.

Such an analysis for the Deschutes River presents some challenges. First, the stratigraphic records of flooding at each of the four sites are different, as are the discharge estimates associated with possibly correlative paleoflood deposits at the two sites of flow estimation. Second, neither of the sites with quantitative estimates of paleoflood discharge is directly comparable to gaged locations on the Deschutes River. Third, the gaged record includes periods of regulated and unregulated flow and therefore is not consistent over the period of record. Each of these issues was treated in a manner to maximize the overall confidence in the results. These complications are typical for studies such as this, and add unquantified uncertainties to the final flood frequency assessment.

Multiple sites. To simplify the issue of multiple sites with different records, we applied only results from the Axford site to the flood frequency analysis and only used paleoflood information on the large floods that were common to multiple sites. We consider the potential reduction in information due to limiting the flood probability distribution to results from a single site to be outweighed by the increased reliability resulting from using only paleoflood bounds that rely on more certain correlations between sites. This approach is supported by the observation that only a few bounds are necessary to significantly improve flood frequency estimates [*Blainey et al.*, 2002; *Levish*, 2002]. The appropriateness of this approach is also bolstered by the overall similarity of the stratigraphic records between all study sites in terms of the timing and relative magnitude of the largest floods. The greatest loss of information due to not considering the Dant site is the estimate for the inferred 1861 flood discharge, although this inference is uncertain. Nevertheless, the 1861 flood is probably represented by one of the high deposits at Axford and thus indirectly included in the analysis.

Relation to gaging records. The closest gaging station to the Axford site is the "Deschutes River near Madras," 30 km upstream at RM 100.1 (Figure 1), for which peak flows have been measured since 1924. The longest record on the Deschutes River is from the Moody gage, 130 km downstream at RM 1.4 near the Columbia River confluence, where annual peak discharge records extend back to 1897 (Figure 2). Three major tributaries join the Deschutes River between the Madras gage and the Axford study site. Shitike Creek and the Warm Springs River both drain the eastern slopes of the Cascade Range and have mostly continuous flow records extending back to 1975 and 1972, respectively. Trout Creek drains the Ochoco Mountains to the east and has no systematic record of streamflow.

Shitike Creek and the Warm Springs River both contribute substantial flow to the Deschutes River, so the gage record at Madras alone does not adequately reflect the peak flows at Axford. Examination of the 1975-1998 annual peak flow records for all of these stations indicates that the total flow at Axford (the combined discharges for the Deschutes River at Madras, Shitike Creek, and Warm Springs River) averages 51 percent of the measured flow at Moody for the same floods (Figure 2). Consequently, we have multiplied the discharges from the Moody gage by 0.51 to establish an approximate systematic record for the period 1897-1998 at Axford. There are uncertainties with this transformation, such as the unknown contributions from Trout Creek and the applicability of such a ratio to the very large floods recorded by the slackwater deposits. However, this relation is broadly consistent with the highest measured flows during the period of overlap in the upstream and downstream records for the 1964 and 1996 floods. For the two large floods in 1964 and 1996, about 75 percent of the peak discharge at Moody was derived from downstream of the Madras gage [*Beebee and O'Connor*, this volume], although it may have been as low as 50 percent without the regulation caused by upstream dams. The incremental increase in drainage area between the Madras gage and the Axford site is about 54 percent of the total area contributing to the Deschutes River between the Madras and Moody gage locations. On this basis and assuming uniform flow generation for area downstream of Madras, the peak discharges at Axford would be expected to be about 65 percent of the Moody discharges. To reflect uncertainty in the local discharge during large floods, we assigned uncertainty (2s) values of ±30% to each gage discharge value for Axford.

Flow regulation. Flows have been regulated in the Deschutes River basin since 1919. Consequently, USGS estimates of flood frequency at the Moody gage are based only on 1898-1919 flow records [*Wellman et al.*, 1993]. Nevertheless, early storage projects were small and substantial flow regulation only began with Bowman Dam on the Crooked River (closed 1960) and Round Butte Dam on the Deschutes River (closed 1964). Both dams stored substantial water during the 1964 flood, perhaps reducing the peak discharge at the Madras and Moody gage locations by 850 m^3/s [*Waananen et al.*, 1971]. During the February 1996 flood, however, the large reservoirs behind both the Bowman and Round Butte dams were much closer to capacity and there was substantially less attenuation of flood discharge [*Fassnacht*, 1998]. For the purposes of flood frequency analysis, we have assumed that the unregulated 1964 peak discharge at Moody would have been about 2750 m^3/s (with a 2s uncertainty of ±50%)(Figure 2), compared to the actual gaged flow of 1910 m^3/s (Figure 2), reflecting *Waananen's* [1971] estimate of reservoir storage. All other annual peak discharges were left unchanged.

Paleohydrologic bounds. The primary manner in which paleoflood data are considered in maximum-likelihood approaches to estimating flood frequency is as a series of constraints, or bounds, on the timing and magnitude of floods. These bounds include information on discharge levels that have and have not been exceeded in specified time periods (Table 2). Non-exceedence bounds are flood discharges that have not been exceeded for a known time period and supply important limiting information for flood frequency distributions in this type of analysis [*Blainey et al.*, 2002; *Levish*, 2002]. The non-exceedence bound assumed from the stratigraphy at Axford is that no flood has exceeded the 3770 m^3/s best-estimate discharge of the Outhouse flood during the last 4865-4490 cal yr BP (Table 2).

Information on specific large paleofloods also constrains the flood frequency distribution [*O'Connell et al.*, in press]. For this analysis, we considered the three largest floods recorded in the stratigraphy at Axford. These floods are the ~4600 cal yr BP Outhouse flood, and the two large floods post-dating 1420 cal yr BP at the top of Section 2. From the age results at Dant, we have assigned ages of ~1300 cal yr BP and <290 cal yr BP to these two floods (Table 2). While many other floods are recorded in the stratigraphy at Axford, these three large floods have left records at multiple sites along the Deschutes River and likely represent the largest floods of the last ~5000 years. For the presumably smaller floods that left many of the lower deposits at Axford, the record is not as likely to be complete, and thus our confidence in the number and timing is not as high. By restricting the analysis to the three largest floods, we only considered paleoflood information deemed complete and reliable, thus reducing the errors and unquantifiable uncertainty owing to incomplete records [e.g., *Blainey et al.*, 2002].

Uncertainty values for corresponding flood discharges were assigned from the ranges of discharges required to overtop corresponding deposits by 0 to 1.2 m (Table 2). The discharge necessary to overtop the deposits by 1.2 m was selected as the best estimate of the paleoflood discharge, a

Table 2. Summary of paleoflood data considered in flood frequency analysis.

Data Type	Minimum Discharge Estimate (m^3/s)[a]	Maximum Discharge Estimate (m^3/s)[b]	Best Estimate for Discharge (m^3/s)[c]	Flood Age, in calendar years BP[d]
Nonexceedence bound[a]	2860	4680	3770	4815-4440
Paleofloods				
<290 cal yr BP	1210	2790	2000	90[e]
~1300 cal yr BP	1060	2560	1810	1300
Outhouse flood[f]	2860	4680	3770	4600

[a]Discharge for flow with a stage equal to elevation of the top of the highest deposit.
[b]Best-estimate discharge plus difference between best-estimate and minimum discharges
[c]Discharge for flow that overtops highest deposit by 1.2 m.
[d]Dendrocalibrated from radiocarbon age and referenced to AD 1950. For flood frequency analysis, which was based on data through AD 2000, 50 yrs were added to each of these ages.
[e]Assigned age reflects likelihood that this flood occurred in 1861.
[f]Entered as a paleoflood in the primary analysis shown in Figure 17a.

required input value for the model. This value was chosen based on the 1.2 m depth of water above the 1996 flood deposits during the peak flood stage. The discharge required to reach the elevation of the deposit provides a minimum limit to the discharge range, and an equivalent difference above the best-estimate discharge was chosen as a reasonable maximum limit. For purposes of estimating the shape of the probability density function about the discharge estimate, the "best-estimate" value, represented by flow overtopping the deposit by 1.2 m, was estimated to be ten times more likely than either of the bounding values of the input discharge range. All analyses were conducted assuming a Log Pearson Type III frequency distribution.

Results

Three specific cases were analyzed (Figure 17, Table 3). The primary analysis (Figure 17a) includes the 94 years of transformed gage data, the non-exceedance bound indicated by the height of the Outhouse flood deposit, and the three large paleofloods, including the Outhouse flood. A secondary analysis (Figure 17b) was performed using the same gage data and the exceedance bound defined by the height of the Outhouse deposit, but not including the Outhouse flood as a specified paleoflood. This case reflects the possibility that the Outhouse flood resulted not from meteorological conditions, but from some type of natural dam failure in the basin, and thus is not appropriately considered as part of the same population of floods. *Beebee and O'Connor* [this volume] specifically addressed this question with the tentative conclusion that the Outhouse flood was indeed a meteorological flood. The third case was for comparative purposes and simply considers the transformed gage data without any paleoflood information (Figure 17c).

All three cases resulted in estimated flood discharges within ±30 percent of each other for floods with annual recurrence intervals of 10 to 10,000 yrs. For recurrence intervals >100 yr, inclusion of the paleoflood data in the primary case results in discharge estimates 20 to 30 percent greater than does the analysis of the transformed USGS gage data alone (Table 3; Figure 17a, 17c). However, the most striking result of including the paleoflood data is the much narrower confidence limits on the calculated distribution function (Figure 17). For example, the 100-yr recurrence interval flood at Axford, determined solely from the transformed Moody gage record is 930 +650/-250 m^3/s. Addition of the paleoflood record results in an estimate of 1120 +310/-240 m^3/s for the 100-yr flood. Excluding the Outhouse flood as a specified meteorological flood results in quantile estimates very similar to those from analysis of the gage record alone (Table 3), but also with much narrower confidence limits (Figure 17b, 17c). At longer recurrence intervals, the improvement in quantile estimates is even greater (Table 3).

These quantitative flood-frequency results from analysis of the Axford stratigraphy are consistent with the overall stratigraphic record of flooding in the lower Deschutes River canyon. The frequency analysis of the combined gage and paleoflood records indicate that the February 1996 flood (about 1060 m^3/s at Axford) was slightly less than the 100-yr

Table 3. Summary of flood frequency results for the Deschutes River (at Axford) using Bureau of Reclamation FLDFRQ3 program [*O'Connell*, 1999; *O'Connell et al.* in press]

Annual Exceedence Probabilities	94-yr Gage Record, 1 non-Exceedence Bound and 3 Paleofloods (primary case)	94-yr Gaged Record, 1 Non-Exceedence Bound and 2 Paleofloods	94-yr Gaged Record
0.1	470	450	430
0.05	620	590	550
0.02	870	810	750
0.01	1120	1020	930
0.005	1420	1270	1150
0.002	1920	1690	1500
0.001	2400	2080	1820
0.0005	2990	2540	2200
0.0002	3970	3300	2820
0.0001	4910	4010	3380

The Outhouse flood was by far the largest flood at the two sites where hydraulic modeling was used to reconstruct paleoflood magnitudes. At Axford, Outhouse flood deposits correspond to a discharge of 2860-3770 m^3/s, a value just slightly greater than associated with correlative deposits at Dant, and much greater than the 1060 m^3/s estimate for the February 1996 flood. The two large late Holocene floods of ~1300 cal yr BP and post-290 cal yr BP had discharges of ~1060-2000 m^3/s and may have been twice the size of the February 1996 flood. Many of the remaining floods preserved in the stratigraphic record at Dant and Axford probably had discharges close to or slightly greater than the February 1996 flood.

These paleoflood data were combined with an adjusted gage record (reflecting the watershed position of the Axford site and regulation of the 1964 flood) to calculate long-term flood frequency. Flood frequency calculations were based on maximum likelihood analysis with a Bayesian approach [*O'Connell*, 1998; *O'Connell, et al.*, 2002]. Key paleohydrologic results constraining the flood frequency distribution were: (1) there have been no floods greater than 2860-3770 m^3/s since 4815-4450 cal yr BP; and (2) there were single floods of 2860-3800 m^3/s about 4600 cal yr BP, 1060-1810 m^3/s about 1300 cal yr BP, and 1210-2000 m^3/s about 140 cal yr BP Compared to analysis of the gage record alone, incorporating the paleoflood information increases flood quantile estimates by about 15 to 30 percent for recurrence intervals ranging from 100 to 10,000 yrs. The increase is much smaller if the Outhouse flood is not considered as a meteorological paleoflood. Perhaps more important for dam safety analysis, addition of the Axford paleoflood data significantly narrows the confidence intervals around the estimated frequency distributions compared to analysis of gage data alone. Confidence in the resulting flood frequency estimates is bolstered by the overall agreement of the calculated return periods of specific floods, such as the February 1996 flood, with the flood stratigraphy at multiple sites along the Deschutes River.

The only apparent gap in the stratigraphic flood record is between 4400 and 3300 cal yr BP, for which there are no dated flood deposits. This period could be a time of few or no large floods on the Deschutes River, or it could be a time period for which deposits were not preserved at any of the study sites. Regardless, the absence of flood deposits from that time period on high, long-lived, surfaces indicates no floods were substantially larger than the February 1996 flood between 4400 and 3300 cal yr BP Gaps in the stratigraphic records at all sites, plus the inherent uncertainty of deposit ages, makes it difficult to speculate about long-term changes in flood frequency and magnitude.

While quantitative flood frequency was assessed for only one site, and flow modeling was conducted for only two of the four sites, stratigraphic analysis of all four sites strengthened the overall conclusions regarding flood frequency and magnitude. All four sites had stratigraphic records of flooding which were slightly different, encompassing different time periods and recording different numbers and sizes of floods in different positions in the basin. Nevertheless, evidence of certain large floods was seen in multiple sections, indicating that the stratigraphic record is likely complete for the largest floods included in the flood frequency analysis. This is an important determination for flood-frequency analysis [e.g., *Blainey et al.*, 2002], and is one that in most situations can be assessed only by study of multiple sites.

Acknowledgments. K. Marshall of Portland General Electric, Inc., provided logistical support of fieldwork and funding for radiocarbon analyses. Additional funding was provided by National Science Foundation Grant EAR-9725336 and U.S. Geological Survey Western Regional Water Resources Grant 97-002 to Ely, and the 2000-2001 Puget Sound Energy Graduate Fellowship in the Department of Geological Sciences, Central Washington University, to Hosman. Radiocarbon dates analyzed by the University of Arizona-NSF Tandem Accelerator Mass Spectrometer were partially funded by that facility. The U.S. Bureau of Reclamation also provided additional funding for radiocarbon analyses. Andrei Sarna-Wojcicki of the U.S. Geological Survey and Nick N. Foit of Washington State University provided tephra identifications. R. Bellivoux, L. McGinnis, E. Shulz, W. Wolfe, J. Green, R. Beebee, G. Grant, J. Curran, J. Hardison, H.

Fassnacht, D. Levish, D. Ostenaa, J. Klawon, and M. Brink assisted in data collection and analysis. R. Beebee, G. Grant, K. House, and J. Klawon provided helpful reviews of the manuscript.

REFERENCES

Baker, V. R., R. H. Webb, and P. K. House, The scientific and societal value of paleoflood hydrology, in *Ancient Floods, Modern Hazards: Principles and Applications of Paleoflood Hydrology*, edited by P. K. House, R. G. Webb, V. R. Baker and D. R. Levish, *Water Science and Application Series*, *5*, 1-19, American Geophysical Union, Washington, DC, 2002.

Barnes, H. H., Jr., Roughness characteristics of natural channels, *U.S. Geol. Surv. Water-Supp. Pap. 1849*, 213 p., 1967.

Blainey, J. B., R. H. Webb, M. E. Moss, and V. R. Baker, Bias and information content of paleoflood data in flood-frequency analysis, in *Ancient Floods, Modern Hazards: Principles and Applications of Paleoflood Hydrology*, edited by P. K. House, R. G. Webb, V. R. Baker and D. R. Levish, *Water Science and Application Series*, *5*, 161-174, American Geophysical Union, Washington, DC, 2002.

Chatters, J. C. and K. A. Hoover, Changing late Holocene flooding frequencies on the Columbia River, Washington, *Quat. Res.*, *26*, 309-320, 1986.

Ely, L. L. and V. R. Baker, Reconstructing paleoflood hydrology with slackwater deposits: Verde River, Arizona, *Phys. Geog.*, *6*(2), 103-126, 1985.

Ely, L. L., Y. Enzel, V. R. Baker and D. R. Cayan, A 5000-year record of extreme floods and climate change in the southwestern United States, *Science*, *262*, 410-412, 1993.

Ely, L. L., Y. Enzel, V. R. Baker, V. S. Kale, and S. Mishra, Changes in the magnitude and frequency of late Holocene monsoon floods on the Narmada River, central India, *Geol. Soc. of Amer. Bull.*, *108*, 1134-1148, 1996.

Engstrom, W. E., The California storm of January 1862, *Quat. Res.*, *46*, 141-147, 1996.

Fassnacht, H., Frequency and magnitude of bedload transport downstream of the Pelton-Round Butte dam complex, lower Deschutes River, Oregon, M.S. thesis, 311 pp., Oregon State University, Corvallis, Oregon, 1998

Feldman, A. D., HEC models for water resources system simulation; theory and experience, *Adv. Hydroscience*, *12*, 297-423, 1981.

Hosman, K. J., Stratigraphic reconstruction of paleoflood frequencies and magnitudes, lower Deschutes River, Oregon, M.S. thesis, 73 pp., Central Washington University, Ellensburg, Washington, 2001.

House, P. K., P. A. Pearthree, and J. E. Klawon, Historical flood and paleoflood chronology of the Lower Verde River, Arizona: Stratigraphic evidence and related uncertainties, in *Ancient Floods, Modern Hazards: Principles and Applications of Paleoflood Hydrology*, edited by P. K. House, R. G. Webb, V. R. Baker and D. R. Levish, *Water Science and Application Series*, *5*, 267-293, American Geophysical Union, Washington, DC, 2002.

Hydrologic Engineering Center, *HEC-RAS River Analysis System User's Manual*, version 2.2, U.S. Army Corps of Engineers, 1998.

Jarrett, R. D. and J. F. England, Jr., Reliability of paleostage indicators for paleoflood studies, in *Ancient Floods, Modern Hazards: Principles and Applications of Paleoflood Hydrology*, edited by P. K. House, R. G. Webb, V. R. Baker and D. R. Levish, *Water Science and Application Series*, *5*, 91-109, American Geophysical Union, Washington, DC, 2002.

Kochel, R. C. and V. R. Baker, Paleoflood hydrology, *Science*, *215*, 353-361, 1982.

Kochel, R. C., and V. R. Baker, Paleoflood analysis using slackwater deposits, in *Flood Geomorphology*, edited by V. R. Baker, R. C. Kochel, and P. C. Patton, pp. 357-376, John Wiley and Sons, New York, 1988.

Levish, D. R., Paleohydrologic bounds: non-exceedance information for flood hazard assessment, in *Ancient Floods, Modern Hazards: Principles and Applications of Paleoflood Hydrology*, edited by P. K. House, R. G. Webb, V. R. Baker and D. R. Levish, *Water Science and Application Series*, *5*, 175-190, American Geophysical Union, Washington, DC, 2002.

Levish, D. R. and D. A. Ostenaa, *Applied Paleoflood Hydrology in North-Central Oregon*, 182 p., Guidebook for Fieldtrip 2, Geological Society of America Cordilleran Section Meeting, Portland, Oregon, 1996.

Miller, G. R., The great Willamette River flood of 1861, *Oregon Hist. Quart.*, *100*(2), 1999.

O'Connell, D. R. H., FLDFRQ3, Three-parameter maximum likelihood flood-frequency estimation with optional probability regions using parameter grid integration, User's Guide (Release 1.1), 19 p., U.S. Bureau of Reclamation (available at ftp://ftp.seismo.usbr.gov/publ/outgoing/geomagic/src/fldfrq3/), 1998.

O'Connell, D. R. H., D. A. Ostenaa, D. R. Levish, and R. E. Klinger, Bayesian flood frequency analysis with paleohydrologic bound data, *Water Resour. Res. 38*, (DOI 10.1029/2000WR000028), 2002.

O'Connor, J. E., and R. H. Webb, Hydraulic modeling for paleoflood analysis, in *Flood Geomorphology*, edited by V. R. Baker, R. C. Kochel, and P. C. Patton, pp. 383-402, John Wiley and Sons, New York, 1988.

O'Connor, J. E., R. H Webb and V. R. Baker, Paleohydrology of pool-and-riffle pattern development: Boulder Creek, Utah, *Geol. Soc. Amer. Bull.*, *97*, 410-420, 1986.

O'Connor, J. E., L. L. Ely, E. E. Wohl et al., A 4500-year record of large floods on the Colorado River in the Grand Canyon, *J. Geol.*, *102*, 1-9, 1994.

Orth, S. A., Refining flood-frequency estimates with paleoflood deposits: John Day River, north-central Oregon, M.S. thesis, 146 pp. Central Washington University, Ellensburg, Washington, 1998.

Orth, S. A. and Ely, L. L., Reconstructing paleoflood history with slackwater deposits: John Day River, north-central Oregon, *Geol. Soc. Amer. Abstr. Prog.*, *30*(7), 1998.

Retallack, G. J., Field recognition of paleosols, in *Paleosols and Weathering Through Geologic Time; Principles and*

Applications, edited by J. Reinhardt and W. R. Sigleo, *Geol. Soc. Amer. Spec. Pap. 216*, 1-20, 1988.

Rhodes, G. B., A small look at the big picture: linking geopotential height anomalies to paleofloods in the Snake River, Idaho and Oregon, M.S. thesis, 214 pp., Central Washington University, Ellensburg, Washington, 2001.

Stedinger, J. R., and V. R. Baker, Surface water hydrology: historical and paleoflood information, *Rev. Geophysics*, *25*, 119-124, 1987.

Stedinger, J. R. and T. A. Cohn, Flood frequency analysis with historical and paleoflood information, *Water Resour. Res.*, *22*, 785-793, 1986.

Stuiver, M. and P. J. Reimer, Extended ^{14}C database and revised CALIB 4.1 ^{14}C age calibration program, *Radiocarbon*, *35*, 215-230, 1993.

Stuiver, M., P. J. Reimer, E. Bard et al., INTCAL98 Radiocarbon age calibration 24,000-0 cal BP., *Radiocarbon*, *40*, 1041-1083, 1998.

Tarantola, A., *Inverse Problems Theory: Methods for Data Fitting and Model Parameter Estimation*, Elsevier, New York, 1987.

Trumbore, S. E., Radiocarbon geochronology, in *Quaternary Geochronology; Methods and Applications*, edited by J. S. Noller, J. M. Sowers, and W. R. Lettis, pp. 41-60, American Geophysical Union, New York, 2000.

Waananen, A. O., D. D. Harris, and R. C. Williams, Floods of December 1964 and January 1965 in the far western states, *U.S. Geol. Surv. Water-Supp. Pap. 1866-A*, 1971.

Webb, R. H., and Jarrett, R. D., One-dimensional estimation techniques for discharges of paleofloods and historical floods, in *Ancient Floods, Modern Hazards: Principles and Applications of Paleoflood Hydrology*, edited by P. K. House, R. G. Webb, V. R. Baker and D. R. Levish, *Water Science and Application Series*, *5*, 111-125, American Geophysical Union, Washington, DC, 2002.

Webb, R. H., J. B. Blainey, and D. W. Hyndman, Paleoflood hydrology of the Paria River, southern Utah and northern Arizona, USA, in *Ancient Floods, Modern Hazards: Principles and Applications of Paleoflood Hydrology*, edited by P. K. House, R. G. Webb, V. R. Baker and D. R. Levish, *Water Science and Application Series*, *5*, 295-310, American Geophysical Union, Washington, DC, 2002.

Wellman, R. E., J. M. Gordon, and R. L. Moffatt, Statistical summaries of streamflow data in Oregon: Volume 2-Annual low and high flow, and instantaneous peak flow, *U.S. Geol. Surv. Open-File Rep. 93-63*, 1993.

Zdanowicz, C. M., G. A. Zielinski, and M. S. Germani, Mount Mazama eruption; calendrical age verified and atmospheric impact assessed, *Geology*, ***27***, 621- 624, 1999.

Kurt J. Hosman and Lisa L. Ely, Department of Geological Sciences, Central Washington University, Ellensburg, WA 98926

Jim E. O'Connor, U.S. Geological Survey, 10615 SE Cherry Blossom Drive, Portland, OR 97216

The Outhouse Flood: A Large Holocene Flood on the Lower Deschutes River, Oregon

Robin A. Beebee

University of Oregon, Eugene, Oregon

Jim E. O'Connor

U.S. Geological Survey, Portland, Oregon

Bouldery cobble bars, massive sand deposits, and stripped bedrock surfaces 5 to 19 meters above summer low flow stages along the lower Deschutes River were left by an exceptional Holocene flood, herein termed the Outhouse flood, which was substantially larger than any historic flow. The flood postdates the 7.6 ka Mazama tephra, and probably predates a 2.9-3.1 ka hearth. A 4.4-4.6 ka piece of charcoal from within sandy flood deposits may more closely represent the age of the flood. Step-backwater modeling at Harris Island, a site 17 km upstream from the Deschutes River confluence with the Columbia River, indicates that this flood had a peak discharge of at least 3800 m^3/s and likely as great as 5660 m^3/s. This is substantially greater than the 2000-3000 m^3/s peak historic discharges of the last 150 years caused by rain-on-snow events. Similar results from two upstream sites also indicate that this flood was substantially larger than historic flows as well as any prehistoric flow of the last 2000 years. Because of its exceptional size and the extensive Quaternary history of natural dam failure floods in the Deschutes River basin, we use multiple criteria to specifically address the question of whether this flood was of meteorological or dam-break origin. The downstream increase in peak discharge determined from the three separate sites of step-backwater analysis, coupled with the absence of any readily identifiable breached natural dam of the proper age, is strong evidence that the flood was indeed meteorological. This conclusion is weakened, however, by the lack of evidence for similar flooding in certain tributaries and adjacent basins.

INTRODUCTION

Geologic evidence of prehistoric large floods (paleofloods) is increasingly being used to support analysis of social and scientific issues such as dam and floodplain safety, century- to millennial-scale climatic variation, and the response of channel morphology to floods. The most commonly studied Holocene paleofloods are those that result from precipitation or snowmelt (meteorological floods). The goal of most paleoflood studies is to collect an extensive enough record of such floods to improve estimates of the recurrence interval of exceptional meteorological events. Such assessments are typically used for evaluating hazards to structures such as dams, or to assess the relations between climate and flood magnitude [*National Research Council*, 1988; *Kochel and Baker*,

A Peculiar River
Water Science and Application 7

10.1029/007WS10

1988; *Jarrett and Tomlinson*, 2000]. In many regions, outburst floods from glacial, moraine, landslide, or manmade dam failures also create both significant hazards and long-lasting channel modification [*Schuster*, 1986; *Costa and Schuster*, 1988; *Costa*, 1988; *Walder and O'Connor*, 1997; *Cenderelli and Wohl*, 2001]. With the exception of certain recurring glacial outburst floods, most outburst floods are treated in the literature on a case-by-case basis as local convergences of phenomena, and not as events with predictable recurrence intervals or regional significance.

Because outburst floods and meteorological floods are treated as separate hazards and geomorphic agents, and have different implications with regard to prediction and mitigation strategies, it may be necessary to distinguish between the two types of floods in conducting paleoflood studies. In regions where outburst floods are known to have occurred, paleoflood analyses should ideally be undertaken with a clear set of criteria to distinguish between floods of different mechanisms in the stratigraphic record, although there are no known examples where this has been done.

In this paper we describe evidence for an exceptionally large Holocene flood in the lower Deschutes River of north central Oregon, and evaluate whether this flood was from a meteorological or a dam-outburst source. Prominent landforms along the lower Deschutes River deposited or shaped by this large flood include islands, boulder bars, rapids, and stripped bedrock surfaces. We have informally named the flood that left these features the "Outhouse flood" for the Bureau of Land Management outhouses laboriously built on many of the bouldery bars to serve recreational river rafters. The distribution of these morphologic features and their interaction with the modern flow regime are discussed in detail in *Curran and O'Connor* [this volume].

BACKGROUND

The Deschutes River drains 26,900 km^2 of north central Oregon before joining the Columbia River 160 km east of Portland (Figure 1). The lower Deschutes River, defined as the downstream 160 km of channel below the Pelton-Round Butte dam complex, flows through a canyon deeply incised into Cenozoic volcanic and volcaniclastic rocks [*O'Connor, Grant, and Haluska*, this volume]. Quaternary volcanism, tectonism, and glaciation contribute to the potential for floods generated by a variety of non-meteorological mechanisms. Pleistocene landslide dam remnants and associated outburst flood deposits have been documented for at least three locations in the lower Deschutes River canyon [*O'Connor et al.*, this volume]. These deposits are distinguished from Outhouse flood deposits by their proximity to the breach site, greater height of deposits above the channel, and greater size of clasts moved, recognizing that there is not a clear distinction in all cases. Other documented Quaternary floods in the Deschutes River basin have resulted from Pleistocene volcanic eruptions, spillover of tectonic basins, and failure of moraine dams in upstream areas. Additional possible flood-generating mechanisms in the drainage basin include failure of lava and ice dams [*O'Connor, Grant, and Haluska*, this volume].

Historically, flow in the lower Deschutes River has been remarkably stable due to an extensive, large-capacity aquifer system and a poorly integrated drainage network in the southern part of the Deschutes River basin [*Manga*, 1996; *Gannett et al.*, this volume]. Aquifers and alpine snowpack in the Cascade Range serve as natural reservoirs that provide year-round flow regulation, such that the seasonal range in runoff is much smaller than for adjacent rivers to the west and east. These factors combine to temper the magnitude of floods derived from both isolated meteorological events, such as winter storms, and from seasonal snowmelt [*O'Connor, Grant, and Haluska*, this volume].

The three largest historic floods on the Deschutes River occurred in the winters of 1861, 1964, and 1996. All of these flows were the result of regional rain-on-snow events that affected multiple basins in the Pacific Northwest and western United States. Both the February 1996 and December 1964 Deschutes River peak discharges were about 2000 m^3/s near the confluence with the Columbia River, although the 1964 flow was substantially reduced by upstream storage reservoirs. Inspection of the lower Deschutes River shortly after the 1996 flood showed abundant Holocene coarse gravel bars, fine-grained floodplain deposits, and erosional trim lines standing several meters above maximum stages achieved by the 1996 flood, indicating that a much larger flood had previously passed down the river. The discharge of the flood was originally estimated as over 5000 and probably closer to 14,000 m^3/s at Harris Island (Figure 1), using a single cross-section and Mannings equation (O'Connor, unpublished data). Because this value is 2.5 to 7 times greater than the largest historic flows, the source and size of the flood became outstanding questions with implications for upstream dam safety as well as channel formation processes and the distribution of aquatic habitats [*Curran and O'Connor*, this volume].

DISTRIBUTION AND MORPHOLOGY OF OUTHOUSE FLOOD DEPOSITS

Evidence for the Outhouse flood has been recognized at sites along most of the 160-km length of the lower

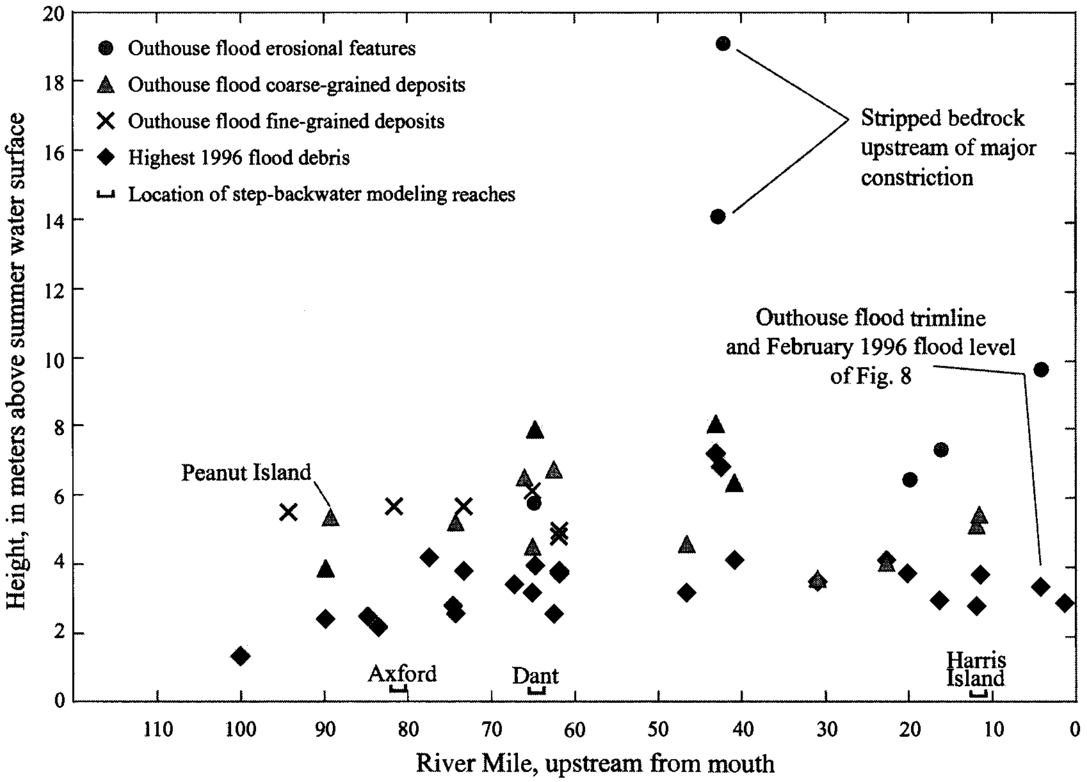

Figure 2. Height of Outhouse flood features (boulder bars and fine-grained deposits) and 1996 flood debris (primarily flotsam and fine woody debris) above summer water level.

Deschutes River (Figures 1 and 2). Depositional features include bouldery cobble bars and fine-grained slackwater deposits. Erosional features, more common in the lower 80 km, include stripped bedrock surfaces and trimlines in thick Pleistocene silt deposits that mantle the banks in the lower canyon. Variation in the height of these features above summer water surface[1] has no discernable downstream trend, but rather is highly dependent on local channel and floodplain width, in a manner similar to the elevations of 1996 flood debris (Figure 2).

Coarse-grained Outhouse flood deposits with surfaces well above historic flood limits are found on the insides of meander bends, and as mid-valley bars and islands (Figures 3 and 4). Maximum bar height varies from 3.5 to 8 m above summer water surface, depending on local channel and floodplain width (Figure 2). The cobbles and boulders are all volcanic rocks, but many of the larger boulders are traceable to local canyon wall lithologies. Boulders are subrounded to rounded, and cobbles are usually well rounded to very well rounded. Limited exposures into coarse-grained Outhouse flood deposits reveal imbricated cobbles and boulders.

Although some of these coarse-grained Outhouse flood deposits could be interpreted as terrace deposits, several attributes point to genesis by an exceptional flood or floods. The bars generally have streamlined shapes and surfaces that begin near summer water level and ramp up in the downstream direction unlike terrace treads, which have steep cut banks facing the river, and are typically flat or gently sloped downstream. The upstream ends of many Outhouse flood bars are mantled with boulders with diameters as great as a meter—much larger than the 3-10 cm gravels found in fill terraces (Figure 5). Maximum clast size consistently diminishes in the downstream direction, similar to patterns observed on other flood-formed bars [e.g. *O'Connor*, 1993]. Individual bars are positioned in zones of diminished flow velocity on insides of valley bends and at canyon expansions, consistent with the hydraulics of a large flood (Figure 4).

[1] Analysis of stages and discharges along the lower Deschutes River indicate that summer water surface (May through September) fluctuates 10-30 centimeters, while discharge fluctuates 15-40 m^3/s.

Table 1. Location and description of radiocarbon dates used in this report. Conventional radiocarbon ages (in ^{14}C yr BP) are calculated on basis of Libby half life for ^{14}C (5568 years). The error stated is ± 1σ on basis of combined measurements of the sample, background, and modern reference standards. Age referenced to AD 1950. Calibrated ages are dendrochronologically calibrated by Beta Analytic Inc. using the INTCAL98 calibration data of *Stuiver et al.* [1998] and a laboratory error multiplier of 1. The 2-sigma range is the intercept of the conventional radiocarbon age ± 2σ with the calibrated calendar time scale curve. The intercept(s) are the intersection of the conventional radiocarbon age with the calibrated calendar time-scale curve. All $^{13}C/^{12}C$ rations were calculated relative to the PDB-1 international standard.

Sample	Site/unit	Material	Conv.^{14}C age BP +/-1sigma	2 sigma cal. range BP (intercepts)	$^{13}C/^{12}C$ Ratio (%)	Laboratory/ ID#
D2-1b	Axford A	charcoal	220+/-40	315 (290) 0	-25.8	Beta 131826
D2-2	Axford B	charcoal	1480+/-40	1420 (1350) 1300	-25.8	Beta 131827
D2-3	Axford C	charcoal	1490+/-45	1516-1426 1424 (1352) 1295	-25.3	UofAz AA36673
D2-5	Axford D	shell	4500+/-45	5310 (5277,5172, 5123,5108,5068, 5055,) 5026 5021-4972	-9.48	UofAz AA36674
5/14/99-2(3)	Axford E	charcoal	5260+/-70	6200 (5995) 5905	-24.1	Beta 131836
D2-10	Axford F	charcoal	4080+/-50	4815 (4540) 4745 4720-4425	-24.9	Beta 131831
D5-10	Dant A	charcoal	140+/-40	290 (265,215,140, 25,0) 5	-24.7	Beta 131834
3/17/00-1(3)	Dant B	charcoal	1836+/-42	1873 (1815,1797, 1775,1757,1739) 1692 1668-1661 1651-1629	-25.3	UofAz AA37926
D5-8	Dant C	charcoal	1310+/-50	1305 (1265) 1155	-26.5	Beta 131833
8/23/00-1(1)a	Dant D	charcoal	2980+/- 40	3310-3000 3260 (3160) 3000	-22.3	Beta 152465
5/17/99-2(1)	Caretaker Flats	charcoal	2850 +/- 50	3090 (2950) 2850	-28.9	Beta 131837

indicators, we use a relationship between shear stress and particle size to estimate depth of overtopping and calculate a "more likely" discharge. Shear stress (τ) is defined as

$$\tau = \gamma D S_e \qquad [1]$$

in which γ is the specific weight of water (9800 N/m), D is the depth in m, and S_e is the local energy gradient. Several relationships between τ and maximum transported particle size have been reported in the literature [*Buffington and Montgomery*, 1997; *O'Connor*, 1993; and *Williams*, 1983 contain summaries]. We use a regression relationship calculated by *O'Connor* [1993] for two reasons. First, the relationship assumes boulder-depositing flow, rather than incipient motion, and the shear stress required to accelerate a particle at rest is substantially greater than that required to keep it in motion. Second, the relationship was developed using the calculated local energy gradient as opposed to channel slope. In reaches upstream of constrictions, such as Dant, energy gradient is often substantially lower than channel gradient, leading to lower values of shear stress along the reach than would be calculated simply using channel slope. The shear stress associated with boulder deposition was related to particle size using the following regression equation:

$$\tau = 0.33 d^{1.12} \qquad [2]$$

where d is the median diameter of the five largest particles in cm [*O'Connor*, 1993]. For d = 30 cm, which is the approximate median diameter of the largest clasts on the highest point of the bars at Harris Island and Dant (e.g.

Table 2. Step-backwater modeling results for paleo- and historic floods, and gaged discharges for the 1964 and 1996 floods. The "natural" peak discharge estimate for the 1964 flood at the Moody gage is obtained by adding the 425 m^3/s rates of storage for Lake Billy Chinook and Prineville Reservoir during the flood [*Waananen et al.*, 1970a] to the gaged peak at Moody. Because it is unknown whether the maximum flow stored in the reservoir would have would have coincided with maximum runoff derived from downstream of the Pelton-Round Butte dam complex, this value for "natural" peak may be an overestimate. The values in parentheses in the Outhouse flood column represent the range of minimum and "more likely" discharges obtained by varying Mannings *n* from 75 –125% of the field-assigned value.

Location	Outhouse Flood (m^3/s)	1861 Flood (m^3/s)	1964 Flood (m^3/s)	1996 Flood (m^3/s)
Madras Gage (RM 100, km 160)	**	**	peak (Dec 28) 450	peak (Feb 8) 541
Axford (RM 82, km 132)	2200-3050 (1850-2400) (2570-3500)	1060 - 1800	**	**
Dant (RM 65, km 104)	2000-3500 (1800-2100) (3400-3700)	1100 - 1700	**	1000 - 1100
Harris Island (RM 11, km 18)	3800-5660 (3370-4250) (5150-6100)	**	**	2040
Moody Gage (RM 1.4)	**	**	peak (Dec 22) 2140 "natural" (Dec 22) 2990	peak (Feb 8) 1990

Figure 5), this implies a minimum shear stress value of 15 N/m. We use this value as a basis for estimating flow depths above Outhouse flood deposits to provide 'more likely' estimates of the peak discharge than the minimum estimates provided by assuming the maximum flow stage just overtopped the deposits. Table 2 summarizes results, including comparison with calculated and gaged discharges for historic Deschutes River floods.

Axford Study Reach

Ten cross-sections were surveyed along an 800-m reach near Axford, OR (Figures 9 and 10, RM 82). This reach was chosen because there is an excellent exposure of fine-grained stratigraphy representing nearly 7000 years [*Hosman et al.*, this volume] (Figure 6). It is not otherwise ideal for modeling for several reasons. First, there is only one site containing paleostage evidence within the reach, thus hindering comparison of calculated water-surface profiles to stage evidence. Second, the position of the site with respect to major tributaries is such that the gaged records of the 1964 and 1996 floods are not directly comparable with results from the site, also hindering assessment of the results. Finally, without a downstream constriction creating a backwater effect, the accuracy of the model is more dependent on the choice of Mannings *n* (discharge varies 550-930 m^3/s over the range of *n* values compared to 300 m^3/s at Dant). Nevertheless, the modeling results indicate that a minimum discharge for the Outhouse flood of 2150 m^3/s was necessary for flow to have achieved a stage represented by the top of the fine-grained deposits. A 'more likely' discharge of 3050 m^3/s is estimated assuming flow overtopped the surfaces by 1.2 m. This depth is based on the average height difference between flotsam from the February 1996 flood (approximating the exact high water surface) and 1.22 m-deep sand and silt deposits from the same flood in this reach [*Hosman*, 2001]. *Hosman et al.* [this volume] use a higher deposit further from the channel at Axford to calculate a discharge of 2860 – 3800 m^3/s for the Outhouse flood. We did not use the surface of this deposit as a paleostage indicator because a charcoal clast from 70 cm depth yielded an age of 1055 – 925 cal. BP, but it is possible that the date does not represent the true age of the deposit and that the Outhouse flood reached this stage.

Dant Study Reach

The Dant reach (RM 65) (Figure 11) has hydraulic conditions much more suitable for discharge estimation, although the gaged records of historic flows do not apply here, either. Several coarse Outhouse flood bars and one well-exposed section of fine-grained sediments are upstream of a substan-

Moody gage (1990 m^3/s, Table 2). One drawback of this reach for modeling purposes is that the 1996 flood split around the two prominent Outhouse flood bars, resulting in flow conditions not entirely suitable for applying a one-dimensional flow model. In addition, the only paleostage indicators for the Outhouse flood are the prominent boulder bars, which would have been submerged at an unknown depth during deposition. Nevertheless, the close fit between discharge modeled for the 1996 flood (2040 m^3/s) and discharge measured at Moody (1990 m^3/s) suggest that the model is reasonable. For the Outhouse flood, a minimum discharge of 3800 m^3/s is calculated assuming the highest boulder bars were just overtopped. A 'more likely' discharge of 5660 m^3/s produces a local shear stress value of 15 N/m^2 with a local energy gradient of 0.001 and a depth of overtopping of 1.5 m.

ANALYSIS OF POSSIBLE SOURCES

The estimated discharges range from 2000 to 5660 m^3/s and show that the Outhouse flood was 1.3 to 3 times larger than the greatest historical floods at each of the three study sites. Furthermore, results reported by *Hosman et al.* [this volume] indicate that the Outhouse flood was substantially larger than any flow of the last 2000 years. Although these discharge estimates for the Outhouse flood are much smaller than the original Mannings equation estimate, the possibility of recurrence of such a flood could substantially affect risk assessment for the Deschutes River. Because of this, the cause of the flood becomes an important consideration. If the Outhouse flood was meteorological, then hazard implications with respect to advance warning, mitigation opportunities, and dam safety are substantially different than if it resulted from a natural dam failure somewhere in the basin. In order to assess whether this flood could indeed have resulted from a meteorological mechanism we address several specific questions: a) Was the downstream behavior of the Outhouse flood more similar to a meteorological flood or an outburst flood?; b) Is there other evidence of an exceptional regional meteorological flood?; c) Is the runoff generation required to produce a meteorological Outhouse flood unreasonable?; d) Are there alternatives to a meteorological explanation for the Outhouse flood that make more sense?

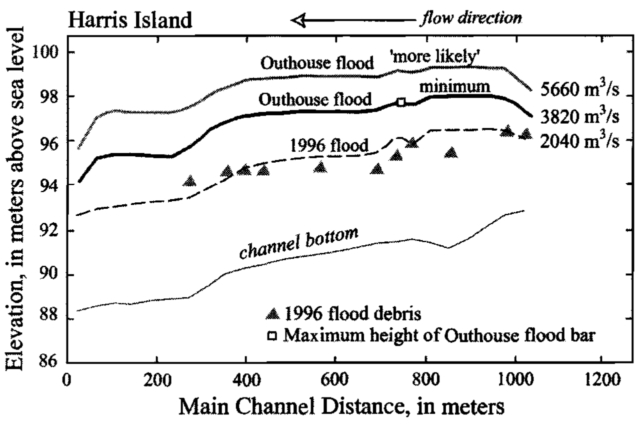

Figure 13. Calculated water-surface profiles and relations to maximum February 1996 stages and the crest of the Outhouse flood bar for the Harris Island reach.

Downstream Flow Behavior

The major hydrodynamic differences between meteorological and outburst floods are the spatial and temporal evolution of peak discharge as the flood translates downstream. The maximum discharge of outburst floods occurs at or near the breach site, and diminishes downstream as the hydrograph is diffused by boundary friction and flow storage in the valley bottom. An empirical equation developed by *Costa* [1988] that defines an envelope curve for the attenuation of discharge downstream for historical failures of constructed dams is

$$Q_x = \frac{100}{10^{(0.0021x)}} \qquad [3]$$

in which Q_x is the discharge at location x, expressed as a percentage of the discharge at the breach location, and x is the distance downstream from location of peak discharge in km. In contrast, tributary input causes most meteorological floods in the Deschutes River basin to increase in discharge downstream (Figure 14). Step-backwater modeling using Outhouse flood features at Axford, Dant, and Harris Island indicates that the peak discharge did increase substantially downstream. The observation that the peak discharges of both the Outhouse flood and the 1996 flood increased substantially between Dant and Harris Island is strong evidence that the Outhouse flood was meteorological as well. More discharge estimates for the Outhouse flood, particularly those that span confluences of significant tributaries such as the Warm Springs and White Rivers, could increase confidence in this conclusion.

Regional Evidence for Exceptional Floods

The atmospheric conditions leading to the largest meteorological floods in the Deschutes River basin commonly

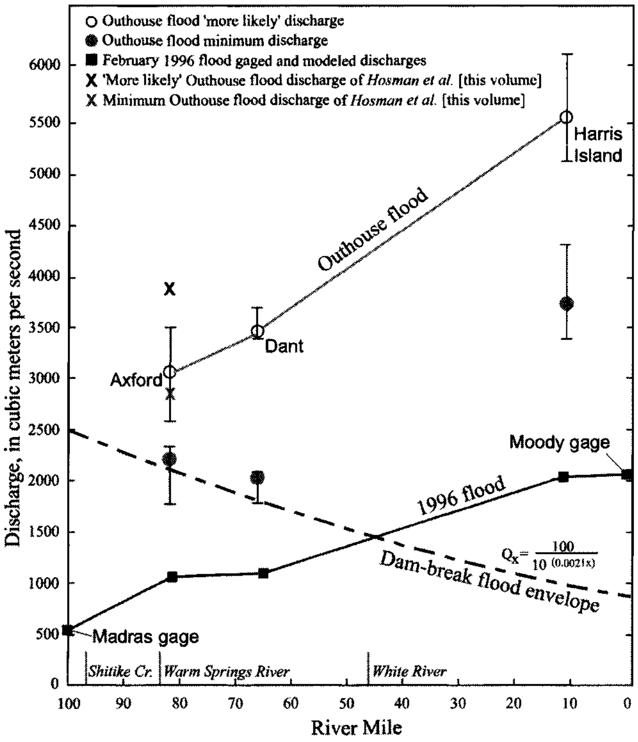

Figure 14. Comparison of downstream discharge evolution between the February 1996 flood measured values, Outhouse flood discharge estimates, and the envelope curve based on historical dam-break floods in narrow valleys [Costa, 1988]. Error bars on the Outhouse flood estimates indicate the range of discharges resulting from changing Mannings n from 75% to 125% of the assigned values.

affect adjacent rivers and occasionally several western states. The region affected depends on the type of storm causing the flooding, and how the storm interacts with the drainage basin. The three largest historic floods of Deschutes River—in December of 1861, December of 1964, and February of 1996—all occurred in midwinter when heavy snowpacks in the Cascade Range were rapidly melted by warm rainstorms. In all three cases, extended periods of low-elevation snow accumulation were followed by intense precipitation and warm temperatures carried into the Pacific Northwest by a subtropical jet stream that shifted north [*Taylor and Hannan*, 1999]. Newspapers reported record flooding on the Willamette and Deschutes Rivers in 1861, as well as heavy snowstorms in California [*The Oregonian*, November 30, 1861]. The winter storms of 1964 caused floods of record on rivers in five western states [*Waananen*, 1970a]. The February 1996 floods were focused in northwest Oregon and southwest Washington and produced large flows on the Willamette River as well as record flows for several eastern Oregon Rivers. These historical data show that large flows on the Deschutes River are usually accompanied by extreme regional flooding. A meteorological source for the Outhouse flood would thus be supported by evidence of contemporaneous flooding in adjacent basins.

Sparse paleoflood data in the region do not provide evidence for an exceptional regional flood at the time of the Outhouse flood. A study of the John Day River (the adjacent river basin to the east) indicates that the largest paleofloods occurred *ca.* 1.6 ka, and the earliest large Holocene flood occurred *ca.* 1.8 ka [*Orth and Ely*, 2000]. A paleoflood analysis of the Crooked River (the major tributary draining the eastern part of the Deschutes River basin) identified the 1861 flood as the largest post-Mazama flood [*Levish and Ostenaa*, 1996]. Similarly, extensive exposures of Mazama tephra capping floodplain stratigraphy along the upper Deschutes River [*Cameron and Major*, 1987] are evidence that there have not been exceptional post-Mazama flows in the southern part of the Deschutes River basin. The absence of evidence for exceptional flooding in other parts of the region, especially the Crooked River and upper Deschutes River basins, weakens the hypothesis that the Outhouse flood resulted from a regional meteorological event.

Are Peak Discharges Too High To Be of Meteorological Origin?

Given the discharge estimates of the Outhouse flood and lack of evidence for similar major flooding in the Crooked River and upper Deschutes River basins, is it still possible that the Outhouse flood resulted from rainfall and snowmelt generated primarily from the northern part of the Deschutes River basin? We assess this by evaluating patterns and volumes of runoff generated during the gaged flows of 1964 and 1996 (Figure 15, Table 3), adjusting for reservoir storage by using flow records from stations above reservoirs. The most striking pattern is that runoff per unit area from western tributaries draining the Cascade Range is an order of magnitude greater than the combined runoff from the Crooked and upper Deschutes River basins. During major historical floods, more than 75 percent of the peak discharge at the mouth of the Deschutes River entered the river in the lowermost 160 km downstream of Lake Billy Chinook. This imbalance between runoff upstream and downstream of Lake Billy Chinook was exaggerated by flow regulation in the Crooked River reservoirs and Lake Billy Chinook in 1964, when less than 7 percent of the peak discharge recorded at the mouth of the Deschutes River was derived from upstream of Lake Billy Chinook. This effect was less pro-

Table 4. Estimates of downstream peak discharge attenuation for specified source volumes and peak discharges for a breach near the location of Peanut Island (RM 89, km 142). The relation of maximum discharge to source volume from *Walder and O'Connor* [1997]. Downstream attenuation based on envelope of *Costa* [1988].

Maximum Discharge (m^3/s)	Reservoir Volume (m^3)	Q_{max} at 5 km	Q_{max} at Axford (12 km)	Q_{max} at Dant (38 km)	Q_{max} at Harris I. (124 km)
2500	$1.07 \bullet 10^7$	2440	2360	2080	1373
3000	$1.40 \bullet 10^7$	2928	2830	2496	1647
3500	$1.76 \bullet 10^7$	3416	3304	2912	1922

accumulation followed by an intense subtropical cyclonic system, even if precipitation was focused primarily on the northern part of the Deschutes River basin. Thus, our assessment is that the apparent size and limited regional extent of the Outhouse flood do not preclude the rainfall-runoff hypothesis. This conclusion could be more completely tested by rainfall-runoff modeling.

Could the Outhouse Flood be an Outburst Flood?

The original working hypothesis developed after discovery of the Outhouse flood features was that there was some sort of outburst flood in the Deschutes River basin. This hypothesis followed from the apparent large magnitude of the flood coupled with the extensive Quaternary history of floods from natural dam failures in the Deschutes River basin [*O'Connor, Grant, and Haluska*, and *O'Connor et al.*, this volume]. Considering the age, magnitude, and geologic setting of the Outhouse flood, the most plausible types of natural dams that could have impounded sufficient water are landslide dams, lava flows, or Pleistocene moraine dams that failed several millennia after formation. The studies by *Levish and Ostenaa* [1996] on the Crooked River and by *Cameron and Major* [1987] along the upper Deschutes River indicate that there have been no exceptional post-Mazama floods debouching from those parts of the Deschutes River basin. These observations limit the possible source areas for an outburst flood to the Deschutes River canyon between Peanut Island (RM 88.9), the upstream-most feature clearly produced by the Outhouse flood (Figure 1), and the study sites of *Cameron and Major* [1987] upstream of RM 180, the Metolius River basin, or the Shitike Creek basin. We have not yet found evidence for middle to late Holocene natural dam failures in any of these areas, although our search has not been thorough.

Without a readily identifiable source for the outburst flood, we can only speculate on possible source conditions based on downstream peak discharge estimates and empirical relations developed from documented natural dam failures. One simple method is to use a regression equation based on documented landslide dam outburst floods. Data from *Walder and O'Connor* [1997] of reservoir volume and peak discharge yield the following relationship:

$$V_o = 116.48 Q_{max}^{1.4615} \ (r^2 = 0.74) \qquad [4]$$

where V_o is volume in m^3, and Q_{max} is discharge in m^3/s. Reservoir volume and downstream attenuation [Eq. 3] were calculated assuming maximum discharges of between 2500 and 3500 m^3/s at Peanut Island (Table 4). According to this regression, the reservoir volume necessary to create the Outhouse flood peak discharge is on the order of 10^7 m^3. For comparison, the volume of Lake Billy Chinook above Round Butte Dam (134 m high) is 6.5×10^8 m^3 and the volume of Lake Simtustus below Round Butte Dam and above Pelton Dam (62 m high) is 4.5×10^7 m^3. The volume values in Table 4 should be viewed as minima because the farther upstream of Peanut Island the dam is located, the greater the volume of impounded water necessary to produce the discharges at Axford, Dant, and Harris Island. This exercise cannot reproduce the increase in discharge downstream indicated by the modeling. Thus, our investigation into the outburst flood hypothesis requires that we discount either the accuracy of the modeled discharge at Harris Island or our original interpretation that the boulder bars were deposited by the same flood that deposited the features at Axford and Dant.

CONCLUSIONS

The Outhouse flood occupies an ambiguous place in the Holocene paleoflood record on the lower Deschutes River and in the Pacific Northwest. Because its inclusion in a flood-frequency analysis could substantially affect the perception of risk from meteorological floods in the Deschutes River, it is important to consider alternative flood-generating mechanisms to explain its large magnitude. Outburst floods from the breaching of natural dams occur in many rivers, especially where tectonic and glacial activity has created landslide-prone conditions. Evidence of several Pleistocene landslide dams in the Lower Deschutes River canyon at first seem to make this alternative an attractive explanation for the Outhouse flood. However, systematically applying criteria to distinguish between meteorological and outburst floods in the ancient record, including evaluating downstream discharge evolution, basin runoff characteristics, and potential sites of breached natural dams, leads us to tentatively infer that the Outhouse flood was from a meteorological source. The strongest evidence for this conclusion is the remarkably similar patterns of downstream increases in peak discharge between the Outhouse flood and historic flows. Counter to this finding is the absence of evidence for similar magnitude floods in other parts of the Deschutes River basin and in the adjacent John Day basin, although evaluation of historical runoff magnitudes suggests that the Outhouse flood could have been generated primarily from the northern Deschutes River basin.

The inference that the Outhouse flood was of a meteorological source could be further tested by (1) more confidently assessing downstream patterns of discharge evolution by finding more sites where precise discharge estimates could be determined, (2) continued searching for potential outburst flood source areas, and (3) identifying evidence for contemporaneous flooding in tributaries draining the northwest part of the basin, which would have to have been major contributors in a meteorological event. These activities are presently underway. Additionally, these criteria for distinguishing between outburst and meteorological floods are being applied in other western rivers, where there are commonly multiple causes for extreme floods.

Acknowledgments. Portland General Electric provided partial support for fieldwork and laboratory analyses for this study. Grant Meyer, Francis Magilligan, and Rebecca Dorsey provided useful comments on an earlier draft.

REFERENCES

Buffington, J. M., and D. R. Montgomery, A systematic analysis of eight decades of incipient motion studies, with special reference to gravel-bedded rivers, *Water Resourc. Res., 33*, 1993-2029, 1997.

Cameron, K. A., and J. J. Major, Reconnaissance investigation of sediment distribution, erosion, and transport in the upper Deschutes River, Deschutes County, Oregon, November 1986, *U.S. Geol. Surv. Water Resourc. Inv. Rep.87-4114*, 24 p., 1987.

Cenderelli, D. A., and E. E. Wohl, Peak discharge estimates of glacial-lake outburst floods and "normal" climatic floods in the Mount Everest region, Nepal, *Geomorphology, 40*, 57-90, 2001.

Costa, J. E., Floods from dam failures, in *Flood Geomorphology*, edited by V. R. Baker, R. C. Kochel, and P. C. Patton, pp. 439-464, John Wiley and Sons, New York, 1988.

Costa, J. E., and R. L. Schuster, The formation and failure of natural dams, *Geol. Soc. Amer. Bull., 100*, 1054-1068, 1988.

Davis, M. B., Discussion of "Sensitivity of natural systems to climatic change" by H. E. Wright, *Character and Timing of Rapid Environmental Change: Prog. Abstr. Amer. Quat. Assoc. 7*, 17, 1982.

Gile, L. H., F. F. Peterson, and R. B. Grossman, Morphological and genetic sequences of carbonate accumulation in desert soils, *Soil Sci., 101*, 347-60 1966.

Hosman, K. J., Stratigraphic reconstruction of paleoflood frequencies and magnitudes, lower Deschutes River, Oregon, M.S. Thesis, Central Washington University, Ellensburg, WA, 78 p., 2001.

Hubbard, L. E., T. A. Herrett, J. E. Poole, G. P. Ruppert, and M. L. Courts, Water Resources Data, Oregon, Water Year 1996, *U.S. Geol. Surv. Water-Data Rep. OR-96-1*, 432 p. 1997.

Jarrett, R. D. and E. M. Tomlinson, Regional interdisciplinary paleoflood approach to assess extreme flood potential, *Water Resourc. Res., 36*, 2974-2984, 2000.

Kochel, R. C. and V. R. Baker, Paleoflood analysis using slackwater deposits, in *Flood Geomorphology*, edited by V. R. Baker, R. C. Kochel, and P. C. Patton, pp. 357-376, John Wiley and Sons, New York, 1988.

Levish, D. R., and D. A. Ostenaa, Applied paleoflood hydrology in North-central Oregon, *U.S. Bur. Recl. Seismotectonic Report 96-7 [Guidebook for field trip 2, April 19-21, 1996, Cordilleran Section Meeting, Geological Society of America]*, Seismotectonic and Geophysics Group, Technical Service Center, Bureau of Reclamation, Denver, Colorado, unpaginated, 1996.

Mack, R. N., N. W. Rutter, V. M. Bryant, and S. Valastro, Reexamination of postglacial vegetation history in northern Idaho, Hager Pond, Bonner Co., *Quat. Res., 10*, 241-255, 1978.

Manga, M., Hydrology of spring-dominated streams and implications for the transmissivity and recharge of Quaternary volcanics in the Oregon Cascades, *Water Resourc. Res.*, 32, 2435-2439, 1996.

National Research Council, *Estimating probabilities of extreme floods*, 180 pp., National Academy Press, Washington, DC, 1988.

O'Connor, J. E., Hydrology, hydraulics and geomorphology of the Bonneville Flood, *Geol. Soc. Amer. Spec. Pap. 274*, 83 pp., 1993.

O'Connor, J. E., and R. H. Webb, Hydraulic modeling for paleoflood analysis, in *Flood Geomorphology*, edited by V. R. Baker, R. C. Kochel and P. C. Patton, pp. 393-402, John Wiley and Sons, New York, 1988.

Orth, S. and L. Ely, Reconstructing paleoflood history with slackwater deposits; John Day River, north-central Oregon (abstract), *Abstracts with Programs—Geol. Soc. Amer.*, 30, 294, 2000.

Schuster, R. L., *Landslide dams: processes, risk, and mitigation*, Geotech. Spec. Pub. no. 3, 164 pp., Amer. Soc. Civ. Eng., New York, 1986.

Sea, D. S. and C. Whitlock, Postglacial vegetation and climate of the Cascade Range, Central Oregon, *Quat. Res.*, 43, 370-381, 1995.

Stuiver, M., P. J. Reimer, E. Bard, et al., INTCAL98 Radiocarbon age calibration, 24,000-0 cal BP, *Radiocarbon, 40*, 1041-1084, 1998.

Taylor, G. H. and C. Hannan, *The Climate of Oregon*, 211 pp., Oregon State University Press, Corvallis, OR, 1999.

U.S. Army Corps Eng. Hydraulic Eng. Center, HEC-RAS River Analysis System (computer program), 1998.

Walder, J. S., and J. E. O'Connor, Methods for predicting peak discharge of floods caused by failure of natural and constructed dams, *Water Resourc. Res.*, *33*, 2337-2348, 1997.

Waananen, A. O., D. D. Harris, R. C. Williams, Floods of December, 1964 and January 1965 in the far western states; Part 1: Description, *U. S. Geol. Surv. Water-Supp.Pap. 1866-A,* 265 pp., 1970a.

Waananen, A. O., D. D. Harris, R. C. Williams, Floods of December, 1964 and January 1965 in the far western states; Part 2: Streamflow and sediment data, *U. S. Geol. Surv. Water-Supp. Pap. 1866-B,* 861 pp., 1970b.

Webb, R. H., and R. D. Jarrett, One dimensional estimation techniques for discharges of paleofloods and historical floods, in *Paleoflood Hydrology*, edited by P. K. House, D. R. Levish, R. H. Webb and V. R. Baker, Amer. Geophys. Un. Water Sci. App. Ser., 2002.

Whitlock, C., A. M. Sarna-Wojcicki, P. J. Bartlein, and R. J. Nickmann, Environmental history and tephrostratigraphy at Carp Lake, southwestern Columbia Basin, Washington, USA, in *Paleoecological Records of the Last Glacial/interglacial Cycle: Patterns of Cause and Change*, edited by A. D. Kershaw and C. Whitlock, *Palaeogeog., Palaeoclim., Palaeoecol., 155*, 7-29, 2000.

Williams, G. P., Paleohydrological methods and some examples from Swedish fluvial environments, I—Cobble and boulder deposits, *Geografiska Annaler, 65A*, 227-243, 1983.

Wright, H. E., Sensitivity of natural systems to climatic change, *Character and Timing of Rapid Environmental Change: Prog. Abstr. Amer. Quat. Assoc. 7,* 12-16, 1982.

Zdanowicz, C. M., G. A. Zielinski, and M. S. Germani, Mount Mazama eruption: calendrical age verified and atmospheric impact assessed, *Geology*, *27*, 7, 621-624, 1999.

Robin A. Beebee, Department of Geological Sciences, University of Oregon, 2410 Cherry Grove Street, Eugene, OR 97403-1272

Jim E. O'Connor, U.S. Geological Survey, 10615 SE Cherry Blossom Drive, Portland, OR 97216

Section III

Geomorphic Effects of Dams on the Deschutes and Other Rivers

Our studies of the Deschutes River were initially motivated by the relicensing of the Pelton-Round Butte hydropower dam complex. These dams are only three of literally hundreds of non-Federal hydropower dams slated for relicensing in the next decades by the Federal Energy Regulatory Commission (FERC) under the Federal Power Act. On the Deschutes River, as elsewhere, relicensing typically involves a suite of studies intended to evaluate the dams' effects on the environment, and provide the technical foundation for the relicensing application as well as any changes in dam operation. Our examination of the downstream effects of the dam complex on the geomorphology of the Deschutes River was only one of multiple studies looking at all types of project effects, including impacts on fish population dynamics, fish passage, water quality, and temperature regimes.

Some background on the dams and relicensing is useful. The Pelton-Round Butte complex consists of two dams (Pelton and Round Butte) and a reregulating structure located on the Deschutes River 160-180 km upstream of its confluence with the Columbia River. The dams were constructed by Portland General Electric between May 1956 and August 1964. Total capacity is 427 megawatts, 408 of which are owned by Portland General Electric, with the remaining capacity owned by the Confederated Tribes of Warm Springs, who installed a 19-megawatt powerhouse on the regulating dam in 1982. The original license issued to Portland General Electric by the Federal Power Commission (the predecessor to FERC) expired December 31, 2001. Initial studies and preparation of the license application began in 1995. A final draft license application was submitted to FERC by Portland General Electric in December 1999 and was amended in June 2001 by a final application amendment jointly submitted by Portland General Electric and the Confederated Tribes of Warm Springs. Currently the project operates under annually issued licenses while FERC reviews and decides upon the final conditions of the relicense, which will have a term of thirty to fifty years.

As specified by the 1986 Electric Consumers Protection Act, FERC must consider both power and non-power interests in evaluating the suitability and terms and conditions of a license application. For U.S. rivers, such non-power interests affected by hydropower operations typically include recreation, reservoir- and river-side development, cultural resources, water quality, and fisheries. For the Deschutes River, fisheries are a major issue. The original facilities were constructed to promote passage of anadromous fish (chinook and sockeye salmon and steelhead, the sea-run form of rainbow trout) to upstream spawning and rearing areas and to allow downstream passage to the Pacific Ocean. These facilities were not successful and, since 1968, passage has been eliminated. Reestablishing passage is being considered as part of future operations. Downstream of the dam complex, the Deschutes River and tributaries support spawning and rearing of remaining anadromous stocks as well as a world-renowned sports fishery targeting native salmon and trout. Thus, a specific question driving much of the research conducted as part of the Pelton-Round Butte relicensing is: "What are the likely effects of past and future dam operations on fisheries in the Deschutes River

A Peculiar River
Water Science and Application 7
10.1029/007WS11

basin?" This question has many facets, but the aspect motivating much of the research presented in this volume is the possible effect of the Pelton-Round Butte dam complex on downstream channel geomorphology and physical habitat conditions.

Aware of other studies on other rivers that showed dramatic changes in channel morphology below dams, such as the erosion of beaches in the Colorado River below Glen Canyon Dam, we anticipated finding similar responses on the Deschutes River. The surprisingly few detectable geomorphic effects below the Pelton-Round Butte dam complex first alerted us to the unique character of the Deschutes River. As discussed in *Fassnacht et al.*, no discernible coarsening of the bed was observed downstream from the dams, nor was there evidence of significant and systematic erosion of islands or the channel bed, even in the reaches immediately below the dams. While unexpected, these results were interpretable in light of the rarity of bedload transport: hydraulic modeling predicted that bedload transport occurred less than 1% of the time in comparison to 5-10% of the time on other gravel-bed rivers. Infrequency of transport was linked to the uniformity of flows without major peaks and with relatively high entrainment thresholds for the coarse bed material.

But as the paper by *Grant et al.* points out, although the studies revealed the Deschutes River to be quite different from other dammed rivers in the absence of downstream response, it does fit within a continuum of rivers and dam effects when viewed across the spectrum of sediment and flow conditions of rivers affected by dams. This offers some hope that by viewing dams within their broader geological and geomorphic settings, downstream effects of dams can be predicted, at least in terms of direction and magnitude, even for peculiar rivers, such as the Deschutes.

Downstream Effects of the Pelton-Round Butte Hydroelectric Project on Bedload Transport, Channel Morphology, and Channel-Bed Texture, Lower Deschutes River, Oregon

Heidi Fassnacht and Ellen M. McClure

Oregon State University, Dept. of Geosciences and Dept. of Civil, Construction, and Environmental Engineering, Corvallis, Oregon

Gordon E. Grant

U.S. Forest Service, Pacific Northwest Research Station, Corvallis, Oregon

Peter C. Klingeman

Oregon State University, Department of Civil, Construction, and Environmental Engineering, Corvallis, Oregon

Field, laboratory, and historical data provide the basis for interpreting the effects of the Pelton-Round Butte dam complex on the surface water hydrology and geomorphology of the lower Deschutes River, Oregon, USA. The river's response to upstream impoundment and flow regulation is evaluated in terms of changes in predicted bedload transport rates, channel morphology, and channel-bed texture. Using a hydraulic model, we predicted discharges between 270 and 460 m³/s would be required to initiate bedload transport. Analysis of morphologic change at a long-term cross-section showed general scour and fill beginning at approximately 250 m³/s. Such bed-mobilizing flows have occurred less than 1% of the time during the 70+-year period of record, substantially less frequently than on other alluvial rivers. Historical streamflow records and bedload transport modeling suggest dam operations have had only minimal effects on the frequency and magnitude of streamflow and bedload transport. Analysis of gage data collected just below the dam complex revealed slow, minor degradation of the channel over the entire period of record, indicating the dams have not noticeably accelerated long-term incision rates. The dams also have had only minimal effect on channel-bed texture, as demonstrated by detailed analysis of longitudinal trends in surface and subsurface grain sizes and bed armoring. This study presents a coherent story of the Deschutes River as a stable alluvial system. This stability appears to be due to a hydrologically uniform flow regime and low rates of sediment supply, neither of which has been substantially altered by the dams or their operation.

INTRODUCTION

Dams alter the movement of water, sediment, wood, and organisms through rivers and can, therefore, have potentially significant effects on alluvial systems. Predicting the magnitude, timing, extent, or duration of dam effects is complex, however [e.g., *Petts*, 1979, 1980; *Williams and*

A Peculiar River
Water Science and Application 7

10.1029/007WS12

Wolman, 1984]. Physical changes to channels downstream of dams can range from bed degradation and narrowing, to changes in channel-bed texture or armoring, to bed aggradation, bar construction, and channel widening, to no measurable change whatsoever [*Petts*, 1979; *Williams and Wolman*, 1984; *Chien*, 1985; *Galay et al.*, 1985; *Gilvear and Winterbottom*, 1992; *Collier et al.*, 1996]. The variability in channel responses downstream of dams reflects the complex interplay between the degree of flow regime alteration, the frequency of flows capable of transporting sediment, and the rate at which new sediment is supplied to the channel relative to the amount trapped by the dam [*Williams and Wolman*, 1984; *Grant et al.*, this volume]. These complex and interacting factors limit our ability to predict the effect of any given dam on the downstream channel. Field and modeling studies are typically required to evaluate downstream changes and relate them directly to a dam and its operation. Such studies are becoming increasingly important as the operating rules and licenses for both Federal and non-Federal dams are renewed, and in light of changing societal expectations and objectives for river management.

This paper examines the downstream effects of the Pelton-Round Butte Hydroelectric Project (hereafter the "Project") on the lower Deschutes River in north-central Oregon (Figure 1). We report and synthesize the results of coordinated studies. Major individual components include a bedload transport study to estimate frequency and magnitude of streamflow and bedload transport prior to and following Project construction [*Fassnacht*, 1998]; a channel morphology study to identify temporal trends and magnitudes of changes in channel cross-section; and a channel-bed texture study to evaluate longitudinal trends in bed-material properties downstream of the Project [*McClure*, 1998]. Results from the channel morphology study complement those from *Curran and O'Connor* [this volume]. Observed responses of the Deschutes River are interpreted in light of the geologic and geomorphic setting of the river.

In the bedload transport study, the percentage of time that threshold transport conditions were equaled or exceeded was calculated based on field data, hydraulic modeling, and analysis of historical streamflow records. The robustness of the modeling results was confirmed by a sensitivity analysis and a detailed analysis of long-term cross-section change in relation to discharge. These results suggested extremely low bedload transport rates that would be difficult to measure directly in the field. To estimate the frequency and magnitude of bedload transport prior to and following Project construction, bedload transport modeling was conducted and evaluated in the context of historical streamflow records.

Although we did not calculate a sediment budget, repeat surveys of Project reservoirs provided first-order estimates of pre-dam sediment supply to the lower river. In addition, field observations were used to assess relative inputs of bed material from tributaries during high flow events.

Effects of the Project on downstream channel morphology and channel-bed texture were examined by using historical cross-sections to measure channel aggradation or scour and using a field program designed to evaluate changes in the grain-size distribution of the channel bed. No pre-dam grain-size measurements exist for the lower Deschutes River. Prior post-dam studies [*Huntington*, 1985] did not retain all particle sizes for measurement, precluding comparison of current particle-size distributions with previous particle-size measurements. It was not possible to obtain representative samples of bed material upstream of the Project due to the location of major tributary confluences and associated fans, and to the large area inundated by the reservoir created by the Project. Consequently, we substituted space for time and examined downstream longitudinal trends in the size of the surface and subsurface bed-material to evaluate the magnitude and extent of channel response. In addition, due to a large flood event that occurred after our first field season, we were also able to evaluate channel response by examining these same longitudinal trends prior to and following a large flood. Taken together, these different lines of evidence present a coherent and consistent story of the Deschutes River and Project effects.

STUDY AREA

The study area is located in the 26,800 km^2 Deschutes River basin in north-central Oregon (Figure 1). The Project (FERC No. 2030), a three-dam hydroelectric complex on the mainstem Deschutes River, is located directly downstream from the confluence of the Crooked, upper Deschutes, and Metolius Rivers (Figure 1). The Project includes Round Butte Dam, at River Mile[1] (RM) 110.1, Pelton Dam (RM 102.6), and the Reregulating Dam (RM 100.1). The study area encompassed the downstream-most 161 km of river extending from the Reregulating Dam to the confluence of the Deschutes and Columbia Rivers (Figure 1). Within this

[1] Units given are metric except for locations, which are given as River Miles (RM), or miles upstream from the river mouth as marked on USGS topographic maps. These values are close to, but not necessarily the same as, actual distances along the present channel. Fractional river miles given herein are based on interpolations between these published river miles.

larger study area, a primary study reach, extending 21 km between the Reregulating Dam and Trout Creek tributary (RM 87.3), was chosen based on the premise that the effects of the Project would be most pronounced in the reach closest to the dams. All field data used in the bedload transport study were collected within this primary study reach; the channel-bed texture study included both the primary study reach and the entire study area.

Geomorphic and Hydrologic Setting

The lower Deschutes River is deeply incised into a 600-800 m deep bedrock canyon comprised of volcanic, volcaniclastic, and sedimentary units [*O'Connor, Grant, and Haluska,* this volume]. Upstream, the upper Deschutes River basin drains highly porous and permeable Pliocene and Pleistocene basalt fields, which are fed by snowfields through a relatively undissected and poorly integrated stream network with many springs [*Manga*, 1996; *Gannett et al.*, this volume]. River widths in the lower river range from 10–170 m, with narrower sections reflecting reaches where the river flows through more resistant rock formations. Floodplains and terraces are rare in these confined reaches but more numerous in unconfined sections. Islands and submerged bars are key morphologic and ecologic features and are commonly associated with tributary fans and channel-margin expansions and constrictions [*Curran and O'Connor*, this volume]. Exposed bars are rare. For the purposes of this study, islands were defined as vegetated mid-channel or channel-margin deposits bounded by water. Vegetation on islands included any combination of trees, shrubs, and grasses. Trees on islands were not cored; however, ages ranged from saplings to decades old. Bars were defined as unvegetated mid-channel and channel-margin deposits usually submerged at mean annual flow.

The quantity, composition, and source of sediment delivered to the lower Deschutes River has varied significantly over geologic and historic time scales [*O'Connor, Grant and Haluska,* this volume]. Recent, proximal sediment sources include canyon-wall landslides and rock falls, and fluvial erosion of previously deposited material from both the main channel and its tributaries. The main-channel bed material is basalt and andesite ranging in size from silt to boulders, with the majority of particles being gravel and cobbles. For most of its length, the lower river has very low sinuosity (<1.2, J. E. O'Connor, U.S. Geological Survey, written communication, 2002) and a very uniform channel gradient [approximately 0.23%, *Aney et al.*, 1967; *McClure*, 1998].

Native riparian species include white alder (*Alnus rhombiofolia*), willow (*Salix spp.*), sedges, rushes, and perennial grasses [*Nehlsen*, 1995]. Although several macrophytes populate portions of the lower Deschutes, coontail (*Ceratophyllum demersum*, identification, S. Gregory, Oregon State University, oral communication, 1998), also known as hornwort, is by far the most abundant, and is concentrated in the reach closest to the Project. This floating macrophyte occupies zones of shallow, slow-moving water [*Haslam*, 1987] and is anchored by shoots penetrating bed material.

The lower Deschutes River experiences only small seasonal variations in discharge because of large groundwater contributions [*Gannett et al.*, 1996; *Gannett et al.*, this volume]. There are two active U.S. Geological Survey (USGS) stream gaging stations on the mainstem lower Deschutes River: station 14092500 (Deschutes River near Madras, Oregon) located at RM 100.1 just downstream from the Reregulating Dam, and station 14103000 (Deschutes River at Moody near Biggs, Oregon) located at RM 1.4 near the mouth (Figure 1). Flow duration curves from the Madras station, for water years 1925-1955 and 1966-1996, illustrate the extraordinary uniformity of river flows (Figure 2). The mean daily discharge with a 10% exceedance probability is less than two times that with a 90% exceedance probability. The difference between the 1% and 99% exceedance probability discharges is less than a factor of three.

Since the Madras gage began operation in 1924, the lower Deschutes River has experienced two exceptionally large floods in December 1964 and February 1996 (Table 1). Both floods occurred as the result of rain-on-snow events. Round Butte Dam caught the peak of the December 1964 flood, which filled the reservoir for the first time, almost a year ahead of schedule.

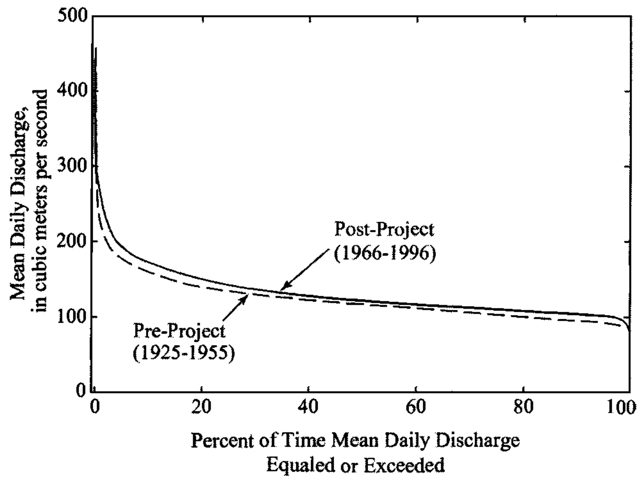

Figure 2. 30-year flow duration curves for pre-Project (water years 1925-1955) and post-Project (water years 1966-1996) time periods.

Table 1. Stream gage and streamflow characteristics of the lower Deschutes River.

	Madras gage (14092500)	Moody gage (14103000)	Reference
Stream gage characteristics			
Period of Record	Jan 1924-June 1933 Aug 1929-Nov 1956 Nov 1957-present	Oct 1897-Dec 1899 Jul 1906-present	1, 2
Location (River Mile)	102.8 102.4 100.1	1.4	1, 2
Drainage Area (km^2)	20,274	27,195	1
Streamflow characteristics (m^3/s)			
Mean Annual Flows			
Range	101-174	121-209	4, 5
Average	128	163	4, 5
Maximum Recorded Flows [a]	637	1,991	1
Largest Flood Peaks [b]			
February 8, 1996			
Instantaneous flow	541	1,991	1
Mean daily flow	504[c]	1,821	1
December 1964	December 28, 1964	December 22, 1964	3
Instantaneous flow	447	1,906	1, 3
Mean daily flow	428	1,767 [d]	3
Minimum Recorded Flows [a]	26	68	1

[a] Instantaneous flow regardless of whether due to storm event or anthropogenic causes.
[b] Flow resulting from storm events only.
[c] Original provisional data listed this value as 510 m^3/s, which was used in our calculations in 1996. Later final data listed this value as 504 m^3/s. The change had a negligible effect on our calculations.
[d] Occurred on December 23, 1964 [*US Department of the Interior*, 1965].

References: 1. *Hubbard et al.* [1997]; 2. *U.S. Department of the Interior* [1994]; 3. *U.S. Department of the Interior* [1965]; 4. U.S. Department of the Interior, U.S. Geological Survey, http://oregon.usgs.gov/www_mans95_dir/man 14092500.html, October, 1997; 5. U.S. Department of the Interior, U.S. Geological Survey, http://oregon.usgs.gov/www_mans95_dir/man 14103000.html, October, 1997.

River Regulation

The Deschutes River is regulated by eight major water storage projects (Figure 1, Table 2) and numerous irrigation diversions; the dams in the basin retain a total of $128 \cdot 10^7$ m^3 of water, 76% of which is permitted annual active storage (though on average only 38% is used). *Permitted annual active storage* is the volume of water that a dam is allowed to retain, and then release at a different time. *Average annual active storage*, or the average storage used, is the actual annual average difference between the minimum and maximum pool elevation recorded each year for a dam's reservoir (D. Ratliff, Portland General Electric, written communication, 2002). The Project's Round Butte Dam impounds the basin's largest reservoir, Lake Billy Chinook, holding over 40% of the total water stored in the basin. However, this dam is responsible for only 11% of the basin's average annual active storage. The Pelton and the Reregulating Dams have no annual active storage. The purpose of the Reregulating Dam is to provide constant discharge to the lower Deschutes River while allowing daily peaking power production from Pelton Dam upstream. To accomplish this, the Reregulating Dam stores water and evens flow on a daily basis. Downstream of the Project, the Deschutes River flows uninterrupted to its confluence with the Columbia River.

Table 2. Storage characteristics of major water storage projects in the Deschutes River basin.

Project (Reservoir)	River	Year Construction Began	Purpose of Dam	Total Storage (10^7 m^3)	Permitted Annual Active Storage (10^7 m^3)	Average Annual Active Storage (10^7 m^3)	Drainage Area (km^2)
Ochoco (Ochoco)	Ochoco Creek	1918 [a, b]	Flood control Irrigation	5.92 [a, b]	5.7 [a, b]	3.26 [c]	750 [b]
Crane Prairie (Crane Prairie)	Deschutes	1922 [d]	Irrigation	6.82 [d, e]	6.6 [d]	3.45 [c]	660 [d, e]
Crescent Lake (Crescent Lake)	Crescent Creek	1922 [d, f]	Irrigation	11.3 [e, g]	11 [e]	3.62 [c]	150 [e]
Wickiup (Wickiup)	Deschutes	1939 [h]	Irrigation	24.7 [g, h]	24.7 [h]	18.0 [c]	660 [g, h] 1,040
Pelton (Lake Simtustus)	Deschutes	1956 [i]	Hydroelectric	3.82 [i]	0.46 [i]	0 [i]	19,950? [e]
Pelton Reregulation	Deschutes	1956 [i]	Flow reregulation Hydroelectric	0.43 [i]	0.31 [i]	0 [i]	20,250 [j]
Bowman (Prineville)	Crooked	1958 [b, k]	Flood control Irrigation	19.1 [b, k]	19 [b, k]	9.38 [c]	7,280 [b]
Round Butte (Lake Billy Chinook)	Deschutes	1962 [i]	Hydroelectric	56.1 [i]	30 [i]	5.42 [l]	19,410 [j]
TOTAL				128	97.8	48.5	

[a] U.S. Army Corps of Engineers, unpublished data (1959).
[b] *U.S. Department of the Interior, Bureau of Reclamation* [1966].
[c] Wayne Skladal, Central Region WRD, Bend, Oregon, written communication, 1999.
[d] K. Gorman, Watermaster, Central Oregon Irrigation District, Bend, Oregon, oral communication, 1997. Original Crane Prairie dam had around the same storage capacity as listed. The dam was rebuilt from 1943 - 1947 improving its structural support. This may refer to the same rebuild that other references cite as occurring in 1940. The hydrologic drainage boundary is uncertain due to inter-basin groundwater exchange.
[e] *Johnson* [1985].
[f] G. Cartwright, Field Supervisor, Tumalo Irrigation District, Bend, Oregon, oral communication, 1997. Storage values are for post-1956.
[g] Northwest Power Planning Council, unpublished data (1986). Values given under total storage are maximum capacity.
[h] *U.S. Department of the Interior, Water and Power Resources Service* [1981].
[i] Portland General Electric, unpublished data (1996).
[j] *Hubbard et al.* [1997].
[k] U.S. Army Corps of Engineers, unpublished data (1961).
[l] Portland General Electric, PGE Hydro Operations Records for Round Butte Dam: 1966-2001, Portland General Electric Company, Portland, Oregon.

Upstream of the Project near Bend, substantial quantities of water are diverted for irrigation, with as much as 94% of monthly streamflow being diverted at the height of the irrigation season [*Fassnacht*, 1998]. However, about 85 m^3/s, or $270 \cdot 10^7$ m^3, of groundwater is estimated to enter the Deschutes system annually below major irrigation diversions and above Lake Billy Chinook [*Gannett et al.*, 1996; *Gannett et al.*, this volume]. This is over five and a half times the annual active storage used in the basin. As a result, even with the presence of the water storage projects and irrigation water withdrawal systems upstream, the lower Deschutes River has been able to maintain its historically stable discharge.

METHODS

Diverse methods were used to examine the Project's effect on the lower Deschutes River. We focused our data collection and analysis on those physical processes and aspects of channel adjustment that we predicted to be most sensitive to Project influences over the time since the Project's construction. Because of the different methods, study locations, and timescales of analysis used, we discuss methods and data analysis separately for each of the study components: bedload transport, channel morphology, and channel-bed texture. The results, which follow the methods section, are organized in a similar fashion.

Bedload Transport

Within the primary study reach, five sites were selected (sites B, D, E, H, and I; Figure 3), representing three hydraulic environments characteristic of the lower Deschutes River: straight, contraction, and expansion zones (Figure 4). Straight zones are reaches where the channel banks are roughly parallel (Figure 4a); contraction zones are those where the channel width decreases abruptly downstream (Figure 4b); and expansion zones are reaches where the channel widens abruptly downstream (Figure 4c). In the Deschutes River channel, contractions and expansions are often the result of tributary alluvial fans constricting the main river channel [*Curran and O'Connor*, this volume; e.g., Figure 4b].

In 1995, cross sections were measured at each site along four to seven transects oriented perpendicular to the main direction of flow (Figure 5); the number of transects measured per site depended on the site's morphologic complexity. Where the water was more than 0.5 m deep, cross-sectional profiles were measured using an Acoustic Doppler Current Profiler (ADCP) mounted on a jet boat. Horizontal positions were calculated from bottom tracking measurements taken along sighted cross sections. Depth resolution of the ADCP is approximately 0.1 m for a single beam [*RD Instruments*, 1996]. The instrument has four beams, each oriented at 20° from vertical. Estimated water depths at the time of measurement were around 2 m, resulting in a relatively small footprint delineated by the four beams. We made four passes per cross section with the jet boat to obtain more data points and to improve our ability to estimate water depth and therefore cross-section shape. On dry land or where the water was less than 0.5 m deep, elevations were surveyed using an electronic total station. Vertical accuracy of cross-section points gathered by the electronic total station is judged to be better than 0.1 m.

Surface particle-size distributions were measured for each site using a modified pebble-count technique [*Wolman*, 1954]. Approximately 100 particles per site were measured along a survey tape oriented parallel to streamflow. Sampling took place on shallow submerged bars, and along

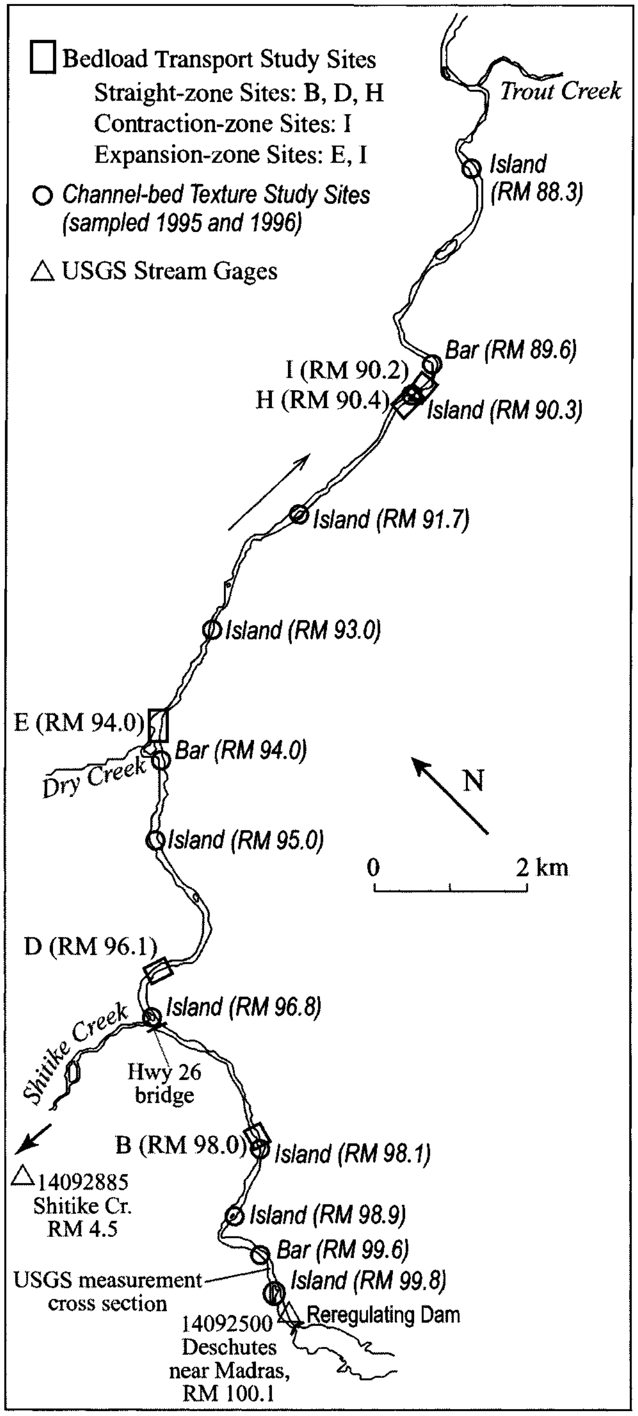

Figure 3. Primary study reach and bedload transport and channel-bed texture study sites. Base map from *Appel* [1986].

island and channel margins within or adjacent to each site; deep, fast moving water precluded sampling the channel bed near the thalweg. Visual underwater inspection of deeper

Table 3. Deschutes River gaging stations used to determine streamflow into Lake Billy Chinook.

River	Location	USGS Station	Reference
Crooked	below Opal Springs, near Culver, Oregon	14087400	*1*
upper Deschutes	near Culver, Oregon	14076500	*2*
Metolius	near Grandview, Oregon	14091500	*3*

References:
1. U.S. Dept. of the Interior, U.S. Geological Survey, http://water.usgs.gov/swr/OR/data.modules/hist.cgi?statnum =14087400, October, 1997;
2. U.S. Dept. of the Interior, U.S. Geological Survey, http://water.usgs.gov/swr/OR/data.modules/hist.cgi?statnum =14076500, October, 1997;
3. U.S. Department of the Interior, U.S. Geological Survey, http://water.usgs.gov/swr/OR/data.modules/hist.cgi?statnum =14091500, October, 1997.

From the Project inflow and outflow hydrographs, the predicted quantity of bedload transported through the sites was calculated using sediment rating curves derived from the bedload transport analysis. Bedload transport calculations for sites located below Shitike Creek confluence and for all transport events except those in 1996, reflect only the bed material moved by streamflow as measured at the Madras gage, since Shitike Creek, which joins the Deschutes upstream of Site D, was ungaged during most transport events.

Channel Morphology

Cross-section measurements have been collected by the USGS at the "Deschutes River near Madras" gage station (14092500) from January 1924 to the present. These measurements were analyzed for changes in channel-bed elevation and cross-sectional area from 1924-1998. Movement of the gage and associated cableway twice in connection with dam construction complicates comparison of channel change between pre- and post-dam time periods. Movement of the measurement cross-section occurred before any dams in the Project were closed, however. Locations and time periods over which measurements were made for the three locations of the Madras gage are shown in Table 1. Channel changes described in this analysis are not meant to represent channel change experienced over the entire study area. Measurement cross-sections are specifically chosen for their stability and are, therefore, expected to show less change than elsewhere in the river. The present location of the gage, however, is representative of the river in the primary study reach.

Minimum streambed elevations from 1924 to 1998 were determined to evaluate the record for evidence of long-term degradation or aggradation at the gage site [*Smelser and Schmidt*, 1998]. In addition, cross-sectional areas were calculated for every third USGS cross-section measurement from 1957 to 1998. Cross-sections prior to 1957 were not included because of the pronounced stability (bedrock) of the streambed at the two gage locations during this time period. Areas were calculated for the part of the cross-section existing below 2 m from an arbitrary datum. This allowed for consistent comparison of data across the range of measured discharges. At some of the larger discharges, cross-section measurement data for one stream bank or the other did not begin until 1 to 1.5 m or more below the datum. Simple linear regressions tested whether observed changes were significant. Temporal trends were examined by looking at changes in cross-section shape and area for measurements bracketing individual high discharge events. Cross-section measurements were also evaluated every 57 m^3/s (2000 ft^3/s) increment in flow, starting at 113 m^3/s, to investigate thresholds of general bed mobility over the cross section.

Channel-Bed Texture

Because islands and bars represent the dominant depositional features in the river, they were sampled to analyze longitudinal trends in bed material size. Sampled sites included islands and bars in comparable hydraulic settings [*Kondolf*, 1997] along which sampling grids could be safely established under low flow conditions. Around each island, four distinctive geomorphic environments were sampled: the head (upstream end), side (abutting main flow), side channel (side bordering secondary channel), and tail (downstream end) (Figure 7). Head and tail environments of selected bars were also sampled (Figure 7). For hydraulic consistency, results presented here focus on comparison of grain-size distributions from heads of islands and bars. Analysis of other geomorphic environments shows similar trends [*McClure*, 1998].

Nine islands and three bars were sampled in the primary study reach in the summer of 1995 (Figure 3) and then resampled in the summer of 1996 to document changes following the February 1996 flood. Eleven island heads in the lowermost 140 km of the river were also sampled during the summer of 1996 to extend the analysis downstream to the Columbia River (Figure 8).

Surface bed material was sampled at each site by measuring the intermediate (b-axis) particle diameter for three standard 100-particle pebble counts conducted on three overlap-

Table 4. Calculated critical discharge (Q_{cr}) ranges and site averages as measured at the Madras gage for Sites B, D, E, H, and I. Ranges indicate the extent of variation found in critical discharge values calculated for individual transects at a site. Site averages are the average of critical discharge values found within the range of values at a site. Bed critical discharges were calculated as an average critical discharge over the channel bed (i.e. using hydraulic depth). Critical discharges for the channel thalweg are included for comparison (i.e. using maximum depth).

Site	RM	Zone Type [a]	Bed Q_{cr} (m^3/s)		Thalweg[b] Q_{cr} (m^3/s)	
			Range	Site average	Range	Site average
B	98.1	S	310-380	340	250-300	270
D	96.1	S	290-380	320	130-200	160
E	94.0	E	240-490	330	80-420	220
H	90.4	S	[c]	[c]	[c]	[c]
I	90.2	C/E	230-490	310	80-230	120

[a] E = expansion zone, S = straight zone, C = contraction zone
[b] Assuming that channel bed here comprised of same sized material as was measured in shallower water
[c] Critical discharge could not be calculated because predicted critical shear stress exceeded the range of shear stresses defined by the Q_{cr} vs τ curve.

We focused on the straight-zone sites (Sites B and D), which most closely fit the assumptions of the one-dimensional hydraulic model. The sensitivity analysis for these two sites showed that individual and simultaneous variation of S_e, D_{50s}, and τ^*_{cr50s} did not substantially alter results of the hydraulic analysis. Critical discharges of 270 m^3/s were obtained for both sites when the three tested parameters were simultaneously varied to decrease critical discharge. Values of 420 m^3/s and 500 m^3/s (average 460 m^3/s), were obtained for Sites B and D respectively, when parameters were simultaneously varied to increase critical discharge. These low and high values (270 m^3/s and 460 m^3/s) represent end members of what we will consider the maximum deviation of the critical discharge value for the examined straight-zone sites in the primary study reach.

Bedload transport of all size classes is predicted to occur close to the entrainment threshold modeled for D_{50}-sized bed material. Using Parker's model, we predicted bedload transport of all evaluated particle sizes to begin between ~300 and 400 m^3/s, with transport rates increasing with discharge (Figure 10). Parker's model was derived for conditions when bedload transport is controlled by hydraulic conditions rather than particle availability [*Parker et al.*, 1982]; therefore, bedload transport rates presented here are those that occur following exceedance of threshold transport conditions and disruption of the channel-bed armor layer rather than just during the initial stage of transport.

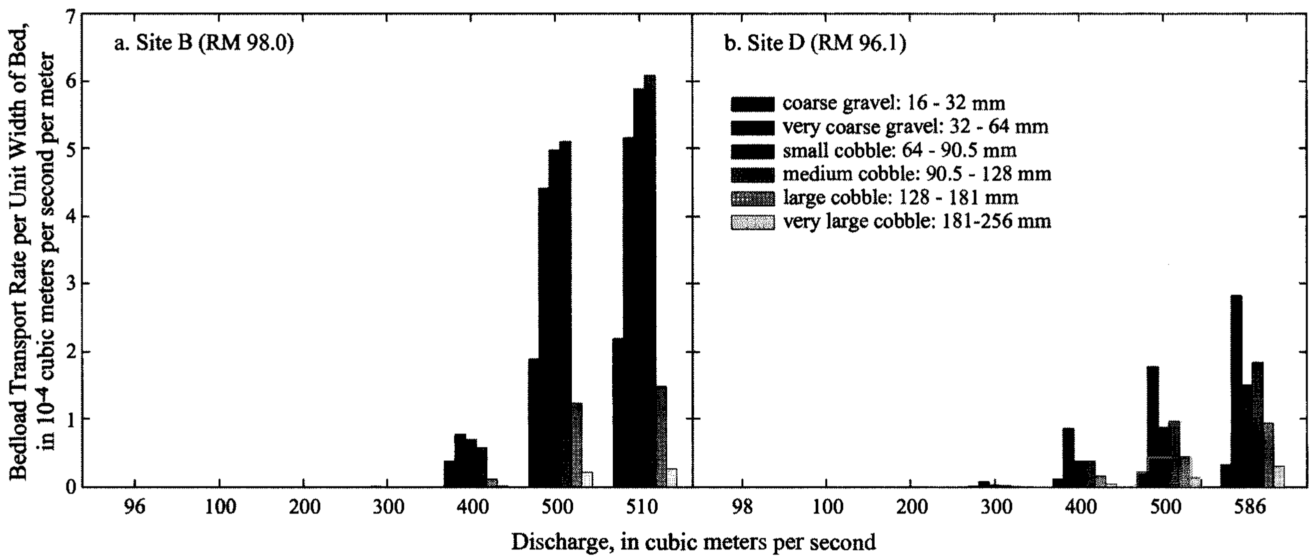

Figure 10. Calculated bedload transport rates per unit gravel-bed width for (a) Site B and (b) Site D.

Frequency and Magnitude of Streamflow and Bedload Transport. Annual flow duration curves showed little change in flow frequency or magnitude over time (Figure 11). Comparison of composite 30-year flow duration curves for the pre- and post-Project time periods similarly revealed that dam effects on hydrology have been slight (Figure 2). These results suggest that Project-induced changes in streamflow did not exist, were subtle, or were operating on time scales other than that of mean daily flow. Differences between the 30-year curves reflect the influence of climate on the two periods: severe drought occurred from the mid-1920s through much of the 1930s, affecting the pre-Project curve, and the largest flood on record affected the post-Project curve. Despite these climatic differences, curves for both time periods are quite similar, underscoring the remarkably stable flow of the Deschutes River prior to and following closure of the Project dams.

Our results predicted that events capable of mobilizing channel-bed material were rare. We found only 26 transport days from 1924 to 1996 (<1% of time) during which mean daily discharge equaled or exceeded 340 m^3/s, the predicted threshold for bedload transport across the sites (Table 5). These estimates are robust with respect to model parameter sensitivity; even our most conservative estimates of parameter values indicated that bedload transport had occurred less than 1% of the time over the 70+-year period of record evaluated (Table 5).

For this same time period, predicted bedload transport rates for Site B generally ranged from 2,000 to 3,000 m^3/yr for the years during which transport was predicted to occur (Figure 12). Two notable exceptions were water years 1965 and 1996 as a result of the December 1964 and February 1996 floods. The 1964 flood was predicted to have transported 6,530 m^3 of bed material and the 1996 flood 14,900 m^3, or 7% and 42% respectively, of all material calculated to have moved through Site B since 1925.

Project Effects on Streamflow and Bedload Transport. Post-Project transport events were predicted to have occurred in December 1964, January 1965, March 1972, February 1982, and February 1996. The 1964 event occurred prior to the Project being fully operational but was included in the analysis because this flood had the largest recorded inflow to the Project (Portland General Electric, 121 S.W. Salmon Street, Portland, OR, unpublished data, 1996), the second highest discharge recorded downstream of the Project [*Hubbard et al.*, 1997], and its peak was captured by Round Butte Dam, whose reservoir was filling for the first time. For simplicity, we refer to the four storms that occurred after the filling of the reservoir as "post-filling" events; all five events together are called "post-dam" events.

Comparing hydrograph shapes for Project inflows and outflows showed that for all post-dam transport events, the Project stored water (inflow > outflow) on the rising limb of the hydrograph and released water (inflow < outflow) during and/or following the hydrograph peak (Figure 13). In all cases but the 1964 event, however, the amount of water stored and released was minimal compared to the overall discharge for the event and, in most cases, most changes in the hydrograph due to the Project occurred below critical discharge predicted for bedload transport. Although changes in the hydrograph at flows less than critical discharge are not important in the context of bedload transport or channel morphologic change, consequences of such flow reduction or enhancement on suspended sediment transport and ecological parameters might exist.

The Project had little effect on the magnitude or timing of post-filling-event flow peaks but delayed the peak of the 1964 event by four days and decreased its magnitude by around 140 m^3/s (Table 6). We consider the Project's effect on the 1964 event unique.

Using Project inflow and outflow discharge values for each post-dam transport event, the quantity of bedload transported per day by these flows was predicted and compared for Sites B and D. The results indicated that, at these sites, the Project slightly increased bedload transport for the four post-filling events and substantially decreased transport for the 1964 event (Table 7). Because Project inflows during the 1964 flood exceeded the upper limits of the sediment rating curve for Site B, transport rates for this event had to be extrapolated.

Channel Morphology

Comparison of USGS historical cross-section measurements for the Madras gage revealed that the channel bed was degrading at a very slow but statistically significant rate both prior to and following construction of the Project as indicated by decreasing minimum streambed elevations (2-sided p-value = 0.05 for 1924–1933; 2-sided p-value << 0.001 for 1929–1956 and 1957–1998) (Figure 14). Although absolute degradation rates between pre- and post-dam time periods cannot be compared because the measurement cross-section was moved when construction began on the Project in 1957, the slopes of the 1929–1957 and the 1957-1998 trend lines are similar. The largest decreases in minimum streambed elevation after 1957 appeared to be associated with high discharge events, particularly those exceeding the predicted critical discharge of 340 m^3/s (Figure 14b). Prior to 1957, the measurement cross-section was located in a boulder- and bedrock-controlled section (USGS, unpub-

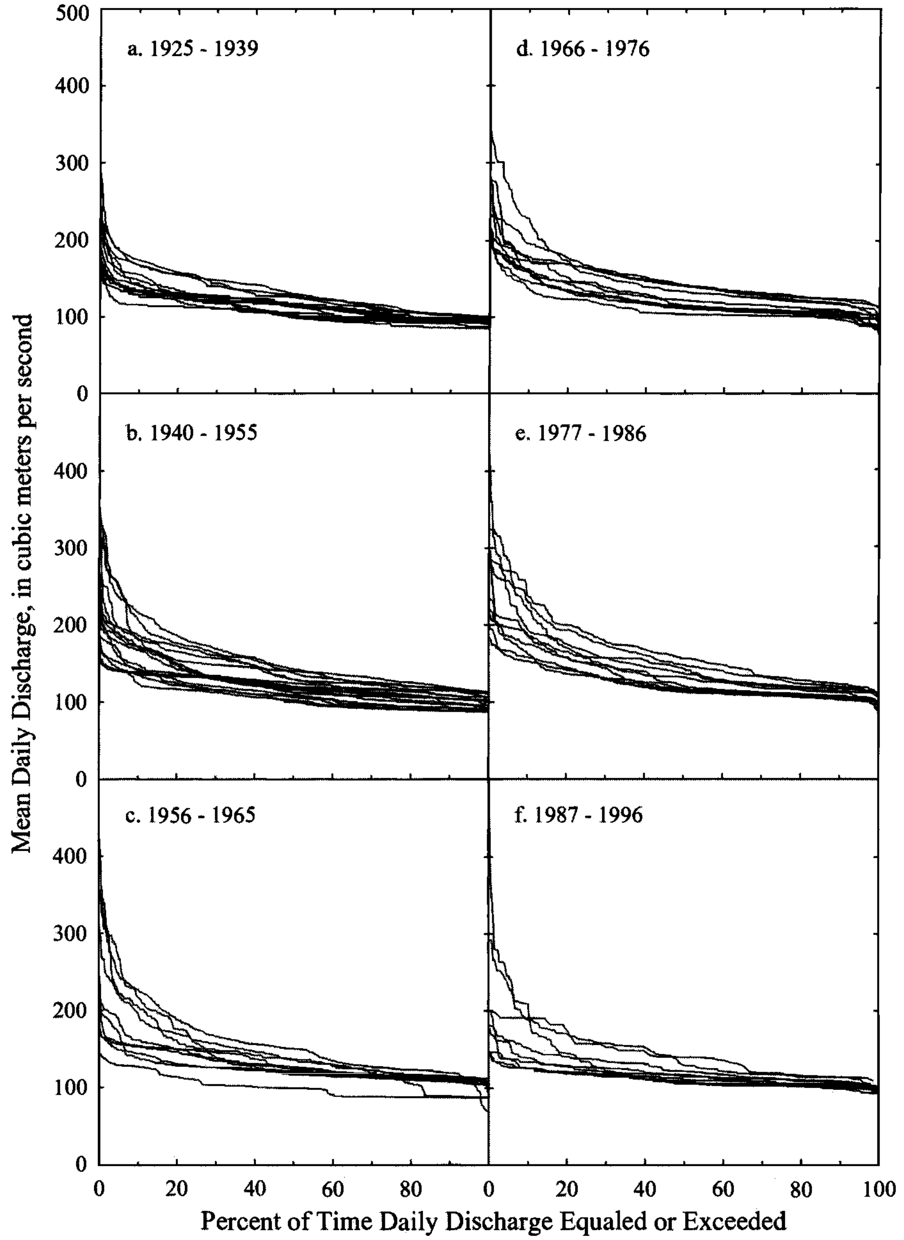

Figure 11. Annual flow duration curves (Deschutes River near Madras gage) for water years (a) 1925-1939, (b) 1940-1955, (c) 1956-1965, (d) 1966-1976, (e) 1977-1986, and (f) 1987-1996.

lished data, 1957) and, therefore, was not as affected by large flood events as the more alluvial post-1957 site (Figure 14). Between 1957 and 1998, net degradation at the channel thalweg was 0.14 m (Figure 14b). Average degradation of the thalweg over the same time period was 0.09 m (Figure 14b). For the post-1957 gage site, cross-sectional area was found to increase with time at a very small but statistically significant rate (2-sided p-value<<0.001), indicating a very slight increase in channel capacity over time (Figure 15). Pre-1957 areas were not calculated because of the extreme stability of the site (Figure 16).

Examination of individual cross sections before, during, and after high discharge events showed channel scour during the events and partial to total refilling of scoured areas

Table 5. Frequency and magnitude of critical discharge exceedance from 1924 to 1996 for calculated critical discharges of 270, 340, and 460 m^3/s.

Q_{cr}[a] (m^3/s)	# days Q[b]$\geq Q_{cr}$	% of record $Q \geq Q_{cr}$	# days $Q > Q_{cr}$ by >10%	>20%
270	181	0.7	96	48
340	26	0.1	6	5
460	1	0.004	1	0

[a] Q_{cr} = critical discharge
[b] Q = discharge

in the following weeks to months (Figure 17). Maximum recorded scour at the Madras gage measurement cross-section was 0.8 m during the February 1996 flood (Figure 17e). Four months later, 0.5 m of the original 0.8 m scour had refilled (Figure 17e). The magnitude of channel "rebound" associated with high discharge events appears to be strongly related to the magnitude of the peak discharge experienced during the event (Figure 18). Similar channel rebound was noted much further downstream at the measurement cross-section for the "Deschutes River at Moody" gage [*McClure*, 1998]

These empirical repeat cross-section surveys suggest that thresholds for general channel-bed entrainment at the Madras gage site are exceeded beginning around 250 m^3/s (Figure 17c, d, e). At this discharge and higher, the entire

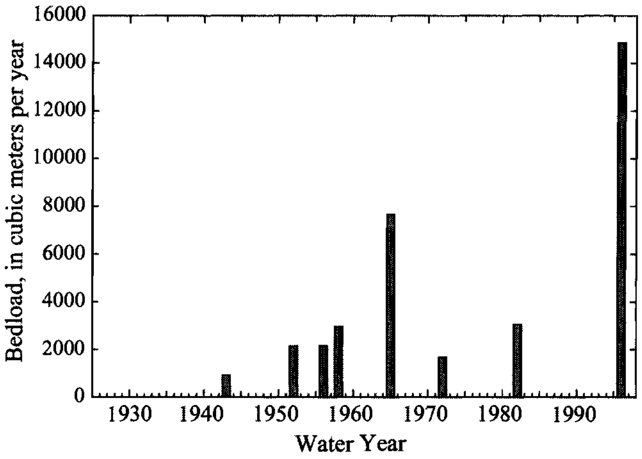

Figure 12. Predicted volume of bedload moved per year at Site B (RM 98.0) during water years 1925-1996.

cross section exhibited change. Channel change was concentrated in the thalweg for smaller discharges of about 150 m^3/s (Figure 17a, b). These results are generally in close agreement with the lower bound of critical thresholds predicted from the hydraulic models for both the cross-section average and the thalweg (Table 4).

Channel-Bed Texture

Results from multiple regression analyses showed few or no significant longitudinal or temporal trends (Table 8). A modest decrease in armoring with distance from the dam was detected but otherwise no clear spatial or temporal trends in grain size emerged.

In the primary study reach, bed surface D_{50} values at island and bar heads ranged from 30 mm to 95 mm (average 70 mm) during 1995 and 1996 (Figure 19a). Results from multiple linear regression showed no significant evidence for a change in surface D_{50} with distance, even after accounting for year and abundance of *C. demersum* (Table 8). In addition, the Trask sorting coefficient showed very little difference in surface particle sorting between sites (Figure 19b). The coefficient generally ranged between 1.3 and 2.7, but reached 5.9 at the island at RM 88.3 in 1995. Better sorting within surface deposits was not observed close to the Project.

Spatial variations in grain size between sites were strongly influenced by abundance of *C. demersum*, which traps sand in an otherwise sand-poor bed. In particular, high levels of the macrophyte were strongly significant in lowering the median grain size in the primary study reach (p-value = 0.006; extra sum of squares F-test) (Table 8). The four lowest D_{50} values represented two sites (islands at RM 88.3 and RM 98.9, Figure 19a) where macrophyte levels were especially high in both 1995 and 1996.

There was also little change in surface grain size as a whole, between years at each site (Figure 20a). Even after accounting for the effects of *C. demersum*, there was no statistical evidence for an overall change in surface D_{50} following the 1996 flood (Table 8).

The bed subsurface D_{50} in the primary study reach was finer than that of the surface and ranged from 5 mm to 50 mm (average 20 mm, Figure 20b). The final statistical model showed no evidence for a longitudinal trend in subsurface D_{50} values when year and the abundance of macrophytes were accounted for in the primary study reach (Table 8).

The final statistical model showed no significant evidence for a temporal change in subsurface D_{50} in the primary study reach (Table 8). The data point representing the bar at RM 89.6 was influential in the regression, however. When

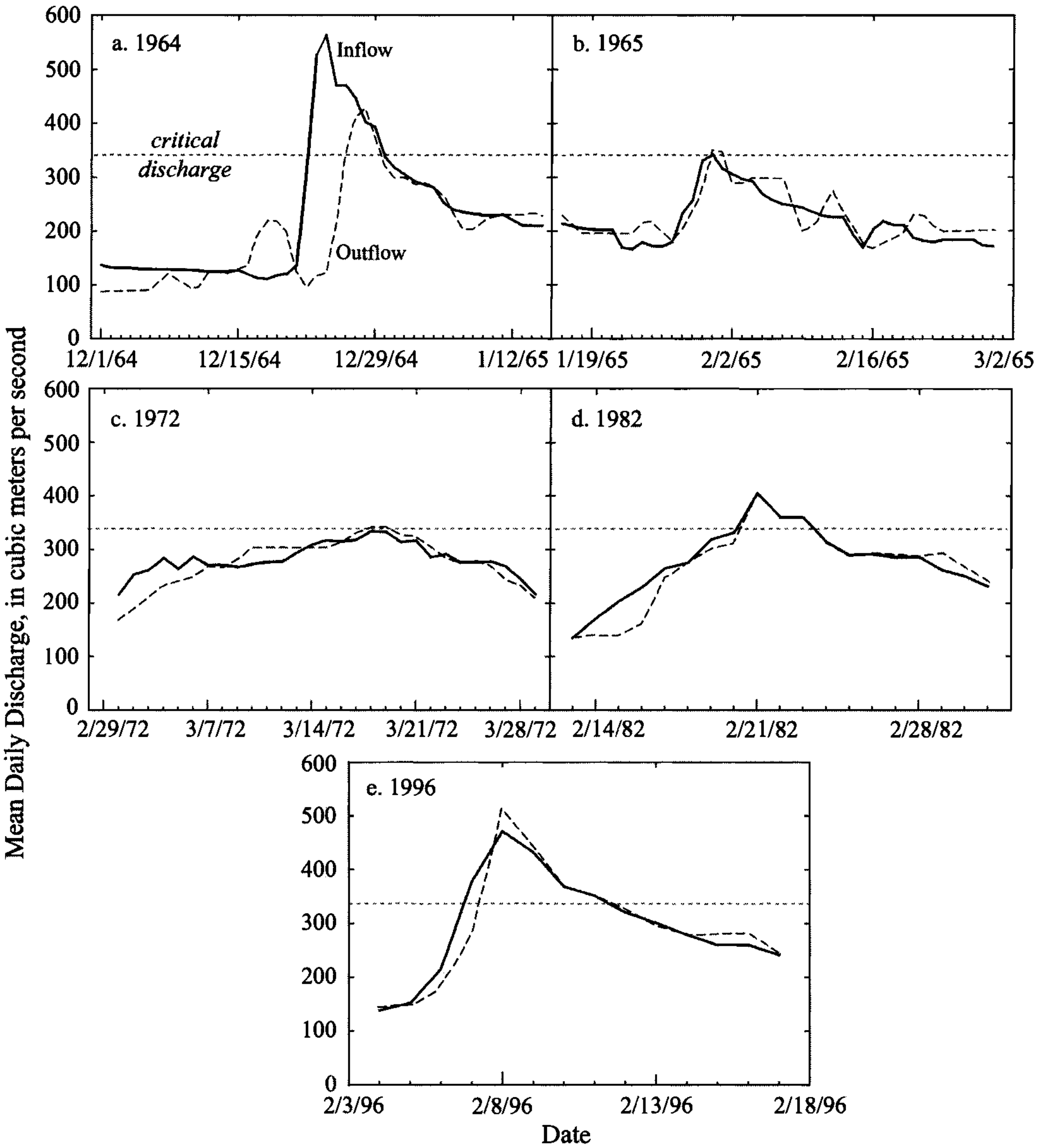

Figure 13. Lake Billy Chinook inflows and Project outflows for all post-dam transport events: (a) December 1964, (b) January 1965, (c) March 1972, (d) February 1982, (e) and February 1996.

removed from the analysis for comparison, the overall decrease in subsurface D_{50} between years was significant (2-sided p-value = 0.012), suggesting that the subsurface may have fined somewhat in response to fine sediment inputs during the flood of February 1996.

Armoring ratios ranged from 1.3 to 11.9 (average 4.0) and generally declined with distance from the Project (Figure 20c). Multiple linear regression showed that the longitudinal trend in armoring was statistically significant (Table 8). The mean armoring ratio was estimated to be 0.16 less with each kilometer from the Project (95% confidence interval between 0.013 and 0.30). Although not statistically significant at p = 0.05, the results indicated that there might also have been an increase in armoring following the February 1996 flood (Table 8). Three of the four sites closest to the Project showed the largest increases in armoring between years (Figure 20c). Data points from 1996 representing the bar at RM 99.6 and the island at RM 98.1 were influential in

Table 6. Timing and magnitude of highest flow peaks for reservoir inflows (Q_{in}) and outflows (Q_{out}) for post-dam transport events. All discharges are mean daily flow.

Transport Event	Magnitude of Highest Flow			Date of Highest Flow		
	Q_{in} (m^3/s)	Q_{out} (m^3/s)	% change	Q_{in}	Q_{out}	Days peak lagged
December 1964	564[a]	428	-32	24 Dec. 1964	28 Dec. 1964	4
January 1965	341[a]	348	2	31 Jan. 1965	31 Jan.1965	0
March 1972	334	343	3	18 Mar. 1972	18-19 Mar. 1972	0
February 1982	405	405	0	21 Feb. 1982	21 Feb. 1982	0
February 1996	471	510	8	8 Feb. 1996	8 Feb. 1996	0

[a] Estimated value due to lack of reservoir water elevation data

Table 7. Total bedload transported by reservoir inflows ($Q_{s\ in}$) and outflows ($Q_{s\ out}$) for five post-dam transport events. Reservoir inflows approximate streamflows that would occur in the absence of the Project. Transport calculations for Site D (except in 1996) do not take into account the discharge contributed by Shitike Creek as the creek was not gaged at this time.

Site	Transport Event	$Q_{s\ in}$ (m^3)	$Q_{s\ out}$ (m^3)	% change in $Q_{s\ in}$
B	December 1964	48,000	6,526	-86
D	December 1964	13,900	4,301	-69
B	January 1965	1,100	1,200	9
D	January 1965	1,400	1,600	14
B	March 1972	0	1,700	--
D	March 1972	0	1,900	--
B	February 1982	3,100	3,100	0
D	February 1982	3,000	3,100	3
B	February 1996	11,700	14,900	27
D	February 1996	9,700	10,400	7

this regression. When the two points were removed separately or in combination, the decrease in armoring with distance from the Project remained significant at the 0.05 level.

In two of these scenarios, there was strong evidence for an increase in armoring between 1995 and 1996. However, when only the point from the island at RM 98.1 in 1996 was removed, the temporal change was not significant at even the 0.1 level. Thus, the model was greatly influenced by these points and the increase in armoring with time cannot be shown conclusively.

Multiple linear regression models constructed for the entire study area showed no significant evidence for a longitudinal trend in surface D_{50}, subsurface D_{50}, or armoring (Table 8, Figure 21). In addition, the Trask sorting coefficient showed very little difference in surface particle sorting between sites over the entire study reach (Figure 22). Thus, bed coarsening or greater sorting was not observed in the primary study reach relative to the lowermost 140 km of the river.

Tributary D_{50} values were generally finer than mainstem values. Of the sampled tributaries, only the Warm Springs River had a coarser grain-size distribution than the mainstem (Figure 23). Grain-size distributions from tributaries generally exhibited similar sorting compared with the mainstem surface bed material.

Most grain-size distributions from the fourteen sampled tributaries were remarkably similar to each other (Figure 23), with D_{50} values averaging 50 mm (range 10–105 mm) and Trask sorting coefficients averaging 2.4 (range 1.4–11.6). However, the two largest tributaries, the Warm Springs and White Rivers, did have particularly distinct grain-size distributions. The White River showed a strongly bimodal distribution, with a high proportion of material

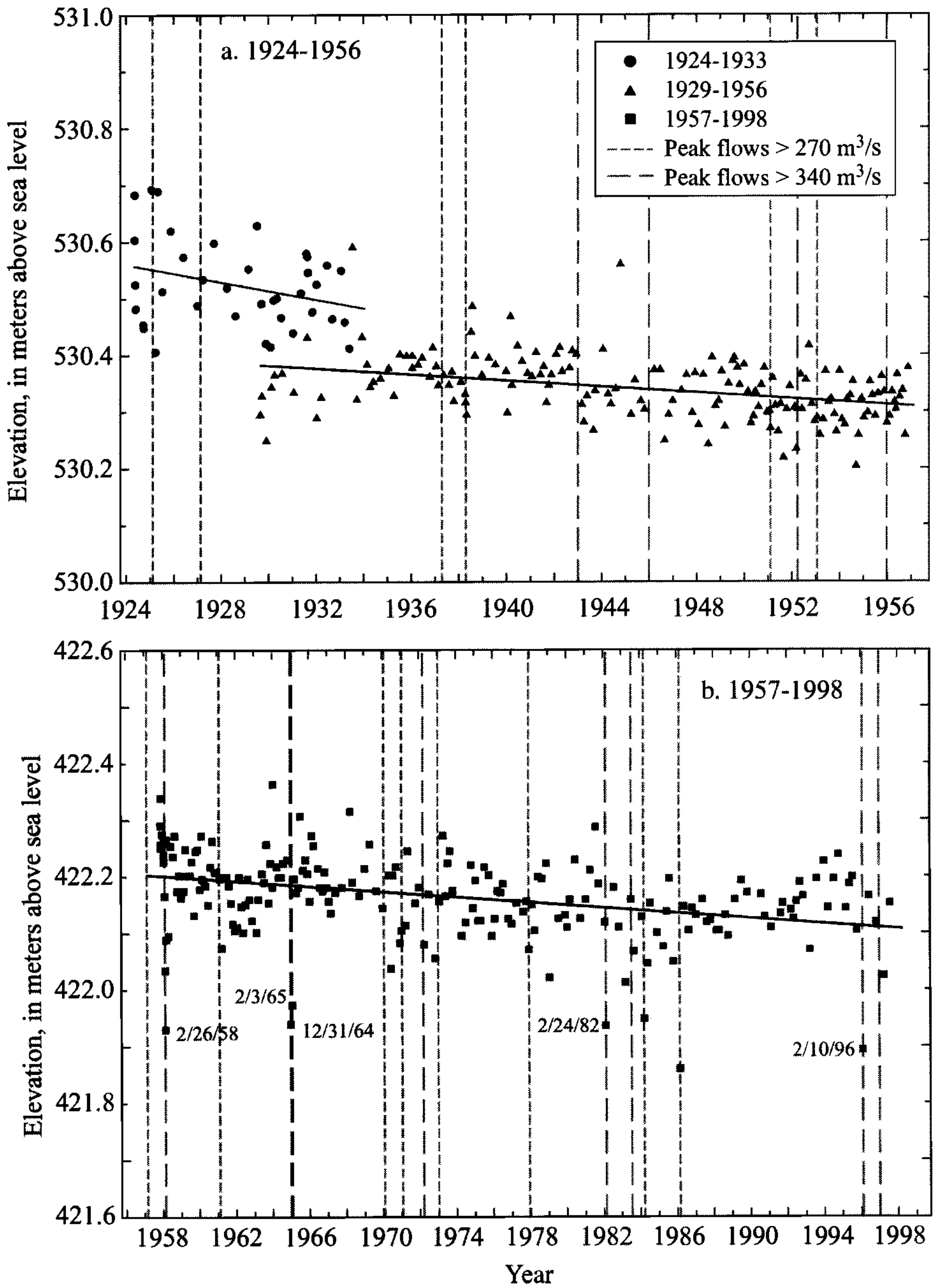

Figure 14. Minimum streambed elevations (i.e., elevation of channel thalweg) of USGS measurement cross-section for the Deschutes River near Madras gage, (a) 1924-1956 and (b) 1957-1998.

less than 2 mm in diameter (Figure 23), presumably sandy material derived from reworked lahar and glacial deposits from Mt. Hood. There was no apparent decrease in D_{50} values in the mainstem Deschutes directly downstream of the White River confluence, however (Figure 24). The Warm Springs River had a relatively coarse grain-size distribution (Figure 23). Despite this, mainstem D_{50} values registered no coarsening downstream of the Warm Springs River confluence (Figure 24). Thus, even where tributaries input the most distinctive bed material to the mainstem, noticeable shifts in the mainstem bed material size did not occur.

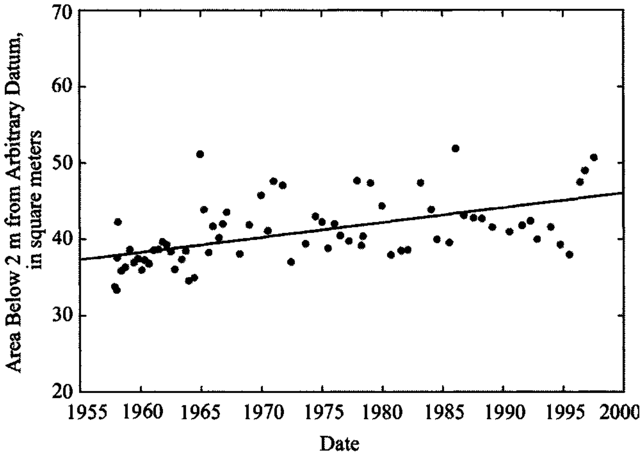

Figure 15. Area of USGS measurement cross-section below 2 meters from arbitrary datum (Deschutes River near Madras gage).

DISCUSSION

Our analyses of bedload transport, channel morphology, and channel-bed texture all consistently characterize the Deschutes River as an unusually stable alluvial river. That stability is reflected in the infrequency of bedload transport events both prior to and following dam construction, the absence of pronounced morphologic or textural change following the record flood in February 1996, and the uniformity of grain size along the channel. Here we consider in detail some aspects of the Deschutes' stability and discuss its causes and implications for assessing the effects of the Project.

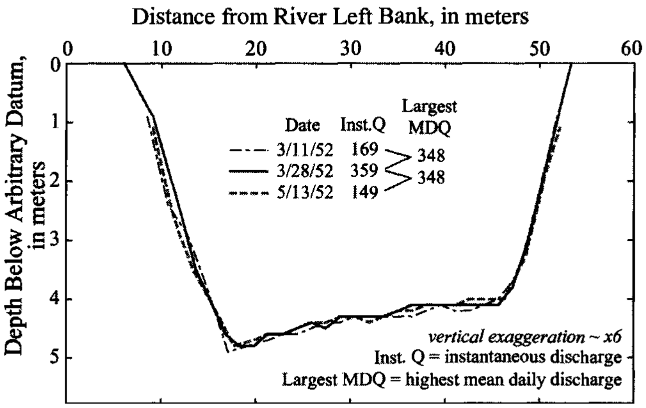

Figure 16. Cross-sectional profiles at the USGS measurement cross-section for the Deschutes River near Madras gage before, during, and after a large flood in March 1952.

Evidence for Channel Stability

Frequency and Magnitude of Bedload Transport. Modeled estimates of critical discharge were generally consistent across sites (Table 4), giving confidence in results of the hydraulic model. General mobility of the channel bed was predicted to begin at discharges of around 340 m^3/s or, incorporating the results of the sensitivity analysis, between 270 and 460 m^3/s for primary study reach sites. These model results were evaluated against a detailed analysis of long-term cross-section change in relation to discharge. The cross-section analysis (1957–1998) showed general mobility of the channel bed beginning around 250 m^3/s, near the lower end of the predicted range (Figure 17). Furthermore, the dates during which bedload transport was predicted to occur (post-1957) coincide with the lowest measured elevations of the channel thalweg at the USGS measurement cross-section (Figure 14), indicating that channel scour did occur during these events, as predicted.

Bedload transport at sites in the primary study reach was predicted to occur less than 1% of the time from 1924 to 1996. The combined effects of reasonable uncertainties of parameters used in the hydraulic modeling did not substantially alter these results. This frequency of transport is much lower than that in other gravel-bed rivers where studies have shown that bed material is typically moved about 5–10% of the time, or several times per year, at flows close to bankfull [*Andrews and Nankervis*, 1995]. The extremely low frequency of bedload transport in the Deschutes River appears to result from the very uniform flow regime, absence of high flows, and coarse gravel-to-cobble substrate with a relatively high entrainment threshold.

The volume of bed material moved was also predicted to be low, generally between 2,000 and 3,000 m^3/year for years in which transport occurred (Figure 12). In comparison, the Kemano River in British Columbia, Canada, a river with similar discharge and particle size to the Deschutes, has an estimated mean annual bedload transport rate of about 50,000 m^3/year [*Church*, 1995]. During water year 1996, the most active year on record, the Deschutes was predicted to have moved only around 15,000 m^3 of bed material (Figure 12, Table 7).

Low predicted frequency and magnitude of bedload transport and no physical evidence for channel aggradation implies that the lower Deschutes River has historically been a sediment-poor system both prior to and following Project construction. This inference is supported by a calculation of sediment discharge rates into Round Butte Reservoir [*O'Connor, Grant and Haluska*, this volume]. Results from a sedimentation survey of this reservoir indicated that about

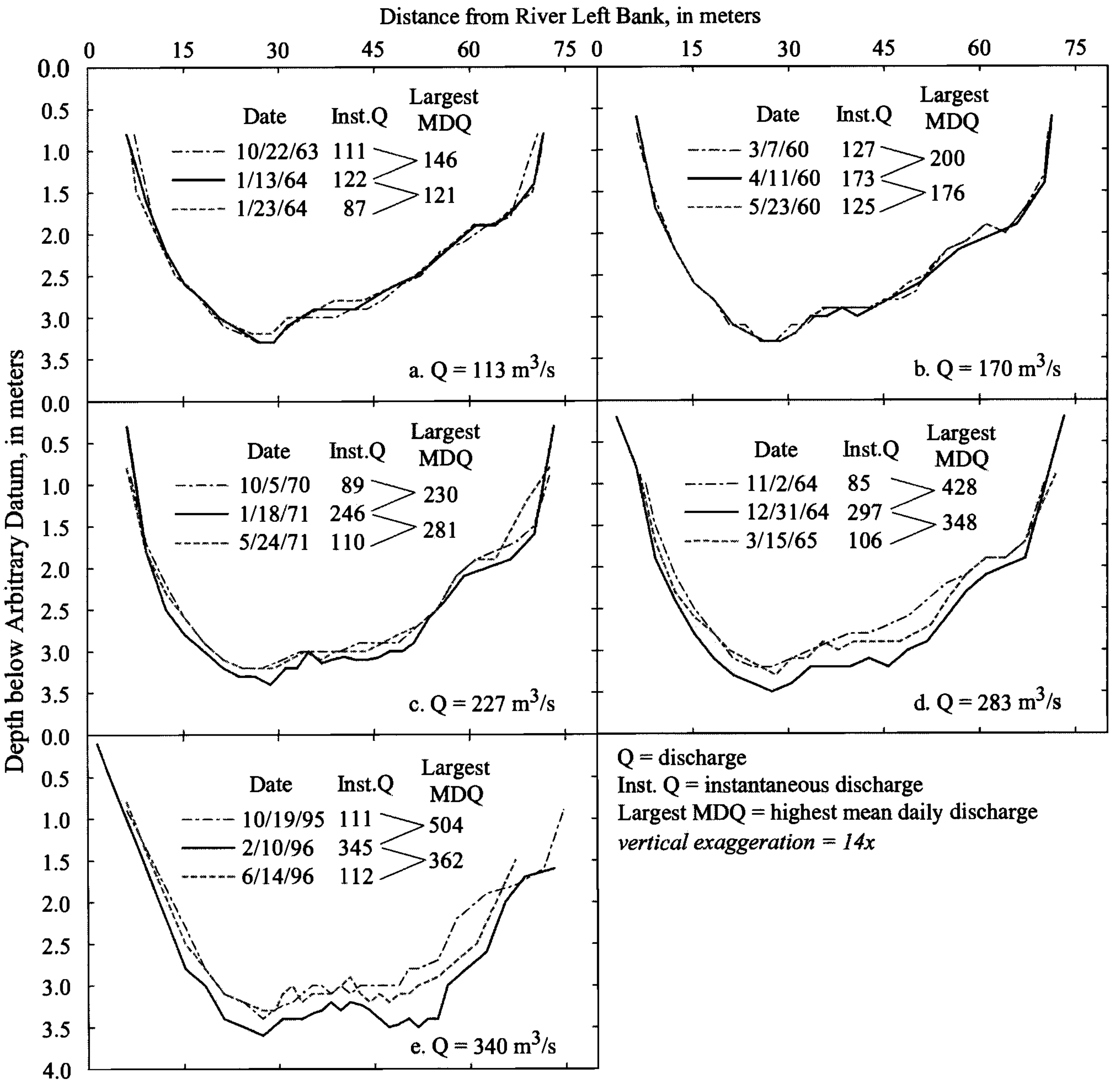

Figure 17. Cross-sectional profiles at the USGS measurement cross-section for the Deschutes River near Madras gage showing degree of bed response for flow events of different sizes.

1,249,000 m^3 of sediment had been captured by Round Butte Dam between 1964 and 1998. This volume is nearly all the sediment of all particle sizes input from the Crooked and Deschutes Rivers to the mainstem lower Deschutes over 34 years. The Metolius River fan was smaller than the detection limits of the survey. Using a sediment density of 2,740 kg/m^3 [*Fassnacht*, 1998], the effective unit sediment supply rate was calculated to be about 11 tonnes/km^2 yr for the 9,740 km^2 drainage basin above Round Butte Dam that directly contributes sediment (J.E. O'Connor, USGS, unpublished data, 1999). This is an extremely low sediment supply rate relative to other rivers (Table 9).

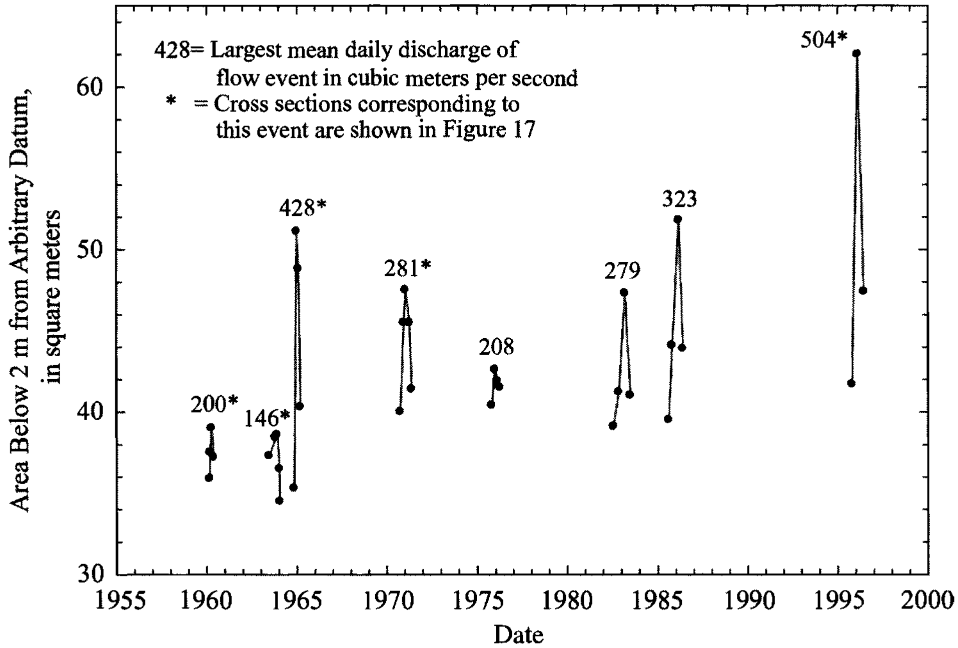

Figure 18. Channel rebound associated with high discharge events, Deschutes River near Madras measurement cross-section 1966-1996.

These recent sediment surveys provide additional support to model predictions of low frequency and magnitude of bedload transport. If sediment supply is low and model predictions were incorrect (that is, if frequency and magnitude of transport were high), we would expect high rates of channel degradation and/or high armoring ratios directly downstream of the Project. Degradation rates just below the Project are about 2.2 mm/year both before *and* after dam closure (Figure 14). This rate of degradation is very low in comparison to those below dams from other selected U.S. rivers (Table 10). Results from the channel-bed textural analysis also did not show any trends in armoring downstream of the Project (Figure 21).

The effects of the flood of February 1996, with the highest recorded peak discharge, provide additional support for interpretations of channel stability. This flood was predicted to have produced transport rates much larger than those from any other recorded event on the Deschutes River. Subsequent field investigations in April, August, and September 1996, indicated that bedload transport did occur during the flood as predicted by the hydraulic and bedload transport modeling. Field evidence of transport included the presence of new gravel and cobble deposits both in-stream and on vegetated islands and floodplains, and the absence of former small islands in the lower river. Although the flood resulted in localized bedload transport and disturbance of vegetation, it did not substantially reorganize channel bars and other surfaces; its most visible effect was the uprooting and breakage of riparian vegetation.

The occurrence of this large flood during the study period allowed us to examine whether the limited geomorphic change in the Deschutes was related to erosion thresholds not being exceeded since Project construction. Coarse-bedded rivers elsewhere have been shown to experience little or no degradation following impoundment because of the general infrequency of mobilizing flows [*Petts*, 1979; *Church*, 1995]. *Petts* [1979] hypothesized that in such "non-mobile channels" a rare large flood, crossing some intrinsic threshold, may be required before channel adjustments will begin. Once that geomorphic threshold has been exceeded, a rapid phase of adjustment might ensue, redistributing channel and floodplain sediments. Critical discharge calculations predicted initiation of bedload transport at a discharge of about 340 m^3/s as measured at the Madras gage. The flood of 1996 had a maximum mean daily flow of about 510 m^3/s at the Madras gage. Despite its slightly less than 100-year return interval [*Hosman et al.*, this volume], the 1996 flood did not appear to be the kind of large resetting flood *Petts* [1979] discussed, as it had little effect on the existing bars and islands. Larger and more infrequent events are apparently

Table 8. Summary of regression results for the Primary Study Reach and lower river. Models shown below table.

Independent variables	Surface D_{50} (mm)		Subsurface D_{50} (mm)		Armoring ratio (mm/mm)	
	Value of β Coefficient	2-sided p-value	Value of β Coefficient	2-sided p-value	Value of β Coefficient	2-sided p-value
Primary Study Reach						
Constant (Low *C. dem.*, 1995)	-34.30	0.68	110.74	0.044[a]	-21.00	0.062
River Kilometer	0.73	0.19	-0.56	0.11	0.16	0.034[a]
YEAR (0 for 1995, 1 for 1996)	6.53	0.32	-6.54	0.14	1.68	0.07
C. demersum: (1 for moderate)	1.54	0.84	n/a[b]	n/a	n/a	n/a
C. demersum: (1 for high)	-28.12	0.0052[a]	n/a	n/a	n/a	n/a
Entire Study Area						
Constant	87.68	<0.0001[a]	30.14	0.0003[a]	2.59	0.07
River Kilometer	-0.13	0.23	-0.08	0.14	0.02	0.14

[a] Statistically significant (<0.05) p-values
[b] n/a = not applicable

Models used:

Primary Study Reach: $|\mu(\text{surface } D_{50})| = \beta_0 + \beta_1(RK) + \beta_2(YEAR) + \beta_3(CD) + \beta_4(CD)$; $|\mu(\text{subsurface } D_{50})| = \beta_0 + \beta_1(RK) + \beta_2(YEAR)$; $|\mu(\text{armor})| = \beta_0 + \beta_1(RK) + \beta_2(YEAR)$

Entire Study Area: $|\mu(\text{surface } D_{50})| = \beta_0 + \beta_1(RK)$; $|\mu(\text{subsurface } D_{50})| = \beta_0 + \beta_1(RK)$; $|\mu(\text{armor})| = \beta_0 + \beta_1(RK)$

where μ = the estimated mean of the grain parameter indicated, RK = River Kilometer, $YEAR$ = year, CD = the level of *C. demersum*, and β values represent coefficients in each regression model (β_0 = y intercept or D_{50} when all other β values equal zero, β_1 = RK, β_2 = 0 for 1995, β_2 = 1 for 1996, β_3 = 1 for moderate levels of *C. demersum*, β_4 = 1 for high levels of *C. demersum*).

responsible for shaping the primary channel features and morphology of the lower Deschutes River.

Channel Features, Vegetation Patterns, and Historical Channel Changes. Channel morphological features and vegetation patterns along the lower Deschutes River and the results of the analysis of historical channel changes all support the interpretation of general channel stability. The river contains very few meander bends and point bars—common features in active alluvial channels. Many of the existing meanders are deeply incised into the lava flows that comprise the steep canyon walls. Tributary fans have built out into the river and constrained the channel. These fans appear to be old, judging from the age of their vegetation and their heavily weathered and desert-varnished boulders, and from the observation that the fans were not substantially modified by the February 1996 flood.

Channel stability is also implied by the scarcity of unvegetated deposits in the river. Islands, tributary fans, and floodplains are covered with grasses, sagebrush (*Artemesia spp.*), willows, sedges, and alders. Alders around 20+ years old can be found lining long stretches of channel banks and along the edges of many islands. These would be unlikely features if the Deschutes were an active alluvial river in which cobble, gravel, and sand deposits were often reworked. Aerial photographs also show stable channel boundaries and island locations [*Curran and O'Connor*, this volume]. Changes that do occur in island and bar morphology following floods tend to be associated with tributary confluences. One of the few islands that is not heavily vegetated is the first island downstream of the Shitike Creek confluence. New gravel was deposited on top and along the sides of this island by the February 1996 flood.

Analyses of historical cross-sections also suggest general channel stability. USGS cross-section measurements for the Madras gage showed extremely limited channel-bed degradation over the period of record (Figures 14, 16, 17). Lateral movement of the channel at the cross-section was minimal (Figures 16, 17). The majority of channel scour noted dur-

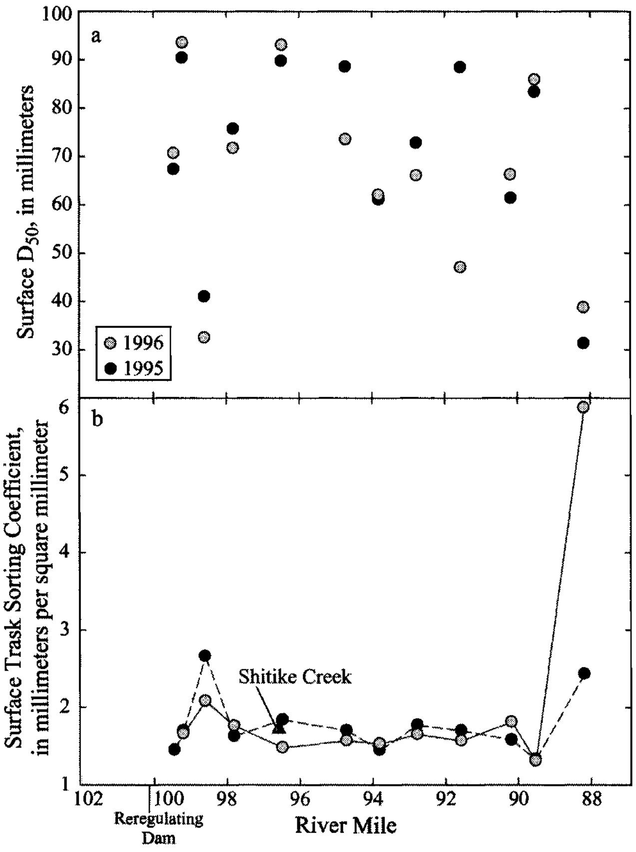

Figure 19. Grain-size data for bar and island heads in the primary study reach in 1995 and 1996: (a) Surface D_{50} values; (b) Trask sorting coefficients for surface bed material.

ing high flow events was refilled in the weeks to months following the event (Figures 17, 18), indicating a state of relative balance between these opposing processes acting on the channel perimeter.

Project Effects on the Geomorphology of the Lower Deschutes River

The results of the bedload transport, channel morphology, and channel-bed texture components of our study provide strong evidence for the intrinsic stability of the Deschutes River system. Within this context of a stable channel environment, we now evaluate the direct effects of the Project on the lower Deschutes River.

Streamflow and Bedload Transport. The low frequency of discharges surpassing the predicted threshold for bedload transport provides a small data set with which to evaluate the downstream effects of the Project on bedload transport frequency and magnitude. Only four transport events were predicted to have occurred during the 30+ years since Round Butte Reservoir was filled. A single high flow event can greatly affect the calculated frequency and magnitude of transport for a given time period (pre- or post-Project). Despite this, our results did not indicate any major natural or anthropogenic changes in the frequency and magnitude of either discharge (Figures 2, 11) or of bedload transport (Figure 12) in the primary study reach following Project construction. Examination of individual events following Project construction did, however, suggest more subtle changes in both discharge and bedload transport at the event scale (Figure 13, Tables 6, 7). Low frequency and magnitude of bedload transport, low sediment supply, and minimal Project-induced effects on streamflow suggest only limited channel degradation, or morphological or textural change, should be expected in the primary study reach following impoundment. Results of the historical cross-section and channel-bed texture analyses support this conclusion (Figures 14-18, 21).

Channel-Bed Texture. No clear longitudinal trend in the surface and subsurface bed-material size distribution emerged in either the primary study reach or entire study area. Data points obtained from the same sites for different years are generally similar to each other; for this reason, finding no longitudinal pattern in surface D_{50} values cannot be attributed to sampling error. Modeling results suggest that downstream distance and year do not significantly influence bed material properties.

The marked uniformity of grain sizes and armoring over the entire course of the river below the dams reflects absence of major changes in channel slope, limited range of grain sizes introduced as bedload by tributaries, and minor hillslope inputs from bedrock canyon walls. No clear differences in grain size were noted upstream and downstream of major tributaries, where changes in longitudinal grain-size distribution patterns due to partially replenished sediment supply might be expected (Figure 24). Several factors account for this longitudinal uniformity: high transport efficiency of fine sediment by the mainstem, opportunities for storage of tributary sediment in alluvial fans at tributary junctions, and similarity of bed-material size ranges between the main channel and tributaries. For example, much of the material transported by the White River during high flow events may be suspended sediment [*U.S. Department of Energy*, 1985], which is easily transported out of the basin by the Deschutes. As a result, the bed of the Deschutes is not noticeably finer downstream of the White River (Figure 24). Coarser bed materials carried by the Warm Springs River are typically deposited within the extensive, coarse fan complex at its confluence with the

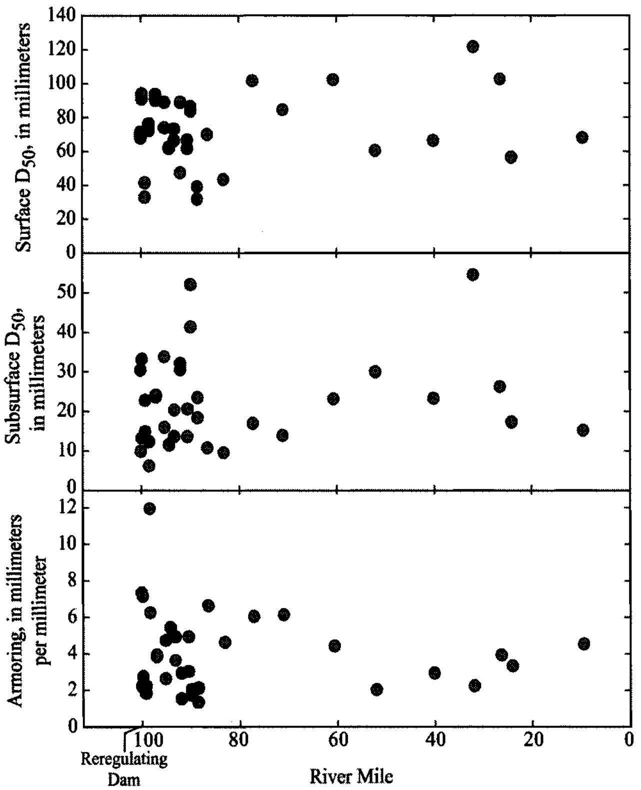

Figure 21. Surface D_{50} values, subsurface D_{50} values, and armoring ratios for bar and island heads along the entire study area in 1996. Note that scales are different for each plot.

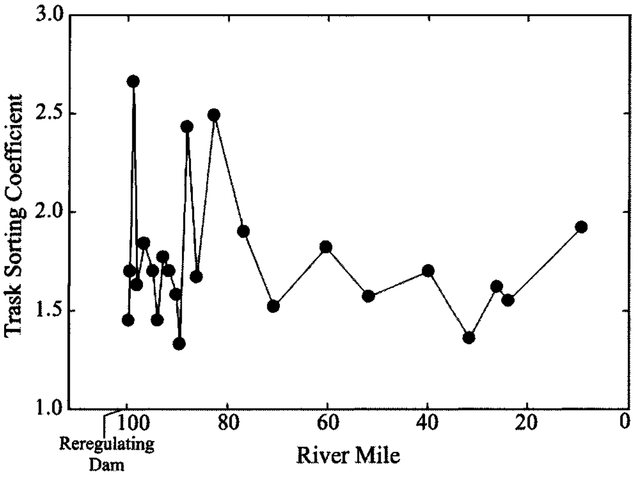

Figure 22. Trask sorting coefficients for surface bed material at bar and island heads along entire study area in 1996.

Deschutes. Sediment derived from the White and Warm Springs Rivers represents material with the largest size deviations from that of the mainstem, but for the most part is not incorporated into mainstem bed material (Figure 24). Some inputs of gravel from Shitike Creek, whose bed material more closely resembles that of the mainstem, appear to be deposited locally within the mainstem, inducing local, minor morphologic changes (for instance, island growth) and textural shifts in the channel bed.

High armoring ratios near the Project (up to 11.9 at RM 98.1) after the 1996 flood appear to have resulted from subsurface fining, as the surface layer did not change significantly between years. This apparent increase in armoring via subsurface fining is contrary to most models of armor development [i.e., *Parker et al.*, 1982; *Dietrich et al.*, 1989]. If sediment supply below the Project were substantially reduced, one would expect selective erosion to cause downstream winnowing of bed material. This would cause the surface grain size to coarsen with time near the Project and for the coarsening front to prograde downstream, particularly during high flow events. Such changes were not observed. Erosion of channel banks and islands by floodwaters may have introduced fine material into the sediment load, although no apparent or adequate source of fine sediment exists in this reach. Fine sediment from sources upstream of Pelton Dam (i.e., Seekseequa Creek; Figure 1) may have contributed fine material to downstream sample sites through turbid water releases from the Project during the February 1996 flood. The flood caused several large headcuts, and substantial erosion and sediment transport out of Seekseequa Creek into the reservoir behind Pelton Dam (C. Gannon, Confederated Tribes of Warm Springs, oral communication, 1999). Consequently, the three high armoring ratios measured near the Project may not be correlated with the Project itself.

Another possible explanation for the apparent fining of subsurface bed material between years is that subsurface sample sizes were smaller than necessary for accurately distinguishing temporal changes. While good precision in the sample mean can be achieved with sample sizes less than those suggested by *DeVries* [1970] and *Church et al.* [1987] for moderately sorted material, the accuracy is much less certain for smaller samples of poorly sorted materials such as fluvial gravel [*Ferguson and Paola,* 1997]. Following the criteria of *Church et al.* [1987], the requisite size of a representative bulk sample of channel-bed subsurface material may be estimated by the largest particles in the surface population, as long as the surface constitutes the same deposit. Using the average surface D_{95} value of 150 mm for sites in the primary study reach, the proposed 0.1% of sample size

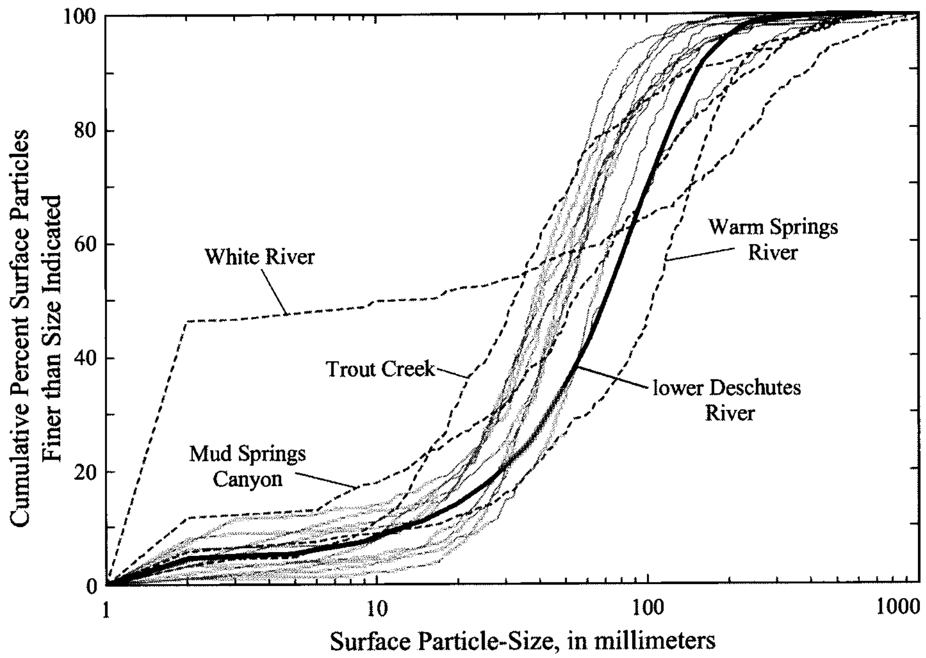

Figure 23. Surface particle distributions of fourteen sampled tributaries of the lower Deschutes River.

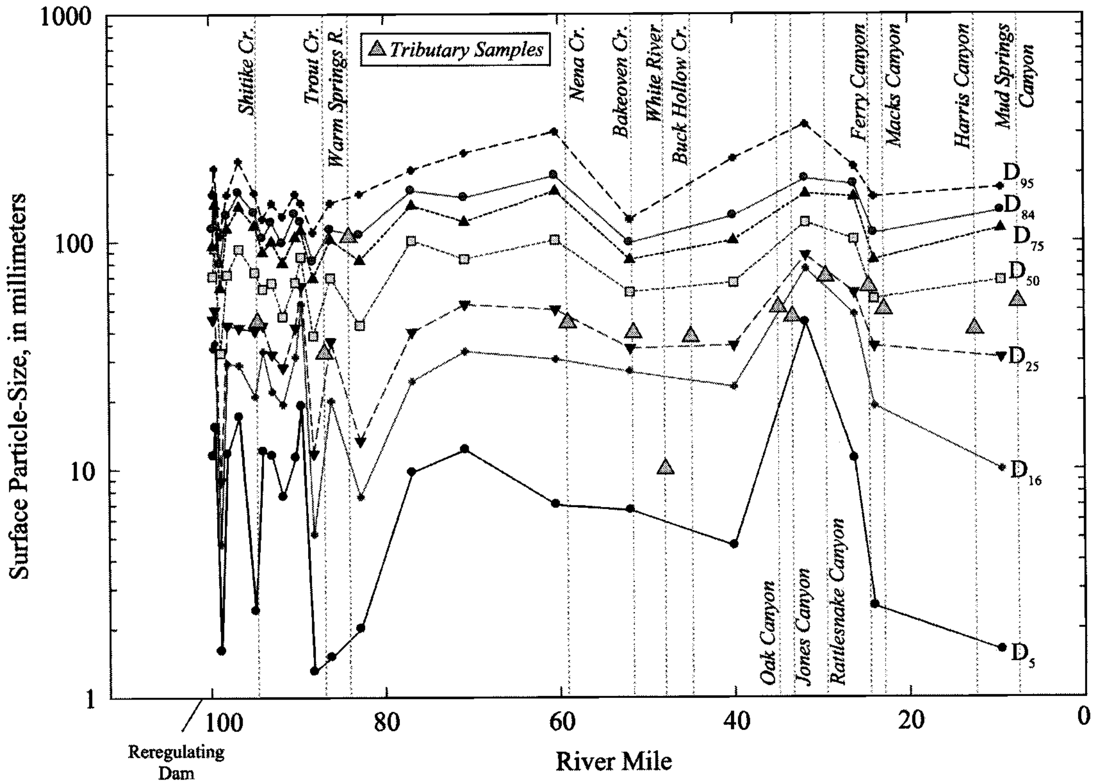

Figure 24. Surface particle percentiles of sample sites over the entire study area in 1996 relative to those of tributary confluences.

Table 9. Sediment discharges for selected North American rivers.

River, Country	Location	Drainage Area (10^6 km^2) *Judson & Ritter* [1964]	*Milliman & Meade* [1983][a]	*This paper*	Sediment Discharge (10^6 t/yr) *Judson & Ritter* [1964]	*Milliman & Meade* [1983][a]	*This paper*	Unit Sediment Discharge (t/km^2/yr) *Judson & Ritter* [1964]	*Milliman & Meade* [1983][ab]	*This paper*
Eel, USA	Scotia, California	0.0081	0.008	...	16	14	...	2048	1750	...
Mad, USA	Arcata, California	0.0013	...	...	2	...	...	1300	...	...
Trinity, USA	Hoopa, California	0.0073	...	...	3	...	...	400	...	...
Snake, USA	Central Ferry, Washington	0.27	...	...	12	...	...	44	...	...
Columbia, USA	Pasco, Washington	0.27	0.67	...	9	8	...	35	12	...
Green, USA	Palmer, Washington	0.0006	...	...	0.06	...	...	108	...	...
Fraser, Canada		...	0.22	...	...	20	...	...	91	...
Yukon, USA		...	0.84	...	...	60	...	...	71	...
Copper, USA		...	0.06	...	...	70	...	...	1167	...
Deschutes, USA	Madras, Oregon	...	...	0.0095	...	...	0.10	...	...	11

[a] Location not provided for these data.
[b] Unit sediment discharge calculated here from data derived from *Milliman and Meade* [1983].

Table 10. Channel-bed degradation rates below dams for selected U.S. rivers[a].

River, Dam, State	Year Dam Closed	Reference Year[b]	Last Year of Data Evaluated	# Dates[c] for which Data Evaluated	Cross-section Distance from Dam (km)	Total Change in Mean Bed Elevation: Range for Years Evaluated (m)	Mean (m)	Standard Deviation (m)	Average Rate of Channel Elevation Change (mm/yr)
Arkansas, John Martin, Colorado	1942	1943	1972	3	3.5	-0.10 to –1.95	-0.82	0.99	-27
Missouri, Fort Peck, Montana	1937	1936	1973	7	9.2	-0.65 to –0.90	-0.74	0.09	-20
Medicine Cr., Medicine Creek, Nebraska	1949	1950	1977	5	0.8	-0.10 to –0.20	-0.18	0.04	-6.4
Smoky Hill, Kanopolis, Kansas	1948	1946	1971	4	0.8	-0.80 to –1.45	-1.16	0.28	-51
Middle Loup, Milburn, Nebraska	1955	1950	1971	13	0.2	-0.60 to –2.65	-1.88	0.58	-115
North Canadian, Canton, Oklahoma	1948	1947	1976	6	1.8	-0.90 to –3.00	-2.05	0.94	-73
Red, Denison, Oklahoma-Texas	1942	1942	1969	4	0.6	-1.25 to –1.60	-1.41	0.15	-52
Deschutes, Pelton-Round Butte, Oregon	1956[d]	1957	1998	211	0.1	0.12 to –0.33	-0.06	0.06	-1.4
channel thalweg only						*0.15 to –0.39*	-0.09	*0.08*	*-2.2*

[a] Data used in calculations obtained from Table 13, *Williams and Wolman* [1984], except data presented for the Deschutes River.
[b] For this year, total change of channel bed is shown as 0 m, and therefore, acts as a reference point for later measurements.
[c] Not including reference year.
[d] Round Butte Dam closed 1962, see Table 2, this paper.

for the largest clast would then require a sample weighing about 5,000 kg per site. Even using a relaxed criterion of 5% would still require 100 kg of bed material. Because of the potential error resulting from sample size, there is no clear evidence for subsurface fining, and consequently an increase in armoring, between years. The substantial labor involved in transporting such large sediment samples from a wilderness river and laboratory time required to process such samples is daunting. A precise description of grain-size distributions of bulk samples remains a difficult problem in studies of gravel-bedded rivers.

Geomorphic Implications of Channel Stability

Within the context of downstream response of a channel to river regulation, there are at least two implications of a stable river. First, a stable river might be able to withstand a relatively wide range of changes in flow with little effect on channel morphology and bed texture because the channel bed, for the most part, remains immobile. This may represent the current situation for the lower Deschutes River, where most changes in streamflow occur at discharges that are less than critical (Figure 13). Even relatively large flows, such as those that occurred in February 1996, are unable to rework the channel substantially, perhaps because of the very low volume of sediment available for transport.

The second implication is that the imprint and consequences of whatever changes *do* occur in the channel may persist for a very long time. For example, if reservoir operations further reduced the already infrequent occurrence of flows near the threshold for bed material transport, textural changes such as increased compaction, cementation, or cohesion of bed materials could result, further reducing bed mobility. Here, not having a disturbance event can be a disturbance event itself [*Junk et al.*, 1989]. On the other hand, changes to the channel morphology induced by surpassing high geomorphic thresholds, such as appears to have occurred during rare and exceptionally large paleofloods, could persist for geologically long periods of time until the next high magnitude disturbance event. Field evidence suggests that, during the Pleistocene and Holocene, mechanisms existed for generating floods much larger than anything recorded over the last seventy-plus years [*Beebee and O'Connor*, this volume; *O'Connor et al.*, this volume]. These mechanisms included outburst floods from large landslide dams, debris flows, and glacially dammed lakes [*O'Connor et al.*, this volume]. The legacy of these floods persists in the major rapids and slope profile breaks at Whitehorse, Buckskin Mary, and Boxcar (Figure 8) [*O'Connor et al.*, this volume], all of which were only slightly modified by the 1996 flood.

It was hypothesized that historically low sediment supply to and transport rates in the Deschutes River would limit textural and morphologic adjustments of the lower river following impoundment. Our results strongly support an inference of low rates of sediment supply and bedload transport. They also confirm very limited textural and morphologic change. The minor hydrological changes noted in the flow record since regulation suggest little change in the frequency of bed-mobilizing flows, and the results of the historical cross-section analysis show no change in the trend of minor channel-bed degradation that preceded Project construction. In other words, both the ratio of post- to pre-Project frequency of mobilizing flows and the ratio of post- to pre-Project sediment supply may be close to 1. In this case, morphologic and textural response downstream from the Project should, for the most part, be small. While it is possible that the morphological manifestations of a reduced sediment supply (i.e., degradation and coarsening of the channel bed) due to gravel being trapped behind the Project have not had a chance to occur, very modest change over the thirty-plus year Project history, which includes some major storms, argues against dramatic changes in the near future.

CONCLUSIONS

Independent analyses of hydraulics and bedload transport, historical streamflow, morphologic change, and channel-bed texture together present a convincing argument that the Pelton-Round Butte Hydroelectric Project has done little to alter the lower Deschutes River's naturally low frequency and magnitude of bedload transport. In a system with low sediment supply, this has resulted in little apparent morphologic or textural response downstream of the Project. The river downstream of the Project appears to be astonishingly stable within its current flow regime and sediment supply, with the low rates of sediment transport keeping pace with the modest inputs of sediment. In a larger context, this study suggests that armoring, degradation, and morphologic change below dams may be limited where sediment transport rates and sediment supply are low.

Many studies of other rivers document armoring and degradation of the channel bed due to reduced sediment supply where flows are still competent to move a large portion of the bed material. In contrast, the Deschutes River represents a unique hydrologic and sedimentologic environment where sediment supply and transport may be limited within time scales defined by the historical flow record.

Acknowledgements. The authors gratefully acknowledge the many people who aided in logistics, field work, and/or field data collection, including Don Ratliff (PGE), Chris Zimmerman (Oregon State University), Scott McCollister (PGE), Eric Schulz (PGE), Tom Herrett (USGS), Tony Sorano (USGS), PGE surveyors Bob Buckley, Jim Tejcka, Gary Reynolds, Larry McGinnis, and Jeff Danielson, and PGE support personnel. A special thanks to the Confederated Tribes of Warm Springs, Jan Luelling, the Deschutes Club, Buck Coe, and Kenny Buck, Sr., who allowed access to the river via private property. Larry Chitwood (Deschutes National Forest) graciously offered use of field equipment as well as laboratory equipment for processing subsurface samples. This work benefited greatly from discussions with Jim O'Connor (USGS), Julia Jones (OSU), and Bob Beschta (OSU). Lisa Ganio and Barbara Marks assisted in the statistical data analysis. Diana Surgeon (North Unit Irrigation District), Larry Zakrajsek (U.S. Bureau of Reclamation), and Scott Lewis (PGE) provided historical information on dams in the Deschutes River basin. Roy Wellman (USGS) and Tom Herrett were of great help in processing ADCP data. Local offices of the Bureau of Land Management and the Oregon Department of Fish and Wildlife served as excellent resources for information and assisted with accessing some study sites.

This material is based upon work supported under a National Science Foundation Graduate Research Fellowship to Heidi Fassnacht, and by funding provided by Portland General Electric to both Heidi Fassnacht and Ellen McClure. Any opinions, findings, conclusions, or recommendations expressed in this publication are those of the authors and do not necessarily reflect the views of the National Science Foundation or Portland General Electric.

REFERENCES

Andrews, E. D., and J. M. Nankervis, Effective discharge and the design of channel-maintenance flows for gravel-bed rivers, *Natural and Anthropogenic Influences in Fluvial Geomorphology, AGU Mon., 89*, 151-164, 1995.

Aney, W. W., M. L. Montgomery, and A. B. Lichens, Lower Deschutes River, Oregon: Discharge and the fish environment, *Lower Deschutes Flow Study Final Report*, Oregon State Game Commission, Portland, Oregon, 1967.

Appel, E. P., Oregon Fishing Map: Lower Deschutes River, Frank Amato Publications, Portland, Oregon, 1986.

Chien, N., Changes in river regimes after the construction of upstream reservoirs, *Earth Surf. Proc. Landf., 10*, 143-159, 1985.

Church, M., Geomorphic response to river flow regulation: Case studies and time-scales, *Regulated Rivers: Research and Management, 11*, 3-22, 1995.

Church, M. A., D. G. McLean, and J. F. Wolcott, River bed gravels: Sampling and analysis, in *Sediment Transport in Gravel-bed Rivers*, edited by C. R. Thorne, J. C. Bathurst, and R. D. Hey, John Wiley and Sons Ltd., New York, 43-88, 1987.

Collier, M., R. H. Webb, and J. C. Schmidt, Dams and rivers: Primer on the downstream effects of dams, *U.S. Geol. Surv. Circ. 1126*, 94 pp., 1996.

DeVries, M., On the accuracy of bed-material sampling, *J. Hydraul. Res., 8*, 523-533, 1970.

Dietrich, W. E., J. W. Kirchner, H. Ikeda, and F. Iseya, Sediment supply and the development of the coarse surface layer in gravel-bedded rivers, *Nature, 340*, 215-217, 1989.

Fassnacht, H., Frequency and magnitude of bedload transport downstream of the Pelton-Round Butte Dam Complex, lower Deschutes River, Oregon, M. S. thesis, Oregon State University, Corvallis, Oregon, 1998.

Ferguson, R. I., and C. Paola, Bias and precision of percentiles of bulk grain size distributions, *Earth Surf. Proc. Landf., 22*, 1061-1077, 1997.

Galay, V. J., R. S. Pentland, and R. A. Halliday, Degradation of the South Saskatchewan River below Gardiner Dam, *Can. J. Civ. Eng., 12*, 849-862, 1985.

Gannett, M. W., D. S. Morgan, and K. E. Lite, Groundwater/surface water interactions in the upper Deschutes basin, central Oregon, abstract, *EOS Trans. AGU, 77*(46), F265, 1996.

Gilvear, D. J., and S. J. Winterbottom, Channel change and flood events since 1783 on the regulated River Tay, Scotland: Implications for flood hazard management, *Regulated Rivers: Research and Management*, 7(3), 247-260, 1992.

Haslam, S. M., *River Plants of Western Europe: The Macrophytic Vegetation of Watercourses of the European Economic Community*, Cambridge University Press, Cambridge, U.K., 512 pp, 1987.

Hubbard, L. E., T. A. Herrett, J. E. Poole, G. P. Ruppert, and M. L. Courts, Water Resources Data, Oregon, Water Year 1996, *U.S. Geol. Surv. Water Data Rep. OR-96-1*, U.S. Geological Survey Water Resources Division, Portland, Oregon, 432 pp., 1997.

Huntington, C. W., *Deschutes River Spawning Gravel Study, Volume I, Final Report*, prepared for U.S. Department of Energy Bonneville Power Administration Division of Fish and Wildlife, Portland, Oregon, 179 pp., 1985.

Johnson, D. M., *Atlas of Oregon Lakes*, Oregon State University Press, Corvallis, Oregon, 317 pp., 1985.

Judson, S., and D. F. Ritter, Rates of regional denudation in the United States, *J. Geophys. Res., 69*, 3395-3401, 1964.

Junk, W. J., P. B. Bayley, and R. E. Sparks, The flood pulse concept in river-floodplain systems, in *Proceedings of the International Large River Symposium*, edited by D. P. Dodge, *Can. Spec. Publ. Fish. Aquat. Sci., 106*, 110-127, 1989.

Kondolf, G. M., Application of the pebble count: Notes on purpose, method, and variants, *J. Amer. Water Resour. Assoc., 33*, 79-87, 1997.

Krumbein, W. C., and F. J. Pettijohn, *Manual of Sedimentary Petrography*, Appleton-Century Company, New York, 549 pp., 1938.

Manga, M., Hydrology of spring-dominated streams in the Oregon Cascades, *Water Resour. Res., 32*, 2435-2439, 1996.

McClure, E. M., Spatial and temporal trends in bed material and channel morphology below a hydroelectric dam complex, Deschutes River, Oregon, M.S. thesis, Oregon State University, Corvallis, Oregon, 1998.

Meyer-Peter, E., and R. Mueller, Formulas for bed-load transport, in *Proceedings of the 2nd Meeting of the International Association for Hydraulic Structures Research*, 39-64, International Association for Hydraulic Research, Stockholm, 1948.

Milliman, J. D., and R. H. Meade, World-wide delivery of river sediment to oceans, *J. Geology*, *91*(1), 1-21, 1983.

Nehlsen, W., *Historical Salmon and Steelhead Runs of the Upper Deschutes River and Their Environments*, Portland General Electric, Portland, Oregon, 78 pp., 1995.

Parker, G., Surface-based bedload transport relation for gravel rivers, *J. Hydraul. Res.*, *28*(4), 417-436, 1990.

Parker, G., P. C. Klingeman, and D. G. McLean, Bedload and size distribution in paved gravel-bed streams, in *Proc. Amer. Soc. Civ. Eng. J. Hydraul. Div.*, *108*(HY4), 544-571, 1982.

Petts, G. E., Complex response of river channel morphology subsequent to reservoir construction, *Prog. Phys. Geog.*, *3*(3), 329-362, 1979.

Petts, G. E., Long-term consequences of upstream impoundment, *Environ. Conserv.*, *7*(4), 325-332, 1980.

RD Instruments, *Acoustic Doppler Current Profiler Principles of Operation, A Practical Primer, 2nd Edition for Broadband ADCPs*, RD Instruments, San Diego, California, 52 pp., 1996.

Rice, S. and M. Church, Sampling surficial fluvial gravels: the precision of size distribution percentile estimates, *J. Sediment Res.*, *66*, 654-665, 1996.

Shields, I. A., Anwendung der Aehnlichkeitsmechanik und der Turbulenzforschung auf die Geschiebebewegung, *Mitteilunguen der Preussischen Versuchsanstalt für Wasserbau und Schiffbau*, translated by W. P. Ott and J. C. van Uchelen, U.S. Dept. of Agriculture Soil Conservation Service Cooperative Lab, California Institute of Technology, Pasadena, California, 36 pp., 1936.

Smelser, M. G., and J. C. Schmidt, An assessment methodology for determining historical changes in mountain streams, *U.S. For. Serv. Rocky Mt. For. Range Exp. Stn., Gen. Tech. Rep. RMRS-GTR-6*, 29 pp., 1998.

U.S. Army Corps of Engineers Hydrologic Engineering Center, HEC-RAS River Analysis System, Hydraulic Reference Manual Version 1.0, U.S. Army Corps of Engineers Hydrologic Engineering Center, California, 131 pp., 1995a.

U.S. Army Corps of Engineers Hydrologic Engineering Center, HEC-RAS River Analysis System, User' s Manual Version 1.0, U.S. Army Corps of Engineers Hydrologic Engineering Center, Davis, California, 150 pp., 1995b.

U.S. Department of Energy, *White River Falls Fish Passage Project, Tygh Valley, Oregon*, Bonneville Power Administration, Division of Fish and Wildlife Final Tech. Rep., Vol. I of III, p. 24, 1985.

U.S. Department of the Interior, Bureau of Reclamation, Reclamation Project Data (supplement), Crooked River project, U.S. Government Printing Office, Washington, D.C., 275 pp., 1966.

U.S. Department of the Interior, U.S. Geological Survey, Water Resources Division, Water Resources Data for Oregon 1965 Part I: Surface Water Records, U.S. Geological Survey Water Resources Division, Portland, Oregon, 359 pp., 1965.

U.S. Department of the Interior, U.S. Geological Survey, Water Resources Division, Description of gaging station 14-0925.00 Deschutes River near Madras, Oregon, 3 pp., 1994.

U.S. Department of the Interior, Water and Power Resources Service, Water and Power Resources Service - Project Data, Deschutes River project, U.S. Government Printing Office, 1463 pp., Denver, Colorado, 1981.

Williams, G. P., and M. G. Wolman, Downstream effects of dams on alluvial rivers, *U.S. Geol. Surv. Prof. Pap. 1286*, 83 pp., 1984.

Wolman, M. G., A method of sampling coarse river bed material, *Trans. Amer. Geophys. Union*, *35*(6), 951-956, 1954.

Heidi Fassnacht, c/o J. E. O'Connor, U.S. Geological Survey, 10615 SE Cherry Blossom Drive, Portland, Oregon, 97216

Gordon E. Grant, U.S. Dept. of Agriculture, Pacific Northwest Research Station, Forestry Sciences Laboratory, 3200 SW Jefferson Way, Corvallis, Oregon, 97331

Peter C. Klingeman, Oregon State University, Dept. of Civil, Construction, and Environmental Engineering, 202 Apperson Hall, Corvallis, Oregon, 97331

Ellen M. McClure, Biohabitats Incorporated, 15 West Aylesbury Road, Timonium, Maryland, 21093

A Geological Framework for Interpreting Downstream Effects of Dams on Rivers

Gordon E. Grant

U.S. Forest Service, Corvallis, Oregon

John C. Schmidt

Department of Aquatic, Watershed, and Earth Resources, Utah State University, Logan, Utah

Sarah L. Lewis

Department of Geosciences, Oregon State University, Corvallis, Oregon

Despite decades of research and numerous case studies on downstream effects of dams on rivers, we have few general models predicting how any particular river is likely to adjust following impoundment. Here we present a conceptual and analytical framework for predicting geomorphic response of rivers to dams, emphasizing the role of geologic setting and history as first-order controls on the trajectory of change. Basin geology influences watershed and channel processes through a hierarchical set of linkages, extending from the drainage basin to the valley and channel, which determine the sediment transport and discharge regimes. Geology also directly shapes the suite of hillslope processes, landforms, and geomorphic disturbances impinging on the channel and valley floor. These factors, in turn, affect the "lability" or capacity for adjustment of the downstream channel, determining the type, direction, and extent of channel adjustments that occur, including incision, widening, and textural changes. We develop an analytical framework based on two dimensionless variables that predicts geomorphic responses to dams depending on the ratio of sediment supply below to that above the dam (S^*) and the fractional change in frequency of sediment-transporting flows (T^*). Drawing on examples from the Green, Colorado, and Deschutes Rivers, we explore how trajectories of geomorphic change, as defined by these two variables, are influenced by the geological setting and history of the river. This approach holds promise for predicting the magnitude and trend of downstream response of other impounded rivers, and can identify river systems where geological controls are likely to dominate.

INTRODUCTION

Because dams influence the two primary factors—water and sediment—that determine the shape, size, and overall morphology of a river, they represent fundamental interventions in the fluvial system. Decades of research on effects of dams on rivers have yielded numerous case studies of down-

A Peculiar River
Water Science and Application 7

10.1029/007WS13

stream response to impoundment, but there are few general models that predict how any particular river is likely to respond once a dam is in place. Geomorphic theory and previous studies provide some basis for predicting general trends, but case studies are distinguished as much by variation as consistency in response [*Williams and Wolman*, 1984].

Dams alter two critical elements of the geomorphic system: the ability of the river to transport sediment and the amount of sediment available for transport. If the transport capacity exceeds the available supply, a sediment deficit exists and the channel can be expected to evacuate sediment from its bed and/or banks. If the transport capacity is less than the available sediment supply, then the channel can be expected to accumulate sediment. There are many adjustable attributes of a channel—its cross-section, bed material, planform, and gradient—and the response of a channel to sediment deficit or surplus varies. [*Petts*, 1980, 1982; *Willams and Wolman*, 1984; *Carling*, 1988; *Brandt*, 2000]. Typical downstream responses can include channel bed aggradation or incision, textural changes such as coarsening or fining of surface grain-size distributions, and lateral adjustments, including both expansion and contraction of channel width.

Grams and Schmidt [2002] showed that the magnitude and style of adjustment varies with geomorphic organization of the fluvial system, even where the magnitude of the sediment budget does not change. Although planform or textural changes can occur, there are also instances where dams have little or no effect on channel morphology [*Williams and Wolman*, 1984; *Inbar*, 1990; *Fassnacht et al.*, this volume]. In such cases, it is often possible to identify *post facto* why the dam had little effect, such as little change in the frequency and magnitude of geomorphically effective flows, presence of bedrock or other resistant channel boundaries, or intrinsically low sediment transport rates.

But despite both theory and ample case studies, there are few means of predicting in advance of construction or investigation which dams will result in small versus large adjustments downstream. Such general predictive models or frameworks are essential as core components of environmental analyses accompanying either new dam construction or assessments of existing dams. The need for such predictions of dam effects is growing as new dams are constructed, particularly in developing countries. During the 1990s, an estimated $32-46 billion was spent annually on large dams, four-fifths of it in developing countries [*World Commission on Dams*, 2000]. In these locales, data and technical resources are limited, prompting the need for general assessment tools and methods. Although virtually no new dams are presently being constructed in the U.S., ongoing relicensing of non-Federal hydropower dams by the Federal Energy Regulatory Commission, reconsideration of operating strategies for Federal dams such as those on the Missouri River [*National Research Council*, 2002], and growing scientific and public interest in dam removal [*Heinz Center*, 2002] are all focusing attention on dams and their downstream effects.

Existing approaches for assessing impacts of dams have almost exclusively emphasized empirical relationships relating pre- to post-dam hydrology to predict response, which is usually defined in terms of some change in channel cross-sectional geometry, grain size, or sediment storage. In their classic paper, *Williams and Wolman* [1984] describe general empirical trends in timing and magnitude of downstream channel adjustments, particularly bed degradation and channel narrowing following dam construction, but variability in downstream response is high, and the authors note many exogenous factors, such as vegetation or bedrock, that can affect these trends. *Brandt* [2000] proposed a classification scheme for distinguishing geomorphic effects downstream of dams based loosely on *Lane's* [1955] conceptualization of the balance between grain size, sediment load, discharge, and channel slope. Though rooted in established principles, this approach relies on determining sediment transport capacity and influx, quantities that may vary spatially in relation to tributary influences and external controls.

Lacking in these approaches, however, is almost any reference to the geological setting of dams and dam-affected reaches as a factor controlling channel response. Motivated by studies of dams in the Deschutes River basin in Oregon [*Fassnacht et al.*, this volume], in this paper we explore the relation between the downstream response of rivers to dams, the overall geologic setting of the watershed, and the specific locations of dams within that watershed. We begin with a framework for interpreting how geology affects both the hydrologic and sediment transport regimes of basins in ways that influence channel morphology downstream from dams, and present a simple model derived from this framework that may be useful for predicting specific directions and magnitudes of downstream effects. Finally, we illustrate these points, drawing on examples from several dammed western rivers, and consider how this framework can be used in a predictive capacity.

A GEOLOGIC FRAMEWORK FOR INTERPRETING GEOMORPHIC EFFECTS OF DAMS

As a means of exploring how geology affects channel response to dams, we begin by examining the role of geology in influencing channels at a range of scales, independent

All of these features result directly from geotechnical properties of the surrounding rock. In the case of large earthflows, landslides, and debris flows, such properties can include the proportion of clay, shear strength, and water-holding capacity and permeability of the regolith and weathered material. Crystalline, highly dense, or cemented rocks, on the other hand, give rise to resistant outcrops. The geotechnical properties of the rock can thus be directly related to the morphology and character of the river canyon [*O'Connor et al.*, this volume].

Geology also controls valley floor and channel features through a second, related mechanism: the specific history of geologically-mediated disturbances of the river bottom. These can include mass movements and debris flows as above, but may also involve more exotic events such as volcanic lahars, lava flows, and glacial-outburst floods. Whether or not a particular river is subject to these events is defined primarily by its geographic setting in relation to volcanoes or glaciers where such events commonly initiate. The Deschutes River in central Oregon, for example, drains the eastern margin of an active volcanic arc located in a northern latitude temperate zone. Because of this, the river canyon has received floods from a wide variety of geological mechanisms, including lahars, glacial outbursts, and landslide dam outbreaks, as well as meteorologically-driven events [*O'Connor et al.*, this volume]. These disturbances are, in turn, recorded in the stratigraphy and distribution of valley bottom features, including floodplains, terraces, flood bars, etc., that both define the current channel morphology, and constrain the channel's lateral and vertical adjustments and movement [*Curran and O'Connor*, this volume].

By this view, geology is an underlying control on both the hydrologic and sediment-transport regimes of a channel as well as the form of the channel itself and, to some degree, the extent to which it can adjust its boundaries. How do dams figure into this framework? We propose that dams both modify the underlying geologically-controlled transport regimes and introduce new processes into the channel system—in essence acting in the latter case as a type of geological disturbance. The consequence is that rivers downstream of dams are responding not only to the "native" discharge and sediment transport regimes but to those introduced by dams as well. A direct corollary of this is that downstream effects of dams on rivers can be scaled by the degree to which the dams change the pre-dam flow and transport regimes. This is not a new concept; most analyses of geomorphic effects of dams have recognized that the effect of any given dam is in some way related to the degree to which it alters the hydrograph and flux of sediment through the system [*Petts*, 1980, 1982; *Willams and Wolman*, 1984; *Carling*, 1988; *Brandt*, 2000]. But we maintain that understanding the geomorphic effect of any given dam requires that the specific changes in hydrology and sediment flux caused by the dam be placed within a larger geological framework which includes broader-scale controls on the source and volume of water and sediment both upstream and downstream of a dam, and the geologically-mediated disturbance regime and history. In short, the downstream effects of a dam cannot be analyzed solely by looking at the dam effects independent of its broader geological setting (Figure 1).

Consider, for example, how the large-scale organization of watersheds and the distribution of runoff- and sediment-producing areas influence the effects of dams in the Colorado River and Rio Grande River basins. In these basins, streamflow arises in the Rocky Mountains at the exterior boundaries of the watershed and sediment is delivered to the mainstem by lower elevation tributaries that drain deserts [*Iorns et al.*, 1965; *Schmidt et al.*, in press]. Thus, streamflow does not significantly increase in the downstream direction despite a downstream increase in sediment delivery to the channel. Dams located in the headwaters of these watersheds control streamflow but not sediment delivery. Further downstream, dams such as Glen Canyon and Hoover Dams on the Colorado and Elephant Butte Dam on the Rio Grande control most of the sediment, as well as water flux. So dams in the headwaters can be expected to have a different range of impacts than those located further downstream, as illustrated below in the contrasting cases of Flaming Gorge and Glen Canyon Dams.

To expand on this, the geological framework greatly influences several key factors determining what we call the "lability" of the downstream channel—its capacity for adjustment. Specifically, the lability of the channel is a function of: 1) the transportability of the bed sediment, which is indexed by its grain size relative to the shear stresses exerted by the flow across the full spectrum of the discharge regime; 2) the erodibility of the bed and banks, as influenced by their cohesiveness and/or the prevalence of bedrock; and 3) the opportunity for lateral mobility, within the limits of the overall width and topography of the valley floor. Taken together, these factors determine where and to what extent channel adjustments below dams (such as incision, widening, and textural changes) can occur, and, as discussed above, all are at least partially under geological control. The grain-size distribution of sediment, for example, reflects both the balance of forces between the flow regime and the sediment supplied from upstream and locally, and the geologically mediated disturbance history. A history of large landslide dam collapse floods, as observed in rivers such as the Deschutes

[*O'Connor et al.*, this volume] and the Middle Fork Salmon [*Meyer and Leidecker*, 1999] can leave coarse bouldery lag deposits along and within the channel that are outside the range of competence of the modern discharge regime. These deposits effectively "freeze" the channel position by constraining both the lateral and vertical movement of the channel. Under these circumstances, dam-imposed changes on either the sediment flux or flow regime are likely to have only minor effects on channel position (although other types of effects are still possible).

Geology may also control sediment sources within a watershed that influence downstream channel changes. On the Trinity River in Northern California, influx of fine-grained sediments derived from a weathered granitic terrain just below the Lewiston Dam results in deposition of sand on the bed of the channel. Prior to reservoir regulation, this sand would have been transported rapidly downstream during high peak flows; post-regulation it is widely stored as patches and deposits within the gravel channel bed, where it affects sediment transport rates and aquatic habitat [*Pitlick and Wilcock*, 2001]. These downstream effects are influenced by, but cannot be uniquely attributed to, flow regime modification at the dam itself, and require a broader view of the dam's location relative to downstream versus upstream sediment sources.

To summarize, *hydrogeomorphic changes*—changes in discharge and sediment-transport regimes—induced by dams and their operation are only part of the equation for predicting downstream impacts. The geological setting of dams within the watershed also contributes, both in the sense that the geology strongly influences the distribution of water and sediment sources within the watershed, and because potential adjustments of the downstream channel are strongly influenced by the geologically-mediated disturbance history (Figure 1).

COMBINING HYDROGEOMORPHIC AND GEOLOGIC CONTROLS TO PREDICT DOWNSTREAM IMPACTS OF DAMS

Given the complexities of factors contributing to channel adjustments downstream of dams, rigorous predictions of dam-related geomorphic impacts have proven difficult [*Brandt*, 2000]. Here we suggest a simple conceptual model of downstream channel changes due to dams in response to both hydrogeomorphic changes and geological controls. We begin by considering dam effects on flow and sediment supply alone. To interpret dam effects, each hydrogeomorphic variable must be scaled by how operation of a dam has influenced it. Although dams can affect the entire flow frequency distribution, a downstream geomorphic response is most likely where the geomorphically effective flow regime [*sensu Costa and O'Connor*, 1995; *Andrews and Nankervis*, 1995] has been altered—that is, a change in the frequency and magnitude of flows that are capable of mobilizing and transporting sediment. Change in these flows can be usefully indexed as the fraction of time T that flows (Q) are greater than the critical flow (Q_{cr}) for sediment transport, expressed as:

$$T = \frac{\sum t_{(Q \geq Q_{cr})}}{\sum t_Q} \tag{1}$$

where t_Q refers to time at flow Q. Changes in the frequency of critical flows can then be compared as the dimensionless ratio (T^*) between the pre-dam (T_{pre}) and post-dam (T_{post}) frequency of sediment-transporting flows:

$$T^* = \frac{T_{post}}{T_{pre}} \tag{2}$$

In general $T^* \leq 1$, since $T_{pre} \geq T_{post}$, both because dams typically suppress peak flows and because coarsening and armoring of bed sediment below dams increases Q_{cr}. Dams that increase daily flows on rivers where sediment transport occurs frequently (as with sand or finer transport regimes) can have $T^* > 1$, as in the Green River example discussed below. Actual calculation of T^* can be difficult, since sediment moves over a range of discharges as a function of the grain-size distribution, and the grain size distribution below a dam may change with time in response to textural adjustments. Although partial sediment transport rates have been calculated for some rivers below dams [e.g., *Andrews*, 1986; *Wilcock et al.*, 1996], the usual practice is to index transport to a specific grain size (D_{50} or similar) and then calculate the frequency of transporting events based on empirical or theoretical sediment transport equations [e.g., *Fassnacht et al.*, this volume].

The question of which grain size T^* should be indexed to relates directly to the specific resource issue under consideration, as discussed below. For example, this grain size will vary depending on whether a dam is being evaluated for its impacts on spawning gravels for fish as opposed to sand beaches for recreationists.

Turning to the effect of dams on sediment supply, most large dams trap virtually all of the sediment delivered from upstream into the reservoir, although trap efficiencies for smaller dams can range from 10-90% or higher [*Brune*,

EXAMPLES OF DOWNSTREAM RESPONSE TO DAMS: THE ROLE OF GEOLOGY

For reasons discussed earlier, precise values of T* and S* can be difficult to obtain. It is possible, however, to use existing literature and inference to plot approximate trajectories of individual dams and rivers in T* and S* space. For example, critical discharges (Q_{cr}) for many gravel-bed channels are at or slightly less than bankfull stage, flows that typically occur several times each year [*Andrews*, 1980, 1983, 1984, 2000], while sand-bed rivers typically have critical discharges that occur much more frequently [*Bennett*, 1995]. Most sand- and gravel-bed rivers for which flow has been significantly regulated would therefore plot towards the right-hand side of Figure 3. Assuming that reservoir trap efficiencies are high, the plotting position on the y-axis will vary in relation to downstream sediment supply. As discussed above, sediment input can change with distance downstream as successive tributaries enter the channel, so that S* typically increases downstream.

By our analysis, interpreting the downstream effects of dams will strongly depend on the downstream trajectories of both T* and S*. In fact, we propose that the slope of the trajectory of change in T* and S* space constitutes a characteristic predictor of the downstream response. Here we focus on how T* and S* change longitudinally for three different rivers, and compare trajectories and downstream responses to dams for the Green, Colorado, and Deschutes Rivers. We consider how these trajectories and responses reflect the underlying geological settings of these three rivers. For comparison we consider both the absolute longitudinal distance (L) and dimensionless distance (L*), the latter scaled by a characteristic length which we take as the channel width (W_c), or $L^* = L/W_c$.

Green River, Utah

Flaming Gorge Dam is located on the upper Green River and completely traps sediment delivered to the river from the mountains and deserts of western Wyoming and the north flank of the Uinta Mountains of Utah. *Andrews* [1986] calculated the change in sediment supply, effective discharge, and sediment transport for pre-dam and post-dam periods, and identified reaches of differing balance between sediment supply and sediment transport capacity. His analyses have been updated and the extent of associated channel changes examined in detail by *Lyons et al.* [1992], *Orchard and Schmidt* [1998], *Allred and Schmidt* [1999], and *Grams and Schmidt* [1999, 2002]. Although some of *Andrews'* [1986] sediment budget numbers have been revised by these more recent studies, we use his 1986 data here because it encompasses the entire 464 km from Flaming Gorge to the Green River (UT) gage; use of this earlier data does not change the underlying story as revealed by later work.

Andrews [1986] defined three different downstream reaches, bounded by USGS gaging stations: Reach 1 from Flaming Gorge Dam to the Jensen gage (termed the Brown's Park reach in this study, with initial flow and sediment measured at the Greendale gage); Reach 2 from the Jensen to the Ouray gage; and Reach 3 from the Ouray to the Green River gage, a total distance of 464 km. *Andrews* [1986] notes that the supply of sediment and water in the basin is not uniform, with most of the water coming from headwater areas in the Wind River Range, while most of the sediment comes from lower tributaries draining the semi-arid Colorado Plateau. In particular, most of the water and sediment in Reach 1 are supplied by the Yampa River at 105 river kilometers below Flaming Gorge.

Although total sediment transport is calculated over the entire discharge range, T* is difficult to calculate directly from the published graphs. However, from visual fitting it appears that sediment transport of the sand fraction that makes up most of the sediment load begins at a discharge of approximately 14 m^3/s (500 ft^3/s) at the different gages [*Andrews*, 1986, Figures 3-4]. Flows of this magnitude were exceeded 90–99% of the time under pre-dam conditions and over 99% of the time under post-dam conditions (since dam operation increased daily low flows) so T* decreased from 1.1 near the dam to very close to 1.0 further downstream (Table 1).

Prior to the dam, sediment discharge past the Greendale gage was calculated as $3.6 \cdot 10^6$ t/yr [*Andrews*, 1986; Table 1]. Flows released from Flaming Gorge reservoir contain no sediment, but large tributaries contribute sediment downstream, so that S*, which we calculate in terms of the volume of sediment delivered to the channel in each reach, rather than the net of supply less transport, increases from 0 at the dam to 3.0 at 464 km downstream (Table 1)(Figure 4a). We use sediment input rather than net input less transport in these calculations since transport may itself be a function of supply [*Topping et al.*, 2000a], which would confound comparisons between rivers.

Andrews [1986] measured changes in channel morphology from aerial photos and cross-sections. If the downstream trajectories of S* and T* are replotted on Figure 5, their correspondence to changes in channel morphology can be evaluated. The lower portion of Reach 1 (Brown's Park) is described as narrowing by 13% and degrading approximately 0.7 m; the sediment budget shows a net depletion of sediment since dam construction. Later work by *Grams et al.*

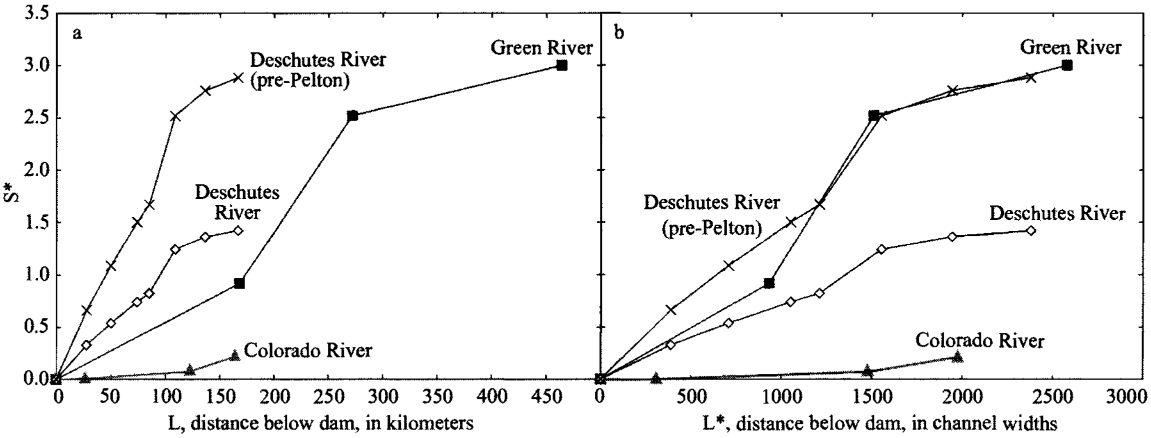

Figure 4. Longitudinal trajectories of change in S* for the Green, Colorado, and Deschutes Rivers below Flaming Gorge, Glen Canyon, and Pelton-Round Butte dams, respectively. Two trajectories are shown for the Deschutes, depending on whether the reference value for the above-dam sediment flux is calculated as pre- or post-upriver dam construction. (a) Absolute distance (L) in kilometers; (b) Non-dimensional distance (L*) equal to L/Wc where Wc is average channel width, and expressed in channel widths.

[2002] could not distinguish between sediment deficit or balance in the segment of the Green River upstream from the Yampa and found no evidence that this reach had degraded during the post-dam period. Downstream from the Yampa River, *Andrews* [1986] and *Grams et al.* [2002] both determined that sediment transport was less than sediment supply.

In Reach 2, both a degree of narrowing similar to upstream (13%) as well as vegetation encroachment and mid-channel bar construction were noted; the sediment budget for this reach indicates that there has been no net accumulation or depletion of sediment since dam construction. Reach 3 is aggrading where the supply of sediment from tributaries is exceeding transport, although the reaches are 10% narrower than prior to dam construction; apparently a new floodplain is being constructed at a reduced channel width.

Further work by *Grams and Schmidt* [2002,] and *Grams et al.* [2002] showed that the Green River has narrowed throughout its length, both upstream and downstream from the Yampa River. Channel organization and bed material exert a large degree of control on the magnitude and style of channel adjustment, but the average magnitude of channel narrowing has been between 15 and 20% throughout.

Table 1. Calculation of T* and S* for the Green River below Flaming Gorge dam from data presented by *Andrews* [Figures 3-7, 1986]. Frequency of sediment transport calculated from sediment rating and flow duration curves, assuming Q_{cr} = 14 m^3/s. S* is calculated using the pre-dam sediment supply rate at Greendale gage as the reference point. Average channel width is 180.00 m.

Reach	Distance below dam in km	in channel widths	% time flow above Q_{cr} Pre-dam	Post-dam	T*	Sediment supply to reach (tons·10^6/yr) Pre-dam	Post-dam	S* (pre)	S* (post)
Outflow from Flaming Gorge (measured at Greendale)	0	0	90.0	99.7	1.1	3.60	0.00	1.00	0.00
1—Greendale-Jensen	168	933.3	90.0	99.7	1.1	6.92	3.31	1.92	0.92
2—Jensen-Ouray	272	1511.1	99.5	99.9	1.0	12.80	9.06	3.56	2.52
3—Ouray-Green River	464	2577.8	99.5	99.9	1.0	17.00	10.80	4.72	3.00

with the Green and Deschutes River data, for which Q_{cr} is estimated on the basis of initial motion, we use the lower bound of the range (200 m³/s), which may still be too high for the Lees Ferry gage based on the sediment rating curve.

This discharge corresponds to a flow duration equaled or exceeded on average 97% of the time during the pre-dam snowmelt season (April-June), but only 40% of the time during the rest of the year; a composite flow duration curve for the entire year was not presented. Since we are interested in whether sand actually moved during the course of the year on an inter-annual basis, rather than the seasonal variation in sand transport that is the focus of the *Topping et al.* [2000a] study, we take the pre-dam value for T_{pre} as 97%, recognizing that a flow duration curve recalculated on an annual (as opposed to seasonal) basis would likely yield a slightly lower value. Using the same threshold of transport and flow duration data, T_{post} is calculated as 80% for the period 1966-98. This gives T* at Lees Ferry a value of 0.82; no data are presented for other gages. We take T* as constant over the entire section, although the authors suggest that it decreases very slightly downstream, since very little water is supplied by tributaries relative to the mainstem flow.

S* is calculated from the sediment budget presented by *Topping et al.* [2000a], showing inputs from the Paria and Little Colorado Rivers along with ungaged tributaries (Table 2). Because the spatial distribution of these tributaries is not shown, the $0.72 \cdot 10^6$ t were apportioned on a distance-averaged basis over the 139 km to the Grand Canyon gage. Channel width was calculated as the average of values given by *Schmidt and Graf* [1990; Table 2] for the upper Grand Canyon.

Because so much of the sediment in the Colorado River prior to the dam was derived from upstream, the increase in S* with distance downstream is small (Figure 4a,b) (Table 2). From data presented in *Topping et al.* [2000a], only 21% of the pre-dam sediment volume at the Grand Canyon gage has been made up on an annual basis by tributary contributions. More recent data suggest that tributaries may make up only 10-15% of pre-dam sediment at this location (D. Topping, personal communication, 2003). Plotting this data in T* and S* space reveals that the upper Colorado River remains entirely within the degradational domain over its entire length, a finding consistent with the many studies that have documented overall erosion of the sand beaches in the upper Grand Canyon [*Schmidt and Graf*, 1990; *Topping et al.*, 2000a,b; *Rubin et al.*, 2002] (Figure 5). Erosion is not uniform along this section, however, and local geologic controls, including the morphology and orientation of debris fans from tributaries, play key roles in determining where erosion and deposition occur, either for beaches or the fans themselves [*Schmidt and Graf*, 1990; *Webb et al.*, 1999; *Pizzuto et al.*, 1999; *Andrews et al.*, 1999].

Deschutes River, Oregon

Data presented by *Fassnacht et al.* [this volume] and *O'Connor, Grant and Haluska* [this volume] permit calculation of S* but not T* for the Deschutes River below the Pelton-Round Butte dam complex, Oregon. There is no suspended-sediment data for this cobble-bedded river, so the analysis of sediment transport by *Fassnacht et al.* [this volume] focuses exclusively on transport of the coarse (gravel to cobble) material that comprises the channel bed. Although both Pelton and Round Butte dams are operated for hydroelectric peaking power production, the downstream re-regulation dam smoothes out discharge variations to the point that the complex has minimal effects on hydrology, with little change in Q_{peak} or Q_{mean}. Because the dam has imposed almost no change on the flow duration curves

Table 2. Calculation of S* for the Colorado River from data presented by Topping et al. [2000] using the pre-dam sediment supply rate at Lees Ferry gage as the reference point. Estimated contributions from ungaged tributaries ($0.72 \cdot 10^6$ tons) are apportioned on a distance-weighted basis between Lees Ferry and Grand Canyon. Average channel width is 83.00 m.

Reach	Distance below dam in km	Distance below dam in channel widths	Sediment supply to reach (tons·10⁶/yr) Pre-dam	Sediment supply to reach (tons·10⁶/yr) Post-dam	S* (pre)	S* (post)
Outflow from Glen Canyon (measured at Lees Ferry)	24	289.1	57.00	0.24	1.00	0.00
1—Lees Ferry-Paria	25.4	306.0	57.01	0.26	1.00	0.00
2—Paria-Little Colorado	122.4	1474.7	60.50	3.74	1.06	0.07
3—Little Colorado-Grand Canyon	163.8	1973.5	68.81	12.01	1.21	0.21

we assume that T* is very close to 1.0 near the dam. The estimated frequency of sediment transport is quite low; depending on the assumptions used in the transport model, critical flows for sediment transport occur from 0.004 to 0.7% of the time over the entire period of record from 1924 – 1996 [*Fassnacht et al.*, this volume].

O'Connor, Grant and Haluska [this volume, Figure 15] show the effect of the Pelton-Round Butte dam complex on sediment supply to the lower Deschutes River in the context of other upstream dams that have diminished sediment supply. Here we consider how S* varies in relation to this history of dam construction on the Deschutes River (Table 3). The Pelton-Round Butte dam complex is both the youngest and downstream-most set of dams on the Deschutes. Construction of upstream dams over the past 80 years has therefore progressively reduced sediment supply to the river below Pelton-Round Butte even before its construction. This raises the question of what the "reference" value for S_A—the above-dam sediment flux—should be for calculating S*. Should it be the upstream sediment flux prior to all dams, or the flux with the other dams in place? It should be the latter if we are focused on the incremental effects of the Pelton-Round Butte dam complex on the river, and the former if we are interested in the overall effects of dams. We plot both trajectories for comparison (Figure 4).

These trajectories show that the rate of increase in S* with downstream distance is higher for the Deschutes River than either of the other two rivers, particularly when the below-dam input is compared with the influx calculated with the upriver dams in place. This rapid increase is due in large part to the geological setting of the Pelton-Round Butte dams. Due to geological factors, basin-wide sediment supply rates for the Deschutes are extremely low, with rates of 4.4-6.1 t/yr·km^2 calculated from reservoir filling rates that are among the lowest in the world [*O'Connor et al.*, this volume]. In addition, much of the water in the upstream reaches of the basin comes from a young (Pleistocene to Holocene) volcanic terrain with little weathering, a high degree of permeability, and a poorly developed drainage network [*Gannett et al.*, this volume]. With upstream dams intercepting much of the remaining sediment before it even reaches the Pelton-Round Butte dam complex, supply rates to the complex are intrinsically low. S* increases rapidly downstream due to both water and sediment influx from tributaries draining the higher and more erodable eastern ramparts of the Cascade Range [*O'Connor, Grant and Haluska*, this volume]. The location of the dam complex at the boundary between two geological terrains, and just downstream from a shift in hydrologic regime from a groundwater to a surface-water dominated system provides a setting where downstream supply of sediment quickly replenishes that intercepted by the dam. With the upriver dams in place, the volume of sediment intercepted by the Pelton-Round Butte dam complex is restored within 40 km (600 channel widths) downstream of the complex, where S* equals 1.0 (Figure 4a,b). For comparison, S* approaches 1.0 at 160 km (1000 channel widths) for the Green River, and from linear regression of the established trend, would require 700 km (8434 channel widths) for the Colorado.

The trajectory of the Deschutes River in T* and S* space is consistent with findings that the degree of geomorphic change in the reaches immediately downstream from the dam was minor. No significant morphologic or textural adjustments were observed in the 160 km downstream of the

Table 3. Calculation of S* for the Deschutes River below the Pelton-Round Butte hydroelectric project, from estimated sediment delivery data presented by *O'Connor, Grant and Haluska* [this volume, Figure 15]. The pre-Pelton reference value of S* is calculated using different values for the above-dam sediment supply (S_A): (1) before construction of any Deschutes dams; (2) following construction of all upstream dams. After closure of Pelton-Round Butte, S* is calculated using either the sediment delivered prior to any dams (3) and following upstream dam construction (4). Average channel width is 70 m.

Reach (in River Kilometers)	Distance below dam: in km	Distance below dam: in channel widths	Sediment supply to reach (tons·10^6/yr): Pre-dam	Sediment supply to reach (tons·10^6/yr): Pre-Pelton	Sediment supply to reach (tons·10^6/yr): Post-dam	S*1 before all dams	S*2 before Pelton Dam	S* after Pelton Dam: S*3, using pre-dam flux	S* after Pelton Dam: S* 4, using pre-Pelton flux
166.4 (at Pelton Dam)	0	0	0.50	0.25	0.00	1.0	1.0	0.0	0.0
139.2	27.2	389	0.66	0.41	0.16	1.3	1.7	0.3	0.7
116.8	49.6	709	0.77	0.52	0.27	1.5	2.1	0.5	1.1
92.8	73.6	1051	0.87	0.62	0.37	1.7	2.5	0.7	1.5
81.6	84.8	1211	0.91	0.66	0.41	1.8	2.7	0.8	1.7
57.6	108.8	1554	1.12	0.87	0.62	2.2	3.5	1.2	2.5
30.4	136	1943	1.18	0.93	0.68	2.4	3.8	1.4	2.8
0 (at Columbia R. confluence)	166.4	2377	1.21	0.96	0.71	2.4	3.9	1.4	2.9

dam [*Fassnacht et al.*, this volume; *Curran and O'Connor*, this volume]. Further inhibiting morphologic adjustments are the coarse bars and terraces that are remnant features of older paleofloods in the canyon due to landslide dam collapses and other flood events; the large cobbles and boulders that make up these deposits resist transport under all but the most exceptional floods [*O'Connor, Grant and Haluska*, this volume; *Curran and O'Connor*, this volume]. As shown within the central region of Figure 5, the history of geological disturbances to the river and valley may dictate the nature of channel adjustments. This history may explain the difference in response between the Deschutes River and the Green River, which displays a similar trend of S^* with nondimensionalized distance downstream (Figure 4b), but which exhibited a more demonstrable, though still modest response. The Green River, having no known history of paleofloods and landslide dam floods, lacks the coarse deposits that would limit channel adjustment; the finer and more easily transported sand-sized sediment in the Green River may be another factor in determining the channel's greater lability than the Deschutes.

IMPLICATIONS FOR INTERPRETING DOWNSTREAM RESPONSES TO DAMS: AN EXAMPLE FROM THE OREGON CASCADES

Along with its heuristic value, the geological framework proposed here provides first-order predictions on likely trajectories of response to dams based on geological setting. As an example, consider the major hydroelectric and flood control dams located in the Willamette River basin, Oregon, the basin adjacent to the Deschutes on the western side of the Cascade Range (Figure 6). While the downstream effects of several of these dams, notably those on the Clackamas River, are being studied as part of the FERC relicensing process, none of them have yet received the extensive geomorphic analysis that has occurred on the Deschutes River. Despite this paucity of data, however, an understanding of the geological setting of these dams provides the basis for interpreting likely directions and magnitudes of downstream response.

The geology of the western side of the Cascade Range can be broadly classified into two regions: the High and Western Cascades [*Ingebritsen et. al.*, 1991; *Grant*, 1997] (Figure 6). The Western Cascades are composed of strongly-weathered basalt and andesite flows from periodic volcanic episodes during the Miocene Era. The steep, highly dissected landscape of the Western Cascades reflects the significant erosion that has occurred in this landscape. Drainage densities are high, averaging 3-4 km/km^2, reflecting an efficient well-organized drainage system [*Wemple et. al.*, 1996]. Streamflows are highly variable, with winter peaks several orders of magnitude larger than low summer base flows. Background sediment yields are on the order of 25 to 50 t/km^2·yr and may increase by as much as an order of magnitude following timber harvest, which is the dominant land use activity [*Grant and Wolfe*, 1991].

In contrast, the High Cascades are much younger geologically and reflect recent volcanic activity rather than erosional forms. Rock is dominated by basalt and andesite, mostly from shield volcano lava flows. In areas of the High Cascades with the most recent volcanic activity, blocky basalt flows are often visible at the surface. Surface hydraulic conductivities in these areas are exceptionally high and often remain high throughout deep permeable volcanic layers. Drainage density in the High Cascades province is significantly lower than in the Western Cascade Province, averaging 1-2 km/km^2. Streamflows are quite uniform throughout the year, with muted winter peaks and high summer base flows. Sediment yields from the western slopes of the High Cascades have not been measured directly, but are likely on the order of 10 – 20 t/km^2·yr, based on eastside reservoir sedimentation rates [*O'Connor, Grant and Haluska*, this volume].

With this broad-scale understanding of the geological setting, we would predict that dams and reservoirs located within or at the western margins of the High Cascade province will trap little sediment, since little is produced by their upstream source areas. Most of the hydroelectric projects are operated as run-of-river, with little storage and flow variation imposed, so the dams impose only minor changes on hydrologic regime. Uniform streamflows and muted peak flows result in low frequency of transport, with or without dams. Therefore, we would predict that T^* will be close to 1.0 and that S^* will rapidly recover to 1.0 downstream of the dams, particularly where dams are located at the boundary with the more erosive terrain of the Western Cascades. Using these simple assumptions and the geologic framework of Figure 3, we would predict only subtle and modest channel changes downstream of dams located within the High Cascades province. In effect, these streams will act similarly to the Deschutes River. Watershed analyses conducted on other dams located at the High/Western Cascades boundary have borne this out [*Stillwater Sciences*, 1998].

The larger flood control dams located on streams whose drainage areas fall mostly or entirely within the Western Cascades may impose a different set of downstream changes than High Cascade dams. Dams located in this region will capture the larger quantities of sediment produced in the Western Cascades, although much of this sediment is silt and clay and thus not likely to substantially affect channel

morphology [*Ambers*, 2001a,b]. Moreover, these flood control dams are operated to suppress winter peaks, so frequency of sediment transport for the coarse fractions (but not necessarily the finer fractions) is likely reduced as well. We would therefore predict that T^* will be less than 1.0, while S^* will recover more slowly than for High Cascade dams. Consequently, we would expect to see downstream reaches below Western Cascade dams plotting in the lower left-hand corner of Figure 3. Since both sediment supply and frequency of transport have been reduced, it is possible that geomorphic response of these streams will also be subtle, but some degree of channel incision or coarsening might be expected. Although a detailed analysis of these streams has not been done, initial analyses are consistent with this interpretation [*Ligon et. al.*, 1995].

CONCLUSIONS

We have only begun to look at the downstream responses of rivers to dams through the lens of the river's geologic setting and history as well as the degree of hydrogeomorphic change imposed by the dams themselves. The examples considered here have only included dams with relatively modest alterations to the hydrology; we need a more exhaustive analysis of the existing case studies that includes dams showing the full range of hydrologic and geomorphic effects. Although our results are preliminary and qualitative, they suggest that our approach may have potential to help predict geomorphic responses to dams, at least in general terms, and to frame further studies and hypotheses.

A key strength of the analytical framework presented here is that it can be flexibly used to meet different management objectives by varying the grain size used in determining $T^*$and S^*. For example, if erosion of sand beaches used as campsites by river runners were the key issue, such as on the Colorado or Snake Rivers, then both variables should be calculated using the critical threshold for sand transport and the rate of sand resupplied from tributaries as the basis for the analysis. If, on the other hand, loss of spawning gravel below dams were the driving concern, then both variables would be calculated using the threshold and resupply rate for gravel. This ability to variously depict the downstream trajectory of rivers in response to loss of specific grain-size fractions and flow alterations offers river managers a more comprehensive way of evaluating tradeoffs between competing management goals.

Detailed geomorphic studies of rivers, such as the Deschutes and the Colorado, are expensive and time-consuming undertakings. With the prospect of new dam construction in developing countries as well as dam removal for those countries with an aging dam infrastructure, these types of studies will continue. Conceptual and analytical frameworks, such as the one presented here, are needed so that these studies can be efficiently and effectively targeted towards the most likely fluvial responses. The testing and refinement of these frameworks then becomes a means of capturing the accumulated knowledge from individual projects and cases. This progression from site-specific studies to conceptual models to hypothesis testing to theory promises to advance not only our understanding of how dams affect rivers, but how rivers themselves evolve and behave.

Acknowledgments. Jim O'Connor's comments were critical to the development of the concepts in this paper. Dave Topping and Pete Wampler provided thoughtful reviews. Tom Lisle, Heidi Fassnacht, and Ellen McClure also contributed. The graphical and editorial assistance of Kathryn Ronnenberg is gratefully acknowledged.

REFERENCES

Allred, T. M. and J. C. Schmidt, Channel narrowing by vertical accretion along the Green River near Green River, Utah, *Geol. Soc. Amer. Bull., 111*(12), 1757-1772, 1999.

Ambers, R. K. R., Using the sediment record in a western Oregon flood-control reservoir to assess the influence of storm history and logging on sediment yield. *J. Hydrol., 244*(3-4), 181-200, 2001a.

Ambers, R. K. R., Relationships between clay mineralogy, hydrothermal metamorphism, and topography in a Western Cascades watershed, Oregon, USA. *Geomorphology, 38*(1-2), 47-61, 2001b.

Andrews, E. D., Effective bankfull discharges of streams in the Yampa River basin, Colorado and Wyoming, *J. Hydrol., 46*, 311-330, 1980.

Andrews, E. D., Entrainment of gravel from naturally sorted riverbed material, *Geol. Soc. Amer. Bull., 94*, 1225-1231, 1983.

Andrews, E. D., Bed-material entrainment and hydraulic geometry of gravel-bed rivers in Colorado, *Geol. Soc. Amer. Bull., 95*, 371-378, 1984.

Andrews, E. D., Downstream effects of Flaming Gorge Reservoir on the Green River, Colorado and Utah, *Geol. Soc. Amer. Bull., 97*, 1012-1023, 1986.

Andrews, E. D., Bed Material transport in the Virgin River, Utah, *Water Resourc. Res., 36*, 585-596, 2000.

Andrews, E.D. and J.M. Nankervis, Effective discharge and the design of channel maintenance flows for gravel-bed rivers, in *Natural and anthropogenic influences in fluvial geomorphology; the Wolman Volume, Geophys. Mon. 89*, edited by J.E. Costa, A.J. Miller, K.W. Potter and P.R. Wilcock, pp. 151-164, American Geophysical Union, Washington, DC, 1995

Andrews, E. D., C. E. Johnston, J. C. Schmidt and M. Gonzales, Topographic evolution of sand bars, in *The Controlled Flood in* *the Grand Canyon, Geophys. Mon. 110*, edited by R. H. Webb, J. C. Schmidt, G. R. Marzolf and R. A. Valdez, pp. 117-130, American Geophysical Union, Washington, DC, 1999.

Brandt, S. A., Classification of geomorphological effects downstream of dams, *Catena*, *40*, 375-401, 2000.

Bennett, J. P., Algorithm for resistance to flow and transport in sand-bed channels, *J. Hydraul. Eng.*, ASCE, 121(8), 578-590, 1995.

Brune, G. M., Trap Efficiency of Reservoirs. *Trans. American Geophysical Union 34*(3): 407-418, 1953.

Carling, P. A., Channel change and sediment transport in regulated U.K. rivers, *Regulated Rivers, 2*, 369-387, 1988

Church, M., Geomorphic response to river flow regulation: case studies and timescales, *Regulated Rivers, 11*, 3-22, 1995

Church, M. and R. Kellerhals, On the statistics of grain size variation along a gravel river, *Can. J. Earth Sci.*, *15*(7), 1151-1160, 1978.

Collier, M., R. H. Webb, and J. C. Schmidt, *Dams and Rivers: A Primer on the Downstream Effects of Dams, U.S. Geol. Surv. Circ. 1126*, 94 pp., 1996.

Costa, J. E. and J. E. O'Connor, Geomorphically effective floods, in *Natural and anthropogenic influences in fluvial geomorphology; the Wolman Volume, Geophys. Mon. 89*, edited by J. E. Costa, A. J. Miller, K. W. Potter and P. R. Wilcock, pp. 45-56, American Geophysical Union, Washington, DC, 1995.

Dietrich, W. E., J. W. Kirchner, H. Ikeda and F. Iseya, Sediment supply and the development of the coarse surface layer in gravel-bedded rivers, *Nature*, *340*(6230), 215-217, 1989.

Galay, V. J., R. S. Pentland and R. A. Halliday, Degradation of the South Saskatchewan River below Gardiner Dam, *Can. J.Civil Eng.*, *12*, 849-862, 1985.

Graf, W. L., Dam nation: a geographic census of American dams and their large-scale hydrologic impacts, *Water Resourc. Res.*, *35*, 1305-1311, 1999.

Grams, P. E. and J. C. Schmidt, Geomorphology of the Green River in the eastern Uinta Mountains, Dinosaur National Monument, Colorado and Utah, in *Varieties of Fluvial Form*, edited by A. J. Miller and A. Gupta, pp. 81-111, John Wiley & Sons, New York, 1999.

Grams, P. E. and J. C. Schmidt, Streamflow regulation and multilevel floodplain formation: channel narrowing on the aggrading Green River in the eastern Uinta Mountains, Colorado and Utah, *Geomorphology*, *44*, 337-360, 2002.

Grams, P. E., J. C. Schmidt, and T. Naumann, Geomorphic adjustment of the Green River and habitat distribution of the Ute-Ladies Tresses Orchid in Red Canyon and Browns Park, Colorado and Utah, Final Report to Dinosaur National Monument and Bureau of Reclamation, Utah State University, Logan, Utah, 80 pp, 2002.

Grant, G. E., 1997. A geomorphic basis for the hydrologic behavior of large river systems, in *River Quality: Dynamics and Restoration*, edited by A. Laenen and D. A. Dunnette, pp. 105-116, CRC Lewis Publishers, Boca Raton, Florida, 1997.

Grant, G. E. and F. J. Swanson, Morphology and processes of valley floors in mountain streams, western Cascades, Oregon. in *Natural and Anthropogenic Influences in Fluvial Geomorphology: the Wolman Volume, Geophys. Mon.No. 89*, edited by J. E. Costa, A. J. Miller, K. W. Potter and P. R. Wilcock, pp. 83-101, American Geophysical Union, Washington, DC, 1995.

Grant, G. E. and A. L. Wolff, Long-term patterns of sediment transport after timber harvest, western Cascade Mountains, Oregon, USA, in *Sediment and Stream Water Quality in a Changing Environment, Proc. of the Vienna IAHS Symp., IAHS Pub. No. 203*, edited by D. E. Walling and N. Peters, pp. 31-40, International Association of Hydrological Sciences, Oxfordshire, United Kingdom, 1991.

Heinz Center, *Dam Removal: Science and Decision Making*, H. John Heinz III Center for Science, Economics, and the Environment, Washington, DC, 221 pp., 2002.

Inbar, M., Effect of dams on mountainous bedrock rivers, *Phys. Geog.*, *11*(4), 305-319, 1990.

Ingebritsen, S. E., R. H. Mariner and D. R. Sherrod, Hydrothermal systems of the Cascade Range, north-central Oregon, *U.S. Geol. Surv. Open-File Rep. 91-0069*, 21 pp., 1991.

Iorns, W. V., C. H. Hembree and G. L. Oakland, Water resources of the upper Colorado River basin—Technical Report, *U.S. Geol. Surv. Prof. Pap. 441*, 370 pp.

Kieffer, S. W., The 1983 hydraulic jump in Crystal Rapid – Implications for river-running and geomorphic evolution in the Grand Canyon, *J. Geology*, *93*, 385-406, 1995.

Lane, E. W., The importance of fluvial morphology in hydraulic engineering, *Proc.Amer. Soc. Civil Eng.*, *81*, 1955.

Leopold, L. B., M. G. Wolman and J. P. Miller, *Fluvial Processes in Geomorphology*, W. H. Freeman, San Francisco, 522 pp., 1964.

Ligon, F. K., W. E. Dietrich and W. J. Trush, Downstream ecological effects of dams: a geomorphic perspective, *Bioscience*, *45*(3), 183-192, 1995.

Lyons, J. K., M. J. Pucherelli and R. C. Clark, Sediment transport and channel characteristics of a sand-bed portion of the Green River below Flaming Gorge Dam, Utah, USA, *Regulated Rivers: Research and Management*, *7*, 219-232, 1992.

Madej, M. A., Development of channel organization and roughness following sediment pulses in single-thread, gravel bed rivers. *Water Resourc. Res.*, *37*(8), 2259-2272, 2001.

Meade, R. H., T. R. Yuzyk and T. J. Day, Movement and storage of sediment in rivers of the United States and Canada, in *Surface Water Hydrology, The Geology of North America, Vol. O-1*, edited by M. G. Wolman and H. C. Riggs, pp. 255-280, The Geological Society of America, Boulder, Colorado, 1990.

Meyer, G. A. and M. E. Leidecker, Fluvial terraces along the Middle Fork Salmon River, Idaho, and their relation to glaciation, landslide dams and incision rates; a preliminary analysis and river-mile guide, in *Guidebook to the Geology of Eastern Idaho*, edited by S. S. Hughes and G. D. Thackray, pp. 219-235, Idaho Museum of Natural History, Pocatello, Idaho, 1999.

National Research Council. Committee on Missouri River Ecosystem Science, *The Missouri River Ecosystem: Exploring the Prospects for Recovery*, National Academy Press, Washington, DC, 188 pp., 2002

Orchard, K. L. and J. C. Schmidt, A geomorphic assessment of the availability of potential humpback chub habitat in the Green River in Desolation and Gray canyons, Utah: final report to the Utah Division of Wildlife Resources, 68 pp., 1998.

Petts, G. E., Complex response of river channel morphology subsequent to reservoir construction, *Prog. Phys. Geog.*, 3, 329-362, 1979.

Petts, G. E., Long-term consequences of upstream impoundment, *Env. Cons.*, *7*(4), 325-332, 1980.

Petts, G. E., Channel changed in regulated rivers, in *Papers in Earth Studies, Lovatt lectures – Worcester,* edited by B. H. Adlam, C. R. Fenn and L. Morris, pp. 117-142, Geo Books, Norwich, United Kingdom, 1982.

Petts, G. E., *Impounded River: Perspectives for Ecological Management*, John Wiley & Sons, Chichester, United Kingdom, 326 pp., 1984.

Pitlick, J. and P. Wilcock, Relations between streamflow, sediment transport, and aquatic habitat in regulated rivers, in *Geomorphic Processes and Riverine Habitat, Water Science and Application Vol. 4*, edited by J. M. Dorava, D. R. Montgomery, B. B. Palcsak and F. A. Fitzpatrick, pp. 185-198, American Geophysical Union, Washington, DC, 2001.

Pizzuto, J. E., R. H. Webb, P. G. Griffiths, J. G. Elliott and T. S. Melis, Entrainment and transport of cobbles and boulders from debris fans, in *The Controlled Flood in the Grand Canyon, Geophys. Mon. 110*, edited by R. H. Webb, J. C. Schmidt, G. R. Marzolf and R. A. Valdez, pp. 53-70, American Geophysical Union, Washington, DC, 1999.

Riggs, H. C. and K. D. Harvey, Temporal and spatial variability of streamflow, in *Surface Water Hydrology, The Geology of North America, Vol. O-1*, edited by M. G. Wolman and H. C. Riggs, pp. 81-96, The Geological Society of America, Boulder, CO, 1990.

Rubin, D. M., D. J. Topping, J. C. Schmidt, et al., Recent sediment studies refute Glen Canyon Dam hypothesis, *EOS*, *83*(25), 273-278, 2002.

Schmidt, J. C. and J. B. Graf, Aggradation and degradation of alluvial-sand deposits, 1965 to 1986, Colorado River, Grand Canyon National Park, Arizona. *U. S. Geol. Surv. Prof. Pap. 1493*, 74 pp., 1990.

Schmidt, J. C., and D. M. Rubin, Regulated streamflow, fine-grained deposits, and effective discharge in canyons with abundant debris fans, in *Natural and Anthropogenic Influences in Fluvial Geomorphology, AGU Geophys. Mon. 89*, edited by J. E. Costa, A. J. Miller, K. W. Potter, and P. R. Wilcock, pp. 177-195, Amer. Geophys. Union, Washington, D.C., 1995.

Schmidt, J. C., B. L. Everitt and G. A. Richard, Hydrology and geomorphology of the Rio Grande and implications for river restoration, in Ecology of the Rio Grande, edited by G. L. Garrett, Texas Tech Publications, Lubbock, Texas, in press.

Stillwater Sciences, *North Umpqua Cooperative Watershed Analysis Synthesis Report*, prepared for Pacificorp, unpublished report, 1998.

Swanson, F. J., R. L. Graham, and G. E. Grant, Some effects of slope movements on river channels, in *Proceedings, International Symposium on Erosion, Debris Flow and Disaster Prevention*, September 3-5, 1985, Tsukuba, Japan, pp. 273-278, 1985.

Topping, D. J., D. M. Rubin, and L. E. Vierra Jr., Colorado River sediment transport. 1. Natural sediment supply limitation and the influence of Glen Canyon Dam, *Water Resourc. Res.*, *36*(2), 515-542, 2000a.

Topping, D. J., D. M. Rubin, J. M. Nelson, P. J. Kinzel III and I. C. Corson, Colorado River sediment transport. 2. Systematic bed-elevation and grain-size effects of sand supply limitation, *Water Resourc. Res.*, *36*(2), 543-570, 2000b.

Webb, R. H., T. S. Melis, P. G. Griffiths and J. G. Elliott, Reworking of aggraded debris fans, in *The Controlled Flood in the Grand Canyon, Geophys. Mon. 110*, edited by R. H. Webb, J. C. Schmidt, G. R. Marzolf and R. A. Valdez, pp. 37-51, American Geophysical Union, Washington, DC, 1999.

Wemple, B. C., J. A. Jones and G. E. Grant, Channel network extension by logging roads in two basins, western Cascades, Oregon, *Water Resourc. Bull.*, *32*(6), 1195-1207.

Wilcock, P. R., A. F. Barta , C. C. Shea, et al., Observations of flow and sediment entrainment on a large gravel-bed river, *Water Resourc. Res., 32*, 2897-2910, 1996.

Williams, G. P., and M. G. Wolman, Downstream effects of dams on alluvial rivers, *Geol. Surv. Prof. Pap. 1286*, 83 pp., 1984.

World Commission on Dams, *Dams and Development: A New Framework For Decision Making: The Report of the World Commission on Dams*, Earthscan Publications, Ltd, London, 2000.

Xu, J., Underlying gravel layers in a large sand bed river and their influence on downstream-dam channel adjustment, *Geomorphology*, *17*, 351-359, 1996.

Gordon E. Grant, U.S. Forest Service, 3200 SW Jefferson Way Corvallis, OR 97331

John C. Schmidt, Department of Aquatic, Watershed, and Earth Resources, Utah State University, Logan,, UT

Sarah L. Lewis, Department of Geosciences, Oregon State University, Corvallis, OR